University of Stavanger

FACULTY OF SCIENCE AND TECHNOLOGY

MASTER'S THESIS

Study programme/specialization: Petroleum Technology/ Drilling and Well Engineering	Spring semester, 2021 Open
Author: Luis Alberto Saavedra Jerez	
Programme Coordinator: Anita Malde Supervisor(s): Dan Sui	
Title of master's thesis: Trajectory Control Optimization Using the RSS Model	
Credits (ECTS): 30	
Keywords: - Rotary Steerable System - Automation - Optimization - Trajectory Control - Deviation Correction - Simulation - Error Model - Ellipse of Uncertainty - Vector of Error	Number of pages: 94 + supplemental material/other: 33 Stavanger, 14.06.2021 date/year

Title page for master's thesis

Faculty of Science and Technology

Abstract

Directional drilling has become a standard method to drill a well since the last decades, mainly caused by directional technologies and methods developments. The next step that the drilling industry is ready to take is to increase its automation levels to reduce their cost and increase the safe environment for field crews.

Moreover, the use of computers has allowed the creation of virtual tools that help drilling staffs visualize and foresee the issues and advantages through different phases from planning to post-analysis. Therefore, the present MSc thesis work focuses on developing a new approach (an in-house directional drilling simulator) to automatically and precisely estimate and control bit positions in real time.

This simulator is called Rotary Steerable System (RSS) Simulator and is based on the Trajectory Control Optimizer (TCO) and the RSS Model. The TCO was developed to plan the optimal trajectory, set the simulation targets, detect the bit deviations and create a correction path to return to the planned trajectory. Each of those processes is fulfilled without any human interaction during the simulation. The second element makes the simulation's calculations on physics including Newton's third law, beam bending analysis, bit force analysis, rate of penetration (ROP) to determine the bit position and then conduct RSS control to steer the bit accordingly. Such model is an upgraded version of the RSS Model developed by the University of Stavanger in 2020.

Besides, the RSS Simulator is a new tool that could interact with external models to interchange data and generate simulations closer to reality according to the factors involved. Furthermore, the simulator considers some uncertainty analysis and adds some noises (systematic and random) to the input data to give a more realistic behavior to the results. Thus, the RSS Simulator is the potential tool that might help the drilling industry walk towards automating most of its processes in the future.

Acknowledgments

I would like to thank Professor Dan Sui from the University of Stavanger for all the support and ideas she made me realize and foresee my potential in the automation area. Furthermore, she has always been kind and respectful, which is some values that I appreciate most from people.

Besides, I want to thank Andrzej Tunkiel for giving me many pieces of advice, not only in my thesis but also in my career. They made me create a point of view that I was not considering before and gave me a brushstroke of reality and potential.

Doing my master's programme in Norway has opened my mind more than I was expecting, not only in academics but also in social life. I have met marvelous friends who have always been happy to share their knowledge without hesitations, and they have always been there when I felt lonely in a new country.

Finally, I want to say big thanks to my family. Although they are on the other side of the world, their love and support were felt every day.

Contents

List of Figures

List of Tables

List of Symbols and Abbreviations

φ	Azimuth
μ	Sliding factor coefficient
a	Distance from the bit to the actuator of the BHA tool (assumed as 0.5 m)
b	Distance from the bit to the upper stabilizer of the BHA (assumed as 2.7 m)
d_E	Distance from the end point to the end attractor point in Beziér curves
DLS_{Bzr}	Dogleg severity of the Beziér calculation
d_S	Distance from the start point to the start attractor point in Beziér curves
E	East coordinate
$Error_{input}$	Error Noise that will be added to the external modules data
Es	Specific energy of the rock
$F_{bit\ azi}$	Total force on the bit for the azimuth component
$F_{bit\ inc}$	Total force on the bit for the inclination component
L_ABZ	MWD: Z-Accelerometer Bias Error – Systematic error
L_ASZ	MWD: Z-Accelerometer Scale Error – Systematic error
L_DSFS	Depth Scale Factor – Systematic error
L_MBXY1	MWD: TF Ind: X and Y Magnetometer Bias – Systematic error
L_MSXY1	MWD: RF Ind: X and Y Magnetometer Scale Factor – Systematic error
Max_{Deg}	Maximum degree of tolerance for the activation of offset
Max_{DLS}	Maximum DLS for the PWP
$Max_{DLS\ Corr}$	Maximum DLS that could be applied to the CP
$maxoff$	Maximum opening offset of the tool (0% to 100%)
Min_R	Minimum radius of EOU
N	North coordinate
$Offset$	Offset applied (percentage of opening of the actuator)
$Offset_L$	Maximum physical opening of the offset
Ran_{Tol}	Range tolerance for searching for the best d_S and d_E value
RF	Ratio factor for the minimum curvature method
ROP_{Axial}	ROP axial
ROP_{Azi}	ROP azimuth
ROP_{Inc}	ROP inclination
RPM	Revolutions per minute
SD_{EOU}	Standard deviation used in the Ellipse of Uncertainty
$Steer$	Steerability of the bit
Sur_{pts}	Survey points for the hold section construction in the PWP
Tol	Tolerance for considering two different segments
Tor	Tortuosity
$Tor_{Max\ Corr}$	Maximum tortuosity that could be applied to the CP
$Tot\ F_{Azi}$	Total force on the bit for the azimuth
$Tot\ F_{Inc}$	Total force on the bit for the inclination

u	Dimensionless parameter iterator, from 0 to 1, used in Beziér curves
V	Vertical coordinate
WOB	Weight on Bit
α	Inclination
Δ	Delta or difference between two measurements
Δt	Time step for the Simulation (Resolution)

BHA	Bottom Hole Assembly
CP	Correction Path
DCOC	Digital Connected Operation Center
DL	Dogleg
DLS	Dogleg Severity
DSATS	Drilling Systems Automation Technical Section
EOU	Ellipse of Uncertainty
HD	Horizontal Displacement
ISCWSA	Industry Steering Committee for Wellbore Survey Accuracy
KOP	Kick-Off Point
LWD	Logging While Drilling
MD	Measured Depth
ME	Minimum Energy
MPC	Model Predictive Control
MWD	Measurement While Drilling
PWP	Planned Well Path
ROP	Rate of Penetration
RP	Reference Path
RSS	Rotary Steerable System
SPE	Society of Petroleum Engineers
TCO	Trajectory Control Optimizer
TVD	True Vertical Depth
VOE	Vector of Error

1 Introduction

Directional drilling has been considered an unusual drilling technique some years ago when vertical drilling was the most common way of performing a drilling job. However, the directional drilling technology and operations have been evolving rapidly over the past decades. Nowadays, it has started to be contemplated as the standard way of drilling for most wells worldwide.

The origin and target zone define the path that the drilling is going to follow or at least try to follow. Since there are many disturbances when the Bottom Hole Assembly (BHA) is steering the direction of the bit, e.g., variations in the rotary walk and build, motor yield variations, target uncertainty, motor variations, gravity, and vibrations. As a result, some directional drillers will compensate for these disturbances, while others will fail to do these tasks and not reach the target properly (Chmela et al., 2020).

Following the projected well path in the drilling plan as much as possible, has brought the necessity to develop some technology to help the drillers to keep on the right track and monitor the drilling parameters. The current level of drilling tools and computers allows the oil industry to start experimenting with total autonomous drilling in some experimental wells.

Consequently, a new trajectory control optimization method has been developed for being used in the Rotary Steerable System Simulator (RSS Simulator) software. This simulator receives some survey points and drilling parameters and performs a simulation that creates the optimal Planned Well Path (PWP), controls the deviation, and corrects it if the deviation is over the maximum tolerance distance value. All the operations are done automatically and without any human intervention since the beginning of the simulation run.

1.1 Future of Drilling Industry

The future of drilling is pointing towards the automation of its operations, which implies that computers and simulators will have a prominent role in the drilling industry, along with the data analysis and its interpretation.

The rapid development of new drilling tools, like MWD, LWD and RSS, shows that the industry is adapting to the future quicker in recent years than in the past century. For instance, until 2006, the primary way to perform directional drilling was using some field engineers and experts on the wellsite. Later, in 2009, remote operations became more popular, where there were some field engineers and some remote engineers who monitor the drilling parameters in real time. In 2017 complete remote actions has been applied to a directional well where two operations were carried with any human intervention (Chatar et al., 2018).

Today there are 12 Digital Connected Operation Centers (DCOCs) that drill directional wells digitally on 350 rigs around the world, allowing the reduction of the crew on the wellsite and reducing the footprint of the directional service provider (Stepnov et al., 2019).

Moreover, the industry is looking for automation to achieve more reliable, safer, and better cost-effective operations. The access to downhole sensors lectures, telemetry in real-time, and the modern RSS system sensors add a complex decision-making situation for a drilling engineer (Demirer et al., 2019). As a result, an algorithm that simplifies that decision-making could be beneficial for the integrity of the well and avoid risky situations that would cost more money to repair.

Despite there are many questions regarding the confidence of a fully autonomous drilling system, it is evident that automation is the objective to reach, as many other industries have already implemented since years ago. Indeed, automation has already become part of our daily lives in other sensitive areas like banking and security. Therefore, the oil industry is preparing for this technology transition (Stepnov et al., 2019).

1.2 Directional Control

The direction control while drilling has a significant influence on the final hitting point inside the reservoir. Therefore, if there is reasonable control of the deviation and a proper correction of it, the possibility of hitting the target zone will increase.

Moreover, steering the bit in the right direction and hitting the geological target many kilometers downhole has caused the drilling engineering to pay more attention to tools and methods to identify the wellbore location and the path created while drilling (Farah, 2013).

The development of an automated directional control tool is challenging since it should consider the approximate position of the bit, the distance from the bit to the planned trajectory, the compensations of the variations in the parameters, and the uncertainty of the position of the tool generated by the depth, azimuth and inclination measure errors.

Once the automated directional control has analyzed the current situation of the drilling and has taken the decision of correcting the actual path towards the planned path again; it should interact with the BHA tool that is responsible for generating an offset opening (using an RSS system) that will turn the direction of the well.

In a typical situation, the directional driller would be responsible for transferring the adequate offset and direction correction to the BHA tool, using some series of measurements like inclination, azimuth, and measured depth from downhole sensors that are usually located 18.3 m (60 ft) behind the bit (Chmela et al., 2020).

However, this complex work, now, must be simulated or imitated by a computer algorithm that will send a signal to the BHA tool, indicating a possible offset opening. After that, the automated control will evaluate the current direction and determine whether the offset opening is enough or not, or if the offset is displacing the tool towards the desired direction.

1.3 2021 Drillbotics® Competition

Drillbotics® is an international competition where universities create a small laboratory drill rig that drills a rock sample autonomously. However, since 2021, a new category has been implemented due to the pandemic of COVID-19. Therefore, the 2021 competition will be divided into two categories: The virtual rig (team A) and the physical rig (team B) (Drillbotics®, 2020).

Particularly, the virtual rig competition will occur in a digital format. It requires the teams to develop a full-scale drilling system and its correspondent deviation control to virtually drill a directional well starting with a given trajectory (SPE & DSATS, 2020).

The University of Stavanger is competing in the 2021 Drillbotics® competition with both teams. Team A is developing a Real-Time Drilling Simulator for the mentioned competition, and the core of this simulator is the RSS Simulator. It is an excellent opportunity to prove and test the RSS Simulator's

limits, comparing its capacity against other simulators from other university teams.

The Drillbotics competitions foment creativity, problem-solving situations, computer programming skills, and implementation of drilling models. Consequently, the present work described in this thesis was developed to create a new approach for automation drilling, but at the same time, it was thought to be used as the principal algorithm for the 2021 Drillbotics® competition.

1.4 Objectives and Scope

The general objective of the thesis is to develop a new approach for simulating directional drillings using the RSS Model and an original automated trajectory control. In the same way, the specific objectives are the following:

- Create a methodology to propose the most optimal planned well trajectory, using just some survey points and some user constraints as initial data.
- Adapt the original RSS Model, described by Saramago and the University of Stavanger, to a new program structure to allow compatibility between the model and the trajectory control.
- Improve and automatize the offset control used in the RSS Model for being controlled only by the PWP target points.
- Create a procedure to detect deviations points in the simulation compared with the PWP, using space vectors and ellipses of uncertainty.
- Create a correction path to return to the nearest survey point on the PWP quickly and safely if the bit trajectory has deviated from the original path plan.
- Program and code the algorithms in a modular way to be compatible with other modules, which will be incorporated in the future for the Drillbotics® competitions.

Furthermore, the scope of the RSS Simulator includes different directional drilling techniques and concepts for calculating the survey points that will define the drilling path. For instance, the execution of Bezier curves in 3D and its optimization, the implementation of the ISCWSA error model, and ellipses of uncertainty will be used for determining the bit deviation, Dog Leg Severity (DLS), tortuosity limitations, and the codification of the simulator in Python language program.

Nonetheless, the RSS simulator has some limitations too. For example, it needs a minimum of 3 initial survey points for representing the curvature section of a well. In addition, it does not consider the gravity force on the tool or any deviation caused by the turning of the bit and requires a particular order of the input surveys for the 2D drilling cases.

2 Theoretical Concepts

Directional drilling involves certain theoretical concepts that must be understood before entering the automation of this process. In this chapter, some of this theory will be explained and described how it is used to support the trajectory control optimization.

2.1 Directional Drilling

The primary use of directional drilling is reaching targets that, due to different causes, cannot be reached or are difficult to access with a vertical well (Farah, 2013). In other words, a well is considered a directional well if there is a specific deviation from the vertical axis that creates some large inclination angle.

The directional drilling implementation situations can vary from optimizing the future production until solving some blowouts. Adams and Charrier indicate some of the specific uses of directional drilling resumed as the following (Adams & Charrier, 1985):

- **Inaccessible locations:** Sometimes, the ideal rig site cannot be accessed due to residential zones, riverbeds, mountains, roads, or another impediment.
- **Multiple wells drilling from a single site:** It is more economical to drill several directional wells from a single well site.
- **Sidetracking:** It is a standard solution for an obstruction (e.g., pack off, a trapped tool, well collapse) in the original well path.
- **Relief well drilling:** To intersect the bottom of a near blowout well; so, the mud and water can help mitigate the blowout pressure.
- **Multiple targets:** If it is necessary to drill through one target and later turn the direction to reach the next target.

Besides, in directional drilling engineering, some technical terminology should be well understood before explaining more detailed information. Farah describes some of the most used terms in drilling engineering in the following terms (Farah, 2013):

- **Azimuth:** Angle between the true North and the plane containing the vertical line from the wellhead and the vertical line through the target (Figure 2.1).
- **Build-up rate:** Angle from the kick-off point where the angle is steadily built up. Usually is measured in °/30 m.
- **Drop-off point:** The point since the inclination of the well begins to tend to vertical.
- **Horizontal Displacement (HD):** The horizontal distance between the vertical lines that pass through the wellhead and the target.
- **Inclination:** Angle between the tangential section of the hole with the vertical axis (Figure 2.1).
- **Kick-off point (KOP):** The depth at which the well deviates from the vertical.
- **Measured depth (MD):** The length of the well along the well path.
- **Tangential or hold section:** Section of a well where the inclination is maintained and the TVD and HD increase.
- **True vertical depth (TVD):** Vertical distance between the rotary table and the survey point. It is essential to mention that the TVD is considered positive when it increases the depth.
- **Well path:** The trajectory left by a directional well drilling in three dimensions.

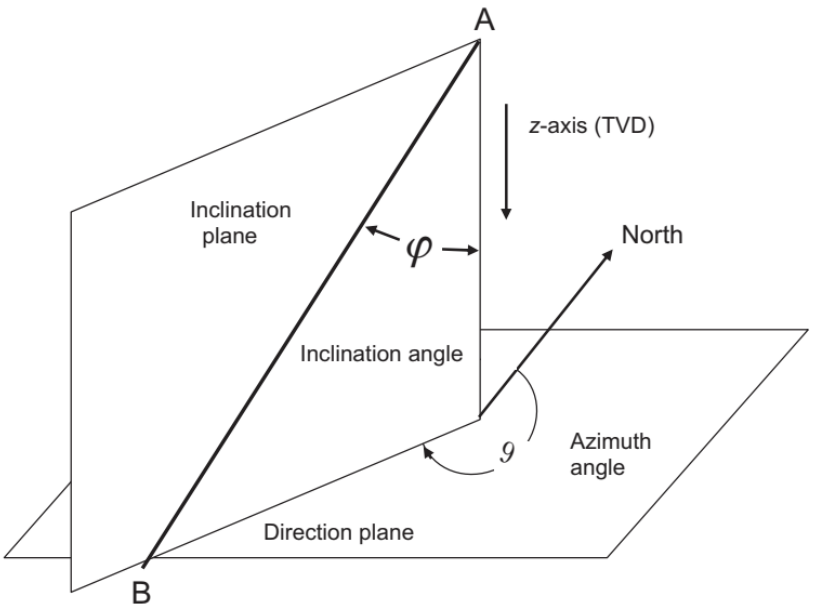

Figure 2.1: Inclination and Azimuth Angles (Mitchell et al., 2011)

Despite the fact that the azimuth can be measured regarding the North and East axis (e.g., N49E or S67W), it is common to measure the azimuth from 0° to 360° starting from the North axis clockwise. Besides, the horizontal plane is divided into four quadrants of 90° each (Mitchell et al., 2011). The azimuth quadrants require special attention since they might need a correction when they are calculated with the tangential survey method later. An example of the four possible direction situations is presented in Figure 2.2.

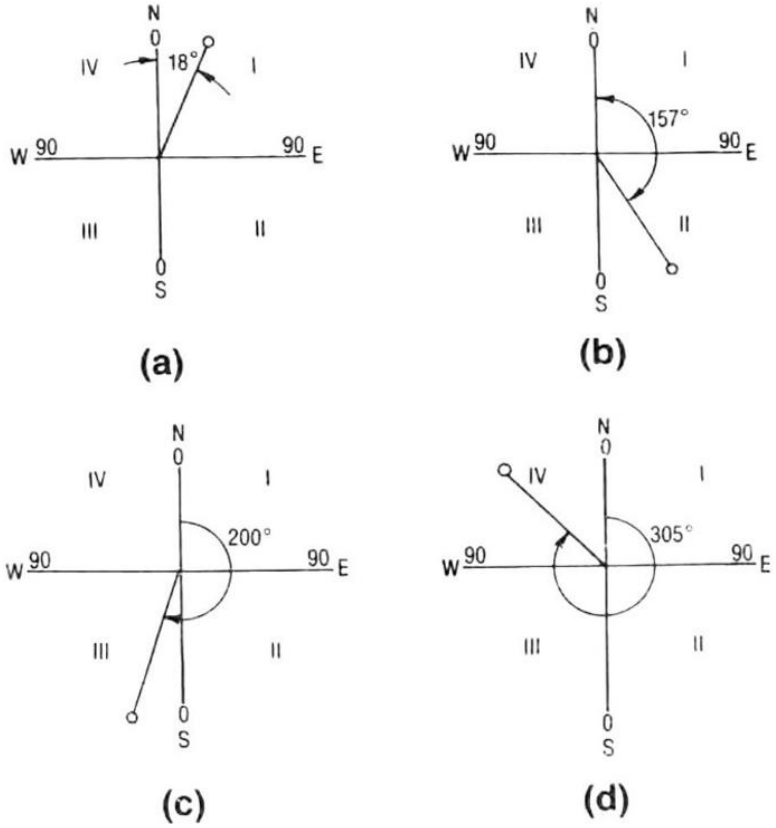

Figure 2.2: Four Quadrants Azimuth Cases (Bourgoyne et al., 1991)

2.1.1 Types of Well Trajectories

A directional well can take different trajectory shapes according to the steering system used and the DLS constraints planned. Nevertheless, there are certain standard types of trajectories that a directional well might follow, depending on the purpose of the well and formation problems that it might encounter in the formations to go through. Bourgoyne et al. describe the common standard types of well trajectories as the next ones (Bourgoyne et al., 1991):

- **Build-and-hold (J type):** The wellbore penetrates the target at the same inclination angle as the hold section (Line A in Figure 2.3).
- **Build-hold-and-drop (S type):** The wellbore increases the inclination, then holds that inclination in the tangential section, and finally, it drops the inclination to enter the reservoir with a vertical section (Line C in Figure 2.3).
- **Build-hold-partial drop-hold (S special type):** Has the same principle as the S shape trajectory, but it penetrates the reservoir at some inclination angle less than the maximum inclination angle for the hold section (Line B in Figure 2.3).
- **Continuous build:** The inclination keeps incrementing right up or through the target (Line D in Figure 2.3).

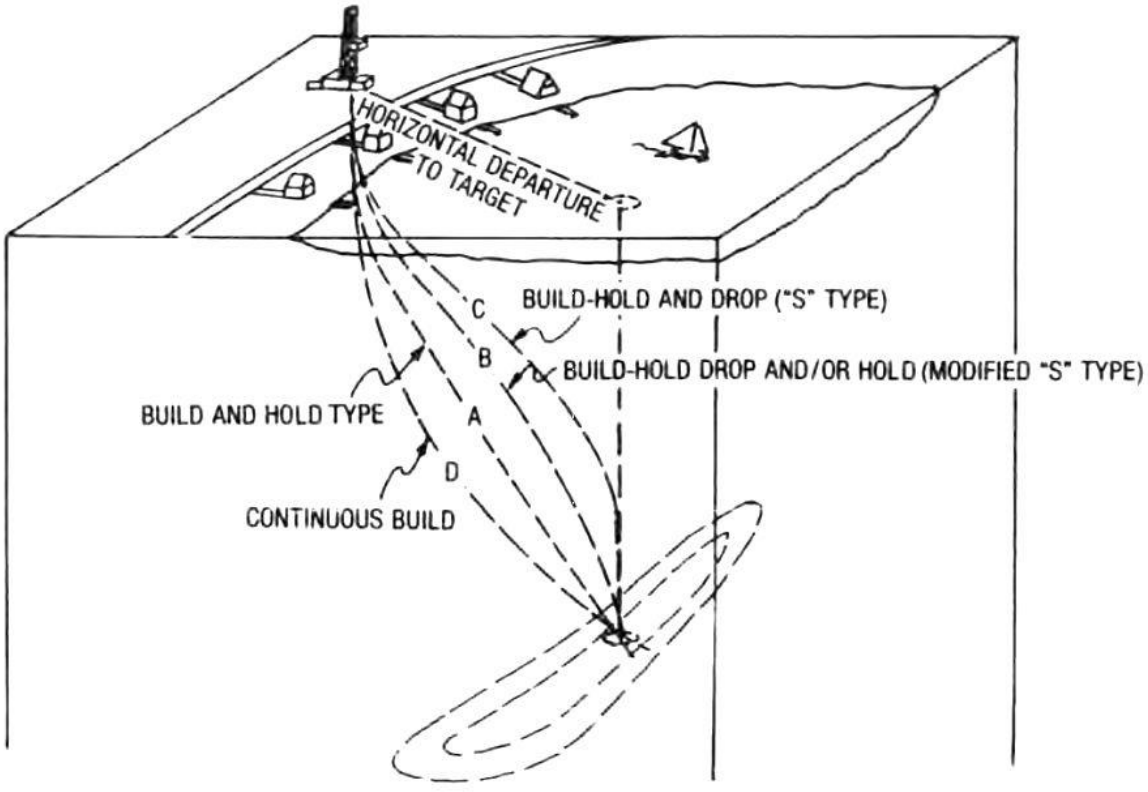

Figure 2.3: Different Directional Well Trajectories (Bourgoyne et al., 1991)

Furthermore, there are other common situations where directional drilling is executed, like the horizontal wells and the extended reach drilling (ERD) (Figure 2.4). Both types of drilling require higher build-up rates, more extended tangent and horizontal sections than the rest of the trajectory types. The inclination angles reached by these two types of paths are more than 60° and are usually between 70° - 90° (Ma et al., 2016).

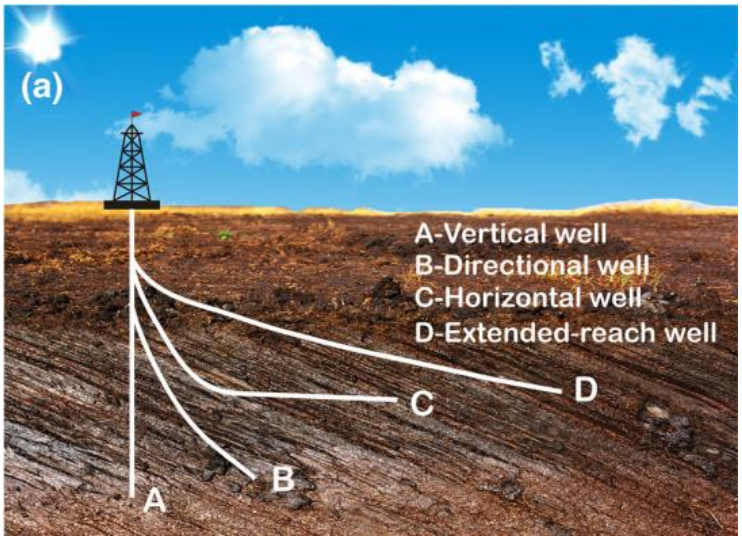

Figure 2.4: Horizontal and ERD Well Types (Ma et al., 2016)

The main advantages for using these techniques are: Increase the area of drainage of the platform, prevention of gas coning or water coning, increasing the penetration of the producing formation, increasing the efficiency of enhanced oil recovery (EOR) methods, and enhance the productivity in fractured reservoirs by intersecting a certain number of fractures (Ma et al., 2016).

2.1.2 Dog Leg Severity and Tortuosity

The steering of a wellbore involves a build-up rate that should be carefully controlled because it could create a sharp dogleg (DL). The DL is a rapid change of direction in the well trajectory, which might produce a stuck of the tool or some problems for running down the casings. The equation that will be used for this study is presented by (Liu & Samuel, 2016):

$$DL = \cos^{-1}(\cos\alpha_{i-1} \cdot \cos\alpha_i + \sin\alpha_{i-1} \cdot \sin\alpha_i \cdot \cos(\varphi_i - \varphi_{i-1})) \quad (2.1)$$

Where:

- $DL =$ dogleg calculated [°]
- $i =$ current survey station
- $i - 1 =$ last survey station (before the actual)
- $\alpha =$ inclination [°]
- $\varphi =$ azimuth [°]

Even though the hold sections are supposed to be straight, the reality is that they present some waves caused by the inaccuracy of the offset system and the disturbs acting against the steering of the tool. If these waves are too large, they could generate a high tortuosity well path that will reduce the drilling efficiency and may be a problem for cuttings transport later.

2.1.2.1 Dogleg Severity

The dogleg severity (DLS) is the wellbore curvature, and it is expressed in °/30 m or °/100 ft (Mitchell et al., 2011). The DLS indicates the build-up or drop rate of a curvature well section.

For instance, a DLS equal to 4.2 °/30 m means that the well is going to have an inclination of 4.2° degrees at the first 30 m after the kick-off point, then an 8.4° after the 60 m, and so on.

The information given by the DLS can be used for estimating: the stress fatigue in the drill pipe, casing wear, casing design loads, and stuck pipe situations. In the same manner, a high DLS has the following consequences (Nkengele, 2019):

- Improper well location of the final path.
- The casing string could have some fitting issues in the curve section.
- Repeated abrasion of the drill string in the DLS location.
- The casing cement may wear unusually quickly due to the higher contact forces.
- Increasing the likelihood of getting stuck or not reaching the target depth.

Moreover, the DLS plays a vital role in the RSS Simulator because it is one of the main constraints for calculating the PWP and the CP, which will be explained later. The DLS is calculated just dividing the Eq. (2.1) by the length between the survey points, or:

$$DLS = \frac{DL}{\Delta MD} \cdot 30 \tag{2.2}$$

Where:

- $DLS =$ dogleg severity calculated $\left[{}^{\circ}/_{30\ m}\right]$
- $\Delta MD =$ distance between 2 survey stations, where the DL has been calculated $[m]$

2.1.2.2 Tortuosity

Tortuosity is a quantitative, geometric concept that determines the deviation of a drilled path from being straight or smooth. Tortuosity is an essential metric of the wellbore quality; however, it is not always an appropriate indicator of the drilling efficiency. What is more, there are two different tortuosities (D'Angelo et al., 2019):

- Macro tortuosity: Tortuosities above 90 ft or 27.4 m (Figure 2.5).
- Micro tortuosity: Tortuosities below the macro-level (Figure 2.5).

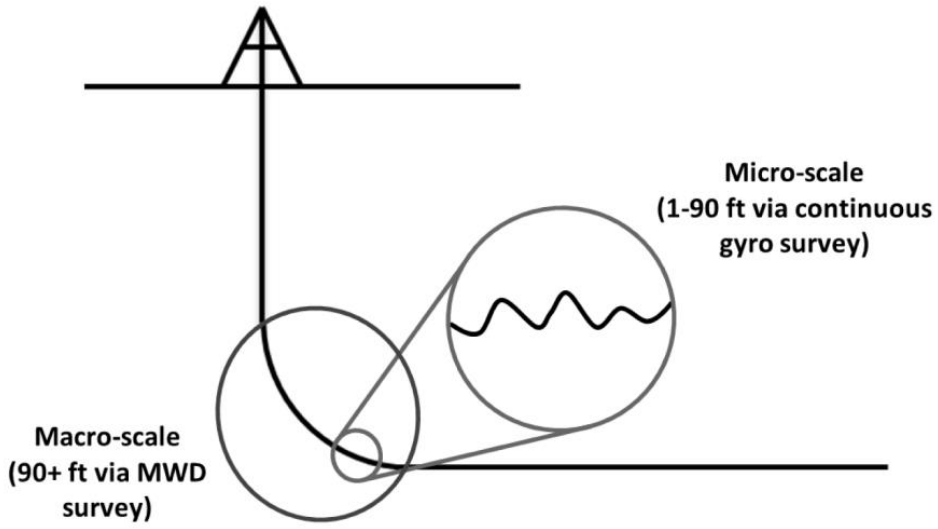

Figure 2.5: Macro and Micro Tortuosities (D'Angelo et al., 2019)

A tortuous well can have some problems like stuck pipe, poor cementation, and early production

equipment failure (Zhou et al., 2016). The tortuosity can be approximated using the following equation (Weijermans et al., 2001):

$$Tor = \frac{\sum_{j=1}^{N} DL_{S_j} - \sum_{j=1}^{N} DL_{P_j}}{MD_{TD} - MD_0} \cdot 30 \tag{2.3}$$

Where:

- Tor = tortuosity calculated $\left[{}^{\circ}/_{30\ m}\right]$
- N = total number of survey stations
- j = survey station
- S = survey
- P = planned
- TD = target depth

The MD_{TD} should be the shortest between the planned path and the drilled path, while the MD_0 is the initial survey point. The tortuosity will play a decisive role in the correction path in the RSS Simulator, which will be explained later.

2.1.3 Survey Points Calculation

The survey points are the locations where some measures are recorded and sent to the surface to inform about the actual bit inclination, azimuth, and depth. The points between two survey points are frequently unknown and can only be approximated through some survey points calculation models (Mittal & Samuel, 2016).

There are plenty of survey points model approximations, but only two will be relevant in the RSS Simulator for the present study. Both are explained in the following sections.

2.1.3.1 Tangential Method

The tangential method uses a straight line to connect two survey points, where this line represents the wellbore. The method is not as accurate as the other models and can only be used when there is no much data available (Farah, 2013). The approximation calculated with this method is seen in Figure 2.6.

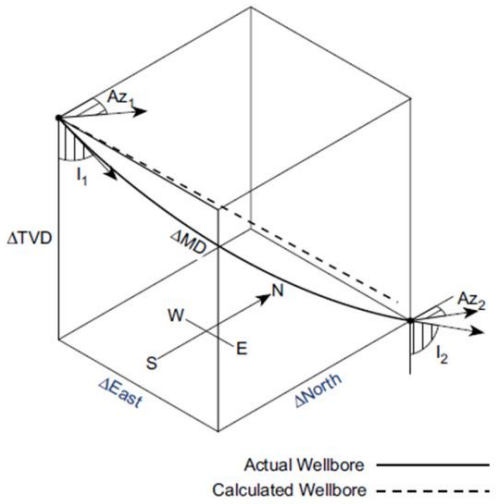

Figure 2.6: Tangential Method (Farah, 2013)

The equations for calculating the differences of the coordinates between both survey points are (Farah, 2013):

$$\Delta V = \Delta MD \cdot \cos \alpha_1 \tag{2.4}$$

$$\Delta N = \Delta MD \cdot \sin \alpha_1 \cdot \cos \varphi_1 \tag{2.5}$$

$$\Delta E = \Delta MD \cdot \sin \alpha_1 \cdot \sin \varphi_1 \tag{2.6}$$

Where:

- $\Delta V =$ vertical coordinate difference $[m]$
- $\Delta N =$ north coordinate difference $[m]$
- $\Delta E =$ east coordinate difference $[m]$

2.1.3.2 Minimum Curvature Method

It is the most widely used since it is simple and accurate. The method assumes that two survey stations lie in a circular arc located plane. In this method, a ratio factor (RF) is used to create a smooth segment (Joshi & Samuel, 2017). The minimum curvature method can be appreciated in Figure 2.7.

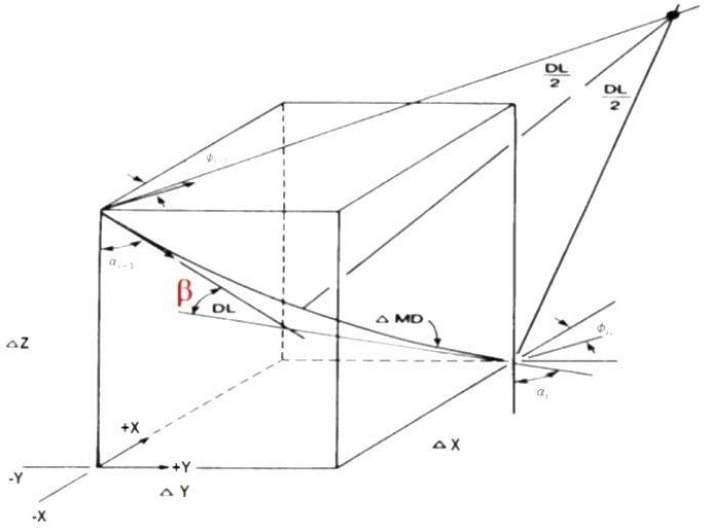

Figure 2.7: Minimum Curvature Method (Joshi & Samuel, 2017)

The equations used for calculating the minimum curvature are the next ones (Farah, 2013):

$$\Delta V = \frac{\Delta MD}{2} \cdot [\cos \alpha_1 + \cos \alpha_2] \cdot RF \tag{2.7}$$

$$\Delta N = \frac{\Delta MD}{2} \cdot [\sin \alpha_1 \cdot \cos \varphi_1 + \sin \alpha_2 \cdot \cos \varphi_2] \cdot RF \tag{2.8}$$

$$\Delta E = \frac{\Delta MD}{2} \cdot [\sin \alpha_1 \cdot \sin \varphi_1 + \sin \alpha_2 \cdot \sin \varphi_2] \cdot RF \tag{2.9}$$

$$RF = \frac{2}{DL} \cdot \tan \frac{DL}{2} \tag{2.10}$$

Where:

- $RF =$ ratio factor

2.2 BHA Steering Systems

The BHA is the tool that is in charge of steering the whole drill string. Through time, the technique used for creating this curvature, in a controlled way, has evolved with the new available technologies each year.

The first directional or deviated wells were made using a jetting technique or through the utilization of a whipstock. The whipstock is a wedge-shaped steel casting with a tapered concave channel down one side that guides the bit against the wall to start the deflection of the string. While the jetting technique is often done in soft formations with a three-roller-cone bit with three nozzles, one of them is bigger than the rest. It starts the deviation washing or eroding the rock with the fluid pressure, and the rock erosion occurs due to the fluid momentum at the bottom of the hole (Mitchell et al., 2011).

However, nowadays, the most widely used techniques are steerable mud motors and rotary steerable systems.

2.2.1 Steerable Mud Motors

The steerable mud motors technology was introduced in 1985, providing the drilling industry the capability to drill more complex and longer well trajectories. Today, most directional wells are drilled using this technology, which also is called point-the-bit (Kuznetcov, 2016).

The mud motors use the fluid power and a bend sub to apply hydraulic pressure to the drill bit, creating a side force that changes the drilling direction (Wiktorski et al., 2017).

The bend sub is configured in the surface with the required angle to create a deviation in the bottom of the well. The whole drill string rotates when it is not required to create an angle yet (Figure 2.8).

The angle construction begins with the sliding operation that happens when the bit is positioned in the desired direction, according to the bend sub, and the rotation stops. Then the fluid pumping that passes through a rotor and stator inside the tool provides a hydraulic power that makes the bit rotate. This means that the drill string stays without rotation except for the bit, which will start to create the build-up section (Kuznetcov, 2016).

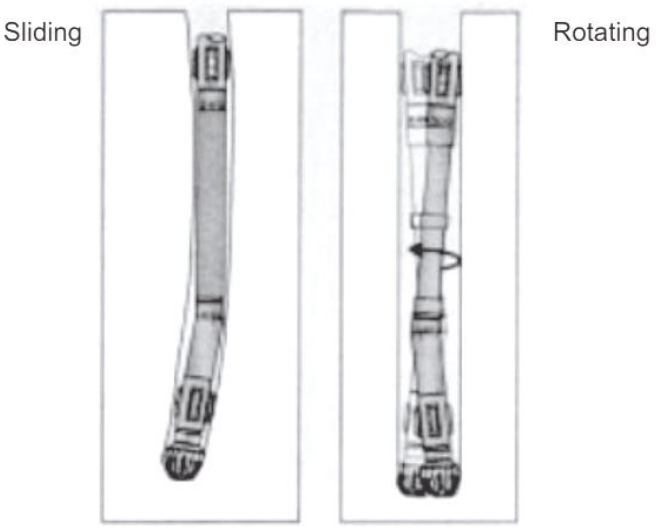

Figure 2.8: Steerable Mud Motor Modes (Mitchell et al., 2011)

2.2.2 Rotary Steerable System

The rotary steerable system (RSS) has been evolving in the past years, but the principle is still the same, which is generating a side force in one of the wellbore walls in order to direct the bit in the opposite direction of the force denominated push-the-bit principle.

The mechanical RSS uses three steering pads that extend to the borehole wall and creates an opposite force that pushes the drill string to the other side, generating reaction forces in the stabilizer and the bit (Figure 2.9) (Wang et al., 2017).

The RSS guide system has two main parts: the control platform and biasing mechanism. The control platform is the "brain" of the system, which controls the direction of the bias mechanism. While the last is an "actuator" that executes the pads extensions according to the correspondent side to apply force (Li et al., 2020).

Moreover, the pads are actioned just when they are getting closer to the correspondent borehole face wall; once they pass this zone, the pad is inactivated and returns to its close state.

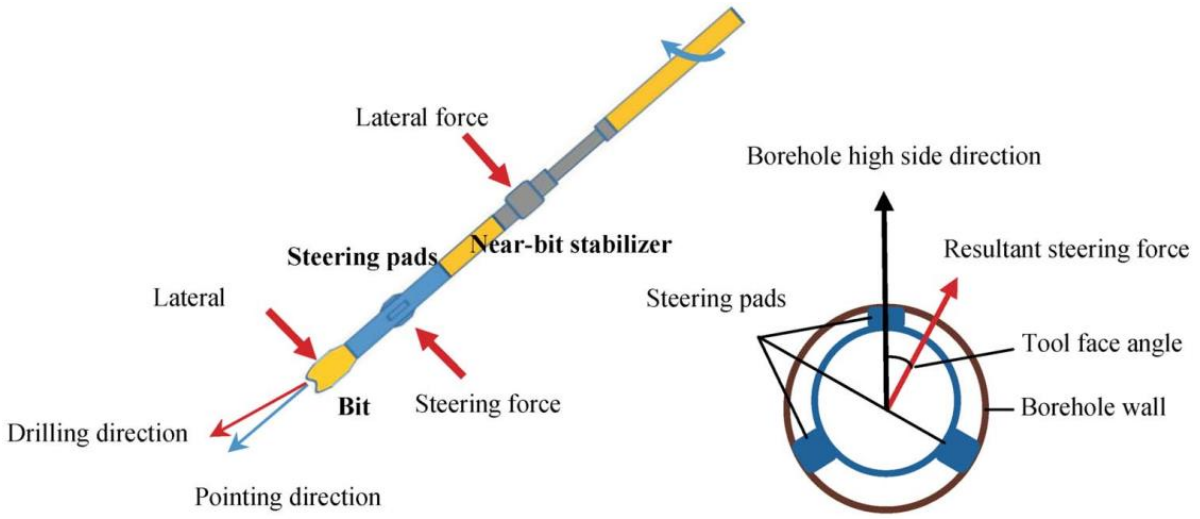

Figure 2.9: Rotary Steerable System (RSS) Tool (Wang et al., 2017)

The rotary steering devices can vary how they accomplish the inclination construction since simply gravity-based orientation systems to more complicated flexure of internal driveshafts or application of forces from pads against the borehole walls (Ruszka, 2003).

2.2.2.1 Canrig OrientXpress® RSS Tool

Canrig Drilling Technology (a company of Nabors) has developed an innovative BHA tool called "OrientXpress® RSS". This tool is interesting since it does not follow the typical 3-pads RSS tool used for a long time. Instead, the OrientXpress® RSS has a cylindrical actuator that "dislocates" from the BHA to create an offset that pushes the bit in the opposite direction, as Figure 2.10 shows.

According to Nabors website, the OrientXpress® RSS actuator enables to drill higher quality wells at lower cost by increasing the downhole maneuverability, borehole quality, and reducing the non-productive time (Nabors Industries Ltd., 2021).

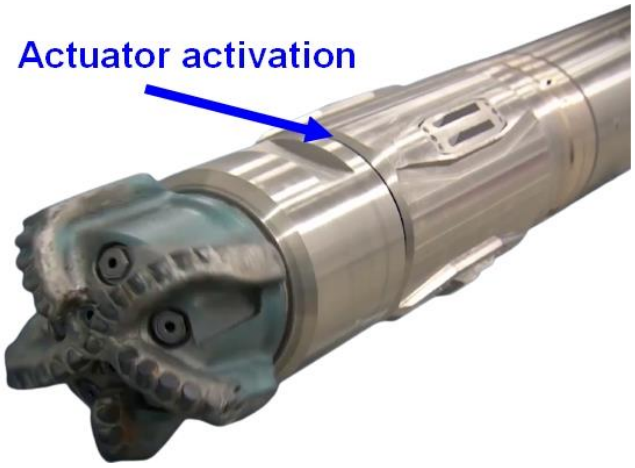

Figure 2.10: OrienXpress® RSS Tool with Active Actuator (Nabors Industries Ltd., 2021)

Moreover, the system is designed to operate in any extended-reach drilling well onshore or offshore, conventional or unconventional, at temperatures up to 347 °F and pressures up to 20000 psi (Stump, 2019).

2.2.3 Differences Between Mud Motors and RSS

Since mud motors and RSS are the most widely steerable technologies nowadays, it is relevant to know the benefits and weaknesses of each one. The advantages and disadvantages described by Wiktorski et al., Kuznetcov, and Ruszka are summarized in Table 2.1 (Wiktorski et al., 2017), (Kuznetcov, 2016) and (Ruszka, 2003).

Table 2.1: Advantages and Disadvantages of Mud Motors and RSS

Steerable Mud Motor	Rotary Steerable System
Advantages	
- Effective steering technique - Reliable - Low cost - Easy to operate - Easy to maintain	- No necessity to stop the rotation, so less possibility of a stuck pipe situation - ROP improvements - Continuous effective hole cleaning - Low tortuosity trajectories - Capable of building complex trajectories - Fewer trips for the BHA change - A more in-gauge wellbore - Improved quality for MWD
Disadvantages	
- Only available for simple trajectories - Limitation for maintaining proper levels of control in particular environments - Low effective ROP - Differential sticking due to in the sliding mode the drill string is not rotating - High tortuosity - Buckling and lock up	- Reliability problems - Significantly more expensive - Require more maintenance hours

The most significant difference between both technologies is that RSS produces a less tortuous well path due to the non-stop rotation of the drill string and the activation of the pads when it is only necessary. In contrast, the mud motor creates a constant tortuous path in the holding sections since it works with a regular bend sub that turns 360° as deep as it goes, as shown in Figure 2.8.

2.3 Drilling Automation

Although the drilling industry has made much progress through time, the automation of its process is something that has not evolved too much if it is compared with other industries like the automobile or food industry.

Nevertheless, the drilling operations have begun to move away from the traditional methods towards automation to achieve more reliable and consistent cost-effective operations (Demirer et al., 2019).

The automated drilling system combines sensors, tool actuators, and a software system that controls the drilling variables in real-time. It improves the drilling performance, wellbore quality, and safety at the rig site through the constant monitoring and analysis of real-time data that supports the decisions of rig personnel in their work (Dashevskiy et al., 2020).

Besides, the evolution of MWD, LWD, and RSS has enabled the automation for drilling an accurate well path in an efficient way (Joshi & Samuel, 2017). Thus, there are many beneficial aspects of the automation of the drilling process, but Coffey and Groover resume them as two big groups (Coffey & Groover, 2020):

- **Drilling consistency:** Drilling automation removes much of the operational variance coming from human interaction.
- **Drilling performance:** Automated systems can act faster than a human directional driller, which means that more precise control is maintained.

Nowadays, the goal of the drilling industry is to continue with automation and have zero crew at the well site (Figure 2.11). Also, the wellsite footprint of drilling operations can be reduced in the near future (Stepnov et al., 2019).

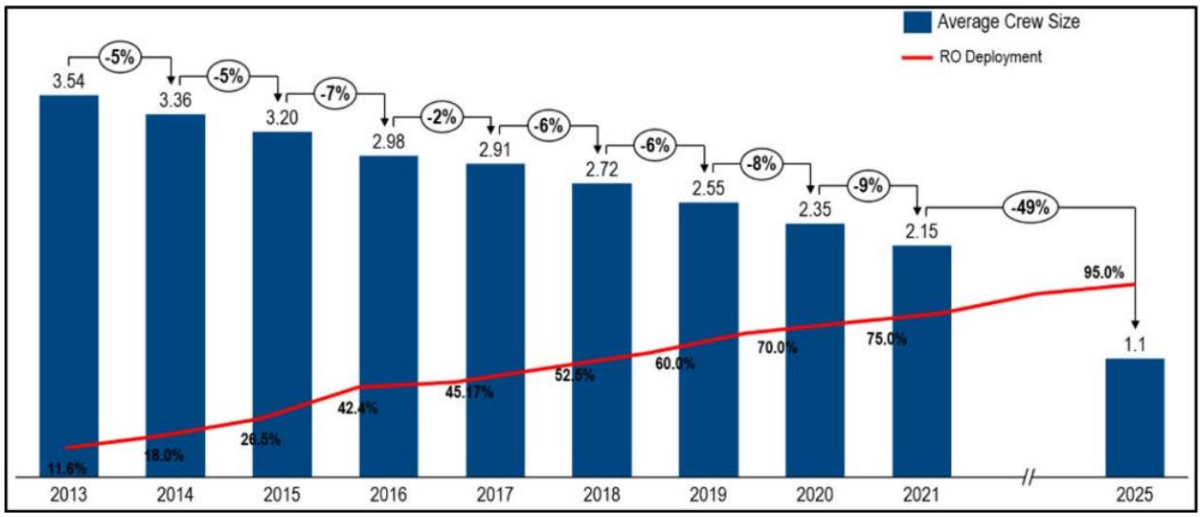

Figure 2.11: Directional Drilling Crew Size Evolution and Ambition (Stepnov et al., 2019)

2.3.1 Levels of Automation

There are different levels of automation; one proper scale for classifying them is presented by Aldred et al., which organizes the automation systems into three big groups (Tiers), according to the grade of interaction between the automation system and the real world (Aldred et al., 2012), as it can be seen in Figure 2.12.

Tier 1 is the less invasive automation system, while Tier 3 is the most autonomous system that could even replace all human interaction in a determined process.

For example, since 2009, some drilling companies have created remote operations centers to support and monitor field engineers during directional drilling operations. Expert drillers cannot be sent to each rig; however, with the remote operations centers, competent experts could be assigned to each rig (Chatar et al., 2018).

Remote operations centers are part of the Tier 2 group since they can control the drilling inputs according to the feedback received and discuss with the field engineers a decision to make.

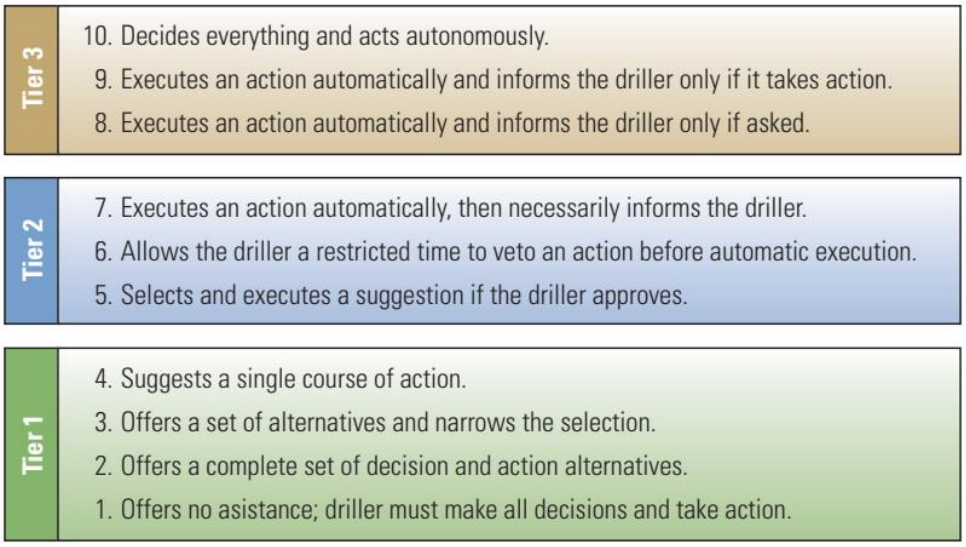

Figure 2.12: Levels of Automation Systems (Aldred et al., 2012)

2.3.2 Closed-Loop Control

Closed-loop control is the process of analyzing the system feedback and performing the necessary corrections in the input variables to change some of the output parameters that must follow a specific restriction value or behavior.

The first step towards drilling automation is to find a control parameter that can quantify the quality of the wellbore, e.g., DLS, tortuosity, or position of the bit (Joshi & Samuel, 2017). Consequently, there must be some set constraints in essential drilling parameters that must be selected by the drilling experts and be monitored by the automated system after each iteration or survey.

According to Going et al., the closed-loop can be implemented in three different options (Going et al., 2006):

- **Option 1:** Send an alarm to the operator along with an external review and wait for manual control execution.

- **Option 2:** Perform the recommended control after the operator's confirmation.
- **Option 3:** Perform the control action and notify the operator that the action is being taken.

2.3.3 Current Directional Control Methods

As it has been discussed before, directional drilling automation has been developing some tools for achieving fully automated drilling, and some of the work done are the following projects and models.

Demirer et al. indicates that the Model Predictive Control (MPC) (Figure 2.13) uses a 3D borehole propagation model that governs the trajectory. The bit position is determined using downhole inclination and azimuth in combination with the depth. The MPC prediction model works with real-time sensor measurements that detect system nonlinearities to predict the next possible bit position and calculate the optimized trajectory until this position (Demirer et al., 2019).

The MPC relies upon future projections of the bit through the propagation algorithm, where the initial condition is estimated at the bit according to the propagation model and the real-time sensor data (Demirer et al., 2019).

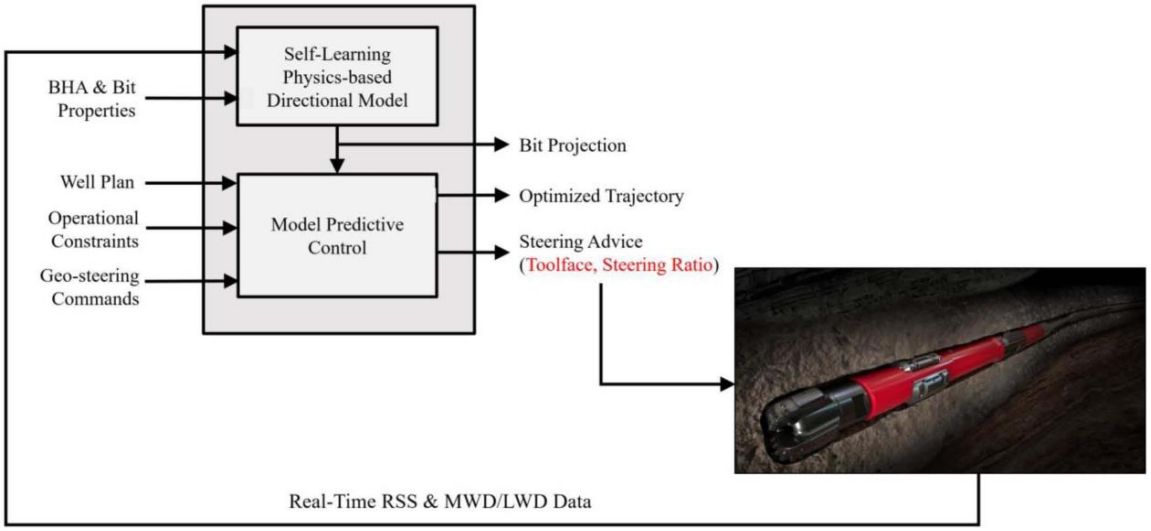

Figure 2.13: Overview of the Model Predictive Control (Demirer et al., 2019)

Moreover, Liu and Samuel created the Wellbore-Trajectory Control using the Minimum Energy Criterion that provides deterministic solutions based on an objective minimum-energy (ME) criterion. The concept is a drilling complexity index that considers the drill string as an elastic beam. The elastic line that bends least while passing through some given points is known as the minimum-energy curve (Liu & Samuel, 2016).

As a result, the algorithm helps choose which correction path is the most adequate to generate the least minimum-energy. It could be combined in a closed-loop algorithm to have an automated trajectory control algorithm.

Another project is the Automated Trajectory Drilling made by Hansen et al. (Figure 2.14) is a semi-autonomous downhole control related to the surface in closed-loop control. The system monitors the actual versus planned path by calculating the achieved real-time build-up and turn gradients to estimate the subsequent directional gradients and tendencies. The system does not use some surface parameters as WOB, flow rate, and RPM in the closed-loop control. They are required to be set manually (Hansen et al., 2020).

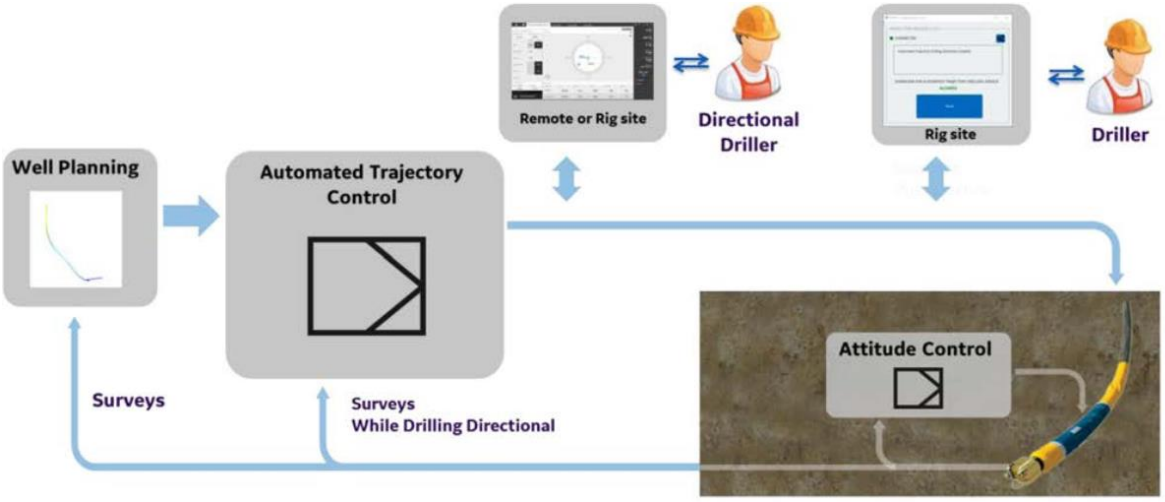

Figure 2.14: Automated Trajectory Drilling Closed-Loop (Hansen et al., 2020)

Finally, Pirovolou et al. indicate that the Trajectory Control System works sending raw data to an acquisition system which provides continuous and static survey information to the software that models the BHA behavior, estimates the current bit position, makes a projection of the next survey, and suggest changes to the toolset when it is necessary (Pirovolou et al., 2011).

The steering application is the core of this model (Figure 2.15), representing the closed-loop followed. This process starts with the data filtration that goes to the analysis of the BHA behavior; then, the bit position is estimated and is compared with the planned trajectory later. Finally, the calculated parameters are used for calculating the steering commands (Pirovolou et al., 2011).

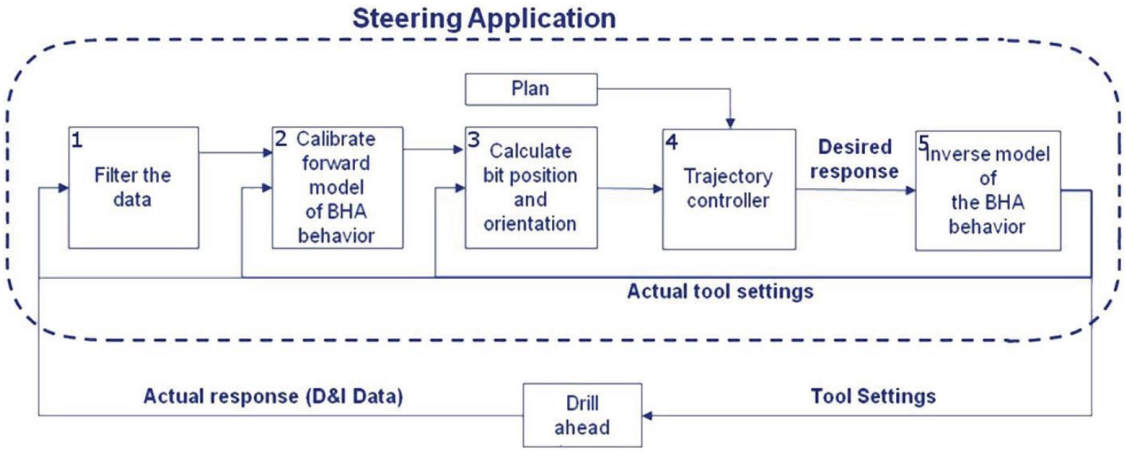

Figure 2.15: Trajectory Control System Closed-Loop (Pirovolou et al., 2011)

3 RSS Simulator Architecture

The Rotary Steerable System Simulator (RSS Simulator) is the evolution of the RSS Model developed by Saramago at the University of Stavanger, complemented with a new Trajectory Control Optimizer (TCO) developed in the present study. In other words, the RSS Simulator is composed of two parts: the updated RSS Model and the developed TCO, as can be seen, more clearly in Figure 3.1.

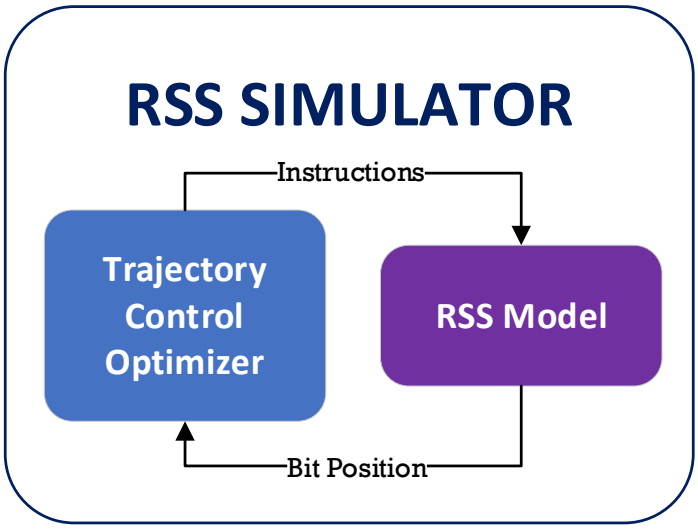

Figure 3.1: RSS Simulator Composition

The TCO is in charge of generating the instructions that are going to be sent to the RSS Model, which will simulate the drilling with the parameters received. After one iteration or time step is simulated by the RSS Model, the current position of the bit will be sent back to the TCO to be analyzed and take the correspondent decision to continue drilling safely and fast.

The RSS Model is an innovative model that simulates the behavior and steering of the drill string based on 3D ROP calculations and the resultant forces. The RSS Model was though for being used with the OrientXpress® RSS developed by Canrig Norway as the actuator of the BHA that creates the angle deviation.

Nevertheless, the RSS Model has a shallow directional control that was too dependent on user decisions. As a result, it was necessary to think and develop an original, automated, and efficient way to control the direction changes and times.

In other words, the original RSS Model had the potential to simulate the drilling aspect of the operation, but it could not simulate the automation of the process because it barely had the tools and the algorithm to deal with this challenge.

The Trajectory Control Optimizer developed is the solution for dealing with the last-mentioned issue. The primary purposes of the TCO are:

- Generate the Planned Well Path (PWP) or trajectories.
- Regulate automatically the BHA tool offset based on the inclination, azimuth, and measured depth.
- Control the deviation of the bit at each survey station in the simulated path.
- Perform a corrective well path if there is a considerable deviation of the bit from the PWP.

- Be flexible to interchange data with other models used in the Real-Time Drilling Simulator in the 2021 Drillbotics® Competition.

Moreover, the TCO considers different models for creating the curvatures, hold sections, deviation determination, and path corrections. The models and their implementation inside the TCO will be explained later in the corresponding chapters. However, the construction of the algorithm was created from scratch using the Python programming language.

The RSS Simulator has the capability to work either in 2D or 3D well trajectories projects based on the initial survey data provided by the user. Also, the RSS Simulator will present the PWP survey points calculated, the simulation results, and the deviation control survey stations. The last item will reflect when the decision (if any) of correcting the actual well path was taken based on comparing the distance from the bit to the PWP line with the correspondent radius of the Ellipse of Uncertainty (EOU) at the bit coordinate.

3.1 Simulator Modules

Despite the RSS Simulator is formed by two principal components (Figure 3.1), a more specific division, based on the different functions that some modules perform, can be made. The RSS Simulator is composed of four modules or functions, which are:

- Planned Well Path (PWP)
- RSS Model
- Deviation Control
- Correction Path (CP)

The modules are called, inside the code, when an adequate situation requires, and they have the characteristic of work as functions that only need some input data to perform their correspondent process and return the expected results.

The relation between the modules is observed in Figure 3.2. The modules are arranged in a closed-loop architecture that controls itself through a deviation control module that decides whether or not the correction is necessary.

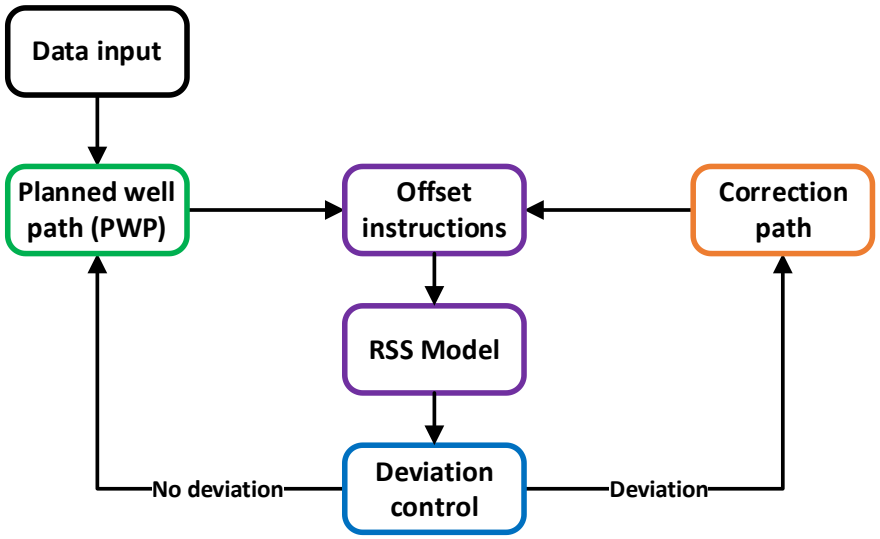

Figure 3.2: Modules Involved in the RSS Simulator Process

The process starts with the data input that represents all the parameters set by the user at the beginning and the given survey coordinates for the expected well trajectory. Among the parameters set by the user, certain constraints will serve as conditions to accomplish specific drilling objectives.

The PWP (green box in Figure 3.2) analyzes the given survey points, introduced as vertical, North, and East coordinates. Then, using the constraints imposed by the user, detects where are the hold and curvature sections, and then it will start to optimize the best curvature shape that follows the conditions given and has the shortest MD. The final well path built by the functions will be the PWP, which is going to be the primary trajectory that the simulation should follow later.

Once the PWP is defined, the next step is to send the direction instructions to the BHA tool through the target inclination and azimuth for the section between two survey stations in the PWP. The offset function (purple box in Figure 3.2), that is inside the RSS Model module, will interpret the target inclination and azimuth and will calculate the correspondent offset value, opening length of the actuator as it is seen in Figure 2.10, and will send this value to the rest of the RSS Model that will simulate the drilling for the next point.

Indeed, the RSS Model (purple box) calculates the next bit position according to the inputs, current bit position, offset instructions, force on the bit calculated, and the results from the 3D ROP equations (explained later). Then, this new bit position will be sent back to the main algorithm that will send it to the next module to check the deviation of the bit.

The following module is the Deviation Control (blue box in Figure 3.2), which determines if the current bit position has deviated from the PWP. This module is very critical since it will be the central control for the closed-loop. The module receives the current bit position calculated by the RSS Model and determines the distance from the bit until the closest orthogonal point on the PWP. It compares this distance against the radius formed by the EOU.

If the distance between the bit and the point on the PWP is longer than the radius of the EOU, the Deviation Control will detect that the bit is too far from the PWP and it needs to be corrected. Therefore, it will call the correction path function. On the contrary, if the length between the bit position and the PWP is shorter than the EOU radius, then the current bit trajectory will not be corrected, and the target inclination and azimuth from the PWP still have relevance to modify the offset function.

When a correction is needed, the Correction Path function (orange box in Figure 3.2) is called, and the actual bit position will be considered the initial point for creating a corrective curved path that will reach some PWP survey station ahead. The correction path must follow some restrictions imposed by the user at the beginning and find the least tortuous and shortest path to return to the PWP.

When the correction path is defined, it will replace the target inclination and azimuth from the PWP with the target inclination and azimuth calculated in the Corrective Path function. Consequently, the offset control will receive a new target inclination and azimuth while the correction is still active. Once the correction has reached its objective survey station on the PWP, the target inclination and azimuth will be acquired again from the PWP, and the process will continue.

3.2 Simulator Flowchart

The modules used in the RSS Simulator are structured and coded in Python using the flow process shown in Figure 3.3. The flowchart is a simplified explanation of the actual Python code, which involves more detailed processes and conditional situations.

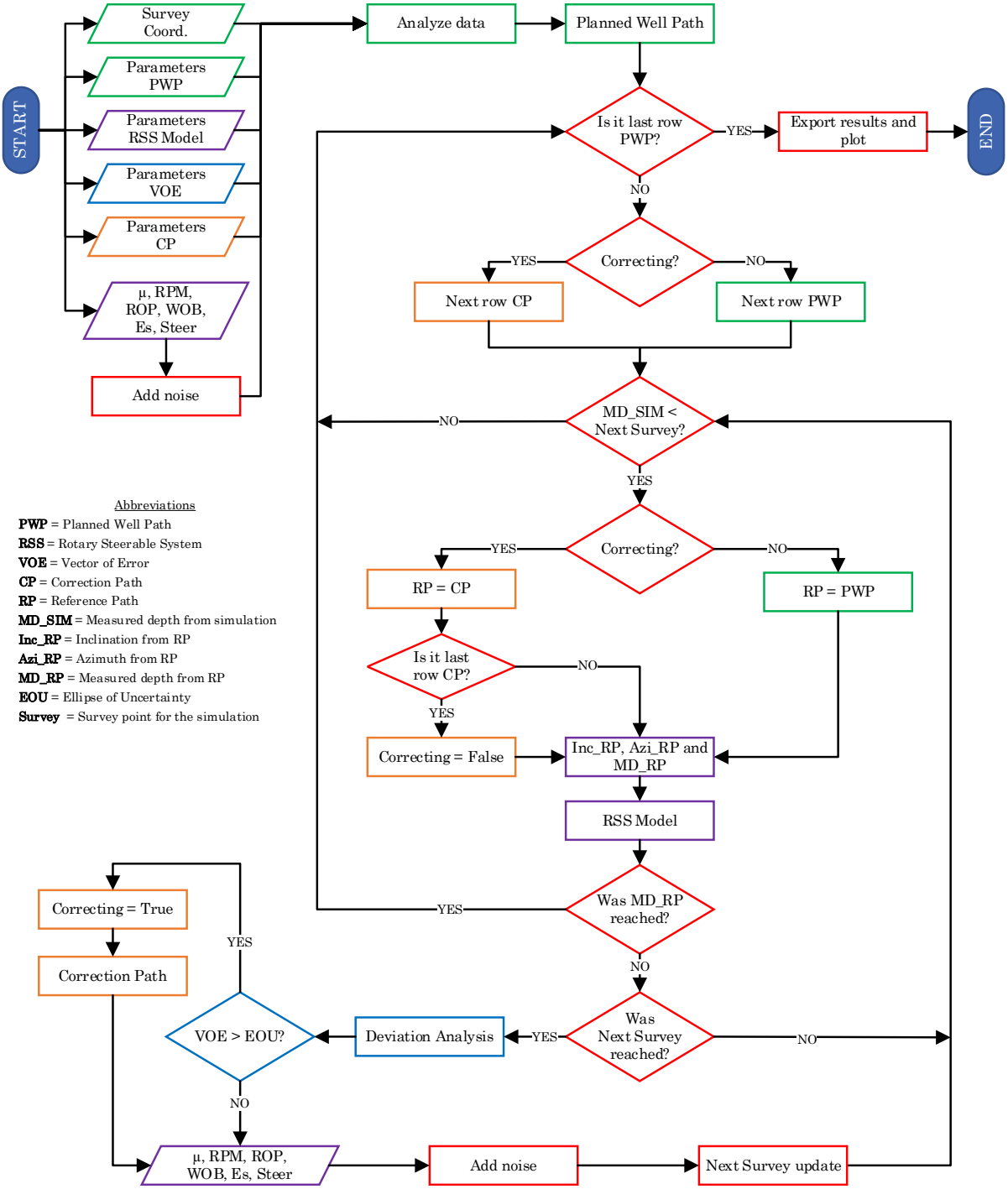

Figure 3.3: RSS Simulator Flowchart

It is essential to follow the colors of the shape contours because they are related to the different modules presented in Figure 3.2. Consequently, the meaning of the colors is the next:

- Green: Related to the PWP function
- Purple: Related to the RSS Model function
- Blue: Related to the Deviation Control function
- Orange: Related to the Correction Path function
- Red: Related to the main algorithm that manages the inputs/outputs, and the rest of the functions

Those meanings will be kept for the rest of the thesis when a figure or table presents the mentioned colors.

The flowchart begins with the data input, as it was mentioned before, but the last group of data (last purple parallelogram) is obtained from other modules calculations that are part of the Real-Time Drilling Simulator developed for the 2021 Drillbotics® competition.

This data group will act as a mean value that will be disturbed a little by adding random noise between 0% and the error percentage decided by the user. The following equation shows the noise added to the transferred data:

$$Data_{rand} = Data_{mean} \pm e \tag{3.1}$$

Where:

- $Data_{rand}$ = data randomized or with noise
- $Data_{mean}$ = data received from other modules
- e = random error added between the range. $e \in (0, Data_{mean} \cdot Error\ percentage)$

For example, if the RPM mean value is 144 and the user sets an error percentage of 15%, then the $Data_{mean}$ is 144, the 15% is 21.6 and the $Data_{rand}$ might be any value between 122.4 and 165.6. Indeed, to get the value of e the Python code performs a uniform distribution between 122.4 and 165.6 and picks a random value and sign. For the example purpose, let us say that the randomly picked value for e is 149.2 then the $Data_{rand}$ will be 293.2. As a result, the RPM that is going to be used in the next simulation iteration is 293.2.

In the same way, this data group will be updated every time a simulated survey point is reached, and the noise procedure is followed again. Adding noise gives the simulation a closer experience to the real world where the data is not perfect and has many disturbances.

Then, the input data is transfer to the PWP function, where it is analyzed, and the PWP is created. The PWP is used as the primary condition to stop the whole iteration of the simulator. Since the PWP is a set of survey stations, they are expressed in a matrix form whose number of rows is the condition that controls the iteration of the program.

When the program finishes the total iterations, it will export a Microsoft Excel file with the PWP, simulation results, and deviation survey points that were obtained during the whole simulation process. Also, the correspondent plots will be generated and shown to the user.

Moreover, the flowchart shows a single condition that is repeated twice. This condition tells the simulator if the current situation is following the PWP or the CP. This decision is crucial for the RSS Model since it will receive the orders from the offset control based on the target inclination and azimuth. Besides, the reference path (RP) will take the form of the PWP or the CP matrix survey stations. As a result, indirectly, the target inclination and azimuth will change according to the option chosen in this step.

Below the RSS Model, there are two conditions, one after the other, where the algorithm decides if the next point will still simulate the next bit position using the current target inclination and azimuth or if a new target inclination and azimuth, either coming from the PWP or the CP, is going to be received.

Furthermore, the deviation analysis or deviation control is done every time the simulation MD has

reached the next simulated survey station. It will decide if the correction path function is required or is acceptable to continue with the next iteration.

The "next survey" phrase that appears in many conditionals refers to the next MD that will simulate a survey point analysis. This variable is determined with an initial MD equal to 0 that will be updated with the delta MD chosen by the user.

3.3 Data Inputs and Outputs

Simulators usually manage many parameters simultaneously; for that reason, it is helpful to organize the different variables that are going to be asked to the user, obtained from the survey stations file, or transferred from other models. As a result, the most relevant inputs and outputs will be shown in a collection of different tables in this section. The complete tables with the whole inputs and outputs parameters can be analyzed in the Appendix A tables.

3.3.1 Inputs

The inputs are asked to the user at the beginning of the algorithm, except for those coming from other external models (Table 3.5), which need to be updated at every survey point.

Table 3.1 shows the parameters needed for the PWP function that where Ran_{Tol} is related with the optimization of the trajectory calculated, and Max_{DLS} is the principal constraint for accepting or rejecting a certain well path.

The RSS Model will receive part of the input parameters from Table 3.2; the other part will come from the external modules. The most relevant variables are the Δt whose manipulation will define the iteration step of the simulation, and the $maxoff$ which determines the percentage of the opening of the actuator of the BHA tool. The user can regulate both variables, and they will have a high impact on the total simulation.

The deviation control will work with the parameters presented in Table 3.3, where all the systematic error variables are used in the ISCWSA Error Model (explained later). The Min_R is important for adjusting the initial tolerance criteria used at the beginning of the well simulation for calculating the radius of the EOU at the initial section.

The correction path function requires the variables of Table 3.4 where the $Max_{DLS\ Corr}$ and $Tor_{Max\ Corr}$ are the main constrains of the corrective trajectory curve. Sometimes it will not be possible to find a correction path due to one or both values are too low to accomplish by the function, and the user should consider higher values.

The variables of Table 3.5 are special since they come from external models that work inside the Real-Time Drilling Simulator. As a result, they will be updated and filled with noise each time a survey point is reached.

Lastly, the original survey data should contain the information shown in Table 3.6 arranged in the same order in the Excel file imported into the Python code. The order of the file is essential for the correct operation of the code in 2D cases.

Table 3.1: Relevant Inputs Used in the PWP Function

Planned Well Path (PWP)		
Parameter	**Symbol**	**Unit**
Tolerance for considering two different segments	Tol	°
Survey points for the hold section	Sur_{pts}	m
Range tolerance for searching for the best D_S and D_E value	Ran_{Tol}	m
Maximum DLS for the PWP	Max_{DLS}	°/30m

Table 3.2: Relevant Inputs Used in the RSS Model Function

RSS Model		
Parameter	**Symbol**	**Unit**
Time step for the Simulation (Resolution)	Δt	s
Error Noise that will be added to the other modules data	$Error_{input}$	-
Maximum opening offset of the tool (0% to 100%)	$maxoff$	-
Maximum physical opening of the offset	$Offset_L$	m
Maximum degree of tolerance for the activation of offset	Max_{deg}	°

Table 3.3: Relevant Inputs Used in the Deviation Control Function

Deviation Control		
Parameter	**Symbol**	**Unit**
Standard deviation used in the Ellipse of Uncertainty	SD_{EOU}	-
Depth Scale Factor – Systematic error	L_DSFS	-
MWD: Z-Accelerometer Bias Error – Systematic error	L_ABZ	m/s2
MWD: Z-Accelerometer Scale Error – Systematic error	L_ASZ	-
MWD: TF Ind: X and Y Magnetometer Bias – Systematic error	L_MBXY1	nT
MWD: RF Ind: X and Y Magnetometer Scale Factor – Systematic error	L_MSXY1	-
Minimum radius of EOU	Min_R	m

Table 3.4: Relevant Inputs Used in the CP Function

Correction Path (CP)		
Parameter	**Symbol**	**Unit**
Maximum DLS that could be applied to the curve	$Max_{DLS\ Corr}$	°/30m
Maximum tortuosity that could be applied to the curve	$Tor_{Max\ Corr}$	°/30m

Table 3.5: Relevant Inputs Coming from External Modules

External Modules (Models)		
Parameter	**Symbol**	**Unit**
Sliding factor coefficient	μ	-
Revolutions per minute	RPM	rpm
Weight on Bit	WOB	N
Specific energy of the rock	Es	Pa
Steerability of the bit	$steer$	-

Table 3.6: Inputs Imported from the Survey Data Points

Survey Data Points (Excel)		
Parameter	**Symbol**	**Unit**
Vertical coordinate	V	m
North coordinate	N	m
East coordinate	E	m

3.3.2 Outputs

The RSS Simulator generates three main outputs presented in a matrix form exported into three different worksheets in the Excel file. The parameters of the three outputs groups are summarized in the following tables. Table 3.7 presents the variables obtained from the PWP function at the end of its analysis, where all the survey points represent a new row in the final PWP. As a result, the variables of the table are, indeed, the columns of the matrix.

In the same way, the parameters in Table 3.8 are the columns obtained after every iteration (row) of the RSS model. The number of the rows or iterations will depend on the value of Δt (Table 3.2), the lower, the more number of iterations.

The last matrix presented informs the variables obtained in the control function, every survey point, where the most relevant value is $Out\ EOU$ (Table 3.9) with the value of 0 or 1. 0 means that the actual bit position is inside the radius of EOU tolerance; while 1 means that the current bit position is too far from the PWP and the distance is bigger than the radius of EOU and correction path should be built.

Table 3.7: Output from the PWP function

Planned Well Path (PWP)		
Parameter	**Symbol**	**Unit**
Vertical coordinate	V	m
North coordinate	N	m
East coordinate	E	m
Measured depth	MD	m
Inclination	α	°

Azimuth	φ	°
Dogleg Severity	DLS	°/30m

Table 3.8: Outputs from the RSS Model Function

Simulation Results		
Parameter	**Symbol**	**Unit**
Measure depth	MD	m
Time	t	min
Inclination	α	°
Azimuth	φ	°
Horizontal Displacement	HD	m
True Vertical Depth	TVD	m
East coordinate	E	m
North coordinate	N	m
Offset applied (percentage of opening of the actuator)	$Offset$	-
Dog Leg Severity	DLS	°/30m
Total force on the bit for the inclination	$Tot\ F_{Inc}$	N
Total force on the bit for the azimuth	$Tot\ F_{Azi}$	N
ROP axial	ROP_{Axial}	m/hr
ROP inclination	ROP_{Inc}	m/hr
ROP azimuth	ROP_{Azi}	m/hr

Table 3.9: Outputs from the Deviation Control Function

Deviation Points Analysis		
Parameter	**Symbol**	**Unit**
Measure depth	MD	m
Vertical coordinate Vector of Error (VEC)	V_{VEC}	m
East coordinate Vector of Error (VEC)	E_{VEC}	m
North coordinate Vector of Error (VEC)	N_{VEC}	m
Length Vector of Error (VEC)	$Length_{VEC}$	m
Vertical coordinate Ellipse of Uncertainty (EOU)	V_{EOU}	m
East coordinate Ellipse of Uncertainty (EOU)	E_{EOU}	m
North coordinate Ellipse of Uncertainty (EOU)	N_{EOU}	m
Length Ellipse of Uncertainty (EOU)	$Length_{EOU}$	m
Boolean that indicates if the bit is in (non-deviated) or out (deviated) of the EOU	$Out\ EOU$	-

3.4 Assumptions and Constraints

As with most simulators, the RSS Simulator has some assumptions and restrictions that should be considered when a project is run. Some of the assumptions involve values used for specific mathematical models or values for calibrating a particular equation.

The assumptions in the RSS Simulator are the following:

- The maximum length of the opening of the actuator or offset of the OrientXpress® RSS BHA tool is 6 mm.
- The deviation control inputs (Table 3.3) are presented in the ISCWSA Error Model Example Excel file located on their web page (ISCWSA, 2016).
- The u value used in the Bezier function is 0.05 when the optimizer is called.
- Only five types of systematic errors will be taken in count for calculating the ISCWSA Error Model.
- The correction path function has an initial D_S and D_E equal to 300 m.
- The correction path optimizer has a set range of 300 samples.
- The maximum DLS of the BHA tool is 15 °/30m.
- The BHA tool is located just after the bit, so there is no necessity of bit projection prediction.
- The simulation follows a planned trajectory because it is assumed that the trajectory is given after some geological considerations have been discussed before initiating the drilling operations.
- The study cases uses some constant external parameters (Table 3.5) since at the moment of the creation of the thesis, the rest of the models of the Real-Time Drilling Simulator are not finished yet.

The limitations or constraints of the RSS Simulator can be summarized as the next ones:

- The survey points input should be arranged in the next order: Vertical, North, and East.
- There must be at least 3 points indicating a holding section in the survey points given and at least 2 points in for indicating a curvature section.
- The gravity and reactive torque have not been taken into count in the forces affecting the bit direction.
- The first and last section of the well should be a hold section.
- The planned trajectory cannot be updated or changed after the simulation has started.
- The formation information was not considered in the simulation, which should be improved in future work with the simulator.
- The simulator did not use a BHA model that might be a good added feature in the future development.

4 Trajectory Design and Optimization

The first step of the RSS Simulator is to calculate and build the most optimal well trajectory based on some given survey coordinates and some given restrictions from the user. This trajectory is called Planned Well Trajectory (PWP), and it will be essential in the simulator since it determines the total number of iterations, directs the simulated action of the BHA tool for moving through space, and is the principal reference for comparison of the ideal path.

The PWP function will create the Planned Well Trajectory. It analyzes the given survey points, identifies the different hold and curved sections, creates the curved sections in the 3D space, and connects each section in the softest and shortest way (optimizes the trajectory).

Therefore, the function presents the final calculation results through survey stations saved in a matrix form. The matrix columns are the most relevant parameters, which were shown in Table 3.7. Every new row of the matrix will represent a new survey point in the trajectory. Also, these survey points will be used for the trajectory plotting at the end of the simulation run.

The number of rows will be the stop condition for the principal while-loop of the RSS Simulator, showed in the flowchart of Figure 3.3. Besides, each row has a specific inclination and azimuth value. At the same time, they will be considered the target inclination and azimuth that will be transferred to the offset control inside the RSS Model function. In other words, every row of the PWP will determine the objective inclination and azimuth that the RSS Model should achieve by the end of the correspondent PWP survey point MD.

The PWP, generated by the function, is the base of the subsequent functions in the simulator and will be deeply explained in the chapter. The description of the function logic will adhere to the process followed by the module from the data input reading until the presentation of the PWP results to the user.

4.1 Cubic Beziér Curves

In order to understand the mathematics behind the curved well section construction, it is necessary to comprehend, first, the Cubic Beziér Curves method. The Cubic Beziér Curves are one of the Beziér Curves' variants, which starts from the linear form until unlimited order. Moreover, the Bezier curves have been implemented in many industries, but also some authors have also adapted this methodology to the drilling industry.

All the concepts, equations, and considerations are obtained from Sampaio's work "Designing 3D Directional Well Trajectories Using Beziér Curves" (Sampaio, 2016). The author has adapted the typical Bezier implementation into a specific Bezier method applied to the 2D and 3D directional well curves.

The Beziér curve is a parametric curve that often it is used in computer graphics to model smooth curves. They were invented by Pierre Beziér in 1962 to be used in automobile design (Joshi & Samuel, 2017).

The simplest Beziér curve is the first-order Beziér curve that only uses two points at the extremes of the line, which are the starting point S and the end point E. The second-order Beziér curve uses three points: S, E and C. The last point is the control point and it is not collinear with the other two points. The third-order Beziér curve utilizes four points, the S, E and two control points C_1 and C_2 that are not collinear with the start and end points (Sampaio, 2016). One of the control points will be related to the start point,

while the other to the end point. As a result, they will be called start control point or attractor C_S and end control point or attractor C_E.

All the Beziér curves have a dimensionless parameter u that goes from 0 to 1, and it will represent the step for the interpolation point B that goes from the start point until the end point. The trajectory that takes the point B will define the Beziér curve, as can be seen in Figure 4.1.

The logic inside this method is to interpolate a point between two given points; for instance, in Figure 4.1, the point I_1 is the interpolation point between S and C_S, I_2 is the interpolation point between C_S and C_E, I_4 is the interpolation point between I_1 and I_2, and B is the interpolation point between I_4 and I_5.

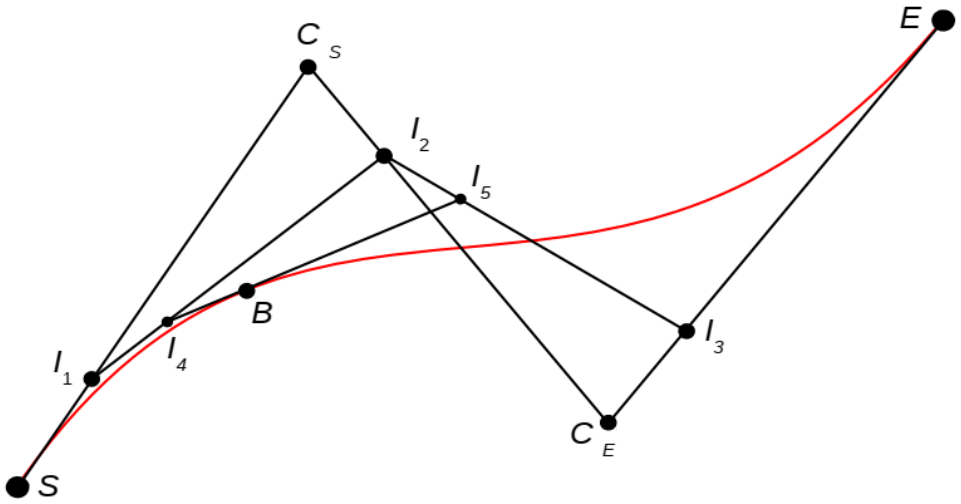

Figure 4.1: Third-order or Cubic Beziér Curve (Sampaio, 2016)

It is interesting to mention that the number of the nested interpolations is the same that the order of the Beziér curve. In the same way, the attractor points will define the shape of the Beziér curve according to their position regarding the start or end points. Sampaio method fix either the C_S or C_E attractor points to follow the direction of the tangential line from the start or end point, respectively. Figure 4.2 presents both cases when the end attractor point C_E is fixed (case a), and when the start attractor point C_S is fixed (case b).

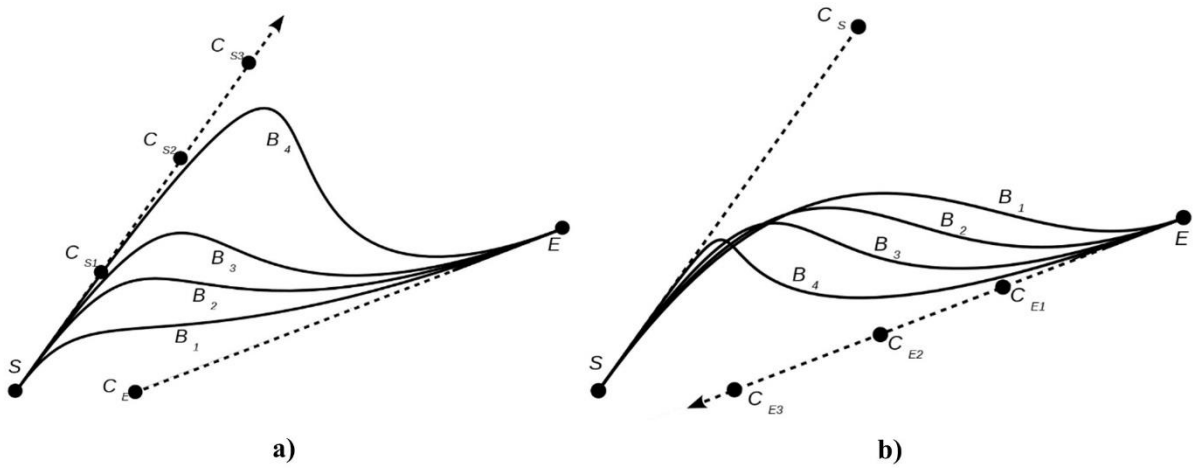

Figure 4.2: Fixed Beziér Attractor Points Alternatives (Sampaio, 2016)

The tangent lines in the last figure can be skew lines (with no intersections but are not parallel) which means that the resulting Beziér curve is a 3D curve that is non-planar (Sampaio, 2016).

The following equation defines the cubic Beziér curve:

$$Bzr_{(u)} = (1-u)^3 \cdot S + 3(1-u)^2 \cdot u \cdot C_S + 3(1-u) \cdot u^2 \cdot C_E + u^2 \cdot E \quad (4.1)$$

Where:

- $Bzr =$ Beziér coordinates $[m]$
- $u =$ dimensionless parameter iterator, from 0 to 1
- $S =$ start point coordinates $[m]$
- $E =$ end point coordinates $[m]$
- $C_S =$ attractor point regarding the Start point $[m]$
- $C_E =$ attractor point regarding the End point $[m]$

Sampaio also uses a unit tangent vector t to determine the inclination and azimuth of the tangential line formed between either the start point and its attractor, or end point and its attractor:

$$t_S = (\cos \alpha_S; \sin \alpha_S \cdot \cos \varphi_S ; \ \sin \alpha_S \cdot \sin \varphi_S) \quad (4.2)$$

$$t_E = (\cos \alpha_E; \sin \alpha_E \cdot \cos \varphi_E ; \ \sin \alpha_E \cdot \sin \varphi_E) \quad (4.3)$$

Where:

- $t =$ unit tangent vector, either using the starting or end point coordinates
- $\alpha =$ inclination of the point [°]
- $\varphi =$ azimuth of the point [°]

With the unit vector t is possible to determine the distance or coordinate location of the correspondent attractor point:

$$C_S = S + d_s \cdot t_s \quad (4.4)$$

$$C_E = E - d_e \cdot t_E \quad (4.5)$$

Where:

- $d_s =$ distance ahead from the start point until the starting attractor $[m]$
- $d_e =$ distance behind from the end point until the ending attractor $[m]$

The MD between the start point and end point is defined by:

$$MD_{Bzr} = \sum_0^i \sqrt{(\Delta V_i)^2 + (\Delta N_i)^2 + (\Delta E_i)^2} = \sum_0^i \Delta l_i \quad (4.6)$$

Where:

- $MD_{Bzr} =$ measured distance between the start and end point $[m]$
- $\Delta V =$ vertical coordinate difference $[m]$
- $\Delta V =$ north coordinate difference $[m]$
- $\Delta V =$ east coordinate difference $[m]$
- $i =$ iteration, according to the u value

For calculating the inclination and the azimuth, Sampaio suggests calculating the unit tangent vector in the following form:

$$t = \frac{\dot{B}}{\sqrt{\dot{B} \cdot \dot{B}}} \tag{4.7}$$

$$\dot{B} = \frac{dB}{du} = -3(1-u)^2 \cdot S + 3(1-u)(1-3u) \cdot C_s + 3(2-3u) \cdot u \cdot C_E + 3u^2 \cdot E \tag{4.8}$$

$$\alpha_{Bzr} = \cos^{-1} t_v \tag{4.9}$$

$$\varphi_{Bzr} = \tan^{-1} \frac{t_e}{t_n} \tag{4.10}$$

Where:

- $t =$ unit vector, composed by $t = (t_v; t_n; t_e)$
- $\dot{B} =$ first derivative of cubic Beziér curve equation

The dot between $\dot{B}$ in Eq. (4.7) means dot product. Moreover, the DLS equation used by Sampaio to calculate this parameter is:

$$k = \frac{1}{\dot{B} \cdot \dot{B}} \ddot{B} - \frac{\dot{B} \cdot \ddot{B}}{\left(\dot{B} \cdot \dot{B}\right)^2} \dot{B} \tag{4.11}$$

$$\ddot{B} = 6(1-u) \cdot S - 6(2-3u) \cdot C_s + 6(1-3u) \cdot C_E + 6u \cdot E \tag{4.12}$$

$$DLS_{Bzr} = 30 \left(\sqrt{k \cdot k}\right) = 30\|k\| \tag{4.13}$$

Where:

- $k =$ k factor
- $\ddot{B} =$ second derivative of cubic Beziér curve equation
- $DLS_{Bzr} =$ dogleg severity of the Beziér point $[°/30m]$

The dot in Eq. (4.11) and (4.13) means dot products between the correspondent vectors.

All the equation variables must be known before applying the Sampaio calculation, except for two variables. d_s and d_E will set the distance of the attractor points, respectively. These variables should be supposed or assumed with an initial value. The PWP function starts the calculation of the Beziér curve with two initial fixed values for d_s and d_E. Nevertheless, it will search for the best combination (explained later in the Optimization of Curvature Sections title) to create a low DLS and short path.

4.2 Planned Well Path Function

The PWP function has been developed based on the cubic Beziér curves and the tangential method for calculating the curve and hold sections survey points, respectively. Inside the code of the RSS Simulator, the PWP function is called at the beginning of the general algorithm (see Figure 3.3) and will return the PWP matrix with the survey points optimized.

The PWP function has three stages (Figure 4.3) for building the optimal well trajectory, starting from the given survey data stations. The first stage is receiving and analyze the survey station's coordinates. The second stage calculates the survey points that will form the PWP starting from the wellhead survey

point until the target survey point. The last stage optimizes the curvature sections while the function is calculating each of these sections (if there are more than one). The holding sections are not optimized since they are just points aligned into a straight.

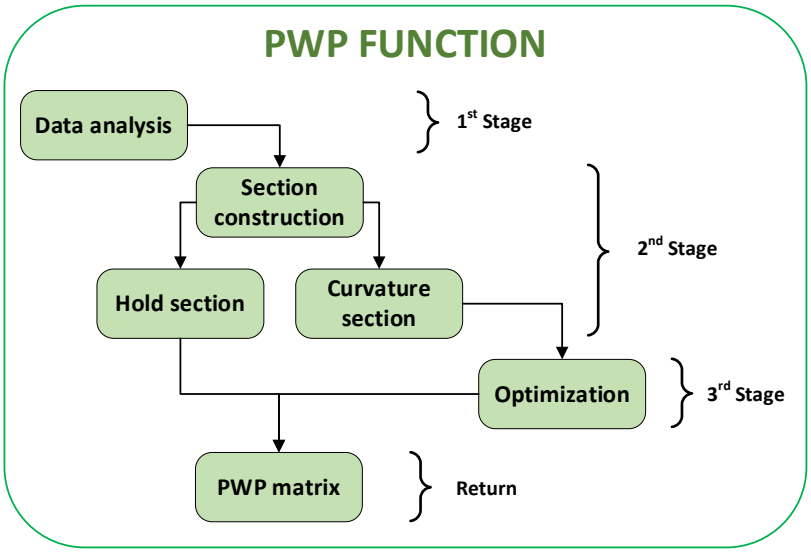

Figure 4.3: PWP Function Stages

4.2.1 Analysis of Survey Points

The objective of the data analysis or given survey stations is to identify and mark when the different sections, that compose a well trajectory, start and finish. By sections, it is meant the hold and curvature segments that exist in a directional well. The relevance of this task is decisive because if a section is not well identified might cause some confusion in the conditionals that the simulator will use later.

The process starts with the data import and the reading of the tolerance value, set by the user at the beginning of the run. Then, the survey points introduced are saved, and the PWP function will put them in their correspondent positions in a 3D space, as seen in Figure 4.4.

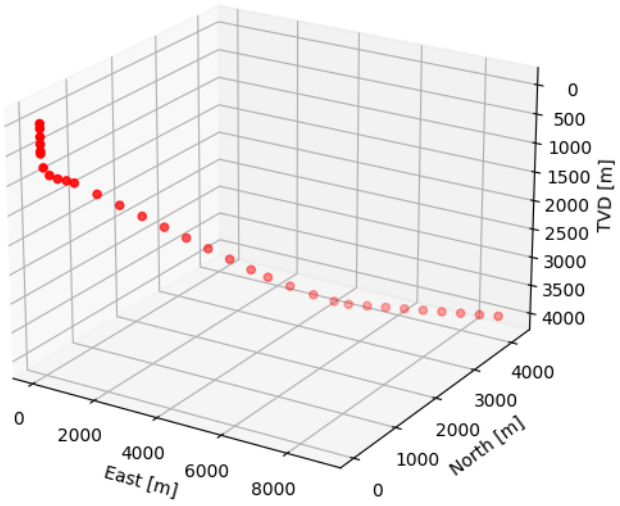

Figure 4.4: Given Data Survey Points Example

Then an imaginary straight is drawn between each two survey stations (magenta lines in Figure 4.5). The inclination and azimuth are calculated based on this imaginary line and the tangential method

equations, Eq. (2.4) and (2.5). Figure 4.5 shows a zoom-in of the last curvature section in Figure 4.4 and provides a more precise explanation of the inclination angles between each two survey stations. The stations in the figure are named with the letter P and the correspondent number of the survey station. Besides, the equations used for the inclination and azimuth approximation are:

$$\Delta MD_i = \sqrt{(V_i - V_{i-1})^2 + (N_i - N_{i-1})^2 + (E_i - E_{i-1})^2} \tag{4.14}$$

$$\alpha_i = \cos^{-1}\left(\frac{V_i - V_{i-1}}{\Delta MD}\right) \tag{4.15}$$

$$\varphi_i = \cos^{-1}\left(\frac{N_i - N_{i-1}}{\Delta MD \cdot \sin\alpha}\right) \tag{4.16}$$

The azimuth value from Eq. (4.16) should be carefully checked since it might need some correction or adjustment depending on the quadrant where it belongs.

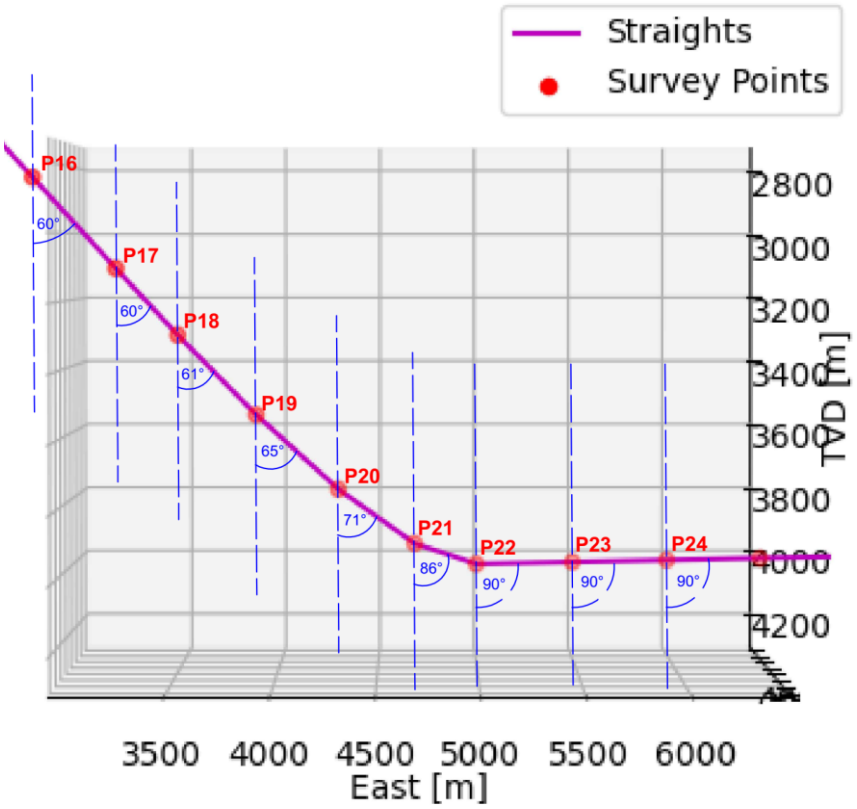

Figure 4.5: Process for Classification of the Sections of the Well

When all the intermediate lines between the points have their inclination and azimuth, the analysis calculates the difference in inclinations and azimuths between two adjacent lines. The difference is compared with the tolerance value, which will result in two possible situations:

- If the tolerance value is bigger than the difference, then the line belongs to a hold section.
- If the tolerance value is lower than the difference, then the line belongs to a curvature section.

For instance, in Figure 4.5, the line between stations P16 and P17 has an inclination of 60°, and the next line also has an inclination of 60°. Supposing that there is a tolerance value of 0.5°, the difference between the inclinations (0°) is less than the tolerance. As a result, the program concludes that this line segment belongs to a hold section.

On the contrary, the line between points P20 and P21 has an inclination of 71°, while the line between points P21 and P22 has an inclination of 86°. The difference of 15° is more than the tolerance value, and it will be considered a curvature section by the program. The same logic is followed for identifying the azimuth segments.

This part of the PWP function will save the section classification and put some corresponding numbers of identification that will be reading by the next section constructor. The section identifiers are 0 for the hold sections and 1 for the curvature sections.

4.2.2 Construction of Hold and Curvature Sections

The construction algorithm used in the PWP function has two parts, as was illustrated in Figure 4.3, the hold section and curvature section construction. The first one calculates a specific number of points on a straight segment that starts and finishes in two specific survey points. The second part, build-up or drops a curvature section from three reference survey points, using the cubic Beziér model.

Therefore, the step that should be made before the calculation is to locate where are the start and end points, for the hold section case and where are the start, middle, and end points for the curvature section. The hold sections have a simpler process to set the PWP survey stations than the curvature sections; thus, the following description will start with the hold sections.

4.2.2.1 Hold Sections

After the data analysis returns the survey points with their correspondent section identifiers, 0 or 1 according to the section classification given by the last analysis, the construction algorithm looks for the first and last rows with the value 0 as section identifier before changing the section.

For example, Figure 4.6 shows a part of the original survey data example given before. In this figure, points P0 and P5 would be taken as the start and end points for the hold section 1. This does not mean that this section will be the only hold section in the entire well. On the contrary, the algorithm is designed to be run every time it finds that an analyzed survey point has been classified as a hold section (e.g. since P10 in Figure 4.6) and looks for the first and last rows with the identifiers.

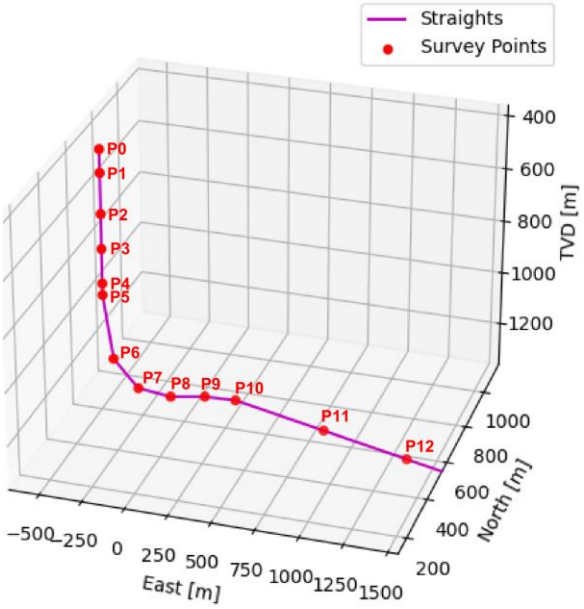

Figure 4.6: Hold Sections Survey Points Example

Once the start and end points have been adequately identified, they are used as the reference points for calculating the space distance between them with Eq. (4.14). This distance is the total distance that must be covered with the construction of the hold section. Consequently, the location of the survey points over this distance depends on the delta distance chosen by the user for the location of the survey points (Sur_{pts}).

The hold sections should change neither inclination nor azimuth; so, the inclination and azimuth calculated by the data analysis part are still valid for this part too. As a result, the inclination, azimuth, and MD (equal to Sur_{pts}) are enough data to obtain the coordinates values (V, N, E) through the tangential method equations.

The result for the hold section construction is a matrix that contains the coordinates, MD, inclination, azimuth, and DLS (equal to 0 for all the hold section survey points) that will form part of the final PWP matrix.

4.2.2.2 Curvature Sections

The other part that is constructed is the curvature section, which can be either for building up or dropping the inclination angle. The model used for estimating the location of the survey points in a curvature segment is the cubic Beziér curves.

As it was said before, the Beziér curves need one starting point S and one end point E to define the length of the curvature that is going to be made. Also, it requires two initial guessed values, which are the distances to the attractor points from S and from E, d_s and d_e respectively. Typically, the user will have to guess these two values, but since the objective of the RSS Simulator is achieving an automatization level, the last option cannot be acceptable.

Therefore, the d_s and d_e initial values are calculated in the code, and the algorithm must find the most optimal combination of values to generate the shortest and lowest DLS. The way of optimizing this process will be explained in the next part of the study. The important results obtained from the optimization are the values of d_s and d_e that will be used to calculate the Beziér curve with the rest of the input data.

Apart from the mentioned input data for the Beziér model, the inclinations and azimuths from the S and E coordinates are necessary. They are significant for the definition of the shape of the Beziér curve because the direction of the start point will influence over the next point and so on until the curve shapes itself to reach the end point.

A more explicit example of the importance of the points inclination and azimuth is perceived in Figure 4.7, where there are two Beziér curves alternatives. Both of them use exactly the same coordinates for the S and E points. The difference between them is that for the first alternative (case a), the inclination and the azimuth for the start point are 34° and 68°, respectively. In the second alternative (case b), the inclination and azimuth at the start point have a value of 74° and 240°, respectively.

In addition, the points S and E need to be selected before calculating the Beziér curves. The methodology is the same as the one explained for the hold section construction. For instance, in Figure 4.6, point P5 is the start point, and point P10 is the end point that will be used in the Beziér calculation. Besides, since the curvature follows a Beziér curve model, the intermediate points between the P5 and P10 are not considered because the curve's trajectory will be different to a certain degree.

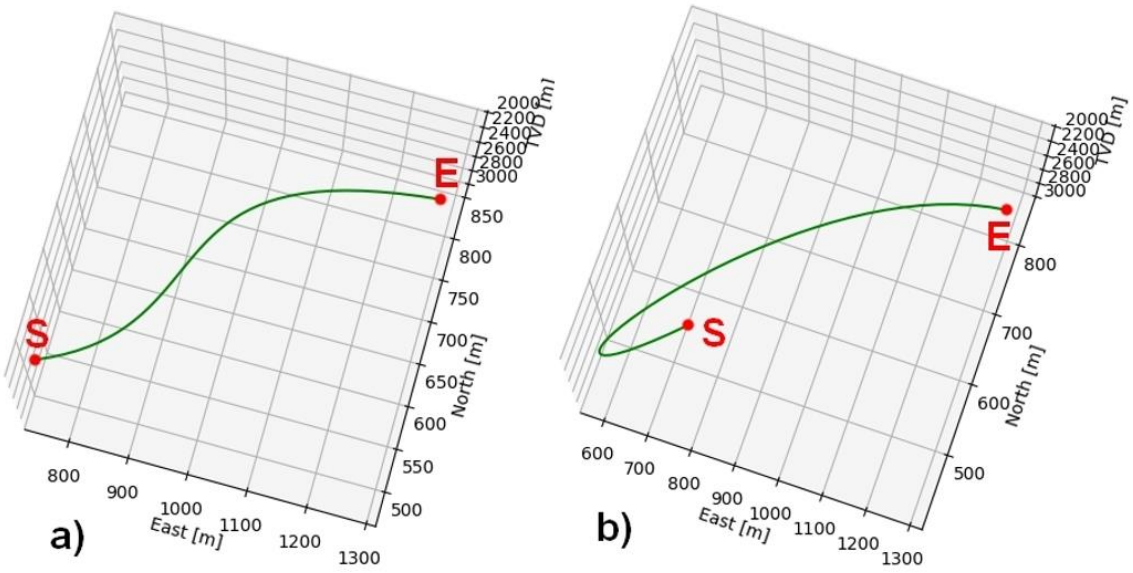

Figure 4.7: Inclination and Azimuth Importance in Beziér Curves

The Beziér model will calculate the survey points' location to build the curvature from the start point to the end point. The distance between the survey points in the curvature section depends on the value u that the user has entered at the beginning of the simulation. If the value of u is low, then the Beziér curve is going to have more survey points.

The Beziér algorithm returns the coordinates (V, N, E), MD, inclination, azimuth, and DLS. All of them are calculated with Eq. (4.1) to (4.13). These survey points are added to the final PWP matrix that will be the Planned Well Path that the rest of the simulator will use as a reference later.

4.2.3 Optimization of Curvature Sections

The cubic Beziér curves change their shape between two points according to the distance of the control points because these will "attract" the line calculated towards them. So, if the distance from the start point or end point is significant, then the curvature will get more aggressive.

The principal purpose of curve optimization is to find the best combination of the distance from the start point to the start attractor d_s, and the distance from the end point to the end attractor d_e. For that goal, the optimization is based on two main constraints:

- **1st condition**: Calculate a Beziér curve where all the survey points generated have a lower DLS value than the maximum DLS imposed by the user at the beginning of the simulation. This limitation assures that the PWP does not have very sharp curve changes that risk the integrity of the drilling operations.
- **2nd condition**: Chose the shortest curve created between the start and end points. In other words, pick the curve that accomplishes the 1st condition and has the lowest total MD value. The length of the curve plays a high relevance while drilling a well due to it will increase the cost of the operations the longer it gets.

The importance of the conditions achieving is transmitted through the values of d_s and d_e selected. Figure 4.8 shows an example comparison between two curves with the same data, except for the values of d_s and d_e. The case a) has a $d_s = 200$ and a $d_e = 220$, while the case b) has a $d_s = 700$ and a $d_e = 640$.

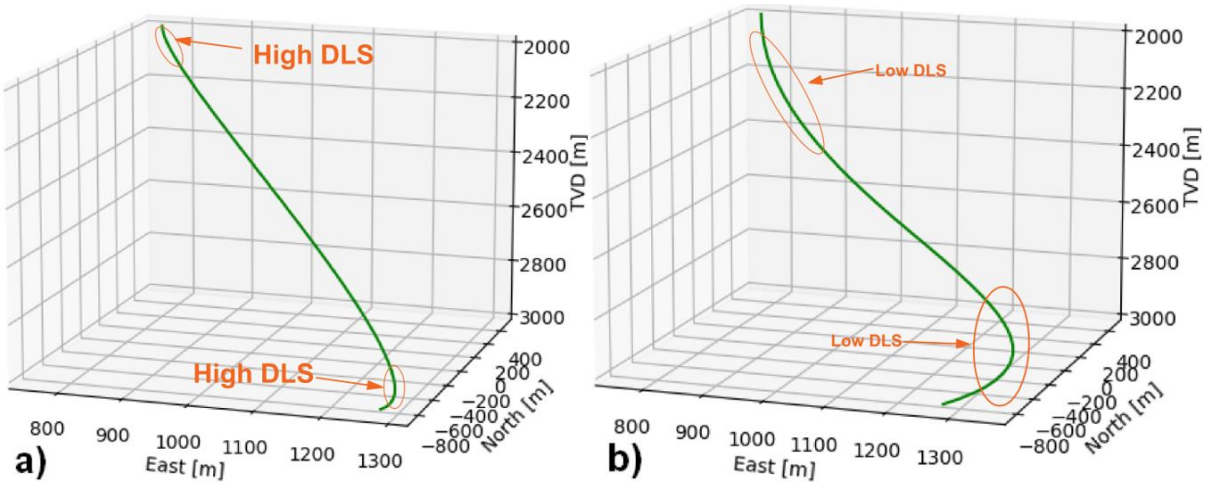

Figure 4.8: *ds* and *de* Values Comparison Example

The following dilemma can be inferred from the last figure: If the distances of the attractor points are close to the *S* and *E* points, then the total MD of the curvature is lower, but the DLS near to the *S* and *E* points will increase and become too sharp. On the contrary, if the distances of the attractor points are further to the *S* and *E* points, then the total MD of the curve is more extensive, but the DLS near to the *S* and *E* points is relatively low and could be tolerable for the operation.

Consequently, the labor of the optimizer is to find the balance between these two extremes situations. In order to perform that task, the optimizer uses the process shown in the flowchart of Figure 4.9.

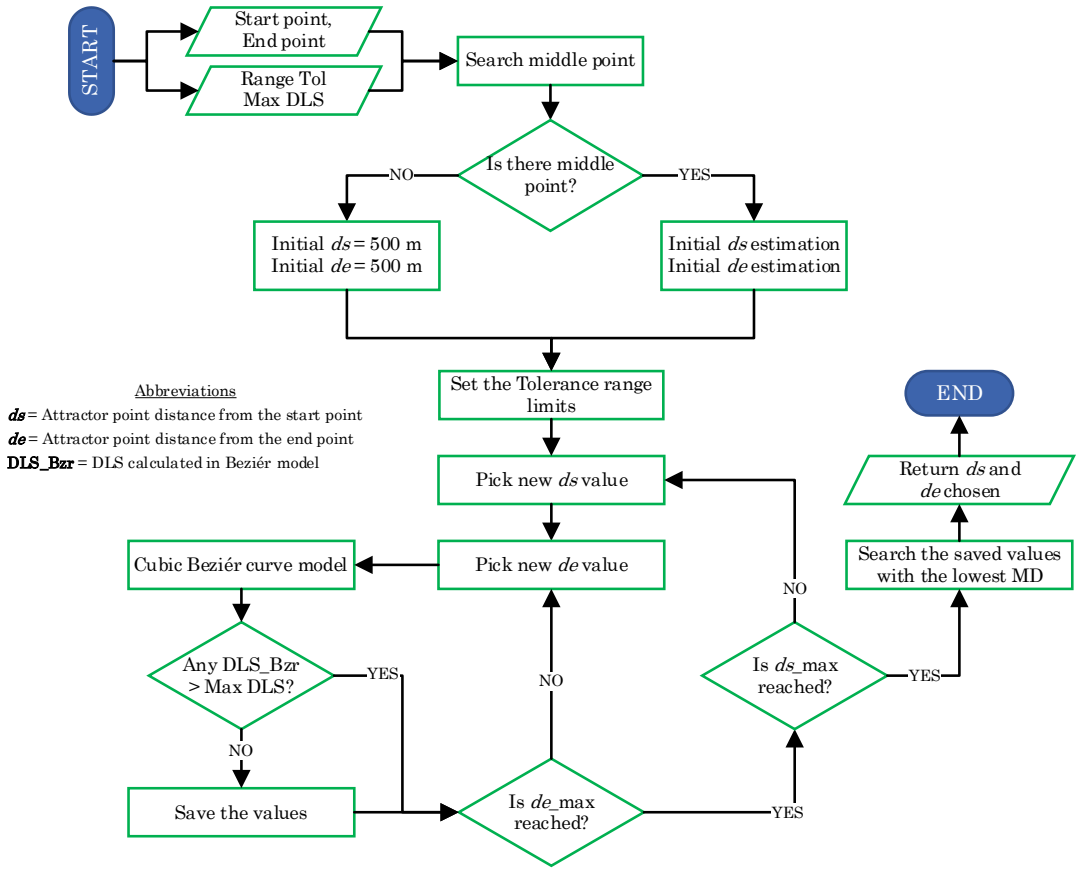

Figure 4.9: *ds* and *de* Optimization Process Flowchart

As it is seen in the last flowchart, the initial data are the S and E points coordinates, and the user set values for the range tolerance and maximum DLS. The range tolerance (Ran_{Tol}) is a numerical value that will be subtracted and added to the initial d_s and d_e estimated values. It sets the lower and upper limits for the different attractor distance combinations. The maximum DLS (Max_{DLS}) is the maximum value that will be compared with all the survey points DLS that are generated each time the Beziér model is called.

The Ran_{Tol} is selected by the user and can be assumed as the maximum and minimum distance that the attractor's points should be. Therefore, it is measured in meters; some good values to try for the range are 300 or 350 m because if the range tolerance is too large, more iterations will be needed for finding the correct combination, and the computational time will increase a lot. On the contrary, if the range tolerance is too low, any combination of attractor points might not be found, and the optimization will not be possible.

Nevertheless, another aspect that should be considered for selecting the Ran_{Tol} adequately is the value of the Max_{DLS}. For instance, if the Max_{DLS} is a low value, there is a significant probability to find the correct combination of attractor points that generates a DLS lower than the Max_{DLS} with a higher Ran_{Tol} value since the range of combinations is larger too. In other words, the user should consider using a higher Ran_{Tol} value as the Max_{DLS} is lower.

In addition, in Figure 4.9, the first step is to approximate initial values for d_s and d_e from the intermediate survey points between S and E points. As a result, the optimizer algorithm searches the middle point between the mentioned extremes from the original survey data points. This step can be done while the data analysis runs and save the coordinates for later.

The distance from S to the middle point is considered as the initial d_s value and the distance from E to the middle point is taken as the initial d_e value (see Figure 4.10).

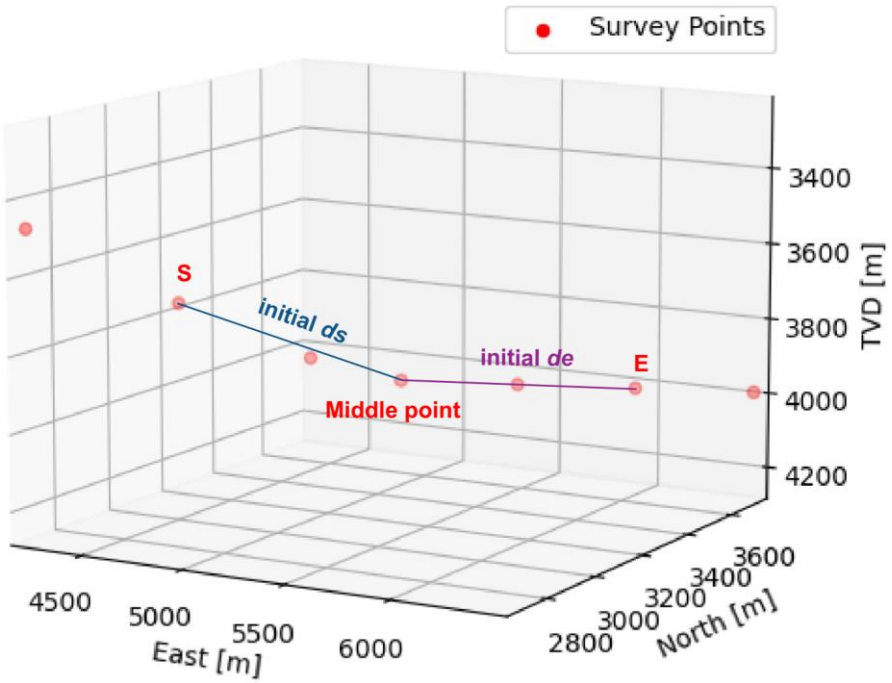

Figure 4.10: Initial *ds* and *de* Estimation Example

The middle point will be the central value in the range combination of d_s and d_e. With the middle point,

it is possible to set the upper and lower range values for the combinations with the following equations:

$$d_{s_{Low}} = initial\ d_s - Ran_{Tol} \quad (4.17)$$

$$d_{s_{Up}} = initial\ d_s + Ran_{Tol} \quad (4.18)$$

$$d_{e_{Low}} = initial\ d_e - Ran_{Tol} \quad (4.19)$$

$$d_{e_{Up}} = initial\ d_e + Ran_{Tol} \quad (4.20)$$

The primary optimization process starts by combining the $d_{s_{Low}}$ and the $d_{e_{Low}}$, and sends them into the Beziér model algorithm. Once the survey points generated in the corresponding Beziér curve are available, the highest DLS_{Bzr} is searched, and it is compared against the Max_{DLS}. If the highest DLS_{Bzr} is lower than the Max_{DLS}, then the values of d_s, d_e and the total MD of the curve are saved for later.

Then the d_e increases 20 m for the next combination, and the process is repeated until the d_e upper limit is reached. After the $d_{e_{Up}}$ reached the d_e value restarts by acquiring the $d_{e_{Low}}$ value and the d_s increases 20 m. The process is an iteration that will mix all the possible combinations between d_s and d_e with a step of 20 m inside the range set before.

After all the thinkable combinations have been made and the values that accomplish the 1st condition were saved, the next step is to search the minimum total MD value between the valid alternatives (Figure 4.11). The point that accomplishes this 2nd condition is determined to be the most optimal combination of d_s and d_e that will not compromise the integrity of the well by not reaching a high DLS, and assures the faster and shortest path to be drilled.

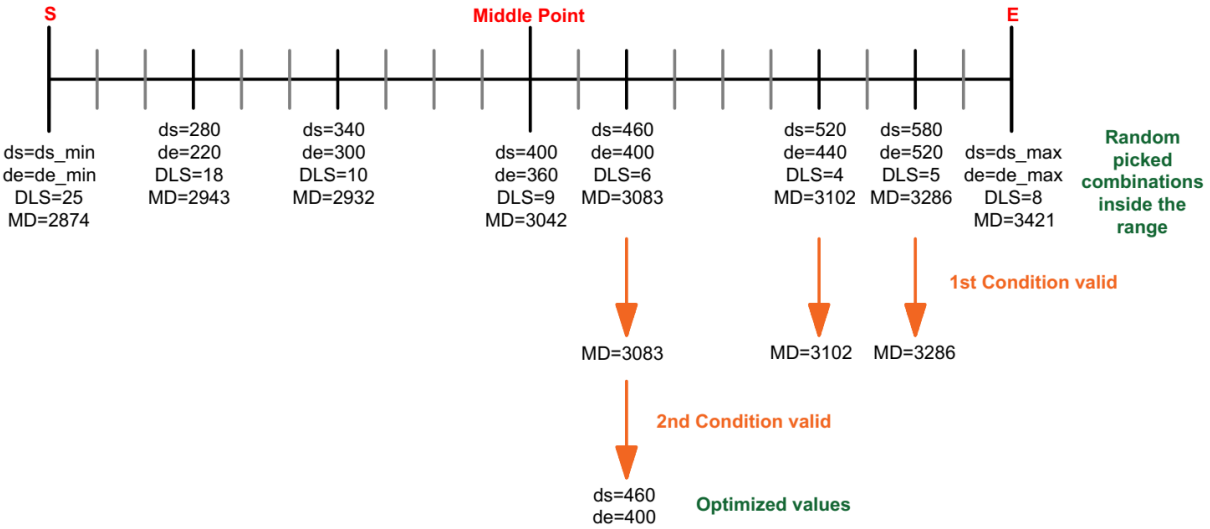

Figure 4.11: Optimization Concept Example

The optimized values of d_s and d_e are transferred to the curve section construction algorithm, which uses them as input parameters for the Beziér curvature model, and obtains the survey points that belong to the curved section in the final PWP.

5 Drilling Simulation with the RSS Model

The RSS Simulator has two general processes described in Figure 3.1, the Trajectory Control Optimizer (TCO) and the RSS Model. The TCO was the principal development of the present thesis, along with the adaptation with the RSS Model. As a matter of fact, Saramago has already presented the RSS Model in the thesis "Rotary Steerable System Modeling and Simulator" developed for the University of Stavanger in 2020.

The principal cause to use the RSS Model inside the RSS Simulator software is the excellent potential and originality that it has developed. However, the model has not been validated yet, and it still needs some improvements and modifications for specific situations.

Consequently, some upgrades were developed in the present work to increase the efficiency of the original RSS Model, but above all, to correct the offset controller, the natural displacement calculation, and the main iteration process thought when it was conceived.

The original offset controller was not available to reach the automation level since it needed to be informed about all the KOP by the user before the simulation and did not make their own decision based on the drilling parameters. Besides, the natural displacement calculation used a linear system of equations that involves very large calculations that reduced the time efficiency of the simulation.

Moreover, the main iteration conditional was very basic, and it was based on the maximum number of iterations instead of a drilling parameter like the MD or the time. It was a significant limitation of the original RSS Model that did not let achieve precise control over the final target reaching condition, since it might neither drill into the target zone due to the maximum iterations has already been reached, nor stop the drill when the target zone has been reached.

The present chapter will describe superficially the procedure followed by the RSS Model explained by Saramago in his work, and if the reader wants to know more about the idea of the model, he or she should recur directly to Saramago's thesis. Besides, the chapter will show the principal upgrades made during the adaptation of the TCO with the RSS Model function.

5.1 RSS Model

Saramago has developed the RSS model in order to simulate the movement and the position of the bit while drilling with the OrientXpress® RSS tool. The model derives the forces on the bit caused by the weight on the bit (WOB) and the bending of the RSS system. With these forces, the model can decompose the traditional ROP definition into 2 or 3 ROPs values, corresponding to the 2D or 3D modeling (Saramago, 2020).

The ROP modeling has been studied for many years, and numerous mathematical models have had the goal to describe the relationship between the rate of penetration (ROP) and several controllable drilling variables; for example, rotary speed of drill string (RPM), weight on bit (WOB), mud weight, pump pressure and pump flow rate (Esmaeili et al., 2012).

Indeed, deterministic models have been developed through the years to predict the ROP based on laboratory experiments, like Bingham, Bourgoyne & Young, Hareland & Rampersad, and Motahhari, Hareland & James. Nevertheless, advances in computational power and machine learning over the years have allowed new data-driven ROP prediction models, which are based purely on data statistics like Hegde & Gray (Hegde et al., 2018).

The operation of the RSS Model function (Figure 5.1) involves some organized steps execution each time the function is called. Despite the original RSS Model having two variants, the 2D modeling and the 3D modeling, only the last variant will be described since the RSS Simulator works in a 3D environment and uses the 3D variant.

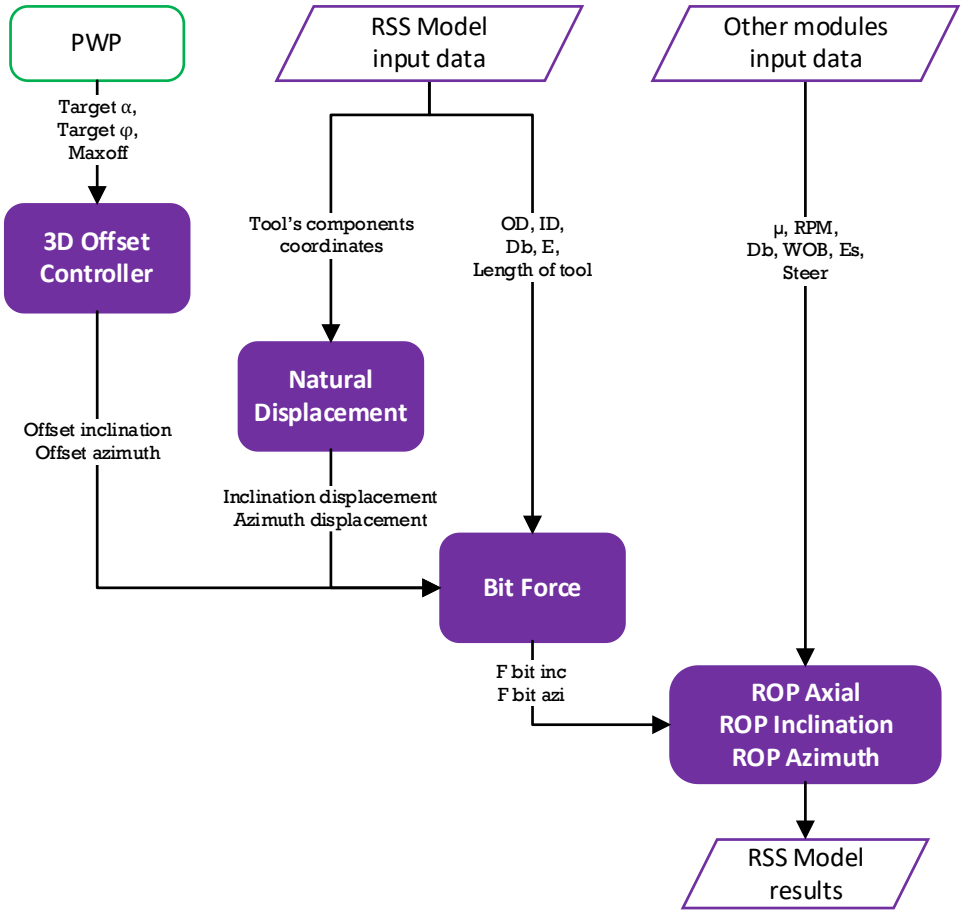

Figure 5.1: RSS Model Operation

5.1.1 3D Offset Controller

The offset controller for the 3D case is the principal function that directs the inclination and azimuth goals to reach or approximate in the next drilling simulation iteration. As it was discussed before, the instructions or the target inclination and target azimuth come from the PWP calculated previously.

The offset controller transforms the target inclination and azimuth values into a particular offset or actuator displacement length. The length of the offset will push the OrientXpress® RSS tool to one side of the borehole with more or less intensity depending on the offset value, as shown in Figure 5.2.

Saramago indicates that the maximum length of displacement in the tool is assumed as 6 mm because the accurate limitation information is reserved for the Canrig Norway company (Saramago, 2020). Nevertheless, the tool's action is still the same and will not vary its behavior during the drilling operation. The offset controller has three situations:

- Fully activate the actuator according to the maximum opening offset percentage ($maxoff$).
- Deactivate the actuator gradually
- Entirely deactivate the actuator.

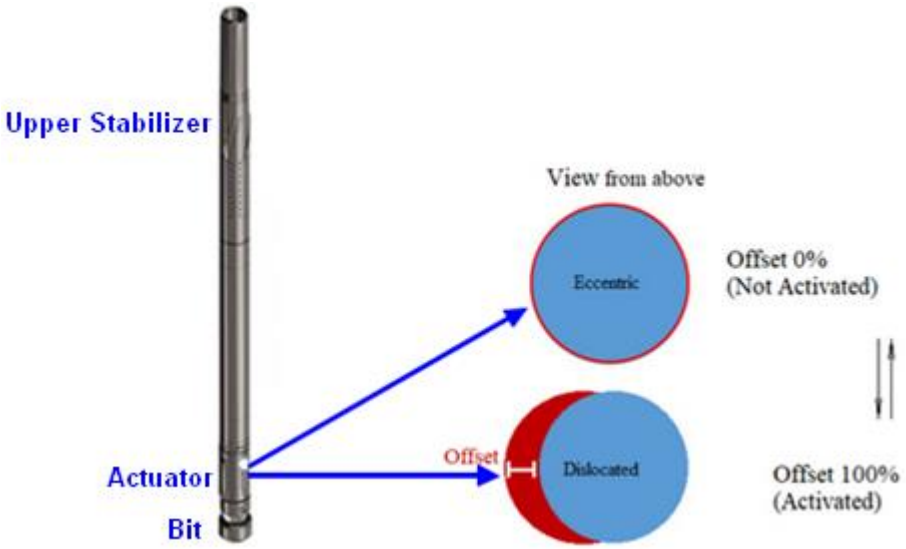

Figure 5.2: Offset Displacement Operation (Saramago, 2020) and (Nabors Industries Ltd., 2021)

The controller increases the complete offset displacement by the determined $maxoff$ that the user has set to be used as maximum. For instance, if the user sets a $maxoff$ of 100%, then the offset will open 6 mm. On the other side, if the user sets a $maxoff$ of 60%, then the offset will open 4.8 mm, which will make the curvature sections longer and softer.

When the bit inclination and azimuth are about to reach the target values, the offset controller gradually decreases the opening value to assure a soft entanglement to the next hold section. Finally, when the hold section is reached, with its correct inclination and azimuth, the offset controller deactivates the opening and keeps it in 0% of opening until another curvature section is beginning to be drilled or there is a necessity of some correction of the trajectory (explained later).

Figure 5.1 indicates that the returned parameters of this function are the offset inclination and the offset azimuth, that is, just the length of the displacement in the axial axis and the length of the displacement in the horizontal axis, respectively. Both offsets will influence the bit force determination in the following steps inside the RSS Model function.

5.1.2 Natural Displacement

The displacement or offset caused by the BHA tool will bend the drill string towards the desired direction. If the displacement is watched from its profile plane, as it is shown in Figure 5.3, it is possible to form two straights lines. One of them connects the middle point from the bit to the upper stabilizer, and it is called “Long line”. The “Short line” connects the middle point from the bit until the actuator of the BHA tool.

Every time the inclination and azimuth change, and the offset of the tool is activated, the two lines create a displacement between them (green vector in Figure 5.3). This displacement is called the natural displacement, and the length will influence the intensity of the force from the BHA actuator to the wellbore walls.

The natural displacement function calculates the magnitude of this displacement using the space vector mechanics and the coordinates of the upper stabilizer (blue square), BHA actuator (orange square), and drill bit (blue point of the drill string).

The natural displacement vector starts in the actuator coordinate and points to the orthogonal point on the long line or vector formed by the stabilizer and the bit. Moreover, the vector does not have magnitude when the drill string is in a hold or vertical section since there is no difference between the two imaginary lines.

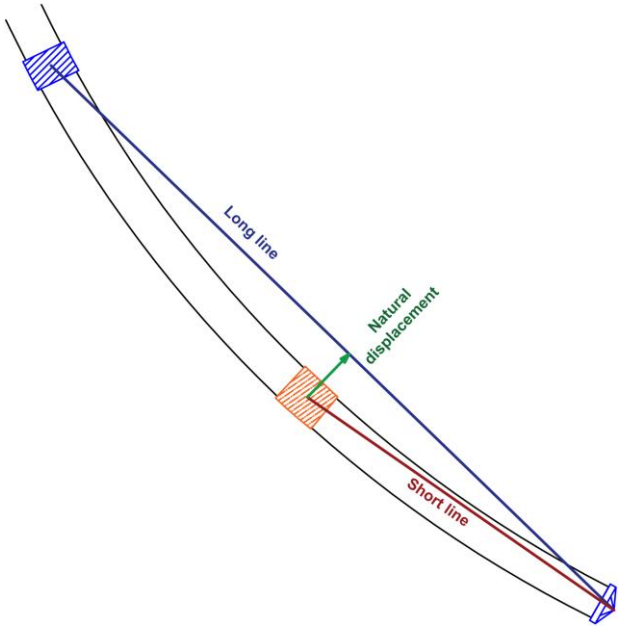

Figure 5.3: Natural Displacement Concept

The natural displacement vector has a magnitude and a direction according to the direction that the drill string is bending, and the vector will define the direction of the forces caused due to the natural displacement. Since the analysis is applied each time the inclination and the azimuth change, the results return two displacement magnitudes, one for the inclination and the other for the azimuth.

5.1.3 Bit Force Estimation

The forces acting over the bit play an important role in creating the trajectory path. They are the physical magnitude that is applied over the wall of the borehole. As a result, a good model for estimating them is needed.

The model chosen by Saramago to model the forces acting on the drill string is the beam bending applied to a steel pipe, where the main idea is the balance of force and momentum (Saramago, 2020). The beam bending scenario used is represented in Figure 5.4, where the W_b and W_a are the reaction forces to the applied punctual load W on the length l of the steel pipe.

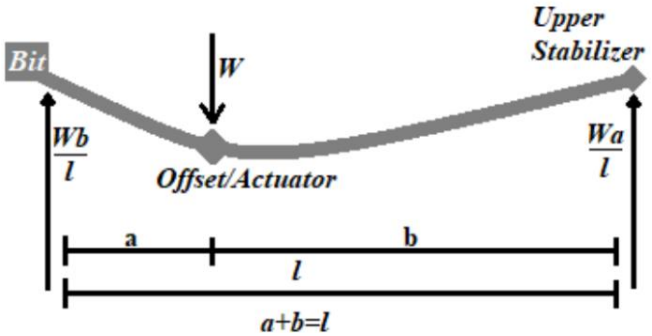

Figure 5.4: Beam Bending Scenario to Model the Drill String Forces (Saramago, 2020)

The details of the derivation of the calculation of the bit forces are in Saramago's work, but the relevant equations for the RSS Model implementation are the following (Saramago, 2020):

$$F_{ND_{azi}} = \frac{3 \cdot ND_{azi} \cdot E \cdot I}{a^2 \cdot b} \tag{5.1}$$

$$F_{ND_{inc}} = \frac{3 \cdot ND_{inc} \cdot E \cdot I}{a^2 \cdot b} \tag{5.2}$$

$$F_{Offset_{azi}} = \frac{3 \cdot Offset_{azi} \cdot E \cdot I}{a^2 \cdot b} \tag{5.3}$$

$$F_{Offset_{inc}} = \frac{3 \cdot Offset_{inc} \cdot E \cdot I}{a^2 \cdot b} \tag{5.4}$$

Where:

- $F_{ND_{azi}}$ = force on the bit due to azimuth natural displacement $[N]$
- $F_{ND_{inc}}$ = force on the bit due to inclination natural displacement $[N]$
- $F_{Offset_{azi}}$ = force on the bit due to azimuth offset $[N]$
- $F_{Offset_{inc}}$ = force on the bit due to inclination offset $[N]$
- ND_{azi} = natural displacement caused by the azimuth change $[m]$
- ND_{inc} = natural displacement caused by the inclination change $[m]$
- $Offset_{azi}$ = offset used in the BHA actuator to reach the target azimuth change $[m]$
- $Offset_{inc}$ = offset used in the BHA actuator to reach the target inclination change $[m]$
- E = elasticity modulus of a steel pipe $[Pa]$
- I = inertia moment $[m^4]$
- a = distance from the bit to the actuator $[m]$. Assumed 0.5 m.
- b = distance from the bit to the upper stabilizer $[m]$. Assumed 2.7 m.

The last set of equations shows two types of forces (each one with an inclination and azimuth component) that act over the bit. The force due to the natural displacement represents the reaction force of the formation contact that is pushing the bit in the opposite direction. The second type is the reaction force produced by the offset opening, which will be transferred to the bit too. A better clarification of the forces and reaction forces directions can be appreciated in Figure 5.5.

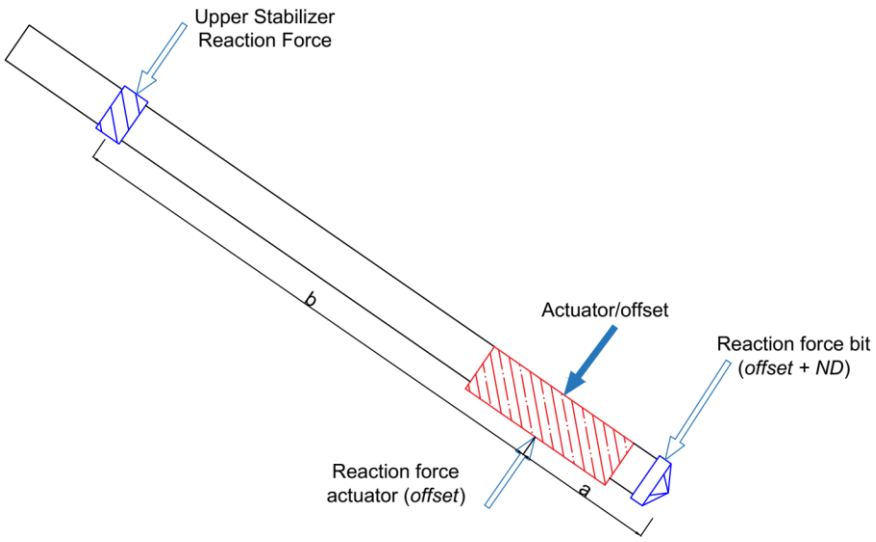

Figure 5.5: Acting Forces on the Bit

The total reaction force over the bit is the principal agent that opposes the bit steering and the force applied to bend the drill string. Consequently, the total force on the bit for the inclination and azimuth directions are:

$$F_{bit\ azi} = F_{ND_{azi}} + F_{Offset_{azi}} \tag{5.5}$$

$$F_{bit\ inc} = F_{ND_{inc}} + F_{Offset_{inc}} \tag{5.6}$$

Where:

- $F_{bit\ azi}$ = total force on the bit for the azimuth component $[N]$
- $F_{bit\ inc}$ = total force on the bit for the inclination component $[N]$

5.1.4 ROPs Calculations

The ROPs calculations are the principal characteristic of the RSS Model because it proposes a new methodology to calculate the bit movement, including its inclination, azimuth, and DLS. The calculation involves three types of ROPs in a tridimensional space (see Figure 5.6, where the blue element is the bit and the red is the rest of the BHA).

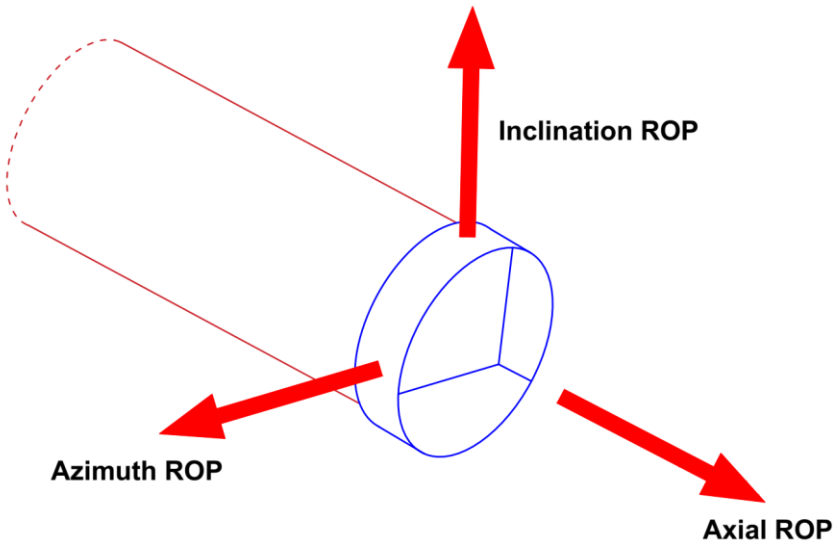

Figure 5.6: 3D ROPs Acting on the Drill Bit

The three ROPs represent the movement of the bit during a specific time step, which agrees with the measuring unit of the ROP (distance over time). Teale proposes the base for the ROPs equations in 1965 where the dependency on the rock mechanics is represented in the value of the energy of the rock (Teale, 1965).

Nevertheless, Saramago adapted this equation of ROP, transforming the original WOB to F_{bit} and it is decomposing the common ROP into an axial ROP, inclination ROP, and azimuth ROP. The idea of the application of the ROPs over the directional drilling is to generate some displacement in the opposite direction of the reaction force to the bit (described before) to overcome this force and start to bend the bit in the desired direction.

The last concept could be analyzed in Figure 5.7 that shows the frontal plane of the bit where the resultant ROP (composed by the inclination and azimuth ROPs) generated by both offsets and the natural displacements from the inclination and azimuth components. The resultant ROP acts against the reaction force on the bit (integrated by the inclination and azimuth components).

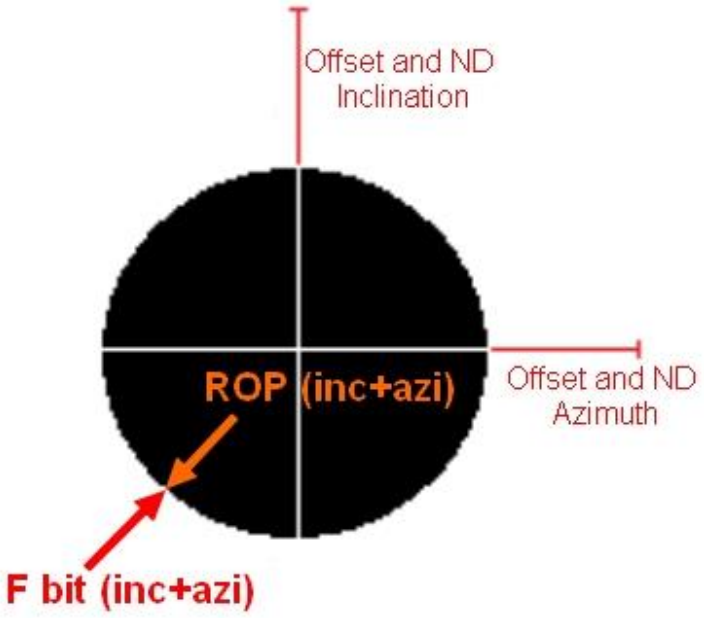

Figure 5.7: Resultant ROP Pushing the Bit Against the Reaction Force on the Bit

The equations that govern the ROP functions are the following (Saramago, 2020), where the units have to be introduced in imperial system, and the ROP calculation will be converted to SI units system:

$$ROP_{axial} = \frac{13.33 \cdot \mu \cdot N}{D\left(\frac{Es}{WOB} - \frac{1}{Ab}\right)} \cdot 0.3048 \tag{5.7}$$

$$ROP_{azi} = \frac{13.33 \cdot \mu \cdot N \cdot steer}{D\left(\frac{Es}{F_{bit\ azi}} - \frac{1}{Ab}\right)} \cdot 0.3048 \tag{5.8}$$

$$ROP_{inc} = \frac{13.33 \cdot \mu \cdot N \cdot steer}{D\left(\frac{Es}{F_{bit\ inc}} - \frac{1}{Ab}\right)} \cdot 0.3048 \tag{5.9}$$

Where:

- ROP_{axial} = ROP in the axial direction $[m/hr]$
- ROP_{azi} = ROP in the azimuth direction $[m/hr]$
- ROP_{inc} = ROP in the inclination direction $[m/hr]$
- Ab = transversal area of the borehole $[in^2]$

The data used by Eq. (5.7) to (5.9) are obtained from external modules or models, except for the forces on the bit and the area of the borehole. The data from the external model is updated every time the simulation reaches a survey point. In other words, when the bit reaches the MD correspondent to a survey station MD, it asks for some new results coming from different analyses used in external modules.

Furthermore, to the mentioned data is added some noise as explained in Eq. (3.1) before. The purpose of this action is to insert some uncertainty into the simulator to approximate the conditions of a real-life drilling environment.

The RSS Model can foretell the next bit position or next bit survey using these equations, calculated in SI units (Saramago, 2020):

$$MD_{(t)} = MD_{(t-1)} + \sqrt{{ROP_{azi_{(t)}}}^2 + {ROP_{inc_{(t)}}}^2 + {ROP_{axial_{(t)}}}^2} \cdot \frac{\Delta t}{3600} \tag{5.10}$$

$$\alpha_{(t)} = \alpha_{(t-1)} + \tan^{-1}\left(\frac{ROP_{inc_{(t)}}}{ROP_{axial_{(t)}}}\right) \cdot \frac{\Delta t}{3600} \tag{5.11}$$

$$\varphi_{(t)} = \varphi_{(t-1)} + \tan^{-1}\left(\frac{ROP_{azi_{(t)}}}{ROP_{axial_{(t)}}}\right) \cdot \frac{\Delta t}{3600} \tag{5.12}$$

$$HD_{(t)} = HD_{(t-1)} + \sin(\alpha_{(t)}) \sqrt{{ROP_{inc_{(t)}}}^2 + {ROP_{axial_{(t)}}}^2} \cdot \frac{\Delta t}{3600} \tag{5.13}$$

$$TVD_{(t)} = TVD_{(t-1)} + \cos(\alpha_{(t)}) \sqrt{{ROP_{inc_{(t)}}}^2 + {ROP_{axial_{(t)}}}^2} \cdot \frac{\Delta t}{3600} \tag{5.14}$$

$$East_{(t)} = East_{(t-1)} + \sin(\varphi_{(t)})(HD_{(t)} - HD_{(t-1)}) \tag{5.15}$$

$$North_{(t)} = North_{(t-1)} + \cos(\varphi_{(t)})(HD_{(t)} - HD_{(t-1)}) \tag{5.16}$$

$$DLS_{(t)} = \frac{\cos^{-1}[\cos(\alpha_{(t)})\cos(\alpha_{(t-1)}) + \sin(\alpha_{(t)})\sin(\alpha_{(t-1)})\cos(\varphi_{(t)} - \varphi_{(t-1)})]}{MD_{(t)} - MD_{(t-1)}} \tag{5.17}$$

Where:

- t = Current iteration position
- $t-1$ = Last iterated position

The equations from (5.5) to (5.17) and the offset applied to the BHA tool will be the results from the RSS Model simulation, whose units can be seen in Table 3.8.The simulation results are transferred to the main algorithm that will send them to the Deviation Control function in the specific moment to verify the simulated bit position regarding the PWP.

5.2 Principal Upgrades

The original RSS Model developed by Saramago in 2020 has a robust architecture; however, it had some procedures that needed to be corrected or modified, especially in the original Python code lines and functions.

Indeed, the original RSS Model had three principal issues that complicated the automation objective. The present work dealt with the problems of adapting the RSS Model with the TCO and preparing the structure to work with external models in the near future. The principal problems to be solved were:

- The Offset control needed the KOPs from the user, and it was not dynamic.
- The main loop was based on a total given iteration number and not on the well drilling parameters.
- The natural displacement calculation used a linear system of equations that involves equations with more than ten terms that reduced the efficiency of the simulation runs.

In the same way, some other minimal processes were corrected or organized more efficiently to improve fluency and computer time consumption.

5.2.1 Offset Control Enhancement

It is important to remember that the RSS Model was developed before the RSS Simulator, which means that the offset control had to work only with some initial instructions given by the user and made the controller not flexible to change or adapt to new trajectory plans. Nevertheless, this was a significant obstacle to reaching the automation level planned for the RSS Simulator. The offset controller function needed to be improved and changed to work autonomously.

As a result, the offset controller was enhanced using the method described in Figure 5.8. The goal of the offset controller is to return the correspondent inclination and azimuth offset to make the BHA tool change the direction of the well.

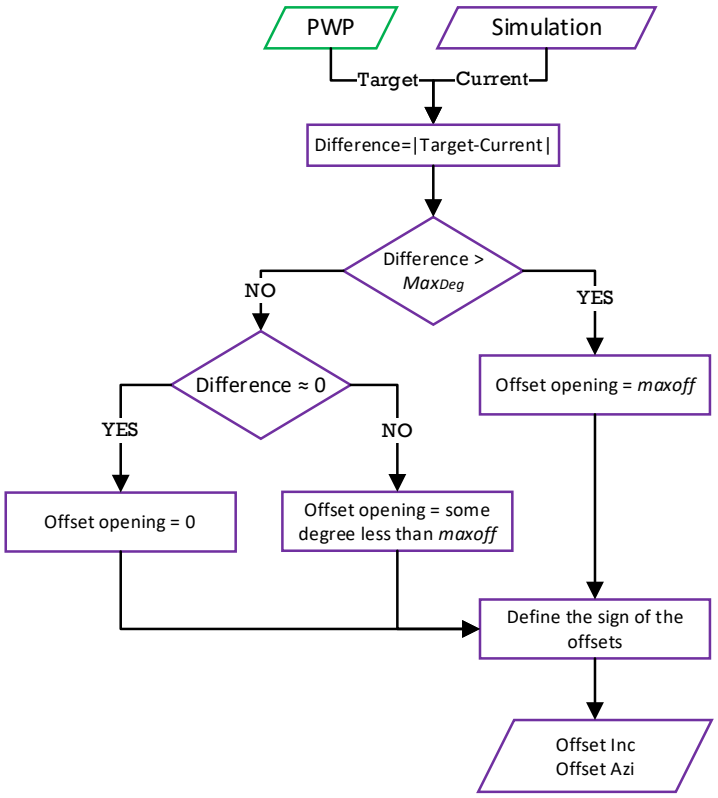

Figure 5.8: Enhanced Offset Control Function Flowchart

The offset controller function begins by receiving the target inclination and azimuth, the current inclination and azimuth, and the maximum offset ($maxoff$) and degree difference (Max_{deg}) set by the user before running the simulator. Then the absolute difference between the target and currents measures is calculated. The difference is compared against some maximum degree reference value (Max_{deg}) set by the user at the beginning.

If the value of the difference is more than the Max_{deg}, then the offset applied to the tool should be the maximum permissible ($maxoff$) like it is described in the following formula:

$$Offset = 1 \cdot maxoff \tag{5.18}$$

Otherwise, the function will determine if the difference is almost 0 or not yet. When the difference is close to 0, the offset could be considered 0 too; but if not, then the offset applies the following formula (Saramago, 2020):

$$Offset = (Target - Current) \cdot 1.5 \cdot maxoff \tag{5.19}$$

Where:

- $Target =$ target inclination or azimuth according to what it is being calculated
- $Current =$ current inclination or azimuth according to what it is being calculated

The offset controller function determines the sign of the offset value depending on the sign of the difference between the target and the current inclinations and azimuths. If the sign is positive, it means that the well needs to build up the angle; otherwise, it needs to drop the angle. The offset controller returns the offset values for the inclination and the azimuth, which will be used in the next simulation parameters.

The last flowchart is just a simplified version of the actual code, which involves other tiny changes made to have a correct execution of the offset control. The comparison between the functionalities or advantages between the original and the enhanced offset control can be appreciated in Table 5.1.

Table 5.1: Differences Original and Enhanced Offset Control

Original	Enhanced
- Needs KOPs inputs from the user - Needs the user to modify the code for each KOP that is present in the well plan - Creates the build-up or drop angle only in the direction set at the beginning of the simulation	- It does not need any user input, but the maximum offset and maximum degree - The target inclination and azimuth can change freely at any time - The offset adapts easier to the different shapes of the curvature - Offset maintains the hold sections more stable - It does not have any maximum number of targets to reach.

5.2.2 Main Loop Change

The RSS Model had been created with a very critical problem that affected the target's accuracy too much. The problem was the structure of the iteration process chosen by Saramago that involves a while-loop that only stopped once the maximum iteration number (set by the user) was reached.

This issue implied that the final point simulated was not always the target point of the drilling plan. For example, if the maximum iteration number were too high, then the simulation would still run even if the target zone was already reached. Nevertheless, if the number were too low, then the simulation would not reach the final zone, and the results would be incomplete.

The solution for this problem was a priority in order to assure good performance of the RSS Simulator. As a result, the whole loop structure was modified, which also involves changing the program's structure and creating new functions. Actually, many operations used to work in the main algorithm, which

hindered the adaptability from working with external models and returning live results to the user.

The main loop change is described in the flowchart of Figure 5.9, where it is painted in red due to it belongs to the main algorithm function. The figure shows a very abbreviate methodology of the actual code intending to show the changes made. A more accurate description of the code is given in the flowchart of Figure 3.3.

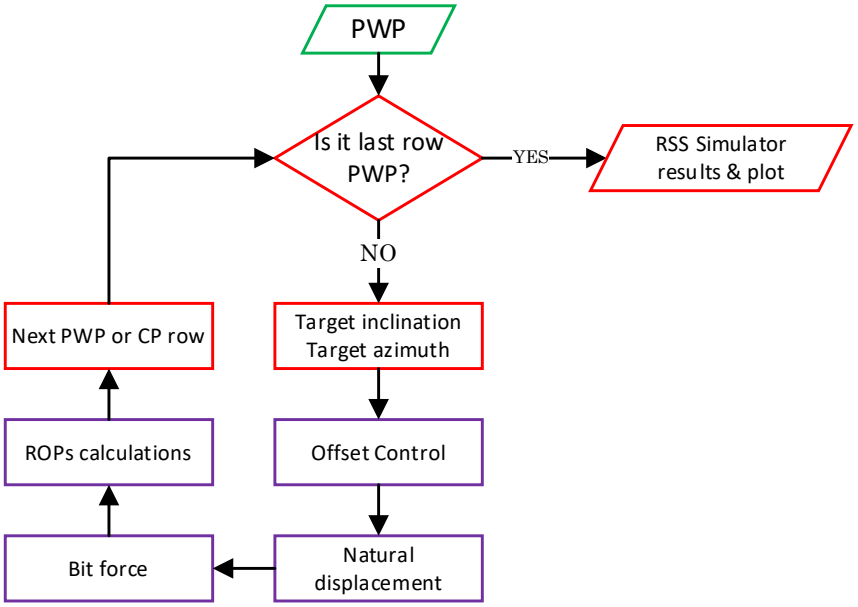

Figure 5.9: Simple Concept of the Enhanced Main Loop

The principal change is that the while-loop is in the function of the number of rows of the PWP based on the input survey points, where the target survey point is the last row of the PWP. In other words, the condition is based on the position of the simulation respected to the last survey station that is the target point.

Besides, the target inclination and azimuth are defined in the main algorithm, and the RSS Model interprets them through the use of the offset control function and the rest of the functions involved in the RSS Model previously described.

The principal differences between the original and the enhanced main loop are presented in Table 5.2.

Table 5.2: Differences Original and Enhanced Main Loop

Original	Enhanced
- The principal condition was the number of iterations - The drilling parameters do not influence the stop point - The target zone could be missed - The different program operations are integrated inside the main algorithm	- The principal condition is related to the target point parameter - Reaching the target point will stop the simulation - The different program operations are separated as functions - Allows the interaction with other external modules

5.2.3 Natural Displacement Algorithm Modification

The natural displacement was conceived following the same principle shown in Figure 5.3 that involves the utilization of two imaginary lines between the bit and the actuator and between the bit and the upper stabilizer.

Owing to both lines have a linear equation that could describe them, Saramago decided to use this approach to obtain the equations from each straight line and create a system of equations that solves the intersection point of a third line formed by the actuators coordinate and one perpendicular point on the "long line", that would represent the natural displacement.

The method involves calculating some equations that contain more than 10 terms and created a very difficult and complicated code algorithm that reduced the computational efficiency. Even though the algorithm used to work well, the margin for some optimization was present. Consequently, the whole method was replaced with vectorial mechanics in a 3D space, but the idea of Saramago is still respected.

Figure 5.10 shows the methodology used for calculating the natural displacement (purple line). Two space vectors are created using the upper stabilizer – bit coordinates (long vector) and the upper stabilizer – actuator coordinates (short vector). Then a third orthogonal vector is created from the head of the short vector towards the long vector. The module of the third vector will be equal to the distance from the actuator to the long vector line and will represent the natural displacement.

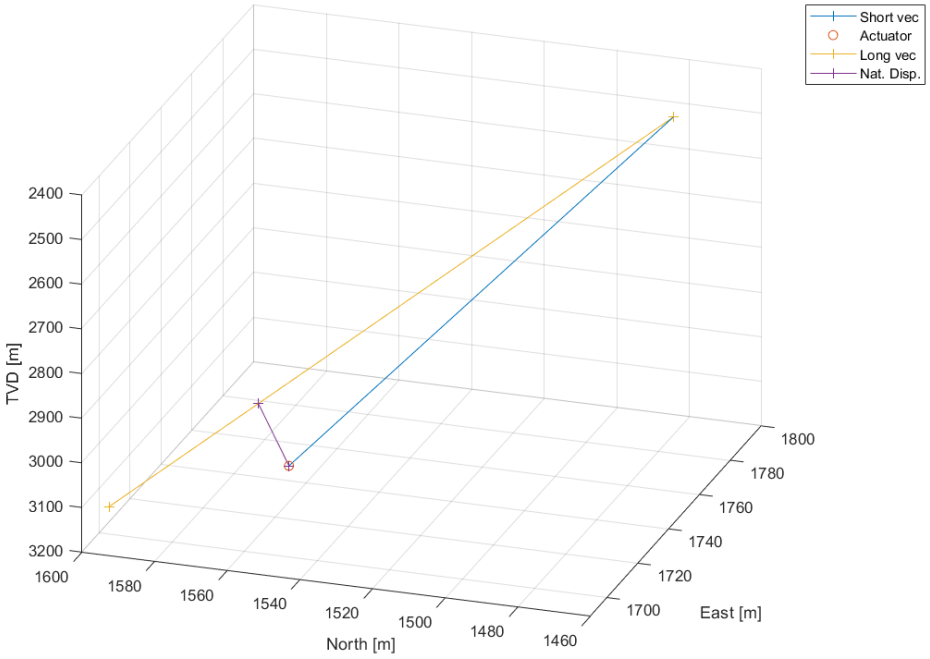

Figure 5.10: Natural Displacement Using Space Vectors

The new methodology is faster and lighter than the original one, increases the efficacy of the computer timing, and helps to understand the program codification. The equations used for this vectorial calculation will be explained in the Vector of Error chapter later.

6 Real-Time Trajectory Control

The Real-Time Trajectory Control oversees the current simulated bit position, determines if the bit direction is deviated from the PWP, and creates a corrective trajectory to return to the initially planned trajectory when it is necessary. Implicitly, the PWP is essential for the control because it is the reference point for comparing the simulated coordinates. As a result, the PWP function and the Real-Time Trajectory Control are part of the TCO. Figure 6.1 presents this concept in a more explicit manner.

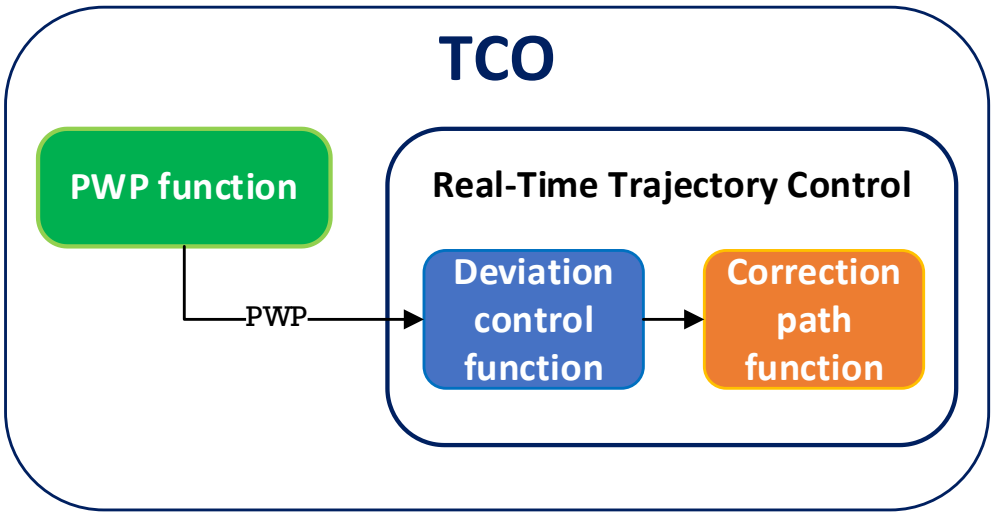

Figure 6.1: TCO Elements

The Real-Time Trajectory Control has two essential functions: The Deviation Control and Correction Path (CP) functions. The first one will be executed at every simulated survey station, as was shown in Figure 3.3. The second function will be called only when the deviation control function detects that the current bit position has deviated.

The objective of the TCO is to ensure to reach (or be close enough to) the target coordinate specified by the user before starting the simulation. The three functions of the TCO work together and sends their results to the RSS Model to set the next bit objective.

6.1 Bit Error Model

Before describing the deviation control, it is required to understand the error model used inside this control function. The error model chosen for the deviation control is the ISCWSA Error Model (Revision 4.3) because the model evaluates the effect of various physical factors that induce some errors in the survey measures and adds uncertainty in the 3D bit position (ISCWSA, 2017b).

The effect of the measured depth, inclination, or azimuth at a specific survey station is evaluated and accumulated with the rest of the individual survey errors to develop a final covariance matrix that gives the final uncertainty in wellbore position (ISCWSA, 2017b). The ISCWSA Error Model analyzes the error according to the type of error involved and quantifies the effect over the directional drilling performance.

The covariance matrix could be used for calculating the ellipse of uncertainty (EOU) in the current survey station, given a confidence level (Adamovitsj, 2020). The EOU is useful for fixing the limits of acceptance of bit deviation if it is compared against the distance from the bit to the closest point on the PWP.

6.1.1 Types of Errors

There are different types of errors in the measuring tools and environments of measurement. The most common classification of error types related to directional surveys is the following (Muhammadali, 2017):

- **Random error:** It is the most natural type of error and the most difficult to predict. The random error act in a random manner that does not follow any frequency to detect it before it happens. To reduce the impact of this error is important to take large amounts of measurements and average out the result. The error will affect the variability of the measure, not the mean value (see Figure 6.2).

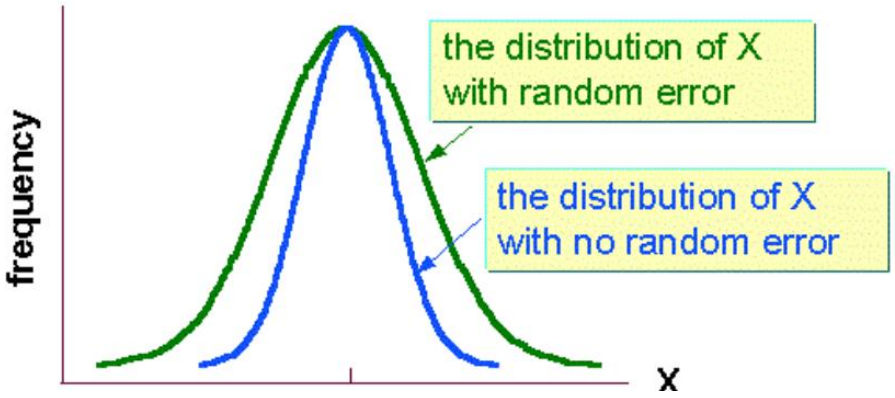

Figure 6.2: Random Error (Trochim, 2006)

- **Systematic error:** It is caused by the system involved in the measurement of the physical parameter. It is a consistent and repeatable error that can be either positive or negative and will be reduced considerably with the calibration of the measurement tools, but it will never be 0. This type of error will affect the mean value of the measurement; this effect is called bias (see Figure 6.3).

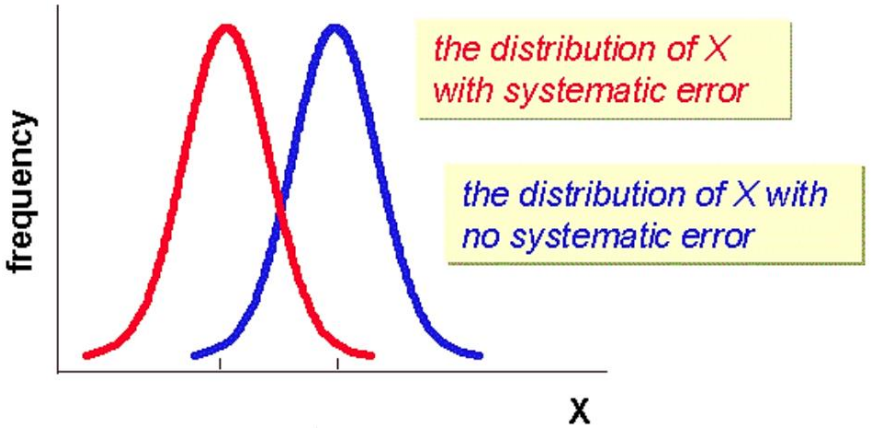

Figure 6.3: Systematic Error (Trochim, 2006)

- **Gross error:** It is a very significant error caused by human negligence and will cause some discrepancies in the measurements. This could happen due to a misunderstanding of the units, operation of the tool, or calculation of parameters with a wrong equation, among other causes.

6.1.2 ISCWSA Error Model Methodology

The purpose of the ISCWSA Error Model is to evaluate the effects and quantify the various factors that might lead to errors in the survey measurements and increment the drilling uncertainty. The errors will be accumulated for each new survey point analyzed and summed to determine the total uncertainty of the wellbore position (Adamovitsj, 2020).

The model has the procedure described in Figure 6.4 that starts with the values established in Table 3.3 and the current survey information like the MD, V, N, E, inclination, and azimuth of the bit. The total covariance matrix produced by the model will be used to calculate the radii of the EOU.

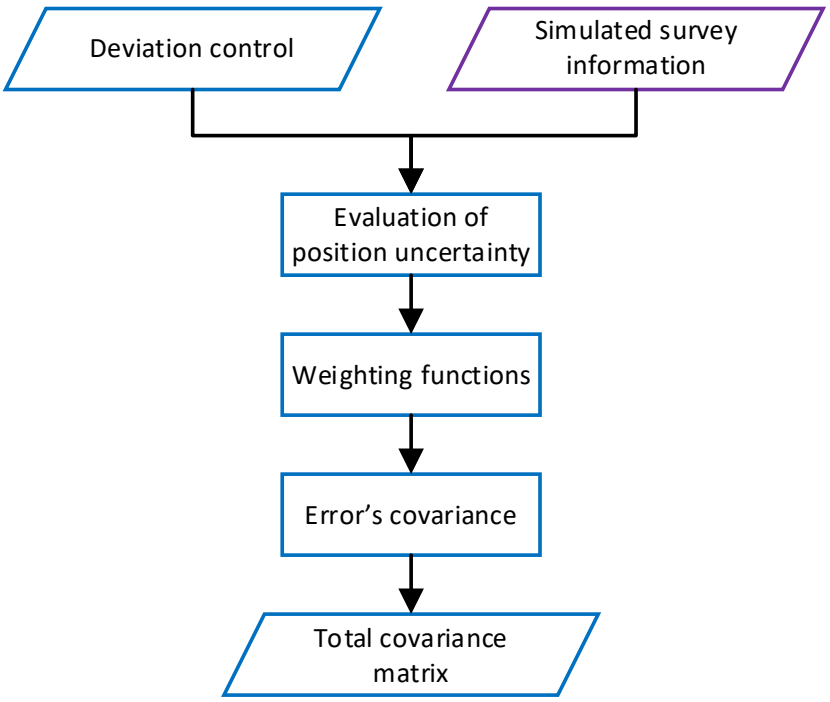

Figure 6.4: ISCWSA Error Model Methodology

The first process of the model is evaluating the position uncertainty regarding the inclination, azimuth, and measured depth of the survey point. The derivation of the following equations can be encountered in the ISCWSA Error Model document itself. Besides, all the equations showed in this chapter are taken from the same source (ISCWSA, 2017b) and the ISCWSA Excel example (ISCWSA, 2016).

The uncertainty in the well position caused by the errors in a survey point is expressed with these 3x3 matrices:

$$\frac{d\Delta r_k}{dp_k} = \frac{1}{2}\begin{bmatrix} \sin\alpha_{k-1}\cos\varphi_{k-1} + \sin\alpha_k\cos\varphi_k & (MD_k - MD_{k-1})\cos\alpha_k\cos\varphi_k & -(MD_k - MD_{k-1})\sin\alpha_k\sin\varphi_k \\ \sin\alpha_{k-1}\sin\varphi_{k-1} + \sin\alpha_k\sin\varphi_k & (MD_k - MD_{k-1})\cos\alpha_k\sin\varphi_k & (MD_k - MD_{k-1})\sin\alpha_k\cos\varphi_k \\ \cos\alpha_{k-1} + \cos\alpha_k & -(MD_k - MD_{k-1})\sin\alpha_k & 0 \end{bmatrix} \quad (6.1)$$

$$\frac{d\Delta r_{k+1}}{dp_k} = \frac{1}{2}\begin{bmatrix} -\sin\alpha_k\cos\varphi_k - \sin\alpha_{k+1}\cos\varphi_{k+1} & (MD_{k+1} - MD_k)\cos\alpha_k\cos\varphi_k & -(MD_{k+1} - MD_k)\sin\alpha_k\sin\varphi_k \\ -\sin\alpha_k\sin\varphi_k - \sin\alpha_{k+1}\sin\varphi_{k+1} & (MD_{k+1} - MD_k)\cos\alpha_k\sin\varphi_k & (MD_{k+1} - MD_k)\sin\alpha_k\cos\varphi_k \\ -\cos\alpha_k - \cos\alpha_{k+1} & -(MD_{k+1} - MD_k)\sin\alpha_k & 0 \end{bmatrix} \quad (6.2)$$

Where:

- $\frac{d\Delta r_k}{dp_k}$ =effect of the errors in the survey measurements in the k station

- $\frac{d\Delta r_{k+1}}{dp_k}$ =effect of the errors in the survey measurements in the $k+1$ station
- k = current survey station
- $k-1$ = last survey station
- $k+1$ = next survey station

The RSS Simulator will approximate the measurements from the $k+1$ survey station since the third survey station after stating the simulation, using the current survey as the $k+1$ station and the last two simulated survey stations as the k and $k-1$ stations.

The next step of the model is to weight the functions according to the observed source and type of error. The ISCWSA model considers plenty of types of errors during the directional drilling measures. However, the present study will consider the following five basic errors related to the depth, inclination, and azimuth:

- Depth Scale Factor – Systematic error ($DSFS$)
- MWD: Z-accelerometer bias error – Systematic error (ABZ)
- MWD: Z-accelerometer scale error – Systematic error (ASZ)
- MWD: TF Ind: X and Y magnetometer bias – Systematic error ($MBXY1$)
- MWD: RF Ind: X and Y magnetometer scale factor – Systematic error ($MSXY1$)

All the errors chosen are systematic since they are repetitive and imply some possible tool inaccuracies that might happen in the real world. It was decided not to include more types of errors from the ISCWSA model because the application of the rest of the errors would imply more profound studies beyond the scope of the thesis.

The correspondent equations matrix for weighting (W) each of the five errors are the following:

$$W_{DSFS} = [MD \quad 0 \quad 0] \tag{6.3}$$

$$W_{ABZ} = \left[0 \quad -\frac{\sin\alpha}{G} \quad \frac{\tan Dip \cdot \sin\alpha \cdot \sin\varphi}{G}\right] \tag{6.4}$$

$$W_{ASZ} = [0 \quad -\sin\alpha \cdot \cos\alpha \quad \tan Dip \cdot \sin\alpha \cdot \cos\alpha \cdot \sin\varphi] \tag{6.5}$$

$$W_{MBXY1} = \left[0 \quad 0 \quad \frac{-\cos\alpha \cdot \sin\varphi}{MF \cdot \cos Dip}\right] \tag{6.6}$$

$$W_{MSXY1} = \left[0 \quad 0 \quad \frac{\sin\alpha \cdot \sin\varphi\ (\tan Dip \cdot \cos\alpha + \sin\alpha \cdot \cos\varphi)}{\sqrt{2}}\right] \tag{6.7}$$

Where:

- W = weighted function
- G = gravity $\left[{}^{m}/_{s^2}\right]$
- Dip = magnetic dip angle [°]
- MF = total magnetic field $[nT]$

Using the procedure in the ISCWSA Excel example, the covariance matrix can be obtained from the error's vectors calculation e and e^*. The covariance matrix is expressed in the North, East, and Vertical axes.

The covariance matrix will be used later to calculate the radii of the ellipses of uncertainty at each

survey station. The covariance matrix has the following form:

$$Cov_{total} = \begin{bmatrix} {\sigma_N}^2 & Cov(N,E) & Cov(N,V) \\ Cov(N,E) & {\sigma_E}^2 & Cov(E,V) \\ Cov(N,V) & Cov(E,V) & {\sigma_V}^2 \end{bmatrix} \quad (6.8)$$

Where:

- σ_N = variance in the north-axis
- σ_E = variance in the east-axis
- σ_V = variance in the vertical axis
- Cov = covariance
- Cov_{total} = total covariance

6.2 Deviation Control

The Deviation Control will apply the bit error model explained before along with the Ellipses of Uncertainty (EOU) and the calculation of a 3D space vector to determine if the simulated bit trajectory is close enough to the PWP or if it needs to be corrected through the change of the directional parameters. The control works with the results from two functions: the PWP from the PWP function and the simulated bit position parameters from the RSS Model function.

Besides, every time the current MD from the simulation reaches the planned survey station, the RSS Simulator performs these special tasks:

- Request new variables from the external modules (variables from Table 3.5).
- Add noise to the new external parameters using Eq. (3.1).
- Run the deviation control function with the current simulated parameters and the PWP.

The first and second tasks are not as vital as the last one because if no new parameters are used, then the last parameters would be still used for the rest of the simulation, which would affect only the uncertainty factor added to the simulator, but not in the structure of it.

In contrast, when the control deviation is deactivated, the simulation will still be running and reaching a final coordinate, but this final coordinate might not be close to the target coordinate. Consequently, the Deviation Control is essential for monitoring the simulation results in real-time, allowing to add a higher probability to reach the target coordinate at the end of the simulation.

The Deviation Control has two groups of functions: the calculation of the Vector of Error (VOE) and the calculation of the Ellipse of Uncertainty (EOU). Both are necessary to create a conditional situation whose result will define if the correction is applied or it is not needed yet.

The Deviation Control function starts by receiving the current bit location drilling parameters like the MD, inclination, azimuth, and coordinates (V, N, E). Moreover, the parameters described in Table 3.3 and the PWP matrix are necessary to have a complete system to compare.

The first step of the deviation control is calculating the ISCWSA Error Model to obtain the total covariance matrix. Later the matrix is used to calculate the radii of the EOU of the actual simulated survey point, and the VOE is obtained using vectorial mechanical analysis. The last step is to compare the lengths of the VOE with the vector formed from to bit position to the EOU radius following the same direction of the VOE.

According to the comparison result, the deviation control will call or execute the Correction Path function or let the simulator continue with the next simulation iteration. The whole described process can be observed in the simple flowchart of Figure 6.5.

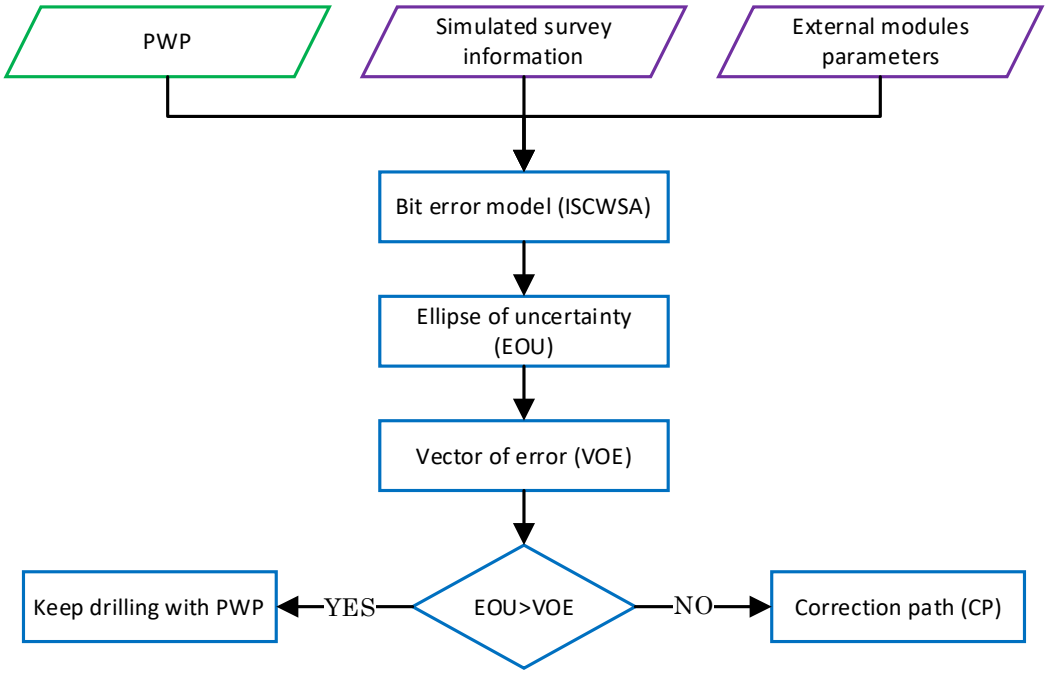

Figure 6.5: Deviation Control Flowchart for Each Survey Station

6.2.1 Ellipse of Uncertainty

The Ellipse of Uncertainty (EOU) is used to quantify the present area of the uncertainty of a specific survey point caused by the errors in the measures made in the directional operation. The inclination error adds a high side dimension, the azimuth error a lateral dimension, and the measured depth error an axis along the wellbore trajectory (Adamovitsj, 2020).

The uncertainty analysis helps to reduce the cost and provides a safe environment for effective and sustainable drilling. Moreover, the EOU radius increases as the depth increments because the uncertainties accumulate at each survey station (Muhammadali, 2017).

The magnitude of the ellipse is in the function of its confidence level expressed by the standard deviation, which assumes that the errors follow a standard distribution. The standard deviations (SD_{EOU}) for different confidence levels and dimensions of the ellipse of uncertainties are shown in Table 6.1.

Table 6.1: Confidence Level for EOU (ISCWSA, 2013)

Probability	**Confidence Level**				
Dimension	68.3%	90.0%	95.0%	99.0%	99.7%
1	0.9999	1.5448	1.9599	2.5758	2.9677
2	1.5151	2.1459	2.4477	3.0348	3.4086
3	1.8779	2.5002	2.7954	3.3682	3.7325

Using the total covariance matrix from Eq. (6.8) and the Eigenvalues applied to the matrix is possible to calculate the major and minor axes of the EOU. However, due to the error model involves a 3D environment, the axes obtained in this case are the major, minor, and height of the ellipsoid of uncertainty. The matrix has the following form (Adamovitsj, 2020):

$$\begin{bmatrix} {\sigma_N}^2 - \lambda_N & Cov(N,E) & Cov(N,V) \\ Cov(N,E) & {\sigma_E}^2 - \lambda_E & Cov(E,V) \\ Cov(N,V) & Cov(E,V) & {\sigma_V}^2 - \lambda_V \end{bmatrix} = 0 \tag{6.9}$$

Where:

- $\lambda =$ Eigenvalue

After solving the three Eigenvalues computationally, it is possible to obtain the three radii using the following equations (Adamovitsj, 2020):

$$R_N = SD_{EOU} \cdot \sqrt{\lambda_N} \tag{6.10}$$

$$R_E = SD_{EOU} \cdot \sqrt{\lambda_E} \tag{6.11}$$

$$R_V = SD_{EOU} \cdot \sqrt{\lambda_V} \tag{6.12}$$

Where:

- $R =$ radius of the ellipse in the correspondent axis

Despite there are three radii, the Deviation Control only uses two of them (North and East) since it works with an ellipse instead of an ellipsoid. The reason for this choice is the utilization of the ellipses in the simulation trajectory. Since the Deviation Control will use a space vector later, there is no necessity to determine the height uncertainty of the ellipsoid because the space vector will take the same direction of the orthogonal plane to the simulated trajectory where the ellipse is positioned (Figure 6.6).

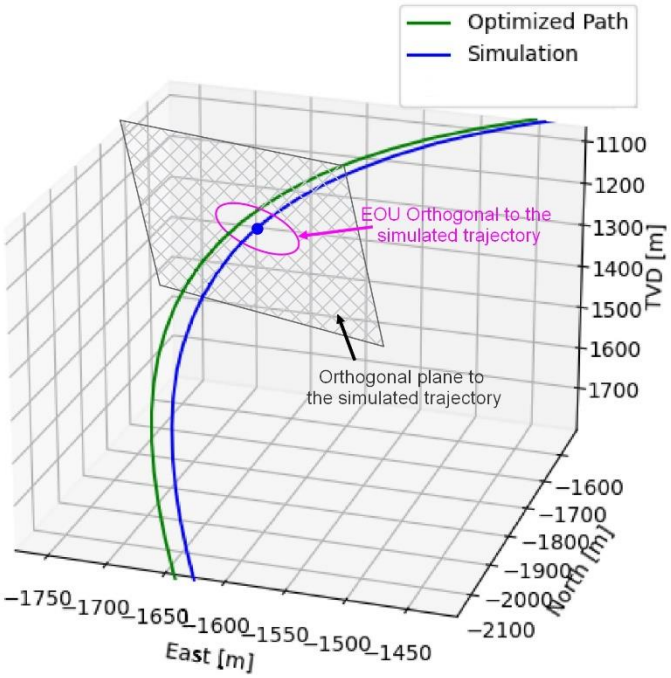

Figure 6.6: EOU Orthogonal Plane Example

As a result, the Deviation Control works only with the R_N and R_E and for simplicity of computational methods, the larger radius between the two is considered as the semi-major axis and the other as the semi-minor axis of the EOU.

6.2.2 Vector of Error

The Vector of Error (VOE) is a 3D vector that starts in the actual bit position on the simulated trajectory and ends in the closest orthogonal point in the PWP trajectory. The module or length of this vector represents the distance from the bit to the perpendicular direction towards the planned trajectory. The distance is the main factor to compare against the EOU radius vector, and it will define the situation of the deviation of the well.

The challenging part of the calculation of this vector is to find the orthogonal direction from some coordinates known. The data necessary for the obtention of the VOE are the current and previous bit position and two survey points (one ahead and one behind the bit position) on the PWP. Both sets of coordinates can be gotten from the simulation results and the PWP matrix, respectively.

Figure 6.7 and Figure 6.8 help visualize the procedure of the VOE function calculation. The bit vector (from the previous to the actual bit coordinate) has an azimuth and an inclination since the bit has a direction at that time. Consequently, it is possible to obtain a perpendicular plane (pink line) to the direction of the blue vector using a third space coordinate situated on the perpendicular plane.

The plane has to be rotated 90° to the azimuth of the bit vector; thus, the reference point for the rotation on the plane is the middle part (pink dash line).

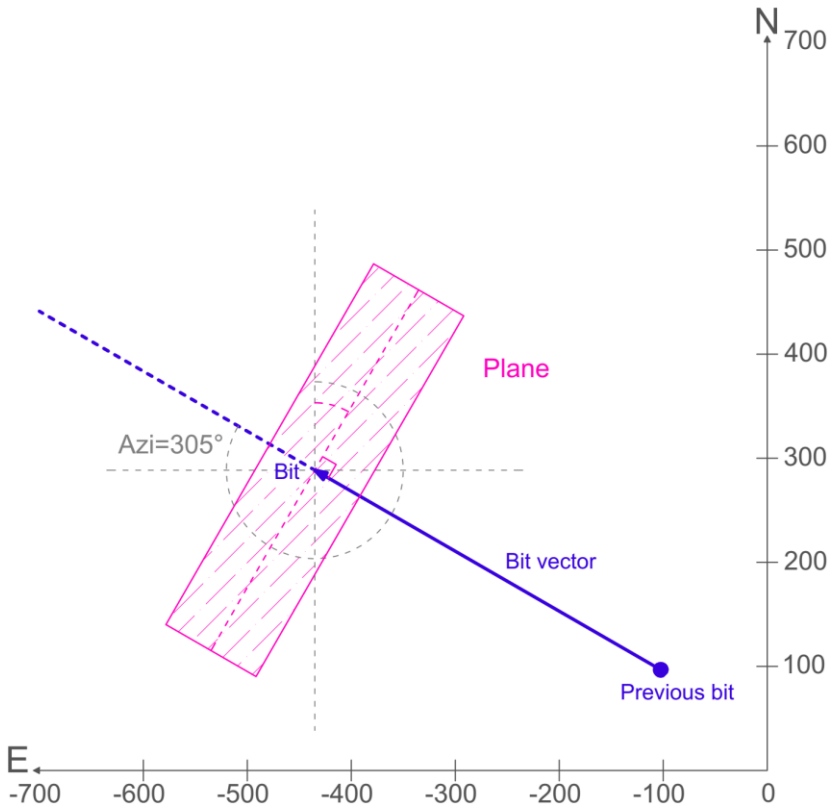

Figure 6.7: Perpendicular Plane in the Azimuth View

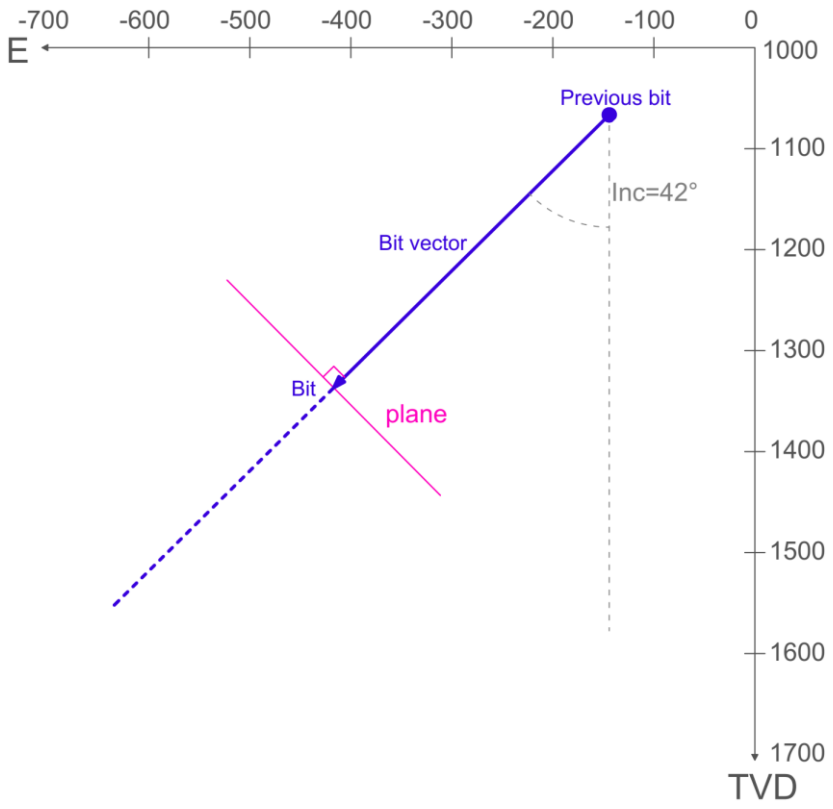

Figure 6.8: Perpendicular Plane in the Inclination View

The principle behind using an imaginary plane is to obtain the equation of the correspondent infinite plane and the search for the intersection coordinate between the plane and a second vector (PWP vector) that crosses that plane. The head of the bit vector and that intersection point will create a third vector, called Vector of Error (VOE), located on the perpendicular plane and will have an orthogonal direction with respect to the bit direction.

The first point for the function is to establish the coordinates positions of the bit survey stations and the correspondent PWP survey stations, to form the bit (blue line) and the PWP (red line) vectors, respectively (see Figure 6.9).

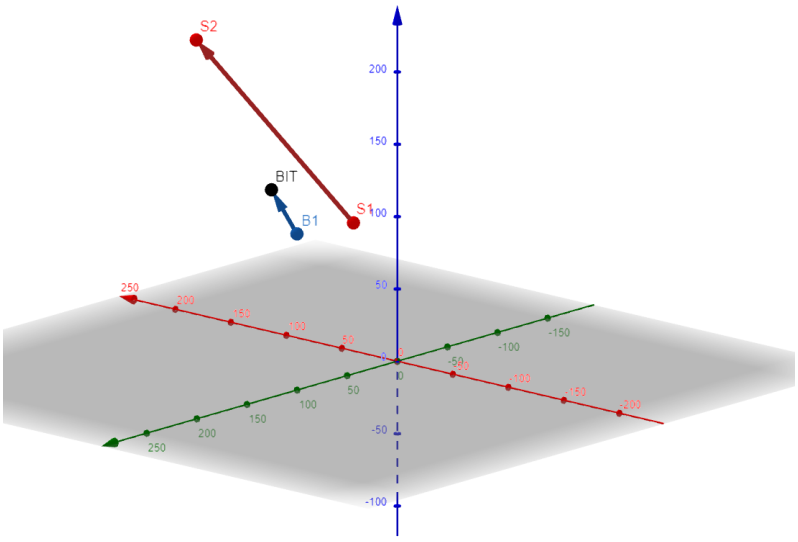

Figure 6.9: Bit and PWP Vectors (Z-axis is inverse to TVD)

Both vectors are obtained with the following equations:

$$\vec{B} = [x_{bit} - x_{b1} \quad y_{bit} - y_{b1} \quad z_{bit} - z_{b1}] \tag{6.13}$$

$$\vec{S} = [x_{s2} - x_{s1} \quad y_{s2} - y_{s1} \quad z_{s2} - z_{s1}] \tag{6.14}$$

Where:

- $\vec{B}$ = bit vector $[m]$
- $\vec{S}$ = PWP vector $[m]$
- x = east coordinate $[m]$
- y = north coordinate $[m]$
- z = vertical coordinate $[m]$
- bit = current bit coordinates (E, N, V)
- $b1$ = previous bit coordinates (E, N, V)
- $s2$ = coordinates (E, N, V) of PWP survey point ahead the bit $[m]$
- $s1$ = coordinates (E, N, V) of PWP survey point behind the bit $[m]$

The next part is to generate a point that belongs to the perpendicular plane to the $\vec{B}$ located in the bit coordinate (see Figure 6.10). The most straightforward point to generate is anyone located on the perpendicular middle line azimuth (pink dash line in Figure 6.7), which involves that the depth of this point ($P0$) can be equal to the depth of the bit coordinate. Using Eq. (2.4) to (2.6) is possible to obtain 3D coordinates with a random MD distance (e.g., 100 m).

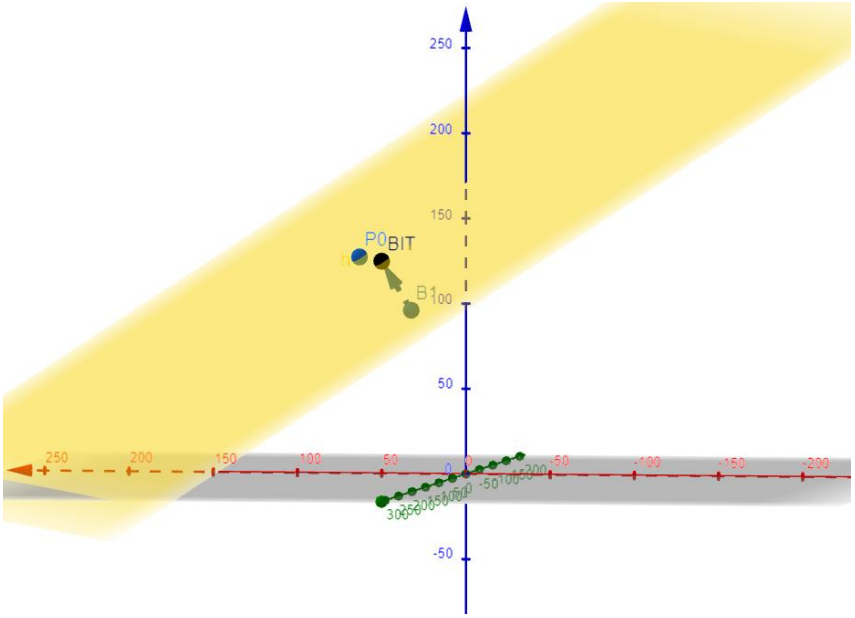

Figure 6.10: Perpendicular Plane to the Bit Formed with 3 Space Points (Z-axis is inverse to TVD)

The equation of the plane is the following:

$$A(x - x_0) + B(y - y_0) + C(z - z_0) + D = 0 \tag{6.15}$$

Where:

- A = X component of the bit vector $[m]$

- $B =$ Y component of the bit vector $[m]$
- $C =$ Z component of the bit vector $[m]$
- $D =$ Scalar number $[m]$
- $0 =$ components from the $P0$ point $[m]$

The value of D can be obtained with the dot product between the $\vec{B}$ and $P0$, like:

$$D = -\left(\vec{B} \cdot P0\right) \tag{6.16}$$

Then the plane equation of Eq. (6.15) can be obtained in the following way:

$$\frac{A}{\|\vec{B}\|}x + \frac{B}{\|\vec{B}\|}y + \frac{C}{\|\vec{B}\|}y + \frac{D}{\|\vec{B}\|} = 0 \tag{6.17}$$

With the equation of the plain obtained, the next step is to get the coordinates of the intersection point (IP) between the plane and $\vec{S}$ using the parametric form of a line:

$$IP = s1 + t \cdot u_S \tag{6.18}$$

$$u_s = \frac{\vec{S}}{\|\vec{S}\|} \tag{6.19}$$

$$t = \frac{-\left(A \cdot s1_x + B \cdot s1_y + C \cdot s1_z + D\right)}{A \cdot u_{s_x} + A \cdot u_{s_y} + A \cdot u_{s_z}} \tag{6.20}$$

Where:

- $IP =$ intersection point on the $\vec{S}$ and the plane $[m]$
- $t =$ scalar factor $[m]$
- $u_s =$ unit vector of $\vec{S}$ (E, N, V) $[m]$

Finally, the resultant vector (Vector of Error) from the bit to the closer orthogonal point on the PWP is obtained with the following equation:

$$\overrightarrow{VOE} = [IP_x - x_{bit} \quad IP_y - y_{bit} \quad IP_z - z_{bit}] \tag{6.21}$$

Where:

- $\overrightarrow{VOE} =$ Vector of Error $[m]$

The distance from the VOE is obtained from the module of the vector ($\left|\overrightarrow{VOE}\right|$) and this value is significant since it will be the one that is compared with the length of the vector of the EOU. The VOE concept looks like Figure 6.11 in a tridimensional space.

Besides, the inclination and the azimuth can be calculated from the VOE because it is a 3D vector with a direction. Those parameters will be useful for calculating a vector from the bit to the perimeter of the EOU, explained later.

This methodology is applied at each simulated survey point where the bit is supposed to be located and works in any section of the trajectory of the well.

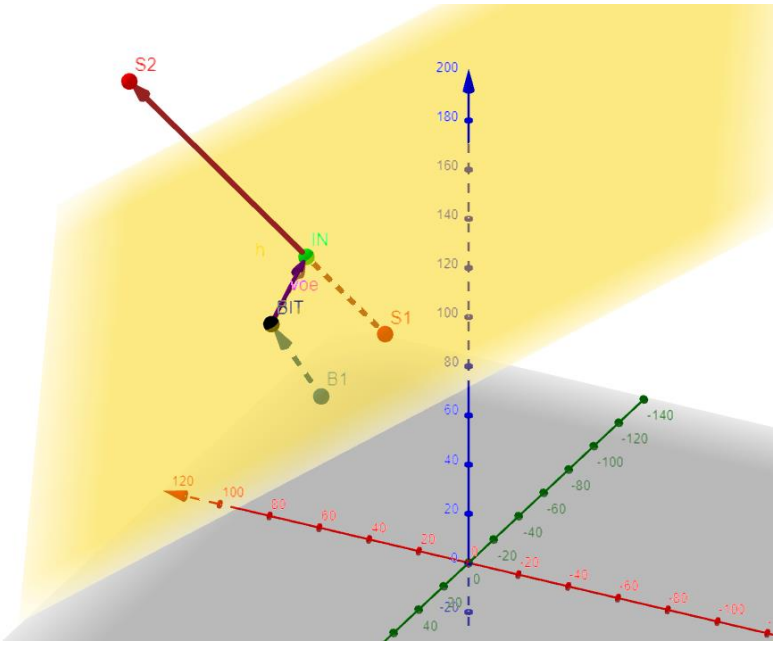

Figure 6.11: Vector of Error Concept (Z-axis is inverse to TVD)

6.2.3 Closed-Loop Implementation

Both parts of the Real-Time Trajectory Control work interconnected for achieving the final or principal target coordinate at the end of the simulation. For this purpose, the way of operating utilizes a closed-loop philosophy that involves analyzing the output of the simulation and adjusting the input for the next iteration frequently.

Implementing the closed-loop structure can be very intricated, depending on how many variables must be controlled. Nevertheless, the closed-loop structure implemented in the RSS Simulator has been designed to control only two parameters: the current bit distance to the PWP and the bit direction. The theoretical closed-loop structure is presented in Figure 6.12, which includes the disturbances generated randomly by the noise added with Eq. (3.1) to create a more realistic simulation environment.

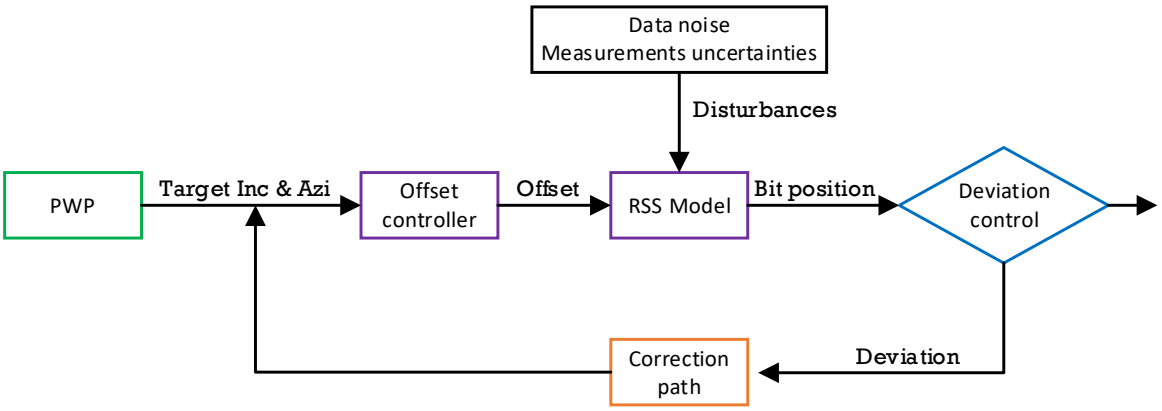

Figure 6.12: Closed-Loop Implementation in the RSS Simulator

The target inclination and azimuth are the variables that will be dynamically changing each time a new section of the well path is reached. However, they also must function as the directions to implement the correction path if the bit deviates. For this reason, the RSS Simulator main algorithm uses “neutral” variables for the target inclination and azimuth information. The variable is filled with the PWP

information when the drilling is going as planned. However, when a deviation is detected, then the algorithm changes the source of recompilation for these neutral variables to be filled with the information from the correction path function until the path returns to the PWP again.

Moreover, the offset controller only cares about receiving the neutral variables, and it interprets their instructions to be sent to the RSS Model. The last model simulates the drilling, using the offset established by the offset controller and working with the rest of the parameters, including the disturbances or noises. Then the bit position simulated is analyzed by the Deviation Control based on the location of the bit and its direction. The Deviation Control will either let it pass to the next simulation or correct the target parameters according to the calculations made in the Correction Path function.

The simplicity of the selection of the target information source makes the RSS Simulator have high flexibility to adapt to have more functionalities in the future since they will not affect the structure of the feedback part of the closed-loop, they will still be based on the location and direction of the bit after the last point simulated.

6.3 Correction Path

The Correction Path (CP) is the last function inside the TCO; it has the main objective of creating a temporary corrective trajectory starting in the actual bit location and reaching some survey station of the PWP in the quickest and least tortuous manner. The CP function creates a small set of temporal survey stations with their coordinates, MD, inclinations, azimuths, and DLS that will be considered a temporal target for the offset controller and, consequently, for the simulation.

The operation of the CP function is described in Figure 6.13, which starts by receiving the actual bit position coordinates, the PWP data survey points, and the DLS and tortuosity constraints previously set by the user.

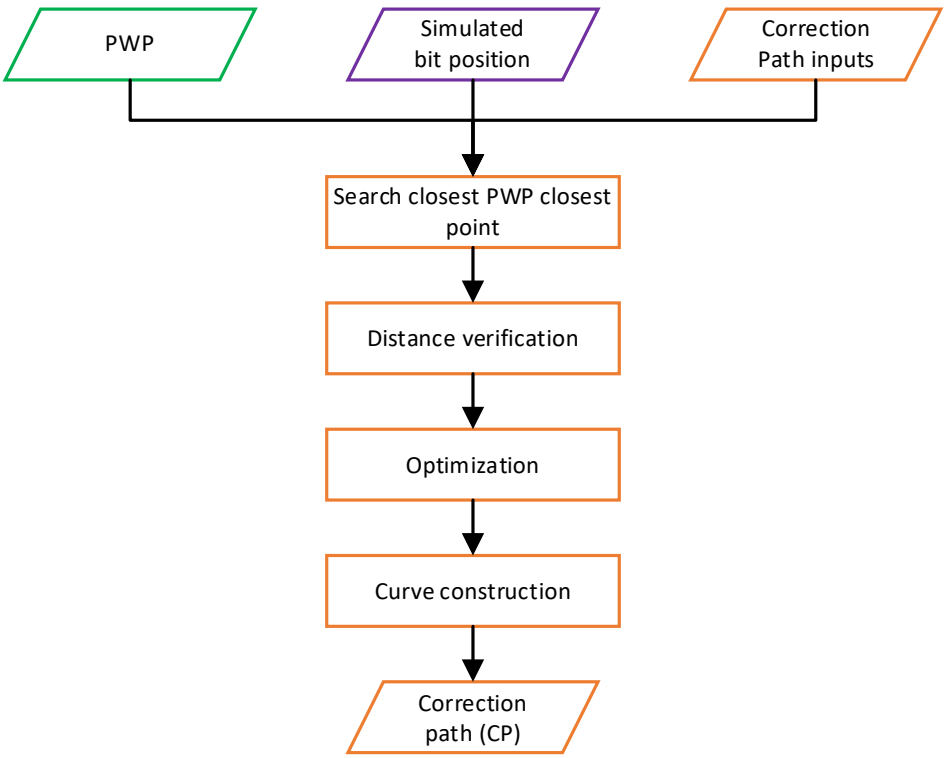

Figure 6.13: Correction Path Function Flowchart

The first process for the correction is to search for the closest point on the PWP that is ahead of the bit coordinate through a minimization process using the PWP survey points and the current bit position. Once the initial survey point has been chosen, the CP function will perform some calculations (explained in the next part) to choose the CP's end point. In other words, the CP searches for the PWP survey point to reach achieving the user conditions.

When the shortest path is found, which does not surpass the maximum DLS and tortuosity defined by the user, the data is transferred to the cubic Beziér curve algorithm to create a curved well path that returns to the original PWP at the reach point.

6.3.1 Reach Point Selection

The reaching point on the PWP plays an important role in the Correction Path since it represents the end point for the corrective trajectory. As a result, the selection of this point should be made carefully because if it is too close to the actual bit coordinate, it may create a sharp curvature with a high DLS. On the contrary, if the reach point is too far from the bit location, it might increase the cost of the operations or drill through a non-planned zone that could cause some problems.

As Figure 6.13 indicated, the first operation is to find the closest survey station from the PWP ahead of the bit coordinate. For this purpose, the algorithm minimizes the distance from the bit to all the PWP survey points to find the one that forms a minimum distance between points. The point encountered is called the “close point”, and its inclination and azimuth are saved for the next process.

Using the bit and close point’s inclinations and azimuths is possible to calculate the DL using Eq. (2.1). Besides, if the DL is divided by the maximum DLS ($Max_{DLS\ Corr}$) established by the user, the distance or the arc length can be obtained. This distance is the minimum distance to create a curvature that respects the $Max_{DLS\ Corr}$, and it is compared with the straight distance between both coordinates (the bit and the close point).

If the minimum distance to create a curvature is higher than the distance between the coordinates, it means that there is not enough space to create a curvature that respects the conditions introduced. As a result, the CP function chooses the next PWP survey station and iteratively performs the same operation until the minimum distance for a curve is less than the straight distance between the bit and the iterated survey station.

The next step is to enhance the curvature quality using the cubic Beziér curves algorithm, explained before, to construct a smoother curve that reaches the PWP. That is to say, an optimization of the corrective curvature design is needed.

The optimization of the Correction Path works similarly to the already described optimization of the PWP function. However, in this case, the optimization is based on one more constrain which is the maximum tortuosity ($Tor_{Max\ Corr}$) set by the user. The optimization tries to find the best combination of the d_s and d_e, used in the Beziér curve calculation that accomplishes the following conditions:

- Do not generate a curve with a DLS superior to the maximum DLS ($Max_{DLS\ Corr}$).
- Create a trajectory with a tortuosity lower than the maximum tortuosity ($Tor_{Max\ Corr}$).
- Build a curvature with the lowest MD that respects the previous two conditions.

The algorithm in charge of the optimization tries different combinations of the d_s and d_e inside a range, that first achieves the DLS condition. Once some promising values have been found, the algorithm

calculates its tortuosity with Eq. (2.3) and determines if it is less than the maximum tortuosity. If there are many candidates, then the third condition is applied, and the one with the lowest MD is chosen as the ideal correction path.

Nevertheless, it might happen that with the bit coordinate and the point chosen on the PWP, that meets the condition of having a minimum distance to create a curvature, one or any of the conditions are not achieved. Therefore, the CP function will look for the next PWP survey station and apply the Beziér optimization until finding a reach point that satisfies the three conditions, and this value will be used to build the correction path curvature.

Figure 6.14 is an example of the procedure just explained, where the first point is the "close point". Since the distance between the bit and this point is not enough to create a curve, the CP function needs to find another further point.

The second point is the one with a minimum distance to build a curvature, it might have a curve with a DLS less than the maximum, but the tortuosity is too much and will not be a good choice for the integrity of the well path.

Finally, the CP function finds the third point, which is the optimized reach point to join the PWP. Using this point, the correction trajectory achieves all the conditions mentioned before. At the same time, the projected trajectories for each point are presented, and it is evident which one is the smoothest and less torturous.

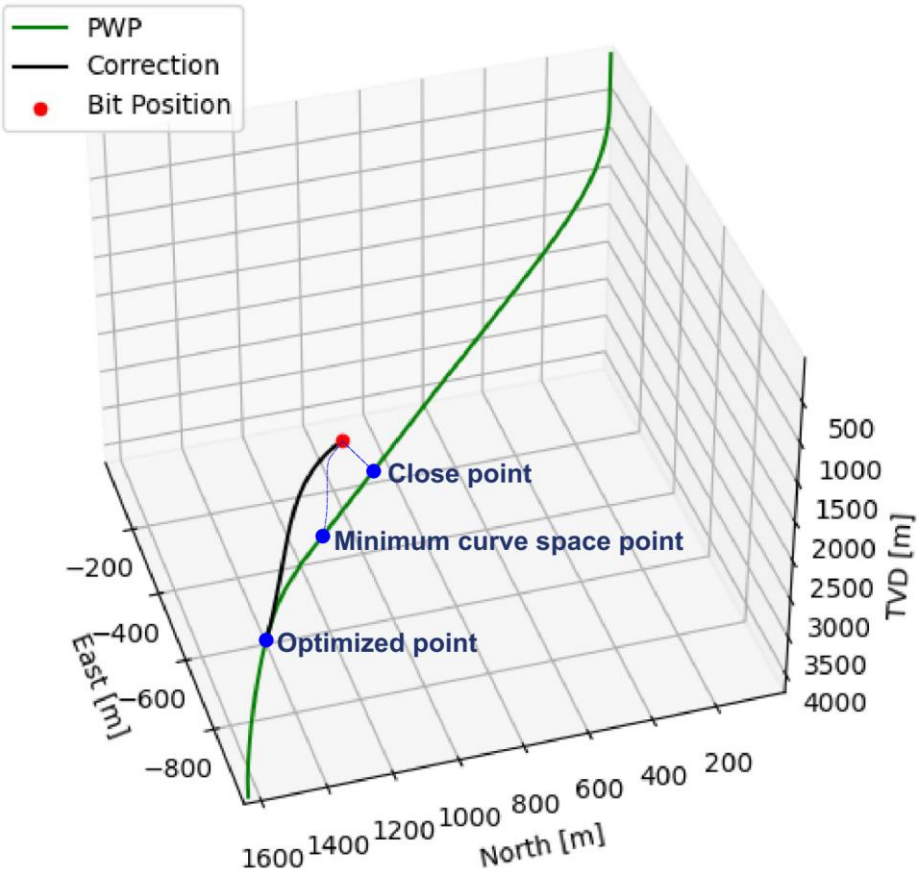

Figure 6.14: Correction Path Optimization Process

6.3.2 Construction of the Correction Path

The description of the reaching point selection finished with the selection of the optimized point for being the common point to rejoin the original trajectory plan. For this objective, the reach point used the Beziér curves algorithm. Nevertheless, the optimization should be fast and should not expend too many computational resources. Consequently, the step, or more precisely, the u value for the Beziér equation, Eq. (4.1), has been set as 0.05, which will give 20 survey points every time a new trajectory is built for being evaluated during the optimization process.

On the contrary, the number of survey points created for the final CP must be more prominent to generate a more detailed curvature. As a result, a new u value is used for the CP, and it is requested by the user at the beginning of the simulation. The u value for the correction path is called $Step_{u\ Corr}$ and it must be a smaller number than 0.05.

The construction of the correction path uses the same Beziér curve methodology with the start point equal to the actual bit coordinate, the end point is the optimized reach point, and the attractor points are the ones calculated for the optimized reach point. All these data are introduced in Eq. (4.1) to (4.13) to generate the CP survey points, as shown in Figure 6.15, where the case a) is the CP profile view, the case b) is the CP superior view.

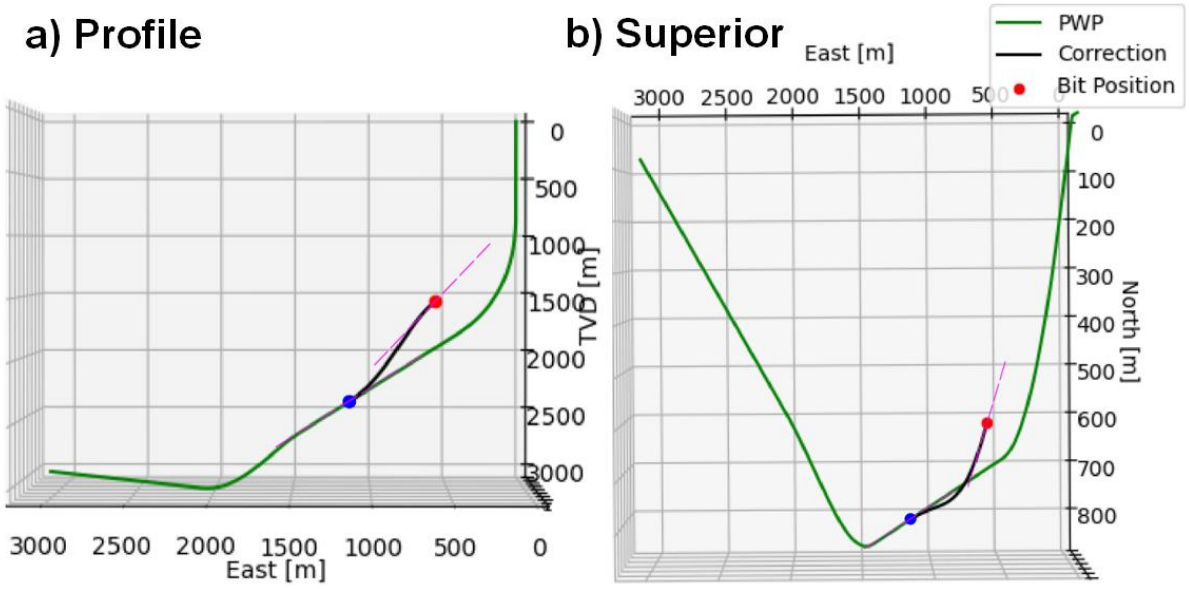

Figure 6.15: Correction Path Inclination and Azimuth

The last figure also shows the difference between the bit and the reach point's inclinations and azimuths (pink lines). As a result, the CP function should change the actual bit's inclination and azimuth into the same inclination and azimuth value of the reach point on the PWP.

The CP function will return a CP matrix with the survey stations that form the curve with their correspondent coordinate, inclination, azimuth, MD, and DLS. The inclination and azimuth are very relevant for the correction because they will be considered the target values that the offset controller needs to reach in the next simulation iteration.

While simulating the CP, the Deviation Control will still verify if the bit follows the CP or if there is the necessity of making a correction of the CP, and another temporal correction trajectory will be generated and considered as the new valid CP to return to the PWP.

6.3.2.1 Limitations and Exceptions

The CP function has some limitations for finding the Correction Path depending on the bit position and direction, and the shape of the PWP. There might be extremes cases where the bit is too far from the PWP because the user was too lenient with the Deviation Control parameters, and the Correction Path cannot be found.

However, if the user sets reasonable deviation control parameters, the bit will be corrected when it is not at a considerable distance from the PWP. Moreover, some other situations might affect the performance of the CP function. Some examples of these situations could be:

- The space for building the curvature is not enough because the minimum distance to the curve construction is more than the available straight distance between the points evaluated.
- The maximum DLS set by the user is too low that any curvature evaluated could achieve a design with a lower DLS.
- The maximum tortuosity value chosen by the user is too small that any trajectory evaluated produces a path with a lower tortuosity value.

Although these exceptions would compromise the CP, they are very unusual, and they could be corrected with a little higher set value of $Max_{DLS\ Corr}$ and/or $Tor_{Max\ Corr}$ from the user.

When the Deviation Control and the Correction Path function have reasonable values for their constrained parameters, the RSS Simulator will correct the trajectory as earlier as needed and avoid having more complicated situations to correct later.

7 Study Cases

The potential of the RSS Simulator can be tested through the simulation of real drilled wells. These wells have their directional drilling plan already concluded, and the initial survey stations can be inferred from it. As a result, this chapter is going to run two simulations in the RSS Simulator Version 2.3 (V2.3), one of them has a 3D trajectory, and the other can be assumed as a 2D trajectory.

It is important to mention that the source of the data for both cases is extracted from the ISCWSA Excel example uploaded on their web page for evaluating clearance scenarios (ISCWSA, 2017a). The Excel file has many well trajectories; the study cases are well 02 and well 03.

Moreover, the interpretation or significance of the results and plots will be given in the following chapter.

7.1 3D Trajectory Case

The 3D case simulated is a well that has a build-up curvature that also changes in the walk rate to finish with an inclination of 85° and azimuth of 190°. The well starts in the origin, used as a reference point, and the target coordinate has a TVD of 1915.22 m, East of -103.74 m and North of -1312.12 m.

As a result, the well trajectory goes to the South-West direction with a vertical section from 0 to 990 m (MD), a curved section from 990 to 2243 m (MD) and a final hold section from 2243 to 2774 m (MD). In addition, the azimuth starts with 175° at the beginning of the curve and finishes with an azimuth equal to 190°.

The most relevant input data used for configuring the simulator is resumed in Table 7.1, and the 95 well survey stations data are available in the Appendix B (see Figure 7.1).

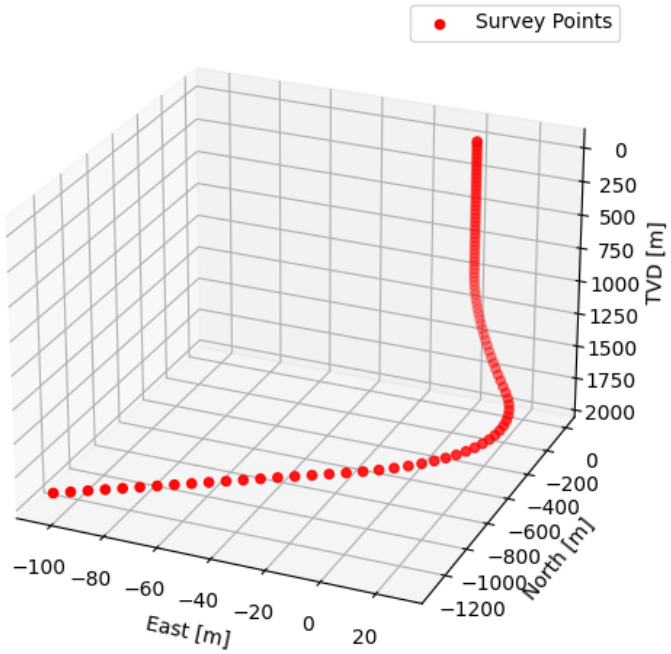

Figure 7.1: Survey Stations Disposition for 3D Case

The well curvature could be optimized according to the maximum DLS allowable. Also, the azimuth changes more than once, which makes the situation more challenging for the simulation.

Table 7.1: Relevant Input Data Used in the 3D Simulation

Parameter	Symbol	Value
Tolerance for considering two different segments	$Tolerance$	0.5°
Range tolerance for searching for the best D_S and D_E value	Ran_{Tol}	300 m
Maximum DLS for the PWP	Max_{DLS}	5.5°/30m
Time step for the Simulation (Resolution)	Δt	60 s
OD of the RSS tool	OD	0.080 m
ID of the RSS tool	ID	0.037 m
Distance actuator - bit	a	0.5 m
Distance actuator - stabilizer	b	2.7 m
Borehole diameter	Db	0.31115 m
Error Noise that will be added to the other modules data	$Error_{input}$	0.1
Maximum opening offset of the tool (0% to 100%)	$maxoff$	0.9
Maximum physical opening of the offset	$Offset_L$	0.006 m
Total magnetic field	MF	50000 nT
Magnetic dip angle	Dip	72°
Standard deviation used in the Ellipse of Uncertainty	SF	2.6
Depth Scale Factor – Systematic error	L_DSFS	0.00056
MWD: Z-Accelerometer Bias Error – Systematic error	L_ABZ	0.004 m/s2
MWD: Z-Accelerometer Scale Error – Systematic error	L_ASZ	0.0005
MWD: TF Ind: X and Y Magnetometer Bias – Systematic error	L_MBXY1	70 nT
MWD: RF Ind: X and Y Magnetometer Scale Factor – Systematic error	L_MSXY1	0.0016
Minimum radius of EOU	Min_R	1 m
Maximum DLS that could be applied to the curve	$Max_{DLS\,Corr}$	6°/30m
Maximum tortuosity that could be applied to the curve	$Tor_{Max\,Corr}$	3°/30m

The $Error_{input}$ will add some uncertainty and noise to the variables from Table 3.5 that come from the external modules. Also, the $maxoff$ is 0.9 which means that the BHA tool actuator is opening only 90% of its total opening capacity; this will affect the curvature section of the well. Moreover, the L_DSFS, L_ABZ, L_ASZ, L_MBXY1 and L_MSXY1 are taken from the ISCWSA Excel example (ISCWSA, 2016).

7.1.1 TCO Results

The results for the TCO part are expressed in the PWP table and the Deviation Control table that can be read in the Appendix B (because of their large data quantity). However, a more dynamic way to

understand the results is with the plots generated by the RSS Simulator, presented in different perspectives in Figure 7.2 and Figure 7.3. Furthermore, the green line represents the PWP that was initially based on the survey stations (red dots), and the blue line is the final simulation trajectory that the RSS Model built following the instructions and deviation correction of the TCO.

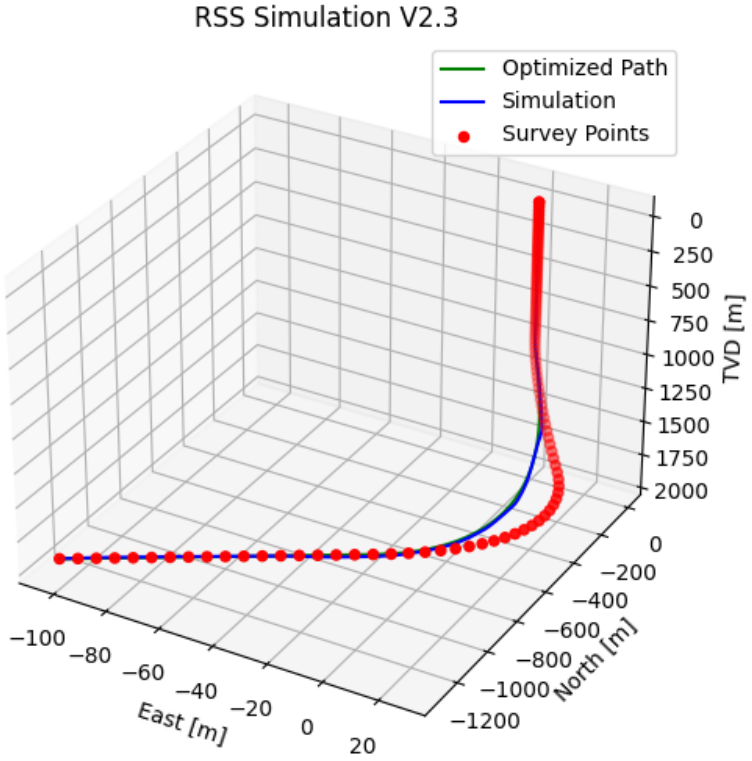

Figure 7.2: RSS Simulation 3D Trajectory General View 1

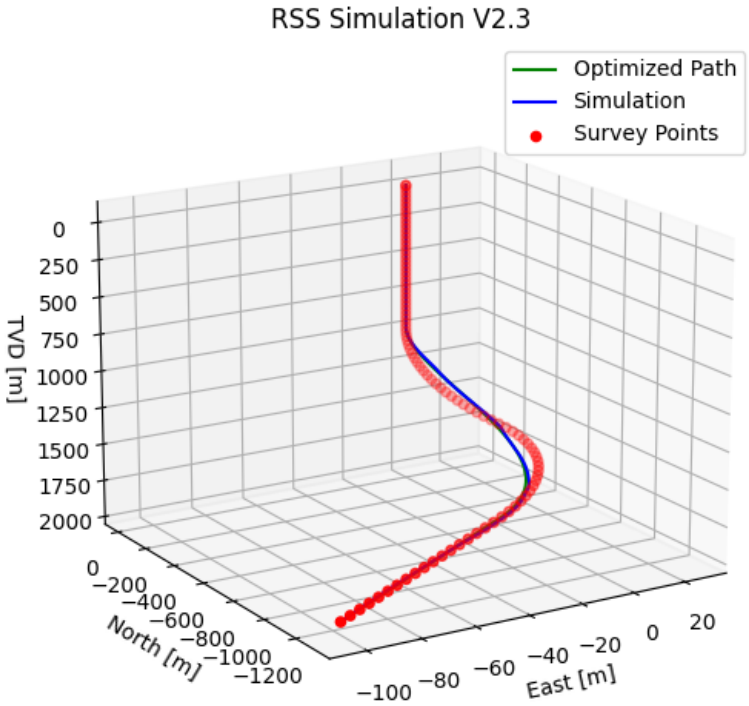

Figure 7.3: RSS Simulation 3D Trajectory General View 2

The profile and the superior view of the simulated trajectory are seen in Figure 7.4 and Figure 7.5, respectively. Both figures show how the RSS Simulator optimized the curvature of the original plan, which might have saved time and money in the actual project.

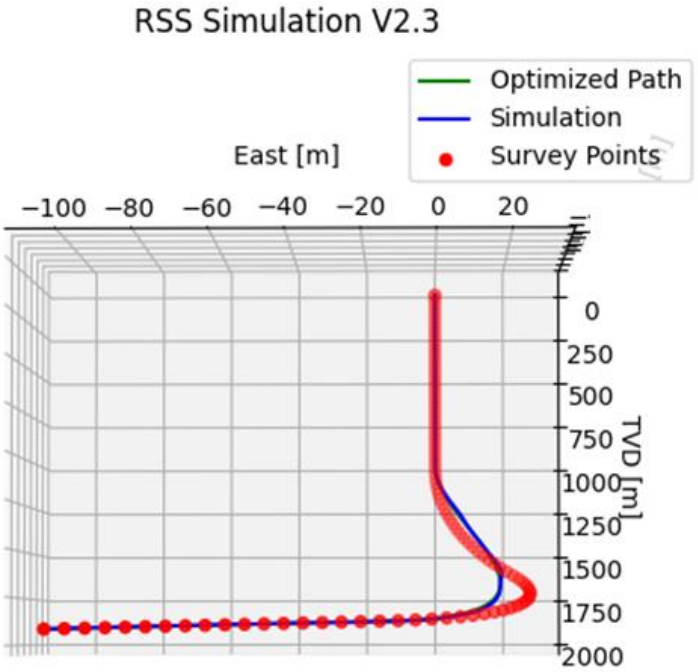

Figure 7.4: Profile View of the 3D Case

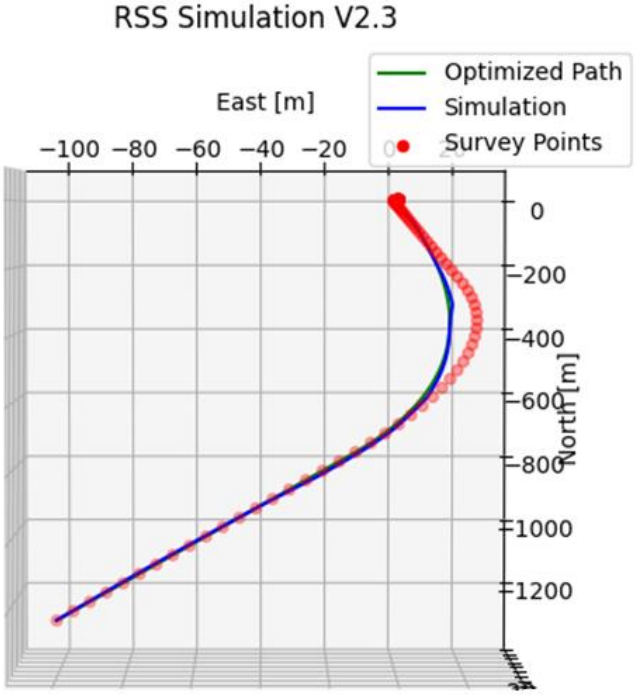

Figure 7.5: Superior View of the 3D Case

The job done by the Real-Time Trajectory Control can be found in the tables from the Appendix B, which indicates which survey points were corrected. Nevertheless, it is better appreciated in the pink ellipses in Figure 7.6, where the simulated trajectory has some corrections that change the direction of the bit and make the simulated trajectory join the PWP again.

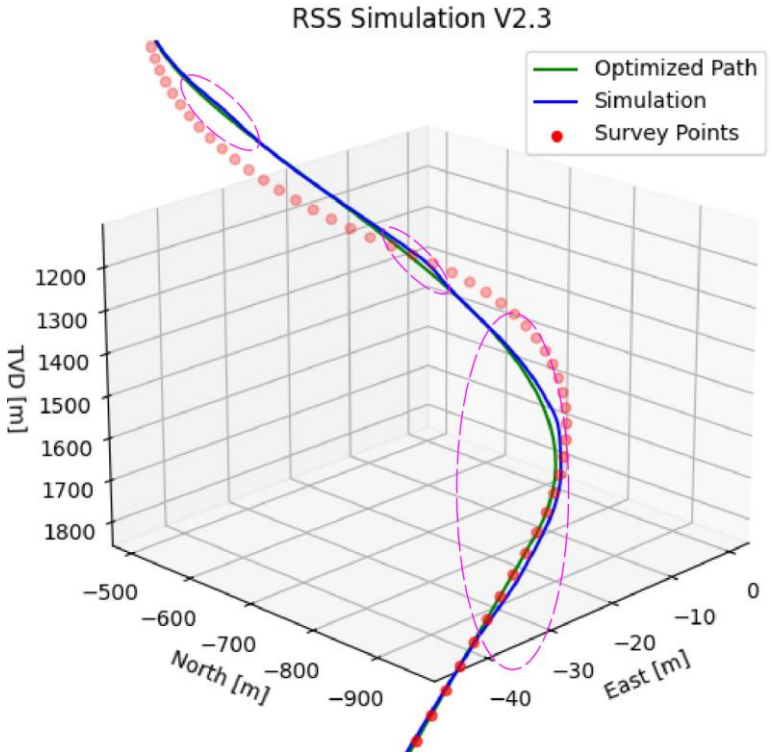

Figure 7.6: Bit Deviation Correction Points in 3D Case

Besides, the target coordinate is reached at the end of the simulation and the distance from the final bit position simulated, and the target are very close. As a result, the software has simulated successfully the project presented, with the data from Table 7.1. There might be many other alternatives to compare by just changing the parameters from the mentioned table.

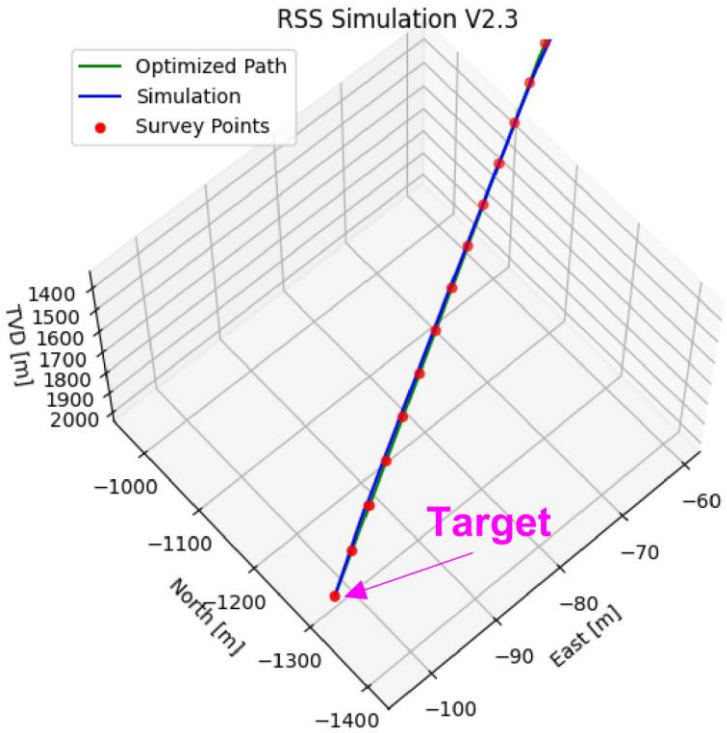

Figure 7.7: Final Target Reach in 3D Case

7.1.2 RSS Model Results

The results of the simulation are presented in the correspondent table in the Appendix B. This table is the short version of the simulation results since the RSS Simulator gives a final simulation table of more than 14000 rows. As a result, only 93 stations (every 30 m) are presented in this table.

The most valuable knowledge that can be obtained from the simulation is the relationship among the variables. The following figures show the performance of certain variables throughout the whole simulation. Since more than 14000 points are plotted, it might not see too many details of the curvatures or peaks of the different parameters. However, some zoomed figures will be offered in the following chapter.

Figure 7.8 shows the inclination changes in the simulation where there is a gradual increment from the vertical direction until a nearly horizontal direction. Figure 7.9 shows the azimuth changes when there is a great change around 990 m.

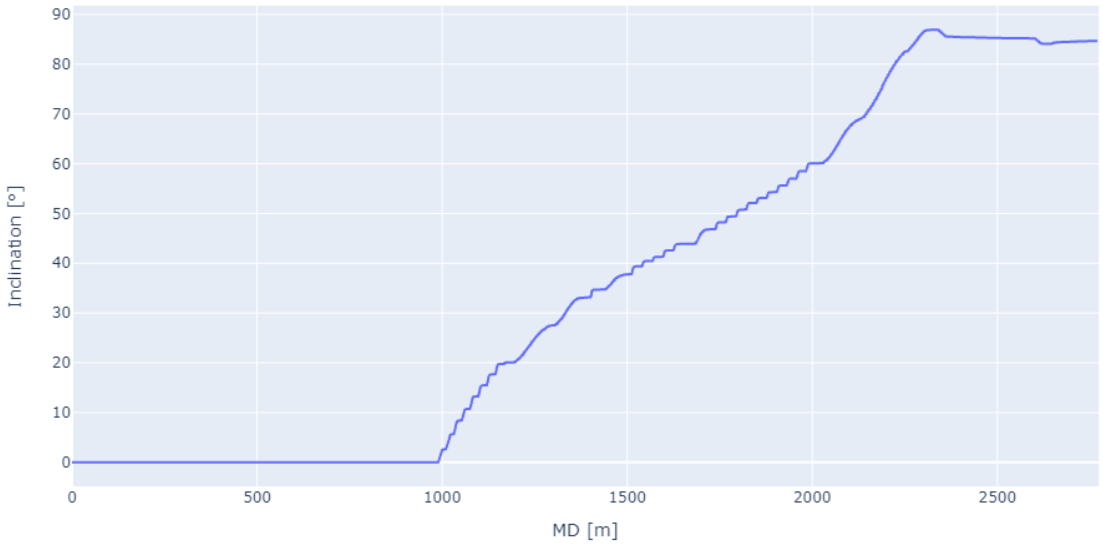

Figure 7.8: Inclination in 3D Case

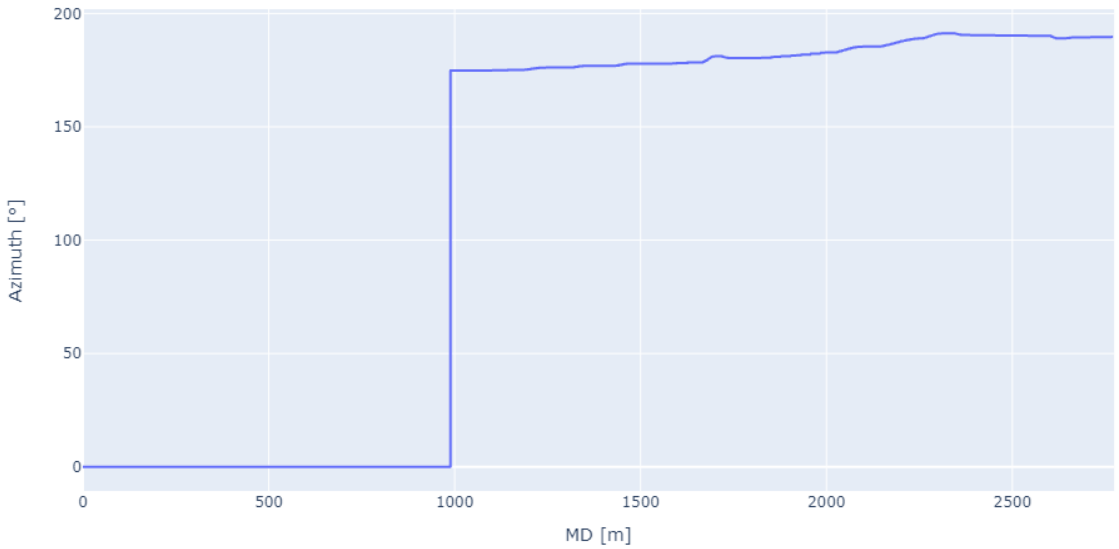

Figure 7.9: Azimuth in 3D Case

One of the most relevant plots is Figure 7.10, which displays the BHA actuator's execution or offset. It tells when the actuator was activated to his maximum opening (set by $maxoff$) and at what moments the offset was gradually deactivated. It is important to remember that the offset behavior indirectly reflects the operation of the TCO algorithm over the simulated BHA tool performance because the TCO sends instructions to the BHA tool for activating and deactivating it at a specific time or depth.

Moreover, the offset behavior will influence the rest of the parameter's actions like the DLS (Figure 7.11) that starts to increment at the same point that the offset acts, and also it is related to which section of the well is being constructed at that time. For example, at the beginning of the curvature, there some DLS with values more than 10°/30m.

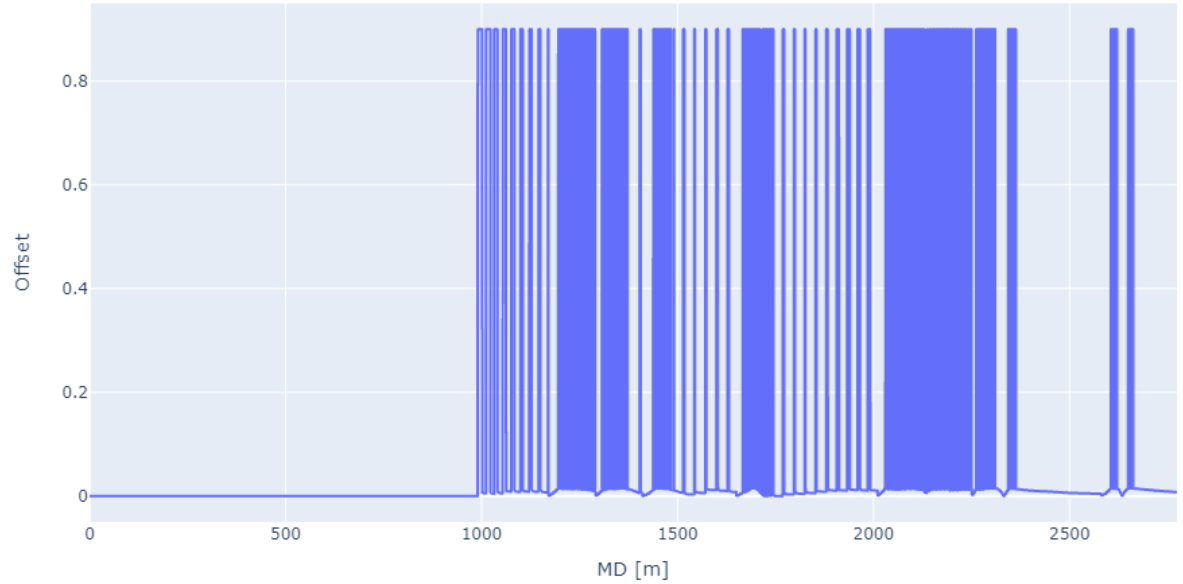

Figure 7.10: Offset Performance in 3D Case

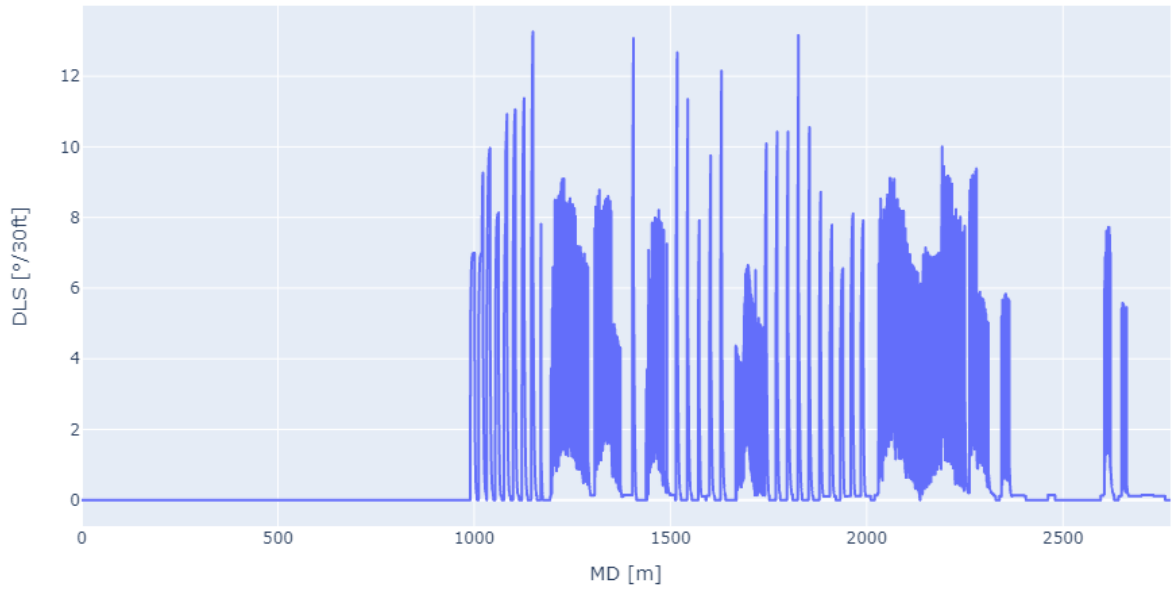

Figure 7.11: DLS in 3D Case

Finally, the ROP axial (Figure 7.12), ROP inclination (Figure 7.13), and ROP azimuth (Figure 7.14) are presented to the user. They are the main result of the simulation model since they are the fundamental parameters for calculating the next bit position, as was described in Eq. (5.10) to (5.17).

The ROP axial presents many oscillations in its behavior; their cause will be explained in the next chapter. However, it can be inferred that there is a frequency in the time when each oscillation appears, and it is related with the number of survey stations simulated.

The ROP inclination and the ROP azimuth have been influenced by the offset and the forces on the bit. Both ROPs indicate that the bit moves to a particular direction either for the inclination plane or for the azimuth plane. When the ROP inclination or azimuth has a positive value that means that the correspondent angle is increasing, and when it has a negative value means a decreasing of the correspondent angle.

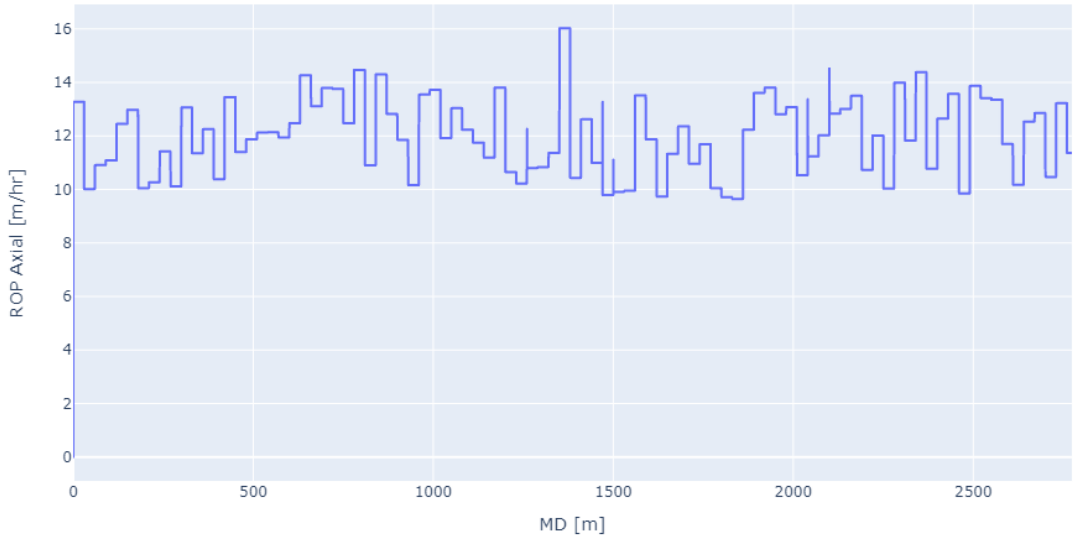

Figure 7.12: ROP Axial in 3D Case

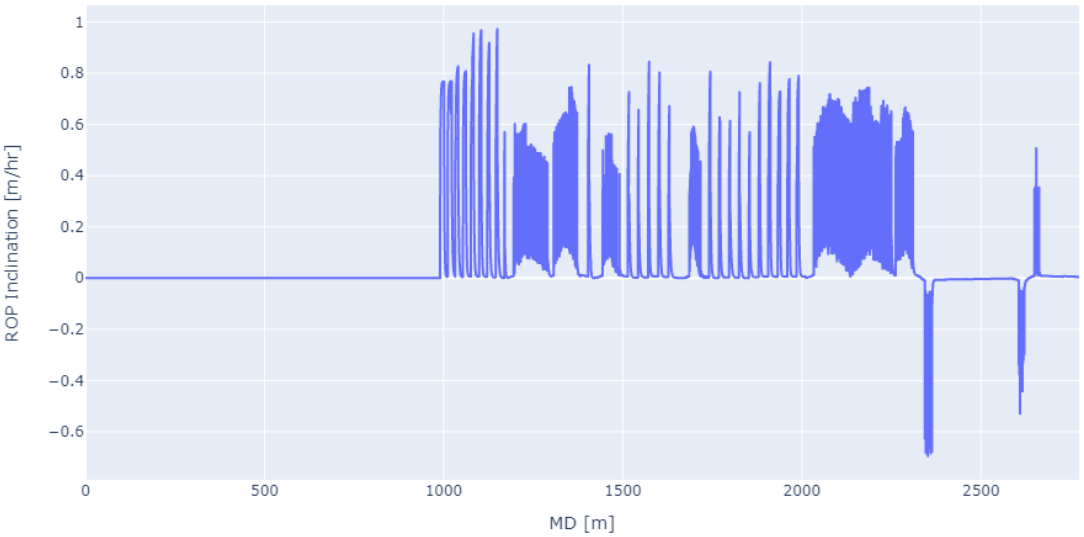

Figure 7.13: ROP Inclination in 3D Case

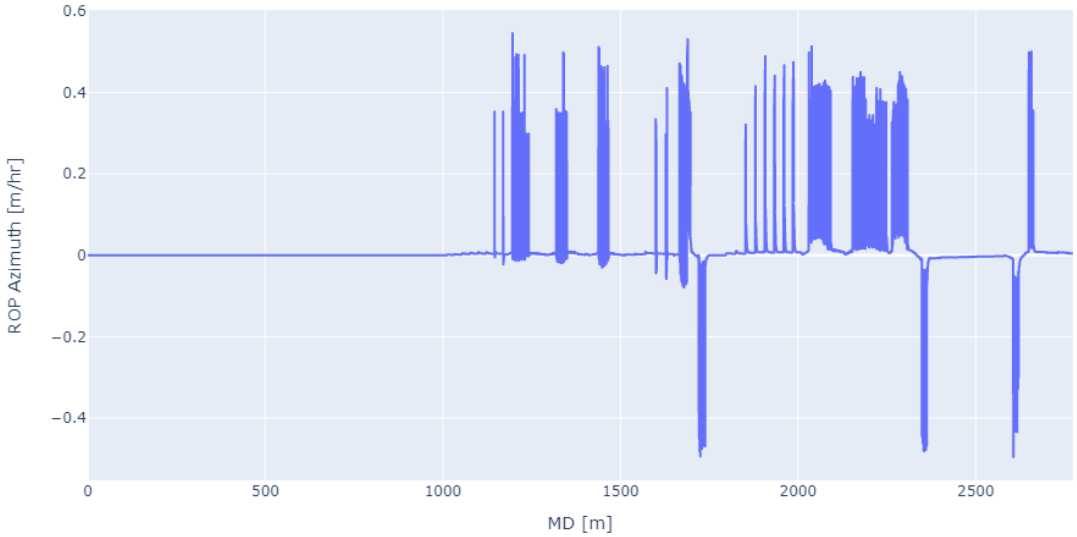

Figure 7.14: ROP Azimuth in 3D Case

7.2 2D Trajectory Case

The 2D case is a J-type well that finishes with an inclination of 90° (horizontal drilling), and the direction of the well is going towards the West (azimuth of 270°). The target coordinate to reach has a TVD of 2002.64 m, East of -1540.52 m and a North of 0 m. The North coordinate does not change in the whole trajectory; consequently, it is considered as a 2D well trajectory.

The well has a vertical section from 0 to 990 m (MD), a curved section from 990 to 2959 m (MD) and a final hold section from 2959 to 3050 m (MD).

The relevant input data used for configuring the simulator is the same as the one used in the 3D case (Table 7.1) except that the $maxoff$ is 0.85 for this case. The well survey stations data for the 2D well are available in the Appendix C (Figure 7.15).

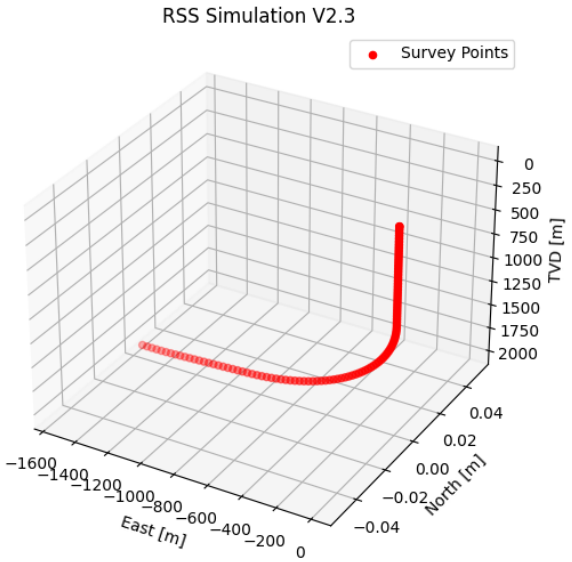

Figure 7.15: Survey Stations Disposition for 2D Case

The well presents only one wide curvature that turns the well from 0° to 90°, and the azimuth does not change since the KOP of the well and keeps constant until the final target.

7.2.1 TCO Results

The TCO created an optimized path (green line in the following figures), and the RSS Model build the simulation line (blue line in the following figures) based on the original survey stations given as input.

Even though in Figure 7.16, the simulated well is presented in a 3D axes plane, the well belongs to a 2D trajectory because the North value coordinate keeps 0 from the beginning until the target coordinate.

Moreover, Figure 7.17 is the profile view of the 2D trajectory, which shows the difference between the PWP and the original survey points. The optimization of the original curvature can be seen clearly, and how this will lead to a shorter well path.

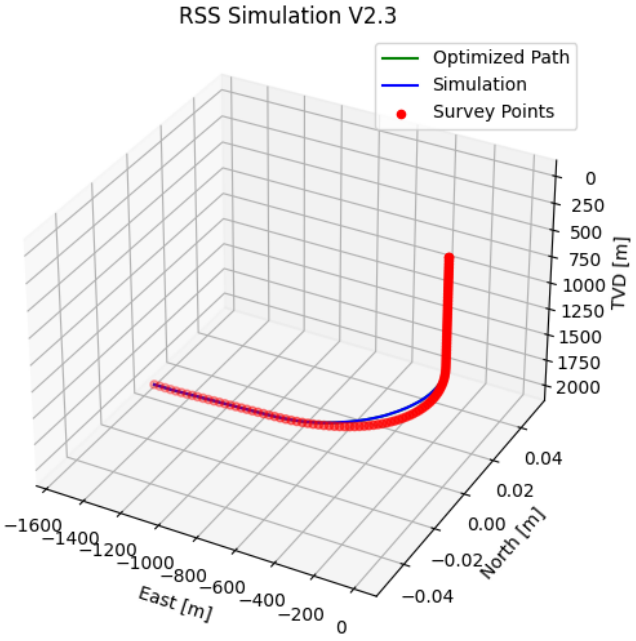

Figure 7.16: RSS Simulation 2D Trajectory General View

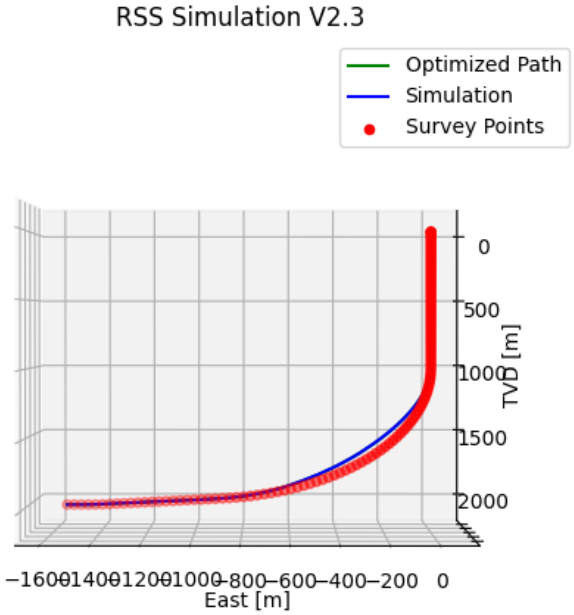

Figure 7.17: 2D Trajectory Profile View

Figure 7.18 shows an example of the real-time trajectory control acting over the simulation trajectory and correcting it to return to the PWP (see pink ellipse). This particular trajectory is not too difficult to simulate, and as a result, the corrections are not too aggressive.

Furthermore, the final coordinate simulated is the same as expected in the original survey station data, as shown in Figure 7.19. It is not very easy to perceive the two straights plotted because, at this point, the simulation was corrected by the TCO. The results of the PWP and the deviation control function are presented in the tables in the Appendix C.

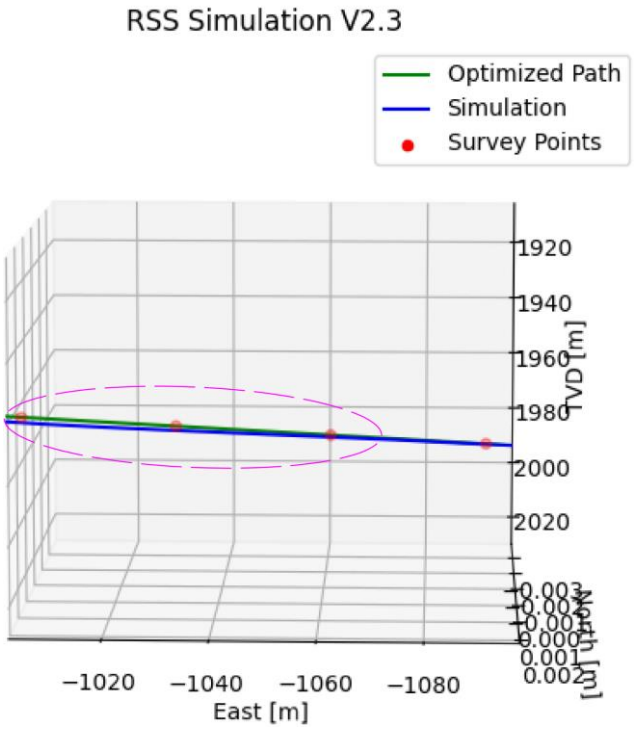

Figure 7.18: Bit Deviation Correction Points in 2D Case

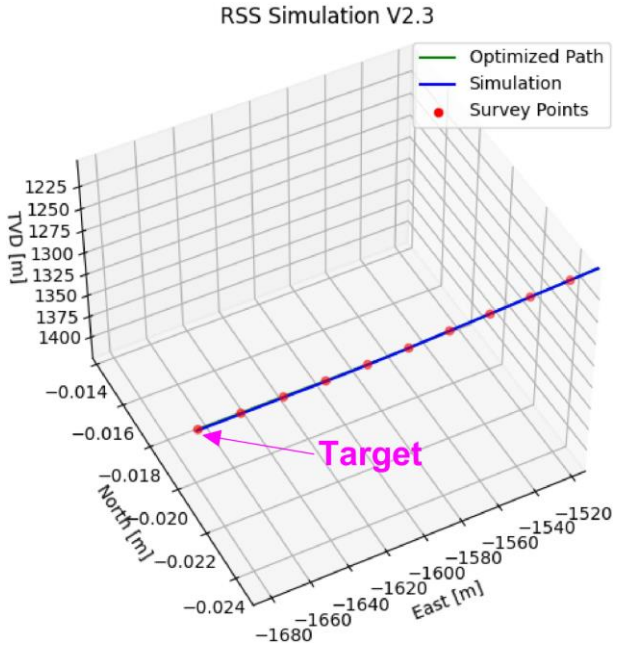

Figure 7.19: Final Target Reach in 2D Case

7.2.2 RSS Model Results

The results from the RSS Model are described in the tables inside the Appendix C. Since it is a 2D case, parameters like azimuth, force in the azimuth direction, or ROP azimuth remain with a 0 value since the beginning until the end, and there is no need to analyze these plots.

The inclination (Figure 7.20) of the 2D case constantly increases until it reaches the 90° value. As the 3D case, the offset behavior (Figure 7.21) is significant for the analysis of the rest of the parameters, and due to the high quantity of data simulated (more than 15000 rows), the resolution is not well appreciated.

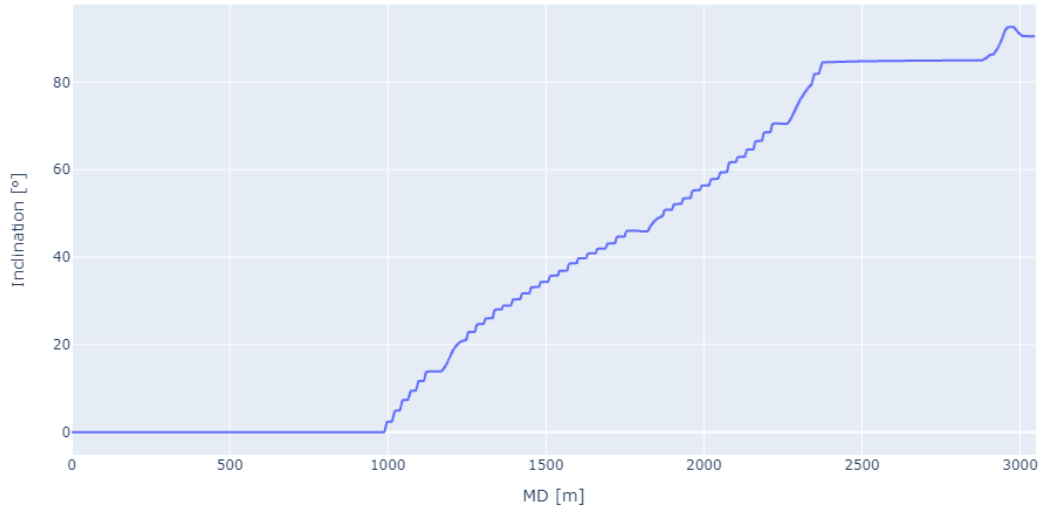

Figure 7.20: Inclination in 2D Case

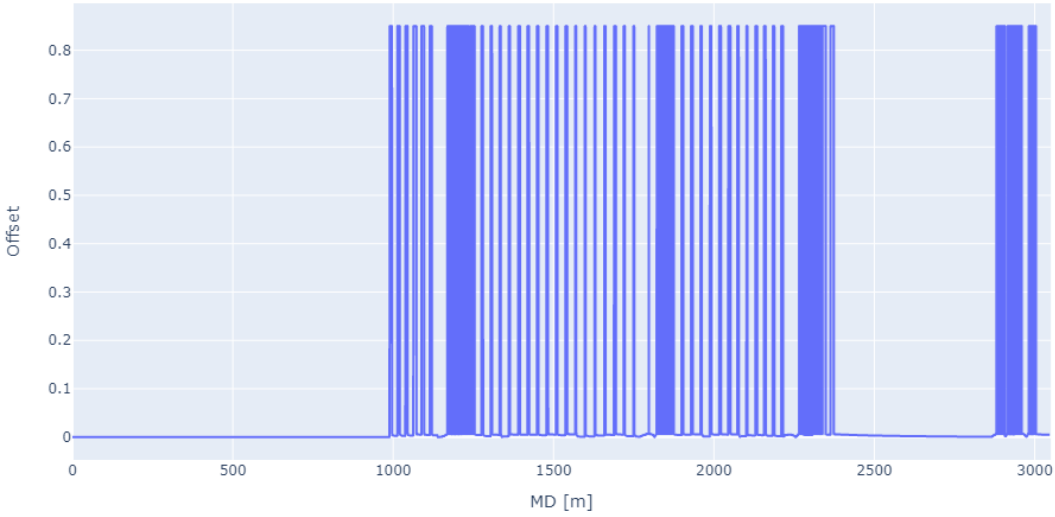

Figure 7.21: Offset in 2D Case

The DLS (Figure 7.22) starts at the same MD of the offset (990 m), and it has two significant increments that reach 14°/30m.

Finally, the ROP axial (Figure 7.23) and the ROP inclination (Figure 7.24) show the change in penetration rate that influences the bit calculation, like was explained before. The different positive and negative peak directions, in the ROP inclination, indicate that the inclination is built up or dropped, respectively.

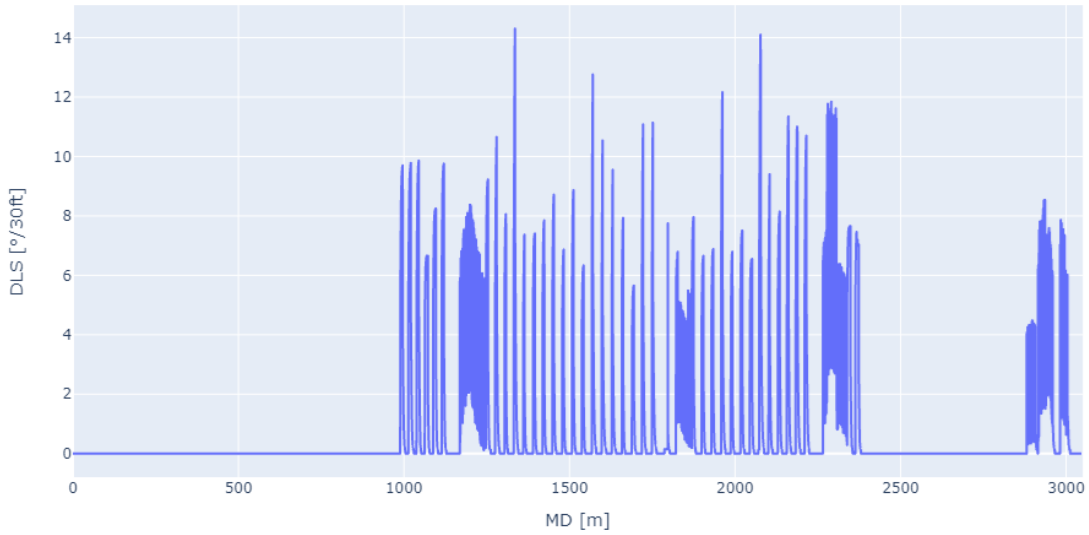

Figure 7.22: DLS in 2D Case

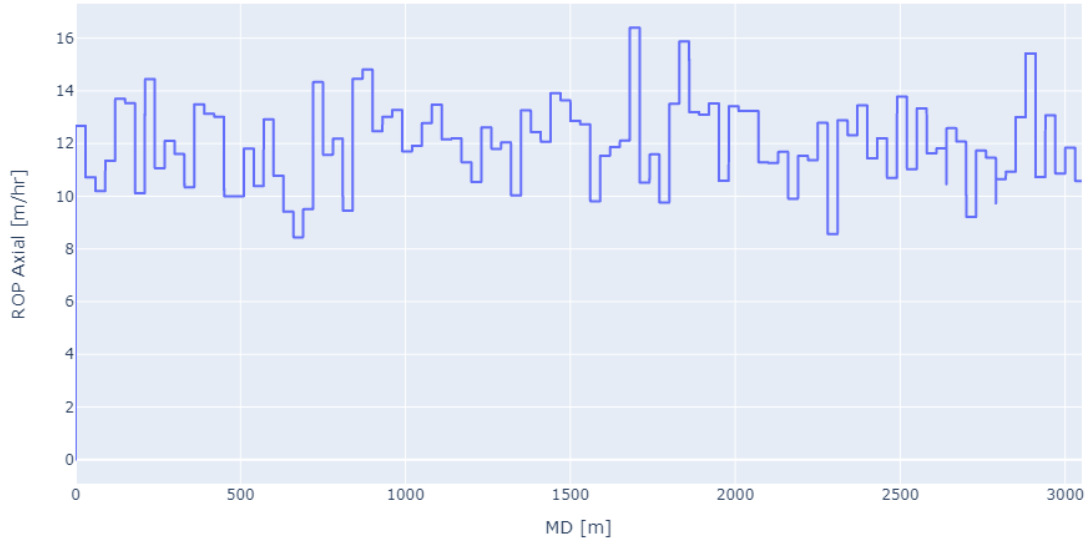

Figure 7.23: ROP Axial in 2D Case

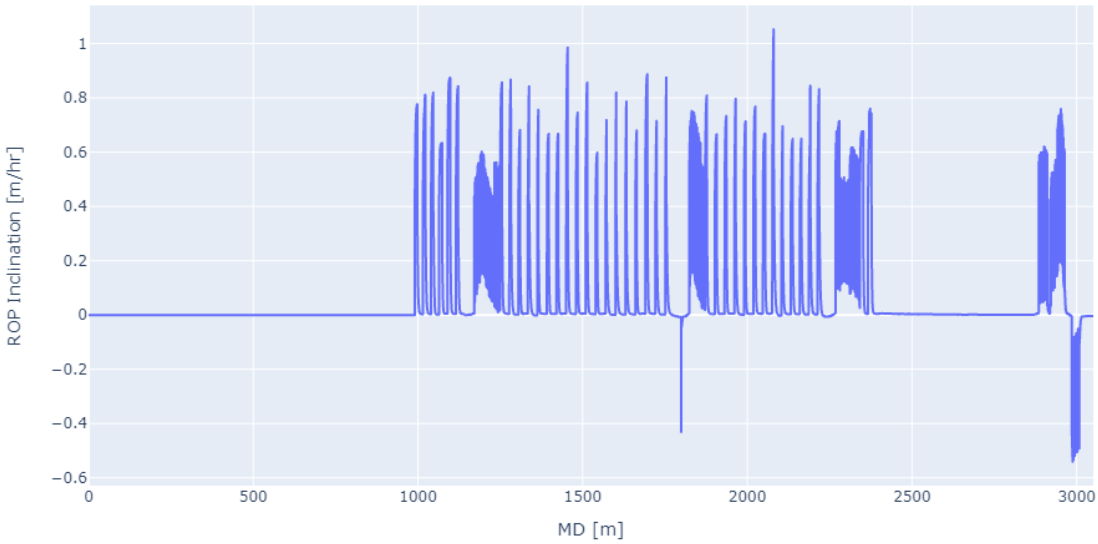

Figure 7.24: ROP Inclination in 2D Case

8 Discussion

The application of the RSS Simulator was tested in the examples presented in the last chapter. However, the analysis of the results is going to be focused just on the 3D example since there is more output information to study. The investigation of the simulator's performance will mark the areas to improve and highlight the strong points.

Consequently, the best method to do the analysis is to compare the same 3D example with the TCO turned off. The initial data will be kept as the same showed in Table 7.1 and the correspondent survey stations. Both situations will show different simulation paths with the TCO on and off that will cause a different error magnitude regarding the PWP. This error will be measured to quantify the implications of using the TCO in simulation projects.

Despite the hold or straight sections of the well do not show many problems to be analyzed, the curvature sections have some issues that need to be figured out and discussed to try to find the cause and probable solution for them.

Moreover, the role that the RSS Simulator will have in the Real-Time Drilling Simulator will be described. Finally, some other possible future applications of the RSS Simulator will be considered in this chapter.

8.1 TCO Performance

The Trajectory Control Optimizer is the new model that needs to be tested and analyzed for the present study. Therefore, the discussion will be more focused on the TCO results than the RSS Model. The TCO was developed to give an automated tool to the industry for reaching the target coordinate without any human intervention.

Consequently, TCO will be tested to check if it can have acceptable results and if the interventions of the Real-Time Trajectory Control over the whole simulation process are adequate or need to be improved. Similarly, the correction path generated should follow certain constrictions and do not generate possible well integrity problems.

It is important to mention that TCO on/off refers to the Real-Time Deviation Control activation or deactivation, which involves the Deviation Control and the Correction Path functions. On the other hand, the PWP function (part of the TCO, too) is always on because it calculates the objectives of the simulation and is used to stop the main simulation loop.

8.1.1 Comparison of the Simulation with the TCO On/Off

The TCO execution during the 3D example was demonstrated since Figure 7.2 to Figure 7.7. Still, a more interesting investigation of the results can be made by comparing the simulation of this example without the participation of the TCO in the Deviation Control process. In other words, the 3D example will be simulated and not be corrected at any survey point to see the final trajectory differences and mainly the target coordinates reached by both simulations.

Figure 8.1 shows the differences in the trajectories when the Deviation Control takes part in the simulation (case a) and when it does not (case b). When the TCO is off, the bit does not have problems in the vertical section, as expected, because no inclination or azimuth forces act over the bit until MD of 990 m.

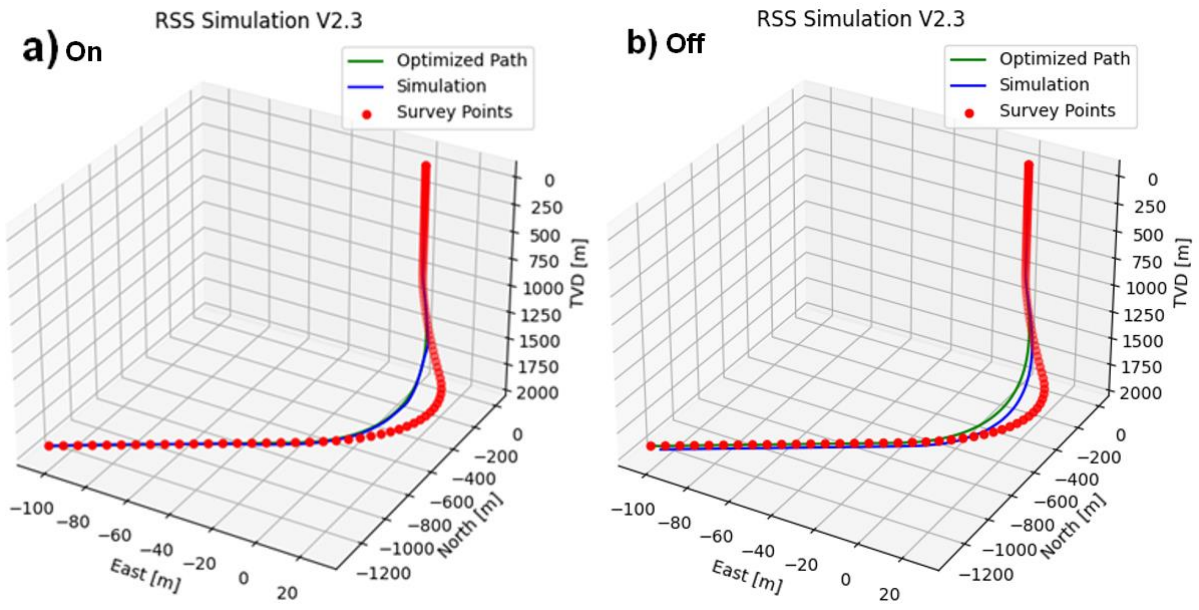

Figure 8.1: Difference of Trajectory Performances TCO On/Off

Nevertheless, the simulation deviates as soon as the curvature builds up and leads to another direction. The deviation increases with every meter drilled during the curvature section because the curvature keeps the same target inclination and azimuth defined since the beginning of the curvature section. Therefore, it is not corrected or compensated with the actual distance of the bit position to the PWP.

The difference between the two trajectories can be appreciated more clearly in Figure 8.2, which is a zoomed view of the curvature section in specific. When the TCO is on, there are significant corrections of the simulation trajectory at the following TVDs: 1378 m, 1565 m, and 1840 m.

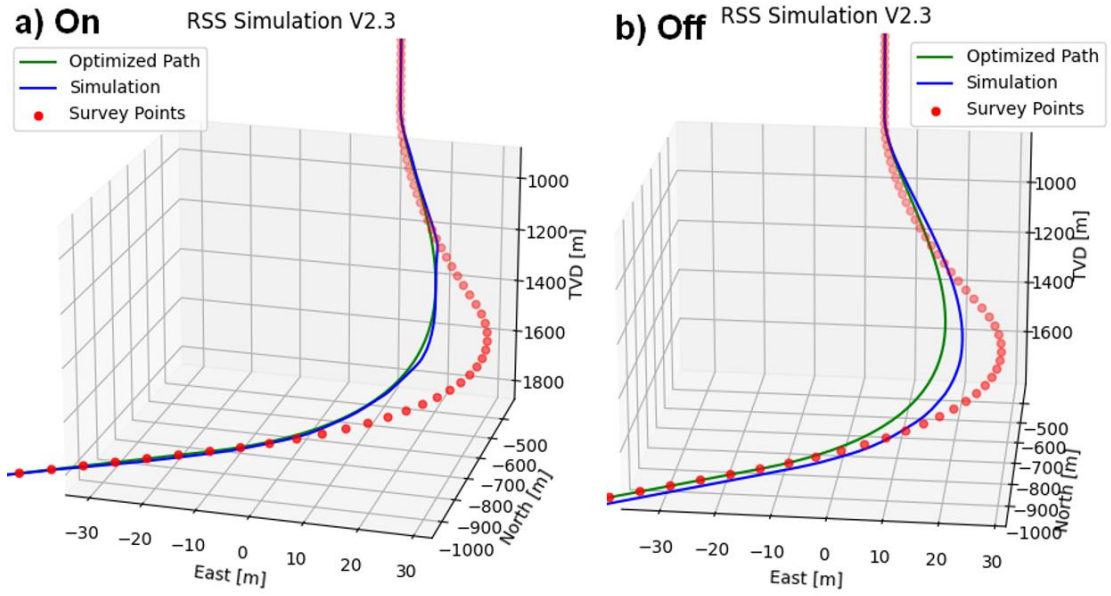

Figure 8.2: Curvature Comparison with the TCO On/Off

Although the three significant deviation corrections of the simulation seem to be the only ones, the results coming from the Deviation Control show that there are more corrections in the MD, as indicated in Table 8.1. The information in the table is just part of the complete Deviation Control table (see the tables in the Appendix B). Table 8.1 indicates only the survey stations where there was some corrective

action. The VOE is the length of the Vector of Error, EOU is the vector from the bit position until the radius of the EOU, and Out EOU just communicate if the VOE is larger than the EOU, which means that the bit is too far from the EOU radius and it is considered as deviated.

Table 8.1: Survey Points Where the Deviation Control Was Activated

Survey	MD [m]	VOE [m]	EOU [m]	Out EOU
39	1170.167076	1.173787019	1	1
43	1290.176142	1.003355378	1	1
47	1410.144327	1.065234878	1	1
55	1650.051439	1.008275231	1	1
67	2010.189395	1.011092639	1	1
71	2130.111409	1.402719389	1	1
75	2250.114095	1.213530351	1	1
86	2580.208975	1.138654067	1	1
93	2773.792962	1.023713604	1	1

The last table presented 9 corrections that were made in the middle of the simulation. The value of EOU keeps constant due to the uncertainty analysis with the inclination, azimuth, and MD values did not affect the Eq. (6.1) and (6.2) too much. As a result, the uncertainty calculated for this well was higher in the curvature sections, but not high enough to surpass the minimum radius for the EOU Min_R imposed by the user, that for this case was 1 m. Nevertheless, the Deviation Control function works as planned because the corrections are made only when the VOE has a higher value than 1 m (for this example).

The corrections are made principally to assure hit the target as close as possible to the one planned. Therefore, an excellent way to evaluate if this purpose is completed is by comparing the final coordinate of the target when the TCO is on and off, as presented in Figure 8.3.

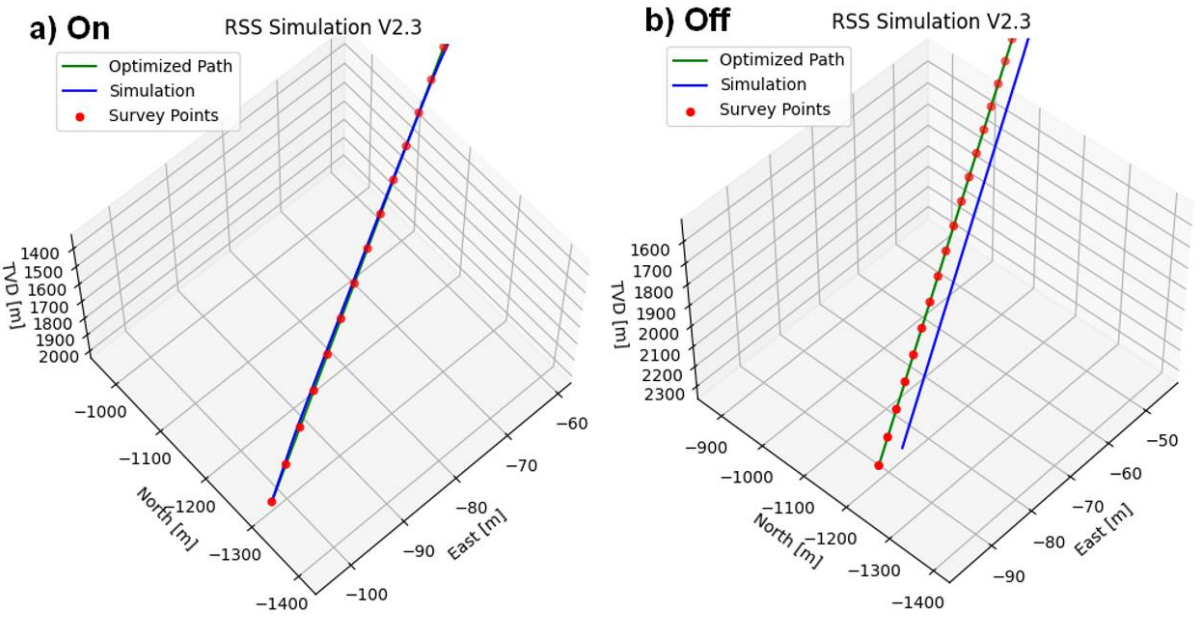

Figure 8.3: Final Target Comparison with the TCO On/Off

The final target coordinate reached with the TCO on is very close to the one planned in the PWP, which will be considered as acceptable. On the other hand, when the TCO is off, the final coordinate reached by the simulation is further than the one planned. As a result, depending on the tolerance set in the drilling plan, it can be accepted or considered a failure. The truth is that without the use of the TCO, the main simulation objective could not be reached, and the implications in real life might bring some others production or reservoir problems.

Until this point, the differences were analyzed from the plots mainly; however, a quantification of the difference between the simulated trajectories with the PWP will be a more accurate way to conclude the performance of the TCO.

As a result, the distances between the survey stations from the PWP and the survey stations of the simulation results should be measured to indicate how close the simulation results are to the PWP, which will be interpreted as how close the simulation is to the trajectory plan. There are two simulation result sets, one with the TCO on and the other with the TCO off. Consequently, each one of the sets should be compared with the PWP survey station's location.

For instance, the PWP survey station number 56 has the following coordinates (V, N, E) in meters (1747.51, -509.55, 13.36), the simulation with the TCO on has (1745, -509.52, 13.89), and the simulation with the TCO off has (1745.27, -513.36, 17.84), then the distances from the PWP to each of the survey stations are:

$$Dist_{TCO\ ON} = \sqrt{(1747.51 - 1747.16)^2 + (-509.55 + 509.52)^2 + (13.36 - 13.89)^2} = 0.64\ m \quad (8.1)$$

$$Dist_{TCO\ OFF} = \sqrt{(1747.51 - 1745.27)^2 + (-509.55 + 513.36)^2 + (13.36 - 17.84)^2} = 6.28\ m \quad (8.2)$$

The same methodology was applied to the rest 80 survey stations in the well. It is essential to mention that the survey stations chosen from the simulation (since it has more than 14000) are the closest ones to the PWP survey points at similar MD value. The complete table with the calculations of each survey station is showed in the Appendix D.

The distances of the points help calculate their mean value and standard deviation for comparing both sets between them. The set that shows lower values will be considered closer to the planned trajectory and more precise. The values of the mean and the standard deviation calculating for both sets are resumed in Table 8.2.

Table 8.2: Mean and SD with TCO On/Off

	Simulation TCO On	**Simulation TCO Off**
Mean	0.8337	3.8757
SD	0.6969	3.3156

The last table indicates that using the TCO in the simulation will generate a lower average distance to the PWP survey stations. It means that the TCO is helping the simulation to follow the planned trajectory and keeps the bit closer to it, compared with the TCO off case.

In the same manner, the lower SD value when the TCO is on means that the probability of having a survey point coordinate that varies a lot from the distance mean value is lower than the TCO off case where there might be some points that are too far from the distance mean value.

8.2 Curvature Sections Analysis

The hold sections of both study cases did not present much trouble for the simulation part, and they were followed according to the PWP target inclinations and azimuths. However, most of the correction points were situated on the curvature sections. Therefore, they generated some changes of direction while making the curvature.

Although the final shape of the curve seems to have some intricated parts that might lead to a well integrity problem, the maximum DLS was 13.26°/30m which is inside the top 15°/30m that the OrientXpress RSS Tool can reach (Nabors Industries Ltd., 2018). However, in an actual drilling project, some other components of the drill string could not be designed to bear the flexion and stresses of this DLS.

The curvature of the well is a critical place where the bit deviation might be corrected by the RSS Simulator. Consequently, it is suitable to analyze if the actual operation of the simulator for correcting the path is the most appropriate or if it can be enhanced for the future.

Therefore, the curvatures of the 3D example will be used to study the curvature and some of its simulated parameters. The first step is looking at the curvature shape of the simulation trajectory (Figure 8.4), where there are some correction points that do not look too smooth. After that, however, they made the bit trajectory to return to the PWP.

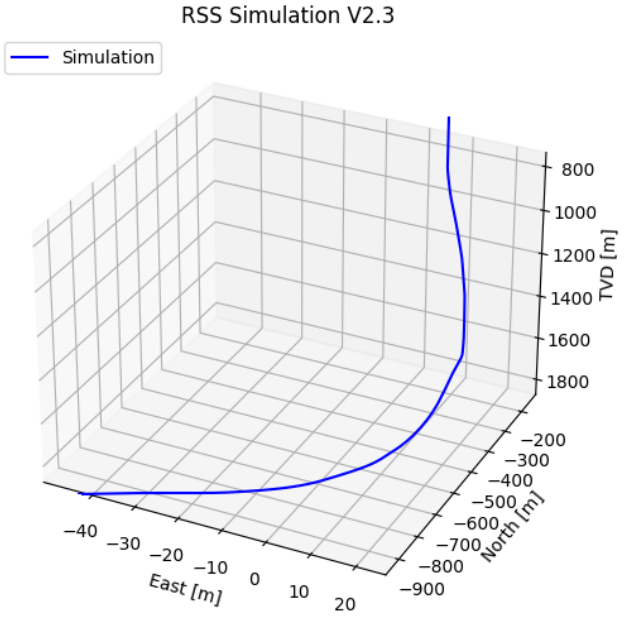

Figure 8.4: Simulation Curvature Shape of 3D Example

Approximately at 1370 m in the TVD axis (closely an MD of 1405 m), there is a noticeable change of direction of the bit. The correction was detected by the Deviation Control and designed by the CP function. The CP follows the constraints set by the user regarding the maximum DLS ($Max_{DLS\ Corr}$) and tortuosity ($Tor_{Max\ Corr}$) which are 6°/30m and 3°/30m, respectively. The DLS calculated with the cubic Beziér curve method should not cause any trouble, for this CP, according to Eq. (4.13).

Nevertheless, the DLS calculated with Eq. (5.17), which is exported as part of the simulation results, shows a high value of 13.07°/30m around the MD of 1405 m, as it can be appreciated in Figure 8.5.

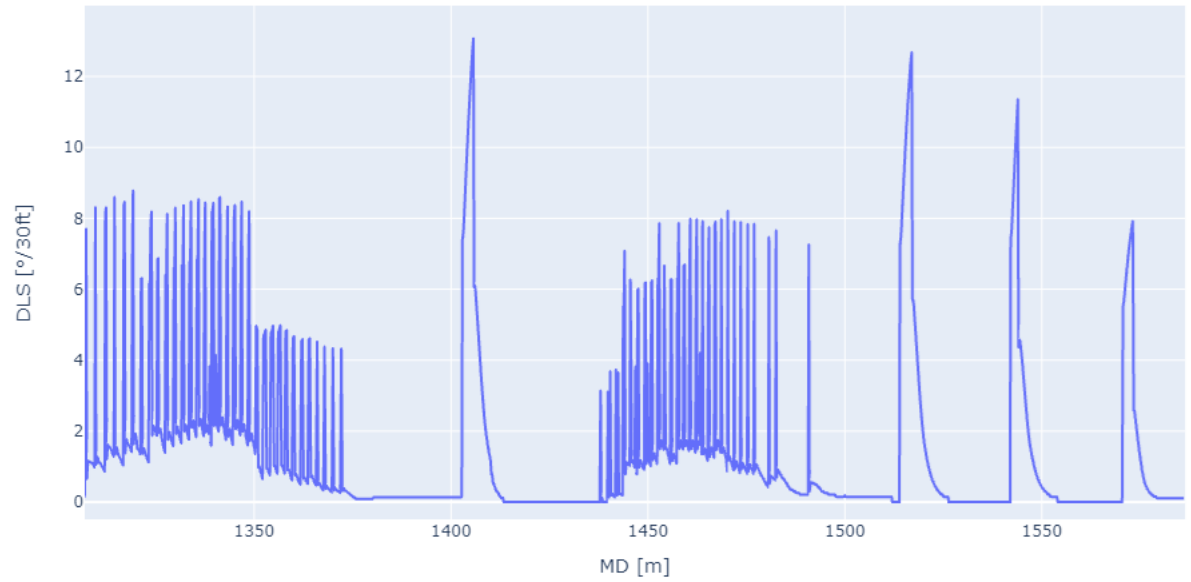

Figure 8.5: Increment of Simulated DLS at MD of 1405 m

As a result, there is some difference in the DLS calculations from the cubic Beziér curves method proposed by Sampaio and the DLS calculation used in the RSS Model by Saramago. The possible solution might be to develop a scale factor between these methods or adapt the Beziér strategy just to calculate the DLS with Eq. (5.17) and examine how accurate this is.

Another interesting area to focus on is the offset behavior during the curvature section. For instance, Figure 8.6 is a zoomed view of the curved section of the 3D example, which describes the activation points where the actuator of the BHA tool was activated.

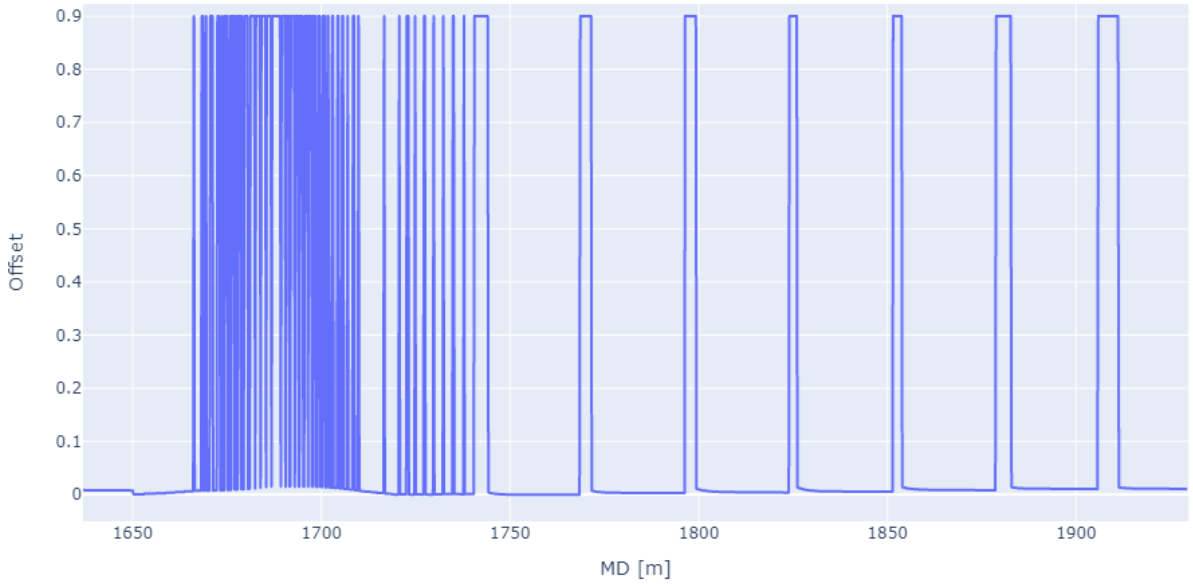

Figure 8.6: Offset Behavior in Part of the Curve Section

The activation of the offset is quick and not progressive at the beginning, but their reduction tends to have a softer finish to return to a value of 0%. The part showed in the last figure is helpful to identify two processes that happen during the simulation of a well trajectory:

- **Correction Path**: (from 1660 m to 1750 m) There are plenty of activations of the offset because the CP gives the target inclinations and azimuths to the offset control function temporarily, and the created curve has a short length.
- **Standard Simulation**: (from1750 m to 1940 m) The activations of the offset are not as frequent as the CP. There are more deactivations zones due to the offset has reached the target inclination and azimuth before receiving new targets.

Despite the offset interventions being correct, the initial application of it can be enhanced and make it more progressive and less quick to not create sudden changes of direction in the curvature. Perhaps the same idea of offset deactivation should be implemented for offset activation. However, the delay caused by a more progressive offset activation might lead to creating a more extended arc curvature that could make it deviate too much from the plan.

Furthermore, the simulation calculations are influenced by the results of the three ROPs involved in the model. For example, the ROP axial (see Figure 8.7) has some oscillations with a particular frequency that equals the space between the simulated survey stations. The fluctuations are caused by the noise added to external input parameters of Table 3.5 with Eq. (3.1).

The random error (e) could have either a positive or a negative value. Consequently, the parameters that come from the external's modules will be modified and will increase or decrease their value. The intention of this practice is to give a certain degree of realism to the simulation.

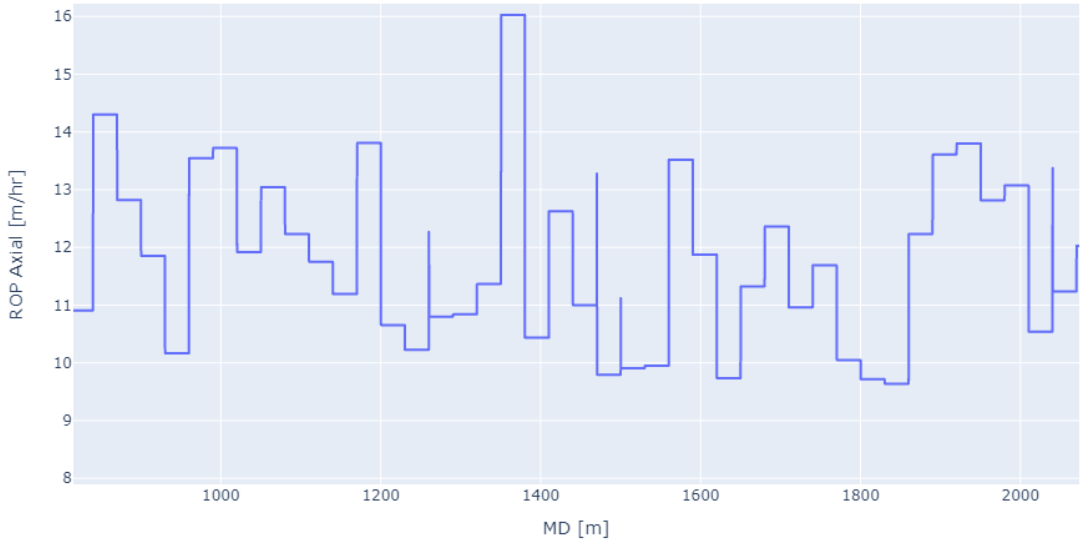

Figure 8.7: ROP Axial Oscillations

The examples showed in the study cases are assuming some values for the μ, RPM, WOB, Es and $Steer$ parameters because the RSS Simulator is not yet integrated with the externals models (they are still in development), but the architecture was designed to facilitate the integration of the rest of the models in the future. As a result, the ROP Axial in the 3D example has an average value for each parameter just mentioned. Still, when the RSS Simulator connects with the rest of the models in the future, there will not be an evident average value for the parameters, but they will still be added the noise.

The ROP inclination and azimuth react to the offset activation because the last one creates a reaction force in the inclination and azimuth planes that are later transferred to the ROPs inclination and azimuth using Eq. (5.8) and (5.9). Thus, when the offset function has the instructions to reach a certain inclination and azimuth, it will determine the direction of the opening of the BHA tool. As a result,

some part of the track change will be positive (increasing the angle inclination or azimuth) or negative (decreasing the angle inclination or azimuth). Figure 8.8 and Figure 8.9 show this phenomenon where the inclination and azimuth are changing due to the offset function is calibrating the intensity of the curvature change.

Figure 8.8 illustrates the ROP inclination at the beginning of the last hold section where the curve is ending, and there are some corrections. On the other side, Figure 8.9 presents a zoomed view of the middle of the curvature after a correction path where the simulation is returning to follow the PWP, and there are some azimuth adjustments.

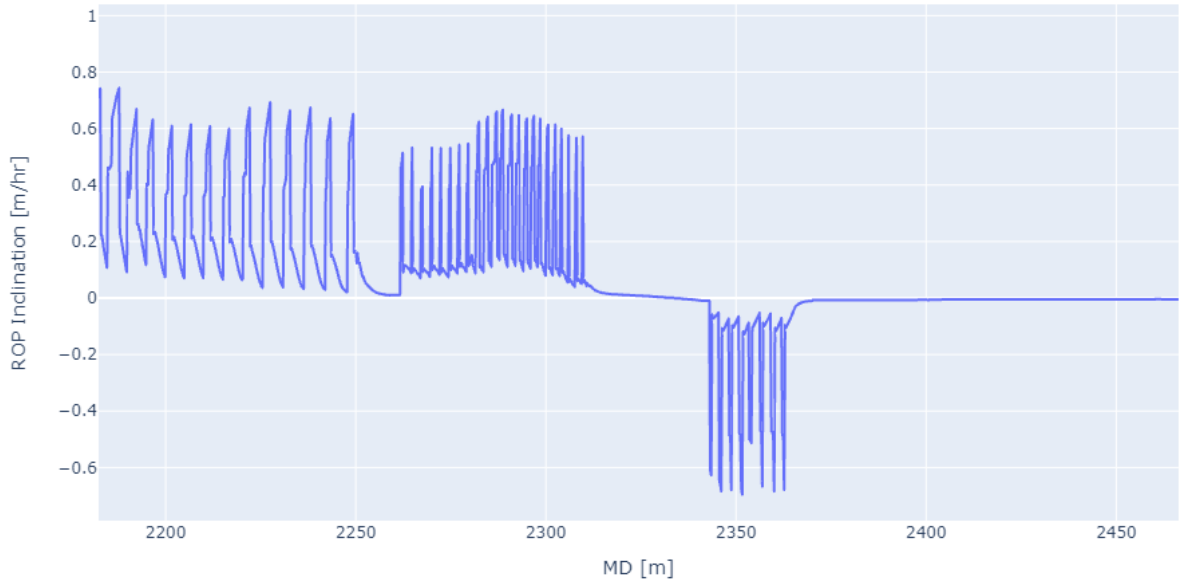

Figure 8.8: ROP Inclination Zoomed View

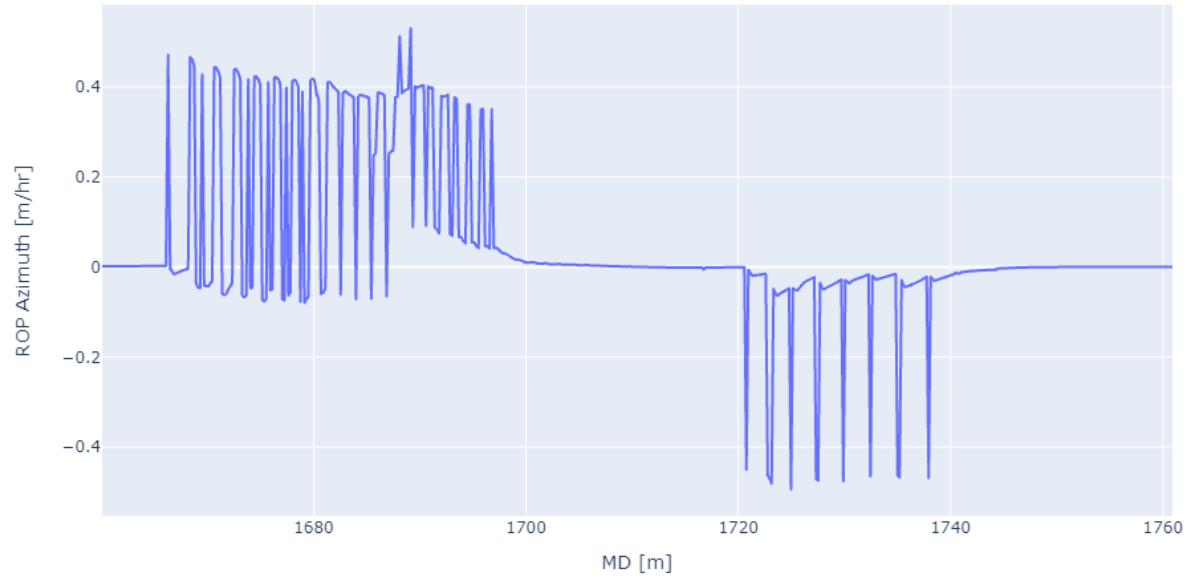

Figure 8.9: ROP Azimuth Zoomed View

The ROPs analysis indicates that the RSS Model works and follows the indications of the TCO and brings good simulation results that accomplish their primary purpose of reaching the target coordinate optimally.

8.3 Future Applications of the RSS Simulator

During the initial stages of the RSS Simulator development, the adaptability to work with external modules was an objective to achieve in the final product. Therefore, the RSS Simulator software architecture allows interaction with the data from external sources and exports the data calculated in the simulator.

The possibility to work as an independent module that only needs some input and gives outputs either at the end of the simulation or after each iteration makes the RSS Simulator have a great versatility to work in different projects.

For instance, the Real-Time Drilling Simulator, developed by the virtual rig team (team A) of the University of Stavanger for the 2021 Drillbotics® Competence, uses the RSS Simulator as the backbone of the project where the rest of the models will be connected. The concept of the Real-Time Drilling Simulator is described in Figure 8.10, where the importance of the RSS Simulator is evident and how it manages the other modules' outputs to return a realistic and automated simulation. In addition, some virtual sensors might simulate the lectures from the accelerometer and magnetometer principally.

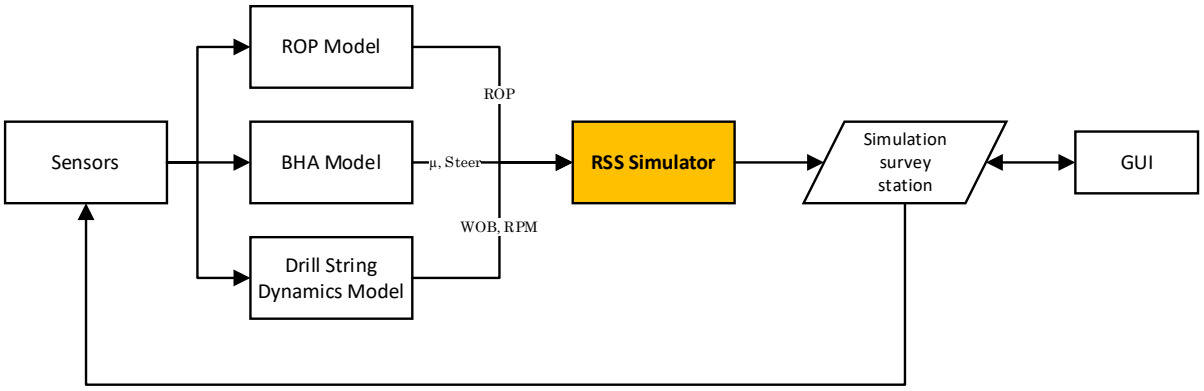

Figure 8.10: Real-Time Drilling Simulator Concept

One great advantage of the RSS Simulator is that each function was developed independently at the beginning. Later, they were joined with the others to properly build the RSS Simulator. Consequently, each function like the PWP, RSS Model, Deviation Control, and CP can work independently in different projects.

For instance, a project looking to generate a well plan trajectory using AI could benefit from the PWP function to set the final survey stations based on the coordinates found by the AI. Besides, there are many possibilities of application of the RSS Simulator or some of its function; some examples are:

- Select the best trajectory alternative among different options using the PWP function to compare the results of each one of them.
- Plan a correction trajectory in an actual drilling project by using the CP function and some other constraints.
- Monitor the bit deviations with the utilization of the Deviation Control function and then apply some correction method when the results from the function indicate a possible deviation position.
- Use the RSS Simulator as the core or complement in a more extensive software tool during a real drilling automation operation to help the industry perform a complete drilling stage without or minimum human interaction.

9 Conclusion and Recommendations

The execution of the RSS Model with the direction of the TCO has resulted in a good simulation execution, and some new features can be added in the software's future. Even though some areas should be enhanced, especially the DLS and the CP in the curvature sections, the outcome is very promising.

One of the main objectives was to assure that the simulations reach (or be very close to) the target coordinate at the end of the simulation run. This objective was fulfilled using the RSS Simulator without any human interaction. The importance of this achievement gives the final product great potential for its use in actual drilling projects.

Moreover, the PWP function creates and, above all, optimizes the original survey stations to reach a faster and safer planned trajectory for the drilling. In the same way, the Deviation Control function detects the bit deviations and warns the simulator about them. The deviations are corrected with the use of the CP function, and it returns to the PWP in most cases.

Indeed, the results obtained when the TCO is on and off show that the use of the TCO brings more possibilities and less uncertainty to reach the target and follow the planned path. However, when the simulation runs without the intervention of the Deviation Control and the CP functions, the simulated trajectory might not end in the location expected and not follow the path projected, which can generate some well integrity issues, reservoir problems, formation faults complications, among other drilling problems.

On the other hand, some features could be upgraded for the future of the software to develop a stronger simulator that considers more inputs or more variability in their functions. Even the structure of the RSS Simulator allows being integrated with another project that requires a particular function from the simulator only. Some recommendations can be made for future study and development of an automated drilling simulator, for example:

- The offset control function (inside the RSS Model) should have a gentler activation of the BHA actuator to avoid sudden curvature changes that might increase the DLS value, like the gradual offset deactivation.
- The force model used in the RSS Model should be improved since the actual is based in the beam bending and might be too simple for a simulation of this level.
- The CP looks for the nearest survey point on the PWP that gives a safe Beziér curve that accomplishes certain limitations of DLS, tortuosity, and length. However, it might be worth studying if it is better to perform the correction path to reach the PWP again in the middle of a curvature, or it is better to contact the PWP in a hold section that will not compromise too much the curve shape, DLS and tortuosity.
- The number of error sources in the ISCWSA Error Model used for calculating the EOU in the Deviation Control function was only five. A deeper study on the errors applied to the simulation will help to enhance the confidence in the simulation results to approximate a real behavior.
- The DLS calculation from the Beziér curves and from the RSS Model should match or at least have a scale factor between them since there are some differences in their values.

The potential of the RSS Simulator for automation in the drilling industry is exciting because it is a new approach to the actual studies in the automation area that plans, drills, detects deviations, and corrects them without the intervention of humans. The simulator is so versatile that it could work with different modules or in various drilling projects. The RSS Simulator could be an initial path that directs towards the future of the drilling automation tools.

10 References

Adamovitsj, M. (2020). *Directional Drilling: Trajectory Design and Position Uncertainty Study for a Laboratory Drilling Rig*. University of Stavanger (UiS).

Adams, N., & Charrier, T. (1985). *Drilling Engineering: A Complete Well Planning Approach*. PennWell Pub. Co.

Aldred, W., Bourque, J., Mannering, M., Chapman, C., du Castel, B., Hansen, R., Downton, G., Hamer, R., Falconer, I., Florence, F., Godinez Zurita, E., Nieto, C., Stauder, R., & Zamora, M. (2012). Drilling Automation. *Oilfield Review*, *Summer 2012*(24), 18–27.

Bourgoyne, A. T., Millheim, K., Chenevert, M., & Young, F. S. (Eds.). (1991). *Applied Drilling Engineering* (2nd ed., Vol. 2). Society of Petroleum Engineers.

Chatar, C., Stepnov, A., Mardyashov, A., & Fedotov, V. (2018). Zero Wellsite Personnel. The First Truly Man-Less Operation for Directional Drilling Services. *September 26, 2018, SPE-191586-MS*, 1–10. https://doi.org/10.2118/191586-MS

Chmela, B., Kern, S., Quarles, T., Bhaduri, S., Goll, R., & Van, C. (2020). *Directional Drilling Automation: Human Factors and Automated Decision-Making*. *SPE-199556-MS*, 1–8. https://doi.org/10.2118/199556-MS

Coffey, S., & Groover, A. (2020). Achieving Automated Directional Drilling Across us Onshore Basins. *Day 3 Thu, March 05, 2020, IADC/SPE-199605-MS*, 19. https://doi.org/10.2118/199605-MS

D'Angelo, J., Ashok, P., van Oort, E., Shahri, M., Thetford, T., Nelson, B., Behounek, M., & White, M. (2019). Unplanned Tortuosity Index: Separating Directional Drilling Performance from Planned Well Geometry. *Day 3 Thu, March 07, 2019*, *SPE/IADC-194099-MS*, 16. https://doi.org/10.2118/194099-MS

Dashevskiy, D., Macpherson, J., Mieting, R., & Wassermann, I. (2020). Advisory System for Drilling: Automatic Procedures Acting on Real-time Data. *Day 2 Wed, March 04, 2020, IADC/SPE-199657-MS*, 11. https://doi.org/10.2118/199657-MS

Demirer, N., Zalluhoglu, U., Marck, J., Gharib, H., & Darbe, R. (2019). A Model Predictive Control Method for Autonomous Directional Drilling. *October 01, 2019, SPE-195917-MS*, 1–7. https://doi.org/10.2118/195917-MS

Drillbotics®. (2020, September 23). *2021 Guidelines/Application Form*. Drillbotics.Com. https://drillbotics.com/guidelines/

Esmaeili, A., Elahifar, B., Fruhwirth, R. K., & Thonhauser, G. (2012). ROP Modeling Using Neural Network and Drill String Vibration Data. *10-12 December 2012*, *SPE-163330-MS*, 13. https://doi.org/10.2118/163330-MS

Farah, O. (2013). *Directional Well Design, Trajectory and Survey Calculations, with a Case Study in Fiale, Asal Rift, Djibouti* (No. 27; Reports 2013, pp. 625–658). United Nations University.

Going, W. S., Anderson, A. B., & Vachon, G. P. (2006). Intelligent Well Technology-The Evolution to Closed-Loop Control. *Offshore Technology Conference*, *OTC 17796*, 9. https://doi.org/10.4043/17796-MS

Hansen, C., Stokes, M., Mieting, R., Quattrone, F., Klemme, V., Nageshwara Rao, K., Wassermann, I., & Zaeper, R. (2020). *Automated Trajectory Drilling for Rotary Steerable Systems*. IADC/SPE International Drilling Conference and Exhibition, Galveston, Texas, USA. https://doi.org/10.2118/199647-MS

Hegde, C., Soares, C., & Gray, K. E. (2018). Rate of Penetration (ROP) Modeling Using Hybrid Models: Deterministic and Machine Learning. *Proceedings of the 6th Unconventional Resources Technology Conference, URTeC: 2896522*, 19. https://doi.org/10.15530/urtec-2018-

2896522

ISCWSA. (2013). *Collision Avoidance Calculations—Current Common Practice*. ISCWSA. https://www.iscwsa.net/media/files/files/b6fb074d/current-common-practice-in-collision-avoidance-calculations-oct-2017.pdf

ISCWSA. (2016, November 14). *Error Model Example File 1—MWDRev4 ISCWSA*. ISCWSA. https://www.iscwsa.net/articles/error-model-example-file-1-mwdrev4-iscwsa/

ISCWSA. (2017a, May 17). *Standard Set of Wellpaths for Evaluating Clearance Scenarios—Excel Workbook*. Www.Iscwsa.Net. https://www.iscwsa.net/articles/standard-wellpath-revision-4-excel/

ISCWSA. (2017b). *Definition of the ISCWSA Error Model Revision 4.3*. ISCWSA. https://www.iscwsa.net/articles/definition-of-the-iscwsa-error-model-revision-43/

Joshi, D. R., & Samuel, R. (2017). Automated Geometric Path Correction in Directional Drilling. *Day 2 Tue, October 10, 2017*, *SPE-187209-MS*, 23. https://doi.org/10.2118/187209-MS

Kuznetcov, A. (2016). *ROP Optimization and Modelling in Directional Drilling Process*. University of Stavanger (UiS).

Li, F., Ma, X., & Tan, Y. (2020). Review of the Development of Rotary Steerable Systems. *Journal of Physics: Conference Series*, *1617*, 7. https://doi.org/10.1088/1742-6596/1617/1/012085

Liu, Z., & Samuel, R. (2016). Wellbore-Trajectory Control by Use of Minimum Well-Profile-Energy Criterion for Drilling Automation. *SPE Journal*, *21*(02), 449–458. https://doi.org/10.2118/170861-PA

Ma, T., Chen, P., & Zhao, J. (2016). Overview on Vertical and Directional Drilling Technologies for the Exploration and Exploitation of Deep Petroleum Resources. *Geomechanics and Geophysics for Geo-Energy and Geo-Resources*, *2*(4), 365–395. https://doi.org/10.1007/s40948-016-0038-y

Mitchell, R. F., Miska, S., Aadnøy, B. S., & Society of Petroleum Engineers (U.S.) (Eds.). (2011). *Fundamentals of Drilling Engineering* (Vol. 12). Society of Petroleum Engineers.

Mittal, M., & Samuel, R. (2016). 3D Downhole Drilling Automation Based on Minimum Well Profile Energy. *Day 3 Wed, September 28, 2016*, *SPE-181381-MS*, 17. https://doi.org/10.2118/181381-MS

Muhammadali, S. (2017). *Error and Ellipses of Uncertainty Analysis in Far North*. Norwegian University of Science and Technology (NTNU).

Nabors Industries Ltd. (2018, July 2). *OrientXpress® Rotary Steering System (Video)*. YouTube. https://www.youtube.com/watch?v=iqsCFzoxv7g&t=28s

Nabors Industries Ltd. (2021). *OrientXpress® Rotary Steering System*. Nabors.Com. https://www.nabors.com/drilling-solutions/directional-automation/automated-wellbore-placement/orientxpress-rotary-steering

Nkengele, J. (2019). *Determination of Dogleg Severity and Side Force for Stuck Pipe Prevention* (TPG 4920). Norwegian University of Science and Technology (NTNU).

Pirovolou, D., Chapman, C. D., Chau, M., Arismendi, H., Ahorukomeye, M., & Penaranda, J. (2011). Drilling Automation: An Automatic Trajectory Control System. *19-21 April 2011*, *SPE-143899-MS*, 8. https://doi.org/10.2118/143899-MS

Ruszka, J. (2003, August). Rotary Steerable Drilling Technology Matures. *Drilling Contractor*, *59*(4), 44–45.

Sampaio, J. H. B. (2016). Designing Three-Dimensional Directional Well Trajectories Using Bézier Curves. *Journal of Energy Resources Technology*, *139*(3), 24.

https://doi.org/10.1115/1.4034810

Saramago, C. (2020). *Rotary Steerable System Modelling and Simulator*. University of Stavanger (UiS).

SPE, & DSATS. (2020). *2020-2021 Drillbotics Guidelines V.3* (Guidelines Version 3; pp. 1–10). Drillbotics®. https://drillbotics.com/wp-content/uploads/simple-file-list/Guidelines/Guidelines-2021/2021-Drillbotics-Guidelines-v3.pdf

Stepnov, A., Chatar, C., El Hawy, A., Cassel, J., Abouassi, B., & Khader, C. (2019). The Digital Directional Drilling Evolution. *November 12, 2019, SPE-197301-MS*, 1–10. https://doi.org/10.2118/197301-MS

Stump, J. (2019, April 1). *New Rotary Steerable Systems Aim to Enhance Drilling Efficiency*. Offshore Magazine. https://www.offshore-mag.com/drilling-completion/article/16763947/new-rotary-steerable-systems-aim-to-enhance-drilling-efficiency

Teale, R. (1965). The concept of specific energy in rock drilling. *International Journal of Rock Mechanics and Mining Sciences & Geomechanics Abstracts*, *2*(1), 57–73. https://doi.org/10.1016/0148-9062(65)90022-7

Trochim, W. (2006, October 20). *Measurement Error*. Conjoint.Ly. https://conjointly.com/kb/measurement-error/

Wang, H., Zhi-Chuan, G., Yu-Cai, S., & De-Yang, L. (2017). Study on Build-up Rate of Push-the-bit Rotary Steerable Bottom Hole Assembly. *Journal of Applied Science and Engineering*, *20*(3), 401–408. https://doi.org/10.6180/jase.2017.20.3.15

Weijermans, P., Ruszka, J., Jamshidian, H., & Matheson, M. (2001). Drilling with Rotary Steerable System Reduces Wellbore Tortuosity. *27 February, SPE/IADC 67715*, 10. https://doi.org/10.2118/67715-MS

Wiktorski, E., Kuznetcov, A., & Sui, D. (2017). ROP Optimization and Modeling in Directional Drilling Process. *Day 1 Wed, April 05, 2017, SPE-185909-MS*, 15. https://doi.org/10.2118/185909-MS

Zhou, Y., Zheng, D., Ashok, P., & va Oort, E. (2016). Improved Wellbore Quality Using a Novel Real-Time Tortuosity Index. *Day 3 Thu, March 03, 2016, IADC/SPE-178869-MS*, 10. https://doi.org/10.2118/178869-MS

Appendix A

The complete list of the input parameters used by the RSS Simulator is presented in the following tables.

Table A1: Inputs Used in the PWP Function

Planned Well Path (PWP)		
Parameter	**Symbol**	**Unit**
Tolerance for considering two different segments	$Tolerance$	°
Survey points for the hold section	Sur_{pts}	m
Step for "u" in the Beziér curve calculation	$Step_u$	-
Range tolerance for searching for the best D_S and D_E value	Ran_{Tol}	m
Maximum DLS for the PWP	Max_{DLS}	°/30m

Table A2: Inputs Used in the RSS Model Function

RSS Model		
Parameter	**Symbol**	**Unit**
Time step for the Simulation (Resolution)	Δt	s
OD of the RSS tool	OD	m
ID of the RSS tool	ID	m
Distance actuator - bit	a	m
Distance actuator - stabilizer	b	m
Borehole diameter	Db	m
Delta between simulated survey points	$Delta_{Sur}$	m
Error Noise that will be added to the other modules data	$Error_{input}$	-
Maximum opening offset of the tool (0% to 100%)	$maxoff$	-
Elasticity modulus	E	Pa
Maximum physical opening of the offset	$Offset_L$	m
Maximum degree of tolerance for the activation of offset	Max_{deg}	°

Table A3: Inputs Used in the Deviation Control Function

Deviation Control		
Parameter	**Symbol**	**Unit**
Gravity	G	m/s2
Total magnetic field	MF	nT
Magnetic dip angle	Dip	°
Standard deviation used in the Ellipse of Uncertainty	SF	-
Depth Scale Factor – Systematic error	L_DSFS	-

MWD: Z-Accelerometer Bias Error – Systematic error	L_ABZ	m/s2
MWD: Z-Accelerometer Scale Error – Systematic error	L_ASZ	-
MWD: TF Ind: X and Y Magnetometer Bias – Systematic error	L_MBXY1	nT
MWD: RF Ind: X and Y Magnetometer Scale Factor – Systematic error	L_MSXY1	-
Minimum radius of EOU	Min_R	m

Table A4: Inputs Used in the CP Function

Correction Path (CP)		
Parameter	**Symbol**	**Unit**
Maximum DLS that could be applied to the curve	$Max_{DLS\ Corr}$	°/30m
Maximum tortuosity that could be applied to the curve	$Tor_{Max\ Corr}$	°/30m
Step for "u" in the Beziér curve calculation	$Step_{u\ Corr}$	-
Boolean that allows that reach point will be on any PWP survey point and not only on the hold sections	$Reach_{all}$	-
Boolean that allows applying the correction path or not	CP_{Active}	-

Table A5: Inputs Coming from External Modules

External Modules (Models)		
Parameter	**Symbol**	**Unit**
Sliding factor coefficient	μ	-
Revolutions per minute	RPM	rpm
Weight on Bit	WOB	N
Specific energy of the rock	Es	Pa
Steerability of the bit	$steer$	-

Table A6: Inputs Imported from the Survey Data Points

Survey Data Points (Excel)		
Parameter	**Symbol**	**Unit**
Vertical coordinate	V	m
North coordinate	N	m
East coordinate	E	m

The outputs coming from the RSS Simulator are shown in the following tables.

Table A7: Output from the PWP function

Planned Well Path (PWP)		
Parameter	**Symbol**	**Unit**
Vertical coordinate	V	m
North coordinate	N	m
East coordinate	E	m
Measured depth	MD	m
Inclination	Inc	°
Azimuth	Azi	°
Dogleg Severity	DLS	°/30m

Table A8: Outputs from the RSS Model Function

Simulation Results		
Parameter	**Symbol**	**Unit**
Measure depth	MD	m
Time	t	min
Inclination	Inc	°
Azimuth	Azi	°
Horizontal Displacement	HD	m
True Vertical Depth	TVD	m
East coordinate	E	m
North coordinate	N	m
Offset applied (percentage of opening of the actuator)	$Offset$	-
Dog Leg Severity	DLS	°/30m
Total force on the bit for the inclination	$Tot\ F_{Inc}$	N
Total force on the bit for the azimuth	$Tot\ F_{Azi}$	N
ROP axial	ROP_{Axial}	m/hr
ROP inclination	ROP_{Inc}	m/hr
ROP azimuth	ROP_{Azi}	m/hr

Table A9: Outputs from the Deviation Control Function

Deviation Points Analysis		
Parameter	**Symbol**	**Unit**
Measure depth	MD	m
Vertical coordinate Vector of Error (VEC)	V_{VEC}	m
East coordinate Vector of Error (VEC)	E_{VEC}	m
North coordinate Vector of Error (VEC)	N_{VEC}	m
Length Vector of Error (VEC)	$Length_{VEC}$	m
Vertical coordinate Ellipse of Uncertainty (EOU)	V_{EOU}	m
East coordinate Ellipse of Uncertainty (EOU)	E_{EOU}	m
North coordinate Ellipse of Uncertainty (EOU)	N_{EOU}	m
Length Ellipse of Uncertainty (EOU)	$Length_{EOU}$	m
Boolean that indicates if the bit is in (non-deviated) or out (deviated) of the EOU	$Out\ EOU$	-

Appendix B

The correspondent tables used for the 3D case study are showed in this appendix. Table B1 was obtained from the ISCWSA Excel example for evaluating clearance scenarios (ISCWSA, 2017a) from the well 03.

Table B1: Input Survey Stations for 3D Study Case

Survey N°	V [m]	N [m]	E [m]
0	0.00	0.00	0.00
1	1.00	0.00	0.00
2	30.00	0.00	0.00
3	60.00	0.00	0.00
4	90.00	0.00	0.00
5	120.00	0.00	0.00
6	150.00	0.00	0.00
7	180.00	0.00	0.00
8	210.00	0.00	0.00
9	240.00	0.00	0.00
10	270.00	0.00	0.00
11	300.00	0.00	0.00
12	330.00	0.00	0.00
13	360.00	0.00	0.00
14	390.00	0.00	0.00
15	420.00	0.00	0.00
16	450.00	0.00	0.00
17	480.00	0.00	0.00
18	510.00	0.00	0.00
19	540.00	0.00	0.00
20	570.00	0.00	0.00
21	600.00	0.00	0.00
22	630.00	0.00	0.00
23	660.00	0.00	0.00
24	690.00	0.00	0.00
25	720.00	0.00	0.00
26	750.00	0.00	0.00
27	780.00	0.00	0.00
28	810.00	0.00	0.00
29	840.00	0.00	0.00
30	870.00	0.00	0.00
31	900.00	0.00	0.00
32	930.00	0.00	0.00
33	960.00	0.00	0.00
34	990.00	0.00	0.00
35	1020.00	-0.35	0.03
36	1049.97	-1.56	0.14
37	1079.88	-3.82	0.33
38	1109.70	-7.11	0.62
39	1139.38	-11.44	1.00
40	1168.89	-16.80	1.47
41	1198.20	-23.18	2.03

42	1227.27	-30.58	2.68
43	1256.05	-38.98	3.41
44	1284.53	-48.38	4.23
45	1312.66	-58.76	5.14
46	1340.41	-70.12	6.13
47	1367.74	-82.43	7.21
48	1394.63	-95.68	8.37
49	1421.03	-109.87	9.61
50	1446.93	-124.96	10.93
51	1472.28	-140.94	12.33
52	1497.05	-157.79	13.81
53	1521.22	-175.50	15.35
54	1544.75	-194.03	16.98
55	1567.62	-213.37	18.67
56	1589.79	-233.50	20.43
57	1611.26	-254.38	22.22
58	1632.01	-275.98	23.84
59	1652.05	-298.27	25.12
60	1671.35	-321.21	26.05
61	1689.89	-344.79	26.63
62	1707.64	-368.97	26.87
63	1724.59	-393.72	26.76
64	1740.72	-419.01	26.30
65	1756.00	-444.81	25.50
66	1770.41	-471.10	24.35
67	1783.94	-497.83	22.85
68	1796.58	-524.97	21.01
69	1808.30	-552.50	18.83
70	1819.10	-580.38	16.31
71	1828.95	-608.57	13.46
72	1837.85	-637.04	10.28
73	1845.79	-665.75	6.77
74	1852.75	-694.68	2.93
75	1858.73	-723.78	-1.22
76	1863.72	-753.02	-5.69
77	1867.72	-782.37	-10.46
78	1870.78	-811.78	-15.52
79	1873.39	-841.21	-20.71
80	1876.00	-870.64	-25.90
81	1878.62	-900.07	-31.09
82	1881.23	-929.50	-36.28
83	1883.85	-958.94	-41.47
84	1886.46	-988.37	-46.66
85	1889.08	-1017.80	-51.85
86	1891.69	-1047.23	-57.04
87	1894.31	-1076.66	-62.23
88	1896.92	-1106.09	-67.41
89	1899.54	-1135.53	-72.60
90	1902.15	-1164.96	-77.79
91	1904.77	-1194.39	-82.98

92	1907.38	-1223.82	-88.17
93	1910.00	-1253.25	-93.36
94	1912.61	-1282.69	-98.55
95	1915.22	-1312.12	-103.74

Table B2: PWP Survey Stations Generated for the 3D Study Case

Survey	V [m]	N [m]	E [m]	MD [m]	Inc [°]	Azi [°]	DLS [°/30m]
0	0.0000	0.0000	0.0000	0.0000	0.0000	0.0000	0.0000
1	50.0000	0.0000	0.0000	50.0000	0.0000	0.0000	0.0000
2	100.0000	0.0000	0.0000	100.0000	0.0000	0.0000	0.0000
3	150.0000	0.0000	0.0000	150.0000	0.0000	0.0000	0.0000
4	200.0000	0.0000	0.0000	200.0000	0.0000	0.0000	0.0000
5	250.0000	0.0000	0.0000	250.0000	0.0000	0.0000	0.0000
6	300.0000	0.0000	0.0000	300.0000	0.0000	0.0000	0.0000
7	350.0000	0.0000	0.0000	350.0000	0.0000	0.0000	0.0000
8	400.0000	0.0000	0.0000	400.0000	0.0000	0.0000	0.0000
9	450.0000	0.0000	0.0000	450.0000	0.0000	0.0000	0.0000
10	500.0000	0.0000	0.0000	500.0000	0.0000	0.0000	0.0000
11	550.0000	0.0000	0.0000	550.0000	0.0000	0.0000	0.0000
12	600.0000	0.0000	0.0000	600.0000	0.0000	0.0000	0.0000
13	650.0000	0.0000	0.0000	650.0000	0.0000	0.0000	0.0000
14	700.0000	0.0000	0.0000	700.0000	0.0000	0.0000	0.0000
15	750.0000	0.0000	0.0000	750.0000	0.0000	0.0000	0.0000
16	800.0000	0.0000	0.0000	800.0000	0.0000	0.0000	0.0000
17	850.0000	0.0000	0.0000	850.0000	0.0000	0.0000	0.0000
18	900.0000	0.0000	0.0000	900.0000	0.0000	0.0000	0.0000
19	950.0000	0.0000	0.0000	950.0000	0.0000	0.0000	0.0000
20	990.0000	0.0000	0.0000	990.0000	0.0000	0.0000	4.6142
21	1010.8280	-0.5643	0.0516	1010.8357	3.0738	174.8124	4.2408
22	1032.0163	-2.2378	0.2017	1032.0906	5.9525	174.9255	3.8900
23	1053.5343	-4.9910	0.4432	1053.7853	8.6464	175.0417	3.5657
24	1075.3511	-8.7946	0.7690	1075.9336	11.1675	175.1611	3.2694
25	1097.4361	-13.6193	1.1721	1098.5431	13.5284	175.2838	3.0013
26	1119.7586	-19.4357	1.6453	1121.6157	15.7420	175.4101	2.7603
27	1142.2879	-26.2145	2.1817	1145.1488	17.8207	175.5399	2.5450
28	1164.9932	-33.9264	2.7740	1169.1354	19.7768	175.6735	2.3533
29	1187.8438	-42.5420	3.4153	1193.5647	21.6217	175.8110	2.1832
30	1210.8090	-52.0319	4.0985	1218.4228	23.3662	175.9527	2.0328
31	1233.8581	-62.3669	4.8164	1243.6931	25.0203	176.0987	1.9001
32	1256.9603	-73.5176	5.5620	1269.3565	26.5933	176.2492	1.7834
33	1280.0851	-85.4547	6.3283	1295.3917	28.0937	176.4044	1.6809
34	1303.2015	-98.1487	7.1080	1321.7757	29.5296	176.5645	1.5912
35	1326.2790	-111.5704	7.8943	1348.4840	30.9081	176.7298	1.5132
36	1349.2868	-125.6904	8.6799	1375.4905	32.2361	176.9006	1.4456
37	1372.1943	-140.4795	9.4578	1402.7682	33.5198	177.0770	1.3875
38	1394.9705	-155.9081	10.2210	1430.2888	34.7651	177.2594	1.3380
39	1417.5850	-171.9471	10.9623	1458.0235	35.9774	177.4481	1.2966
40	1440.0069	-188.5670	11.6746	1485.9425	37.1619	177.6434	1.2625
41	1462.2056	-205.7386	12.3510	1514.0156	38.3235	177.8456	1.2354
42	1484.1502	-223.4324	12.9842	1542.2121	39.4669	178.0552	1.2148

43	1505.8102	-241.6192	13.5673	1570.5008	40.5966	178.2725	1.2005
44	1527.1547	-260.2695	14.0932	1598.8504	41.7169	178.4980	1.1922
45	1548.1532	-279.3542	14.5547	1627.2295	42.8321	178.7321	1.1900
46	1568.7748	-298.8437	14.9448	1655.6063	43.9465	178.9753	1.1936
47	1588.9888	-318.7088	15.2564	1683.9493	45.0643	179.2282	1.2032
48	1608.7645	-338.9201	15.4825	1712.2270	46.1897	179.4913	1.2189
49	1628.0713	-359.4484	15.6159	1740.4082	47.3273	179.7652	1.2410
50	1646.8784	-380.2641	15.6496	1768.4618	48.4813	180.0507	1.2696
51	1665.1550	-401.3381	15.5764	1796.3572	49.6566	180.3484	1.3053
52	1682.8705	-422.6410	15.3894	1824.0643	50.8579	180.6592	1.3484
53	1699.9942	-444.1434	15.0815	1851.5537	52.0904	180.9838	1.3996
54	1716.4953	-465.8159	14.6455	1878.7966	53.3595	181.3233	1.4597
55	1732.3431	-487.6294	14.0744	1905.7652	54.6711	181.6786	1.5293
56	1747.5069	-509.5543	13.3611	1932.4327	56.0313	182.0509	1.6096
57	1761.9560	-531.5614	12.4985	1958.7734	57.4469	182.4413	1.7017
58	1775.6597	-553.6213	11.4796	1984.7631	58.9251	182.8511	1.8068
59	1788.5872	-575.7046	10.2972	2010.3794	60.4737	183.2819	1.9264
60	1800.7079	-597.7822	8.9443	2035.6016	62.1012	183.7352	2.0621
61	1811.9910	-619.8245	7.4138	2060.4112	63.8167	184.2128	2.2157
62	1822.4058	-641.8023	5.6987	2084.7922	65.6300	184.7166	2.3891
63	1831.9216	-663.6862	3.7918	2108.7315	67.5516	185.2487	2.5843
64	1840.5077	-685.4468	1.6861	2132.2194	69.5927	185.8114	2.8033
65	1848.1333	-707.0549	-0.6255	2155.2499	71.7651	186.4075	3.0477
66	1854.7678	-728.4811	-3.1501	2177.8214	74.0807	187.0398	3.3190
67	1860.3805	-749.6961	-5.8948	2199.9372	76.5517	187.7115	3.6178
68	1864.9405	-770.6704	-8.8666	2221.6063	79.1898	188.4262	3.9437
69	1868.4173	-791.3748	-12.0727	2242.8440	82.0058	189.1880	4.2945
70	1870.7800	-811.7800	-15.5200	2263.6727	85.0086	190.0013	0.0000
71	1875.1303	-860.8333	-24.1706	2313.6727	85.0086	190.0013	0.0000
72	1879.4806	-909.8865	-32.8212	2363.6727	85.0086	190.0013	0.0000
73	1883.8309	-958.9398	-41.4718	2413.6727	85.0086	190.0013	0.0000
74	1888.1812	-1007.9931	-50.1224	2463.6727	85.0086	190.0013	0.0000
75	1892.5315	-1057.0464	-58.7730	2513.6727	85.0086	190.0013	0.0000
76	1896.8818	-1106.0996	-67.4237	2563.6727	85.0086	190.0013	0.0000
77	1901.2321	-1155.1529	-76.0743	2613.6727	85.0086	190.0013	0.0000
78	1905.5825	-1204.2062	-84.7249	2663.6727	85.0086	190.0013	0.0000
79	1909.9328	-1253.2594	-93.3755	2713.6727	85.0086	190.0013	0.0000
80	1915.2200	-1312.1200	-103.7400	2773.6723	85.0086	190.0013	0.0000

Table B3: Simulation Result (Shorth Version) for the 3D Study Case

	MD [m]	Time [min]	Inc [°]	Azi [°]	HD [m]	TVD [m]	East [m]	North [m]	Offset []	DLS [°/30m]	Tot Force inc [N]	Tot Force azi [N]	ROP Ax [m/hr]	ROP Inc [m/hr]	ROP Azi [m/hr]
0	0.0000	0.0000	0.0000	0.0000	0.0000	0.0000	0.0000	0.0000	0.0000	0.0000	0.0000	0.0000	0.0000	0.0000	0.0000
1	30.0961	136.0000	0.0000	0.0000	0.0000	30.0961	0.0000	0.0000	0.0000	0.0000	0.0000	0.0000	13.2777	0.0000	0.0000
2	59.9693	315.0000	0.0000	0.0000	0.0000	59.9693	0.0000	0.0000	0.0000	0.0000	0.0000	0.0000	10.0134	0.0000	0.0000
3	89.9606	480.0000	0.0000	0.0000	0.0000	89.9606	0.0000	0.0000	0.0000	0.0000	0.0000	0.0000	10.9114	0.0000	0.0000
4	120.0752	643.0000	0.0000	0.0000	0.0000	120.0752	0.0000	0.0000	0.0000	0.0000	0.0000	0.0000	11.0862	0.0000	0.0000
5	149.9486	787.0000	0.0000	0.0000	0.0000	149.9486	0.0000	0.0000	0.0000	0.0000	0.0000	0.0000	12.4472	0.0000	0.0000
6	180.0043	926.0000	0.0000	0.0000	0.0000	180.0043	0.0000	0.0000	0.0000	0.0000	0.0000	0.0000	12.9775	0.0000	0.0000
7	209.9738	1105.0000	0.0000	0.0000	0.0000	209.9738	0.0000	0.0000	0.0000	0.0000	0.0000	0.0000	10.0457	0.0000	0.0000
8	240.0777	1281.0000	0.0000	0.0000	0.0000	240.0777	0.0000	0.0000	0.0000	0.0000	0.0000	0.0000	10.2639	0.0000	0.0000
9	269.9660	1438.0000	0.0000	0.0000	0.0000	269.9660	0.0000	0.0000	0.0000	0.0000	0.0000	0.0000	11.4223	0.0000	0.0000
10	299.9877	1616.0000	0.0000	0.0000	0.0000	299.9877	0.0000	0.0000	0.0000	0.0000	0.0000	0.0000	10.1123	0.0000	0.0000
11	329.9836	1754.0000	0.0000	0.0000	0.0000	329.9836	0.0000	0.0000	0.0000	0.0000	0.0000	0.0000	13.0631	0.0000	0.0000
12	359.9214	1912.0000	0.0000	0.0000	0.0000	359.9214	0.0000	0.0000	0.0000	0.0000	0.0000	0.0000	11.3580	0.0000	0.0000
13	389.9254	2059.0000	0.0000	0.0000	0.0000	389.9254	0.0000	0.0000	0.0000	0.0000	0.0000	0.0000	12.2526	0.0000	0.0000
14	420.0538	2233.0000	0.0000	0.0000	0.0000	420.0538	0.0000	0.0000	0.0000	0.0000	0.0000	0.0000	10.3783	0.0000	0.0000
15	450.0946	2367.0000	0.0000	0.0000	0.0000	450.0946	0.0000	0.0000	0.0000	0.0000	0.0000	0.0000	13.4511	0.0000	0.0000
16	479.9149	2524.0000	0.0000	0.0000	0.0000	479.9149	0.0000	0.0000	0.0000	0.0000	0.0000	0.0000	11.3963	0.0000	0.0000
17	509.9816	2676.0000	0.0000	0.0000	0.0000	509.9816	0.0000	0.0000	0.0000	0.0000	0.0000	0.0000	11.8716	0.0000	0.0000
18	540.0865	2825.0000	0.0000	0.0000	0.0000	540.0865	0.0000	0.0000	0.0000	0.0000	0.0000	0.0000	12.1245	0.0000	0.0000
19	570.0317	2973.0000	0.0000	0.0000	0.0000	570.0317	0.0000	0.0000	0.0000	0.0000	0.0000	0.0000	12.1399	0.0000	0.0000
20	600.0767	3124.0000	0.0000	0.0000	0.0000	600.0767	0.0000	0.0000	0.0000	0.0000	0.0000	0.0000	11.9384	0.0000	0.0000
21	630.0167	3268.0000	0.0000	0.0000	0.0000	630.0167	0.0000	0.0000	0.0000	0.0000	0.0000	0.0000	12.4750	0.0000	0.0000
22	659.9741	3394.0000	0.0000	0.0000	0.0000	659.9741	0.0000	0.0000	0.0000	0.0000	0.0000	0.0000	14.2654	0.0000	0.0000
23	689.9229	3531.0000	0.0000	0.0000	0.0000	689.9229	0.0000	0.0000	0.0000	0.0000	0.0000	0.0000	13.1078	0.0000	0.0000
24	720.0383	3662.0000	0.0000	0.0000	0.0000	720.0383	0.0000	0.0000	0.0000	0.0000	0.0000	0.0000	13.7986	0.0000	0.0000
25	750.0682	3793.0000	0.0000	0.0000	0.0000	750.0682	0.0000	0.0000	0.0000	0.0000	0.0000	0.0000	13.7541	0.0000	0.0000
26	780.0097	3937.0000	0.0000	0.0000	0.0000	780.0097	0.0000	0.0000	0.0000	0.0000	0.0000	0.0000	12.4756	0.0000	0.0000
27	809.9008	4061.0000	0.0000	0.0000	0.0000	809.9008	0.0000	0.0000	0.0000	0.0000	0.0000	0.0000	14.4634	0.0000	0.0000
28	839.9576	4226.0000	0.0000	0.0000	0.0000	839.9576	0.0000	0.0000	0.0000	0.0000	0.0000	0.0000	10.9082	0.0000	0.0000
29	869.9376	4352.0000	0.0000	0.0000	0.0000	869.9376	0.0000	0.0000	0.0000	0.0000	0.0000	0.0000	14.3031	0.0000	0.0000
30	900.0903	4493.0000	0.0000	0.0000	0.0000	900.0903	0.0000	0.0000	0.0000	0.0000	0.0000	0.0000	12.8204	0.0000	0.0000
31	929.9235	4644.0000	0.0000	0.0000	0.0000	929.9235	0.0000	0.0000	0.0000	0.0000	0.0000	0.0000	11.8542	0.0000	0.0000

32	959.9365	4821.0000	0.0000	0.0000	0.0000	959.9365	0.0000	0.0000	0.0000	0.0000	0.0000	0.0000	10.1644	0.0000	0.0000
33	989.9069	4954.0000	0.0000	0.0000	0.0000	989.9069	0.0000	0.0000	0.0000	0.0000	0.0000	0.0000	13.5459	0.0000	0.0000
34	1019.8898	5085.0000	4.5603	174.8164	1.2240	1019.8589	0.1106	-1.2190	0.9000	6.9902	28077.2794	53.1757	13.7210	0.7676	0.0014
35	1049.9400	5236.0000	8.3916	174.8348	4.7386	1049.6952	0.4276	-4.7192	0.0054	0.0000	271.4269	68.1037	11.9200	0.0064	0.0016
36	1079.9397	5374.0000	11.6292	174.8688	10.0006	1079.2255	0.8998	-9.9600	0.9000	7.8717	28375.8712	193.7036	13.0429	0.7814	0.0053
37	1109.9412	5521.0000	15.4471	174.9237	17.0758	1108.3761	1.5292	-17.0072	0.0092	0.2921	877.0599	150.1933	12.2296	0.0264	0.0045
38	1139.9259	5674.0000	17.6707	174.9781	25.6031	1137.1180	2.2795	-25.5014	0.0084	0.0000	121.5699	149.4584	11.7505	0.0031	0.0038
39	1169.9803	5835.0000	19.9073	175.1731	35.4637	1165.5048	3.1297	-35.3253	0.9000	7.4658	20795.4912	-275.1549	11.1922	0.5452	-0.0072
40	1200.0851	5966.0000	20.2621	175.3257	45.7881	1193.7832	3.9955	-45.6133	0.0145	0.7007	2690.7561	-143.5904	13.8077	0.0773	-0.0041
41	1229.9208	6134.0000	22.6923	176.0409	56.6622	1221.5617	4.8068	-56.4571	0.0135	2.0898	5274.6349	-308.5209	10.6525	0.1379	-0.0081
42	1259.9269	6310.0000	25.5401	176.1716	68.9506	1248.9323	5.6374	-68.7174	0.0131	1.1763	3228.8207	159.2538	10.2242	0.0716	0.0035
43	1289.9962	6477.0000	27.3716	176.2107	82.3988	1275.8253	6.5299	-82.1359	0.0099	0.8755	2686.5642	55.6064	10.7963	0.0592	0.0012
44	1319.9868	6643.0000	28.5019	176.2733	96.3433	1302.3763	7.4483	-96.0501	0.0143	1.8399	4707.9016	-163.9473	10.8392	0.1256	-0.0044
45	1349.9178	6801.0000	31.6971	176.8896	111.3354	1328.2743	8.3304	-111.0162	0.0142	1.6283	4628.7753	-56.0442	11.3647	0.1224	-0.0015
46	1379.9579	6914.0000	33.0506	176.9286	127.5327	1353.5729	9.2032	-127.1899	0.0123	0.0910	330.1802	118.4042	16.0249	0.0107	0.0038
47	1409.9704	7086.0000	34.6571	176.9566	144.0329	1378.6413	10.0831	-143.6666	0.0049	1.2657	3295.8462	73.3876	10.4345	0.0803	0.0018
48	1440.0254	7229.0000	34.7254	177.0519	161.1453	1403.3485	10.9886	-160.7551	0.9000	3.1080	348.4263	18841.9174	12.6256	0.0093	0.5065
49	1469.9159	7392.0000	36.8614	177.8183	178.5614	1427.6347	11.7410	-178.1547	0.0141	1.2787	3632.0191	170.4477	10.9995	0.0901	0.0042
50	1500.0349	7576.0000	37.7420	177.8605	196.8798	1451.5423	12.4301	-196.4602	0.0090	0.1489	417.2941	42.4402	9.7955	0.0087	0.0009
51	1529.9499	7757.0000	39.3650	177.8735	215.4887	1474.9618	13.1231	-215.0562	0.0033	0.0000	108.3076	46.6178	9.9078	0.0023	0.0010
52	1559.9706	7938.0000	40.4492	177.9038	234.7533	1497.9846	13.8335	-234.3077	0.0061	0.0000	112.4018	89.0448	9.9506	0.0025	0.0020
53	1590.1050	8072.0000	41.2767	177.9456	254.4905	1520.7549	14.5488	-254.0320	0.0117	0.0000	242.6971	156.3620	13.5178	0.0074	0.0048
54	1619.9940	8223.0000	42.5895	178.1154	274.5130	1542.9435	15.2284	-274.0429	0.0101	0.0000	152.6831	150.9326	11.8740	0.0038	0.0037
55	1650.0514	8408.0000	43.8729	178.3884	295.1771	1564.7683	15.8395	-294.6978	0.0078	0.0000	49.6920	118.1477	9.7353	0.0011	0.0026
56	1680.0674	8567.0000	43.8803	179.3822	315.9771	1586.4030	16.3511	-315.4913	0.9000	3.8502	217.3243	16749.3692	11.3252	0.0054	0.4149
57	1709.9609	8712.0000	46.6254	181.1192	337.1505	1607.4912	16.1051	-336.6623	0.9000	5.5703	20983.2963	-1.4068	12.3631	0.4959	0.0000
58	1739.9426	8876.0000	46.8235	180.3667	358.9983	1628.0204	15.7864	-358.5075	0.0012	0.1882	50.9889	-799.7650	10.9595	0.0012	-0.0188
59	1769.9491	9030.0000	48.4942	180.3456	381.3126	1648.0810	15.6511	-380.8214	0.9000	7.5458	24545.8616	1.2768	11.6925	0.6015	0.0000
60	1799.9610	9209.0000	50.3259	180.3534	404.0950	1667.6170	15.5134	-403.6034	0.0101	4.1553	12443.8206	175.8978	10.0483	0.2441	0.0034
61	1829.9297	9394.0000	51.9991	180.4401	427.3456	1686.5246	15.3546	-426.8535	0.0076	1.8987	4470.3508	316.9363	9.7161	0.1042	0.0074
62	1859.9760	9581.0000	53.0720	180.8302	451.1165	1704.9000	15.1247	-450.6232	0.0092	0.3706	992.1523	343.1396	9.6390	0.0197	0.0068
63	1889.9090	9728.0000	54.2605	181.1424	475.1513	1722.7386	14.7274	-474.6546	0.0112	0.1192	345.9543	268.9385	12.2327	0.0092	0.0071
64	1920.0638	9861.0000	55.6114	181.5223	499.7736	1740.1425	14.1646	-499.2704	0.0112	0.1072	250.1792	259.9580	13.6102	0.0073	0.0076
65	1949.9717	9991.0000	56.9874	181.8829	524.6342	1756.7641	13.4208	-524.1197	0.0120	0.1057	237.1019	265.6345	13.8000	0.0063	0.0070
66	1979.8978	10131.0000	58.5102	182.3395	549.9706	1772.6839	12.4613	-549.4378	0.0109	0.1138	222.9411	254.7634	12.8146	0.0060	0.0069

67	2009.9715	10269.0000	60.0784	182.7923	575.9067	1787.9010	11.2508	-575.3456	0.0104	0.1116	213.2372	246.4123	13.0733	0.0058	0.0067
68	2040.0460	10440.0000	60.6220	183.3584	601.9990	1802.8540	9.9204	-601.4038	0.0134	1.0265	1940.5609	1992.9068	10.5368	0.0492	0.0505
69	2070.0575	10600.0000	63.7447	184.7862	628.5006	1816.9235	8.0287	-627.8371	0.0147	2.5134	6512.5095	2121.9321	11.2360	0.1772	0.0577
70	2099.9397	10749.0000	67.1004	185.3913	655.6912	1829.3038	5.5759	-654.9167	0.0143	1.1820	3348.8194	360.8497	12.0269	0.0987	0.0106
71	2129.8973	10889.0000	68.9260	185.4878	683.5018	1840.4374	2.9369	-682.6018	0.9000	6.3001	19659.2753	234.7041	12.8297	0.6043	0.0072
72	2160.0354	11028.0000	71.2097	185.9109	711.7929	1850.8159	0.1946	-710.7597	0.9000	6.2568	22460.3431	2735.4272	13.0060	0.6128	0.0745
73	2190.0022	11161.0000	75.0158	187.0476	740.4581	1859.5221	-3.0367	-739.2416	0.9000	5.4574	16098.2621	13782.6285	13.5092	0.4472	0.3827
74	2220.0711	11329.0000	79.2785	188.2211	769.7924	1866.0887	-6.9796	-768.3092	0.0116	0.9799	2855.5169	703.5076	10.7329	0.0636	0.0157
75	2249.9138	11478.0000	82.3386	189.0441	799.2557	1870.8005	-11.4359	-797.4333	0.0141	1.9460	5949.4515	1239.8418	12.0140	0.1601	0.0333
76	2280.0587	11658.0000	84.3784	190.0027	829.1801	1874.4128	-16.2831	-826.9621	0.0142	2.5213	5348.5264	3181.5378	10.0352	0.1272	0.0756
77	2309.9200	11786.0000	86.7752	191.1722	858.9525	1876.6403	-21.8095	-856.2164	0.0148	0.5212	1984.6674	759.3775	13.9916	0.0552	0.0211
78	2339.9190	11938.0000	86.8982	191.2488	888.9070	1878.2738	-27.6433	-885.5974	0.0083	0.1233	-257.5047	-160.3720	11.8275	-0.0070	-0.0043
79	2370.0903	12064.0000	85.5476	190.5683	919.0072	1880.3005	-33.3489	-915.1516	0.0130	0.1014	-313.5551	-317.1497	14.3843	-0.0100	-0.0101
80	2400.0687	12231.0000	85.4435	190.4592	948.8929	1882.6558	-38.8013	-944.5356	0.0105	0.1354	-295.6788	-310.4316	10.7707	-0.0064	-0.0067
81	2430.0006	12373.0000	85.3891	190.4021	978.7291	1885.0484	-44.2024	-973.8789	0.0092	0.0000	-194.0771	-204.1079	12.6473	-0.0047	-0.0049
82	2460.0768	12506.0000	85.3436	190.3542	1008.7069	1887.4784	-49.6024	-1003.3663	0.0081	0.0000	-172.0943	-181.0119	13.5682	-0.0046	-0.0048
83	2489.9720	12688.0000	85.2702	190.2771	1038.5018	1889.9250	-54.9372	-1032.6798	0.0063	0.0000	-181.2772	-190.4738	9.8556	-0.0037	-0.0039
84	2519.9653	12818.0000	85.2400	190.2454	1068.3923	1892.4064	-60.2614	-1062.0923	0.0056	0.0000	-118.2208	-124.4630	13.8740	-0.0031	-0.0033
85	2549.9370	12952.0000	85.2131	190.2169	1098.2600	1894.9007	-65.5662	-1091.4851	0.0050	0.0000	-103.5723	-109.0641	13.4167	-0.0027	-0.0028
86	2579.9864	13087.0000	85.1887	190.1913	1128.2041	1897.4149	-70.8708	-1120.9555	0.0044	0.0000	-91.5381	-96.4076	13.3548	-0.0024	-0.0025
87	2610.0466	13241.0000	84.8616	189.8438	1158.1557	1899.9576	-76.1459	-1150.4390	0.0142	1.3483	-3450.3140	-2651.5519	11.7004	-0.0852	-0.0655
88	2640.0754	13418.0000	84.0807	189.0213	1188.0306	1902.9771	-80.9091	-1179.9314	0.0084	0.0000	180.8799	199.7231	10.1783	0.0036	0.0040
89	2669.9581	13561.0000	84.4110	189.4069	1217.7616	1905.9761	-85.6695	-1209.2788	0.0141	0.1163	317.1025	314.7086	12.5376	0.0081	0.0080
90	2699.9532	13701.0000	84.4944	189.4896	1247.6163	1908.8749	-90.5710	-1238.7283	0.0121	0.1134	277.0107	275.0050	12.8573	0.0074	0.0074
91	2729.9871	13873.0000	84.5874	189.5818	1277.5139	1911.7315	-95.5247	-1268.2128	0.0099	0.1394	268.7028	266.6305	10.4630	0.0054	0.0054

Table B4: Deviation Control Survey Points for the 3D Study Case

	MD [m]	V VOE [m]	N VOE [m]	E VOE [m]	Length VOE [m]	V EOU [m]	N EOU [m]	E EOU [m]	Length EOU [m]	Out EOU*
0	0.0000	0.0000	0.0000	0.0000	0.0000	0.0000	0.0000	0.0000	0.0000	0.0000
1	30.0961	30.0961	0.0000	0.0000	0.0000	31.0961	0.0000	0.0000	1.0000	0.0000
2	60.1362	60.1362	0.0000	0.0000	0.0000	59.1362	0.0000	0.0000	1.0000	0.0000
3	90.1424	90.1424	0.0000	0.0000	0.0000	91.1424	0.0000	0.0000	1.0000	0.0000
4	120.0752	120.0752	0.0000	0.0000	0.0000	121.0752	0.0000	0.0000	1.0000	0.0000
5	150.1560	150.1560	0.0000	0.0000	0.0000	151.1560	0.0000	0.0000	1.0000	0.0000

6	180.0042	180.0042	0.0000	0.0000	0.0000	179.0042	0.0000	0.0000	1.0000	0.0000
7	210.1412	210.1412	0.0000	0.0000	0.0000	211.1412	0.0000	0.0000	1.0000	0.0000
8	240.0777	240.0777	0.0000	0.0000	0.0000	239.0777	0.0000	0.0000	1.0000	0.0000
9	270.1564	270.1564	0.0000	0.0000	0.0000	271.1564	0.0000	0.0000	1.0000	0.0000
10	300.1562	300.1562	0.0000	0.0000	0.0000	301.1562	0.0000	0.0000	1.0000	0.0000
11	330.2013	330.2013	0.0000	0.0000	0.0000	331.2013	0.0000	0.0000	1.0000	0.0000
12	360.1107	360.1107	0.0000	0.0000	0.0000	361.1107	0.0000	0.0000	1.0000	0.0000
13	390.1296	390.1296	0.0000	0.0000	0.0000	391.1296	0.0000	0.0000	1.0000	0.0000
14	420.0538	420.0538	0.0000	0.0000	0.0000	421.0538	0.0000	0.0000	1.0000	0.0000
15	450.0946	450.0946	0.0000	0.0000	0.0000	449.0946	0.0000	0.0000	1.0000	0.0000
16	480.1048	480.1048	0.0000	0.0000	0.0000	481.1048	0.0000	0.0000	1.0000	0.0000
17	510.1795	510.1795	0.0000	0.0000	0.0000	511.1795	0.0000	0.0000	1.0000	0.0000
18	540.0865	540.0865	0.0000	0.0000	0.0000	539.0865	0.0000	0.0000	1.0000	0.0000
19	570.0317	570.0317	0.0000	0.0000	0.0000	569.0317	0.0000	0.0000	1.0000	0.0000
20	600.0767	600.0767	0.0000	0.0000	0.0000	601.0767	0.0000	0.0000	1.0000	0.0000
21	630.0167	630.0167	0.0000	0.0000	0.0000	631.0167	0.0000	0.0000	1.0000	0.0000
22	660.2118	660.2118	0.0000	0.0000	0.0000	661.2118	0.0000	0.0000	1.0000	0.0000
23	690.1413	690.1413	0.0000	0.0000	0.0000	691.1413	0.0000	0.0000	1.0000	0.0000
24	720.0383	720.0383	0.0000	0.0000	0.0000	721.0383	0.0000	0.0000	1.0000	0.0000
25	750.0682	750.0682	0.0000	0.0000	0.0000	751.0682	0.0000	0.0000	1.0000	0.0000
26	780.0097	780.0097	0.0000	0.0000	0.0000	781.0097	0.0000	0.0000	1.0000	0.0000
27	810.1418	810.1418	0.0000	0.0000	0.0000	811.1418	0.0000	0.0000	1.0000	0.0000
28	840.1394	840.1394	0.0000	0.0000	0.0000	839.1394	0.0000	0.0000	1.0000	0.0000
29	870.1760	870.1760	0.0000	0.0000	0.0000	869.1760	0.0000	0.0000	1.0000	0.0000
30	900.0903	900.0903	0.0000	0.0000	0.0000	899.0903	0.0000	0.0000	1.0000	0.0000
31	930.1211	930.1211	0.0000	0.0000	0.0000	931.1211	0.0000	0.0000	1.0000	0.0000
32	960.1059	960.1059	0.0000	0.0000	0.0000	959.1059	0.0000	0.0000	1.0000	0.0000
33	990.1327	990.1327	-0.0036	0.0003	0.0036	990.1327	-0.9958	0.0911	1.0000	0.0000
34	1020.1189	1020.0848	-1.2954	0.1172	0.0583	1020.0458	-2.2330	0.1956	1.0000	0.0000
35	1050.1387	1049.9180	-4.5283	0.4026	0.2231	1050.0092	-3.7628	0.3064	1.0000	0.0000
36	1080.1575	1079.4938	-9.6996	0.8446	0.3149	1079.6137	-9.0374	0.7160	1.0000	0.0000
37	1110.1451	1108.6982	-16.5537	1.4109	0.5371	1108.8064	-16.1164	1.3048	1.0000	0.0000

38	1140.1218	1137.5395	-24.7858	2.0686	0.8381	1137.5848	-24.6360	2.0269	1.0000	0.0000
39	1170.1671	1166.0577	-34.3278	2.8039	1.1738	1166.0019	-34.4849	2.8529	1.0000	1.0000
40	1200.0851	1193.7389	-45.7396	3.9410	0.1445	1193.4767	-46.4875	3.6188	1.0000	0.0000
41	1230.0984	1221.5824	-56.9034	4.6558	0.4331	1221.3952	-57.3981	4.4520	1.0000	0.0000
42	1260.0973	1248.8226	-69.3970	5.3678	0.7158	1248.7180	-69.6377	5.2588	1.0000	0.0000
43	1290.1761	1275.5756	-83.0624	6.1791	1.0034	1275.5770	-83.0596	6.1803	1.0000	1.0000
44	1320.1674	1302.4517	-96.2991	7.3928	0.1929	1302.1033	-96.9807	7.1371	1.0000	0.0000
45	1350.1072	1328.2150	-111.5093	8.1236	0.4987	1327.9934	-111.9051	7.9102	1.0000	0.0000
46	1380.2250	1353.3934	-127.9855	8.8487	0.8465	1353.3203	-128.1034	8.7830	1.0000	0.0000
47	1410.1443	1378.2587	-144.5875	9.6610	1.0652	1378.2909	-144.5372	9.6872	1.0000	1.0000
48	1440.0254	1403.3093	-160.8160	10.9076	0.1087	1402.9879	-161.3159	10.2432	1.0000	0.0000
49	1470.0992	1427.5741	-178.5653	11.4831	0.4495	1427.3201	-178.9335	11.1622	1.0000	0.0000
50	1500.0349	1451.1423	-196.9973	12.0366	0.7768	1451.0273	-197.1517	11.9236	1.0000	0.0000
51	1530.1151	1474.6294	-215.7558	12.7095	0.8602	1474.5546	-215.8525	12.6417	1.0000	0.0000
52	1560.1364	1497.7564	-234.8569	13.3505	0.7468	1497.6363	-235.0066	13.1854	1.0000	0.0000
53	1590.1050	1520.4477	-254.4091	13.9279	0.7887	1520.3654	-254.5101	13.7616	1.0000	0.0000
54	1620.1919	1542.8176	-274.5049	14.4374	0.9023	1542.7882	-274.5404	14.3513	1.0000	0.0000
55	1650.0514	1564.6032	-294.9011	14.8659	1.0083	1564.6045	-294.8994	14.8739	1.0000	1.0000
56	1680.0674	1586.3962	-315.5020	16.2036	0.1480	1586.3575	-315.5632	15.3547	1.0000	0.0000
57	1710.1670	1607.4174	-337.0223	15.7540	0.4602	1607.1649	-337.2690	15.3456	1.0000	0.0000
58	1740.1252	1627.7016	-359.0553	15.6133	0.6313	1627.4424	-359.2974	15.5127	1.0000	0.0000
59	1770.1443	1647.8046	-381.3322	15.6458	0.5453	1647.4664	-381.6361	15.6422	1.0000	0.0000
60	1800.1285	1667.3867	-404.0217	15.5529	0.4462	1666.9680	-404.3809	15.6029	1.0000	0.0000
61	1830.0917	1686.4436	-427.1277	15.3252	0.2344	1685.8536	-427.6067	15.2323	1.0000	0.0000
62	1860.1367	1705.0140	-450.7364	14.9489	0.1755	1705.0962	-450.6649	14.1316	1.0000	0.0000
63	1890.1129	1722.9717	-474.7303	14.4121	0.3441	1723.1890	-474.5591	13.8174	1.0000	0.0000
64	1920.0638	1740.3067	-499.1437	13.6998	0.5090	1740.4651	-499.0215	13.2514	1.0000	0.0000
65	1950.2017	1757.0944	-524.1567	12.7887	0.6766	1757.1923	-524.0822	12.4896	1.0000	0.0000
66	1980.1114	1773.0544	-549.4274	11.6733	0.8447	1773.1020	-549.3920	11.5297	1.0000	0.0000
67	2010.1894	1788.3464	-575.2934	10.3192	1.0111	1788.3427	-575.2960	10.3293	1.0000	1.0000
68	2040.0460	1802.7065	-601.4793	9.7421	0.2434	1802.2481	-601.7140	9.1878	1.0000	0.0000
69	2070.0575	1816.5442	-628.0072	7.5844	0.6084	1816.3002	-628.1167	7.2985	1.0000	0.0000

70	2100.1401	1828.7526	-655.3214	4.8233	0.9925	1828.7479	-655.3231	4.8178	1.0000	0.0000
71	2130.1114	1839.5749	-683.0827	1.9149	1.4027	1839.8445	-683.0017	2.2028	1.0000	1.0000
72	2160.0354	1850.6416	-710.8066	0.0170	0.2533	1850.1276	-710.9450	-0.5067	1.0000	0.0000
73	2190.0022	1859.1271	-739.3125	-3.4755	0.5946	1858.8579	-739.3609	-3.7746	1.0000	0.0000
74	2220.0711	1865.5381	-768.3401	-7.6689	0.8828	1865.4649	-768.3442	-7.7605	1.0000	0.0000
75	2250.1141	1870.0815	-797.6034	-12.4242	1.2135	1870.2127	-797.6079	-12.2558	1.0000	1.0000
76	2280.0587	1874.2174	-826.9508	-16.4974	0.2902	1873.7395	-826.9231	-17.0215	1.0000	0.0000
77	2310.1532	1876.1632	-856.3842	-22.3726	0.7158	1875.9685	-856.3601	-22.5783	1.0000	0.0000
78	2340.1162	1877.6456	-885.6940	-28.3460	0.9267	1877.5951	-885.6864	-28.3985	1.0000	0.0000
79	2370.0903	1879.9430	-915.1005	-33.7407	0.5329	1879.6296	-915.0557	-34.0842	1.0000	0.0000
80	2400.0687	1882.5521	-944.5203	-38.9289	0.1651	1882.0280	-944.4426	-39.5741	1.0000	0.0000
81	2430.0006	1885.1566	-973.8875	-44.1079	0.1439	1885.8000	-973.9385	-43.5455	1.0000	0.0000
82	2460.0768	1887.7735	-1003.3952	-49.3116	0.4153	1888.1889	-1003.4360	-48.9022	1.0000	0.0000
83	2490.1362	1890.3889	-1032.8859	-54.5123	0.6411	1890.6409	-1032.9111	-54.2581	1.0000	0.0000
84	2520.1966	1893.0043	-1062.3769	-59.7131	0.8279	1893.1246	-1062.3889	-59.5906	1.0000	0.0000
85	2550.1606	1895.6113	-1091.7735	-64.8972	0.9928	1895.6164	-1091.7740	-64.8921	1.0000	0.0000
86	2580.2090	1898.2257	-1121.2528	-70.0959	1.1387	1898.1292	-1121.2432	-70.1951	1.0000	1.0000
87	2610.0466	1900.1128	-1150.4538	-75.9884	0.2216	1900.6579	-1150.5058	-75.4351	1.0000	0.0000
88	2640.0754	1903.3213	-1179.9519	-80.5642	0.4877	1903.6829	-1179.9734	-80.2019	1.0000	0.0000
89	2670.1671	1906.0507	-1209.4861	-85.6560	0.0722	1906.7483	-1209.5140	-85.0449	1.0000	0.0000
90	2700.1675	1908.6612	-1238.9217	-90.8470	0.3364	1908.1990	-1238.8881	-91.3220	1.0000	0.0000
91	2730.1614	1911.2881	-1268.3480	-96.0324	0.6648	1911.0563	-1268.3299	-96.2738	1.0000	0.0000

*Out EOU: 1 = Out of the EOU, 0 = Inside the EOU.

Appendix C

The tables used for the 2D case study are showed in this appendix. Table C1 was obtained from the ISCWSA Excel example for evaluating clearance scenarios (ISCWSA, 2017a) from the well 02.

Table C1: Input Survey Stations for 2D Study Case

Survey N°	V [m]	N [m]	E [m]
0	0.00	0.00	0.00
1	1.00	0.00	0.00
2	30.00	0.00	0.00
3	60.00	0.00	0.00
4	90.00	0.00	0.00
5	120.00	0.00	0.00
6	150.00	0.00	0.00
7	180.00	0.00	0.00
8	210.00	0.00	0.00
9	240.00	0.00	0.00
10	270.00	0.00	0.00
11	300.00	0.00	0.00
12	330.00	0.00	0.00
13	360.00	0.00	0.00
14	390.00	0.00	0.00
15	420.00	0.00	0.00
16	450.00	0.00	0.00
17	480.00	0.00	0.00
18	510.00	0.00	0.00
19	540.00	0.00	0.00
20	570.00	0.00	0.00
21	600.00	0.00	0.00
22	630.00	0.00	0.00
23	660.00	0.00	0.00
24	690.00	0.00	0.00
25	720.00	0.00	0.00
26	750.00	0.00	0.00
27	780.00	0.00	0.00
28	810.00	0.00	0.00
29	840.00	0.00	0.00
30	870.00	0.00	0.00
31	900.00	0.00	0.00
32	930.00	0.00	0.00
33	960.00	0.00	0.00
34	990.00	0.00	0.00
35	1020.00	0.00	-0.31
36	1049.98	0.00	-1.40
37	1079.91	0.00	-3.43
38	1109.76	0.00	-6.39
39	1139.50	0.00	-10.29
40	1169.11	0.00	-15.11
41	1198.56	0.00	-20.86
42	1227.80	0.00	-27.52

43	1256.83	0.00	-35.10
44	1285.61	0.00	-43.57
45	1314.10	0.00	-52.95
46	1342.29	0.00	-63.21
47	1370.15	0.00	-74.35
48	1397.64	0.00	-86.35
49	1424.74	0.00	-99.21
50	1451.43	0.00	-112.90
51	1477.68	0.00	-127.43
52	1503.46	0.00	-142.77
53	1528.75	0.00	-158.91
54	1553.52	0.00	-175.83
55	1577.75	0.00	-193.51
56	1601.42	0.00	-211.95
57	1624.50	0.00	-231.11
58	1646.97	0.00	-250.99
59	1668.80	0.00	-271.56
60	1689.98	0.00	-292.81
61	1710.49	0.00	-314.70
62	1730.30	0.00	-337.23
63	1749.40	0.00	-360.36
64	1767.76	0.00	-384.08
65	1785.38	0.00	-408.36
66	1802.22	0.00	-433.19
67	1818.29	0.00	-458.52
68	1833.55	0.00	-484.35
69	1848.00	0.00	-510.64
70	1861.61	0.00	-537.37
71	1874.39	0.00	-564.51
72	1886.31	0.00	-592.04
73	1897.37	0.00	-619.93
74	1907.54	0.00	-648.15
75	1916.84	0.00	-676.67
76	1925.23	0.00	-705.47
77	1932.72	0.00	-734.52
78	1939.29	0.00	-763.79
79	1944.95	0.00	-793.25
80	1949.69	0.00	-822.87
81	1953.50	0.00	-852.63
82	1956.48	0.00	-882.48
83	1959.09	0.00	-912.36
84	1961.71	0.00	-942.25
85	1964.32	0.00	-972.14
86	1966.94	0.00	-1002.02
87	1969.55	0.00	-1031.91
88	1972.17	0.00	-1061.79
89	1974.78	0.00	-1091.68
90	1977.40	0.00	-1121.57
91	1980.01	0.00	-1151.45
92	1982.62	0.00	-1181.34

93	1985.24	0.00	-1211.22
94	1987.85	0.00	-1241.11
95	1990.47	0.00	-1270.99
96	1993.08	0.00	-1300.88
97	1995.70	0.00	-1330.77
98	1998.31	0.00	-1360.65
99	2000.64	0.00	-1390.56
100	2002.15	0.00	-1420.52
101	2002.64	0.00	-1450.52
102	2002.64	0.00	-1480.52
103	2002.64	0.00	-1510.52
104	2002.64	0.00	-1540.52

Table C2: PWP Survey Stations Generated for the 2D Study Case

Survey	V [m]	N [m]	E [m]	MD [m]	Inc [°]	Azi [°]	DLS [°/30m]
0	0.0000	0.0000	0.0000	0.0000	0.0000	0.0000	0.0000
1	50.0000	0.0000	0.0000	50.0000	0.0000	0.0000	0.0000
2	100.0000	0.0000	0.0000	100.0000	0.0000	0.0000	0.0000
3	150.0000	0.0000	0.0000	150.0000	0.0000	0.0000	0.0000
4	200.0000	0.0000	0.0000	200.0000	0.0000	0.0000	0.0000
5	250.0000	0.0000	0.0000	250.0000	0.0000	0.0000	0.0000
6	300.0000	0.0000	0.0000	300.0000	0.0000	0.0000	0.0000
7	350.0000	0.0000	0.0000	350.0000	0.0000	0.0000	0.0000
8	400.0000	0.0000	0.0000	400.0000	0.0000	0.0000	0.0000
9	450.0000	0.0000	0.0000	450.0000	0.0000	0.0000	0.0000
10	500.0000	0.0000	0.0000	500.0000	0.0000	0.0000	0.0000
11	550.0000	0.0000	0.0000	550.0000	0.0000	0.0000	0.0000
12	600.0000	0.0000	0.0000	600.0000	0.0000	0.0000	0.0000
13	650.0000	0.0000	0.0000	650.0000	0.0000	0.0000	0.0000
14	700.0000	0.0000	0.0000	700.0000	0.0000	0.0000	0.0000
15	750.0000	0.0000	0.0000	750.0000	0.0000	0.0000	0.0000
16	800.0000	0.0000	0.0000	800.0000	0.0000	0.0000	0.0000
17	850.0000	0.0000	0.0000	850.0000	0.0000	0.0000	0.0000
18	900.0000	0.0000	0.0000	900.0000	0.0000	0.0000	0.0000
19	950.0000	0.0000	0.0000	950.0000	0.0000	0.0000	0.0000
20	990.0000	0.0000	0.0000	990.0000	0.0000	0.0000	3.3873
21	1014.3417	0.0000	-0.5724	1014.3484	2.6669	270.0000	3.1855
22	1038.9532	0.0000	-2.2718	1039.0186	5.2061	270.0000	2.9913
23	1063.8051	0.0000	-5.0712	1064.0276	7.6222	270.0000	2.8070
24	1088.8676	0.0000	-8.9438	1089.3875	9.9210	270.0000	2.6338
25	1114.1110	0.0000	-13.8627	1115.1057	12.1089	270.0000	2.4727
26	1139.5058	0.0000	-19.8011	1141.1856	14.1929	270.0000	2.3239
27	1165.0222	0.0000	-26.7321	1167.6265	16.1800	270.0000	2.1872
28	1190.6306	0.0000	-34.6288	1194.4248	18.0771	270.0000	2.0624
29	1216.3013	0.0000	-43.4643	1221.5735	19.8914	270.0000	1.9490
30	1242.0047	0.0000	-53.2118	1249.0632	21.6295	270.0000	1.8464
31	1267.7111	0.0000	-63.8444	1276.8817	23.2979	270.0000	1.7539
32	1293.3909	0.0000	-75.3353	1305.0152	24.9030	270.0000	1.6708
33	1319.0145	0.0000	-87.6575	1333.4476	26.4507	270.0000	1.5966
34	1344.5520	0.0000	-100.7843	1362.1614	27.9467	270.0000	1.5307

35	1369.9740	0.0000	-114.6886	1391.1373	29.3963	270.0000	1.4723
36	1395.2507	0.0000	-129.3438	1420.3552	30.8047	270.0000	1.4211
37	1420.3525	0.0000	-144.7228	1449.7935	32.1768	270.0000	1.3766
38	1445.2497	0.0000	-160.7989	1479.4298	33.5173	270.0000	1.3382
39	1469.9126	0.0000	-177.5451	1509.2409	34.8305	270.0000	1.3058
40	1494.3117	0.0000	-194.9346	1539.2027	36.1208	270.0000	1.2789
41	1518.4173	0.0000	-212.9406	1569.2908	37.3923	270.0000	1.2574
42	1542.1996	0.0000	-231.5360	1599.4800	38.6489	270.0000	1.2409
43	1565.6291	0.0000	-250.6942	1629.7451	39.8945	270.0000	1.2294
44	1588.6761	0.0000	-270.3882	1660.0604	41.1331	270.0000	1.2227
45	1611.3109	0.0000	-290.5911	1690.4000	42.3683	270.0000	1.2208
46	1633.5039	0.0000	-311.2761	1720.7381	43.6038	270.0000	1.2236
47	1655.2254	0.0000	-332.4163	1751.0487	44.8435	270.0000	1.2311
48	1676.4457	0.0000	-353.9849	1781.3060	46.0911	270.0000	1.2436
49	1697.1353	0.0000	-375.9549	1811.4845	47.3504	270.0000	1.2609
50	1717.2644	0.0000	-398.2995	1841.5588	48.6253	270.0000	1.2835
51	1736.8034	0.0000	-420.9919	1871.5040	49.9199	270.0000	1.3113
52	1755.7226	0.0000	-444.0051	1901.2957	51.2382	270.0000	1.3448
53	1773.9924	0.0000	-467.3123	1930.9101	52.5846	270.0000	1.3841
54	1791.5832	0.0000	-490.8867	1960.3241	53.9636	270.0000	1.4298
55	1808.4652	0.0000	-514.7012	1989.5154	55.3798	270.0000	1.4822
56	1824.6087	0.0000	-538.7292	2018.4630	56.8381	270.0000	1.5418
57	1839.9843	0.0000	-562.9437	2047.1466	58.3437	270.0000	1.6090
58	1854.5621	0.0000	-587.3179	2075.5475	59.9021	270.0000	1.6846
59	1868.3126	0.0000	-611.8248	2103.6485	61.5188	270.0000	1.7690
60	1881.2061	0.0000	-636.4376	2131.4340	63.2000	270.0000	1.8630
61	1893.2128	0.0000	-661.1295	2158.8903	64.9519	270.0000	1.9671
62	1904.3033	0.0000	-685.8736	2186.0061	66.7810	270.0000	2.0821
63	1914.4477	0.0000	-710.6429	2212.7723	68.6941	270.0000	2.2084
64	1923.6165	0.0000	-735.4107	2239.1828	70.6980	270.0000	2.3464
65	1931.7800	0.0000	-760.1501	2265.2342	72.7999	270.0000	2.4966
66	1938.9086	0.0000	-784.8342	2290.9270	75.0067	270.0000	2.6588
67	1944.9725	0.0000	-809.4360	2316.2652	77.3250	270.0000	2.8328
68	1949.9421	0.0000	-833.9289	2341.2571	79.7612	270.0000	3.0175
69	1953.7879	0.0000	-858.2858	2365.9158	82.3207	270.0000	3.2116
70	1956.4800	0.0000	-882.4800	2390.2593	85.0079	270.0000	0.0000
71	1960.8309	0.0000	-932.2903	2440.2593	85.0079	270.0000	0.0000
72	1965.1818	0.0000	-982.1007	2490.2593	85.0079	270.0000	0.0000
73	1969.5327	0.0000	-1031.9110	2540.2593	85.0079	270.0000	0.0000
74	1973.8836	0.0000	-1081.7213	2590.2593	85.0079	270.0000	0.0000
75	1978.2345	0.0000	-1131.5317	2640.2593	85.0079	270.0000	0.0000
76	1982.5854	0.0000	-1181.3420	2690.2593	85.0079	270.0000	0.0000
77	1986.9363	0.0000	-1231.1524	2740.2593	85.0079	270.0000	0.0000
78	1991.2872	0.0000	-1280.9627	2790.2593	85.0079	270.0000	0.0000
79	1995.6381	0.0000	-1330.7730	2840.2593	85.0079	270.0000	0.0000
80	1998.3100	0.0000	-1360.6500	2870.2555	84.9906	270.0000	1.1590
81	1998.5214	0.0000	-1363.0853	2872.6999	85.0859	270.0000	1.1820
82	1998.7262	0.0000	-1365.4901	2875.1134	85.1820	270.0000	1.2053
83	1998.9243	0.0000	-1367.8646	2877.4963	85.2786	270.0000	1.2289
84	1999.1160	0.0000	-1370.2093	2879.8487	85.3759	270.0000	1.2528

85	1999.3012	0.0000	-1372.5243	2882.1711	85.4738	270.0000	1.2771
86	1999.4802	0.0000	-1374.8099	2884.4638	85.5724	270.0000	1.3016
87	1999.6529	0.0000	-1377.0665	2886.7269	85.6715	270.0000	1.3264
88	1999.8196	0.0000	-1379.2942	2888.9609	85.7712	270.0000	1.3515
89	1999.9803	0.0000	-1381.4934	2891.1659	85.8715	270.0000	1.3768
90	2000.1351	0.0000	-1383.6643	2893.3424	85.9723	270.0000	1.4023
91	2000.2841	0.0000	-1385.8073	2895.4905	86.0736	270.0000	1.4281
92	2000.4274	0.0000	-1387.9225	2897.6106	86.1754	270.0000	1.4540
93	2000.5651	0.0000	-1390.0104	2899.7030	86.2778	270.0000	1.4801
94	2000.6973	0.0000	-1392.0710	2901.7679	86.3805	270.0000	1.5064
95	2000.8241	0.0000	-1394.1049	2903.8056	86.4837	270.0000	1.5327
96	2000.9456	0.0000	-1396.1121	2905.8165	86.5874	270.0000	1.5591
97	2001.0620	0.0000	-1398.0930	2907.8009	86.6914	270.0000	1.5855
98	2001.1732	0.0000	-1400.0478	2909.7589	86.7957	270.0000	1.6119
99	2001.2794	0.0000	-1401.9770	2911.6909	86.9004	270.0000	1.6383
100	2001.3808	0.0000	-1403.8806	2913.5972	87.0053	270.0000	1.6645
101	2001.4773	0.0000	-1405.7590	2915.4781	87.1105	270.0000	1.6906
102	2001.5692	0.0000	-1407.6125	2917.3339	87.2159	270.0000	1.7165
103	2001.6564	0.0000	-1409.4414	2919.1649	87.3214	270.0000	1.7421
104	2001.7392	0.0000	-1411.2459	2920.9713	87.4271	270.0000	1.7674
105	2001.8175	0.0000	-1413.0263	2922.7534	87.5328	270.0000	1.7923
106	2001.8916	0.0000	-1414.7829	2924.5115	87.6385	270.0000	1.8167
107	2001.9615	0.0000	-1416.5159	2926.2460	87.7443	270.0000	1.8406
108	2002.0273	0.0000	-1418.2257	2927.9571	87.8499	270.0000	1.8638
109	2002.0890	0.0000	-1419.9125	2929.6450	87.9554	270.0000	1.8863
110	2002.1469	0.0000	-1421.5767	2931.3101	88.0607	270.0000	1.9079
111	2002.2010	0.0000	-1423.2184	2932.9527	88.1657	270.0000	1.9286
112	2002.2514	0.0000	-1424.8379	2934.5731	88.2704	270.0000	1.9483
113	2002.2982	0.0000	-1426.4356	2936.1714	88.3747	270.0000	1.9668
114	2002.3415	0.0000	-1428.0117	2937.7481	88.4786	270.0000	1.9840
115	2002.3814	0.0000	-1429.5665	2939.3034	88.5818	270.0000	1.9998
116	2002.4180	0.0000	-1431.1002	2940.8376	88.6845	270.0000	2.0140
117	2002.4514	0.0000	-1432.6132	2942.3510	88.7864	270.0000	2.0265
118	2002.4817	0.0000	-1434.1058	2943.8438	88.8875	270.0000	2.0371
119	2002.5090	0.0000	-1435.5781	2945.3164	88.9877	270.0000	2.0457
120	2002.5334	0.0000	-1437.0305	2946.7690	89.0869	270.0000	2.0521
121	2002.5550	0.0000	-1438.4632	2948.2019	89.1851	270.0000	2.0560
122	2002.5739	0.0000	-1439.8766	2949.6154	89.2820	270.0000	2.0574
123	2002.5902	0.0000	-1441.2709	2951.0098	89.3776	270.0000	2.0560
124	2002.6040	0.0000	-1442.6464	2952.3854	89.4718	270.0000	2.0516
125	2002.6154	0.0000	-1444.0034	2953.7424	89.5644	270.0000	2.0439
126	2002.6245	0.0000	-1445.3421	2955.0812	89.6554	270.0000	2.0328
127	2002.6315	0.0000	-1446.6629	2956.4019	89.7446	270.0000	2.0179
128	2002.6363	0.0000	-1447.9659	2957.7050	89.8318	270.0000	1.9991
129	2002.6391	0.0000	-1449.2515	2958.9906	89.9170	270.0000	1.9761
130	2002.6400	0.0000	-1450.5200	2960.2591	90.0000	270.0000	0.0000
131	2002.6400	0.0000	-1500.5200	3010.2591	90.0000	270.0000	0.0000
132	2002.6400	0.0000	-1540.5200	3050.2591	90.0000	270.0000	0.0000

Table C3: Simulation Result (Shorth Version) for the 2D Study Case

	MD [m]	Time [min]	Inc [°]	Azi [°]	HD [m]	TVD [m]	East [m]	North [m]	Offset []	DLS [°/30m]	Tot Force inc [N]	Tot Force azi [N]	ROP Ax [m/hr]	ROP Inc [m/hr]	ROP Azi [m/hr]
0	0.0000	0.0000	0.0000	0.0000	0.0000	0.0000	0.0000	0.0000	0.0000	0.0000	0.0000	0.0000	0.0000	0.0000	0.0000
1	29.9837	142.0000	0.0000	0.0000	0.0000	29.9837	0.0000	0.0000	0.0000	0.0000	0.0000	0.0000	12.6692	0.0000	0.0000
2	60.0403	310.0000	0.0000	0.0000	0.0000	60.0403	0.0000	0.0000	0.0000	0.0000	0.0000	0.0000	10.7229	0.0000	0.0000
3	89.9512	486.0000	0.0000	0.0000	0.0000	89.9512	0.0000	0.0000	0.0000	0.0000	0.0000	0.0000	10.1969	0.0000	0.0000
4	119.9924	645.0000	0.0000	0.0000	0.0000	119.9924	0.0000	0.0000	0.0000	0.0000	0.0000	0.0000	11.3435	0.0000	0.0000
5	150.0908	777.0000	0.0000	0.0000	0.0000	150.0908	0.0000	0.0000	0.0000	0.0000	0.0000	0.0000	13.6989	0.0000	0.0000
6	180.0927	910.0000	0.0000	0.0000	0.0000	180.0927	0.0000	0.0000	0.0000	0.0000	0.0000	0.0000	13.5347	0.0000	0.0000
7	209.9188	1087.0000	0.0000	0.0000	0.0000	209.9188	0.0000	0.0000	0.0000	0.0000	0.0000	0.0000	10.1105	0.0000	0.0000
8	239.9430	1212.0000	0.0000	0.0000	0.0000	239.9430	0.0000	0.0000	0.0000	0.0000	0.0000	0.0000	14.4463	0.0000	0.0000
9	270.0625	1375.0000	0.0000	0.0000	0.0000	270.0625	0.0000	0.0000	0.0000	0.0000	0.0000	0.0000	11.0662	0.0000	0.0000
10	299.9247	1523.0000	0.0000	0.0000	0.0000	299.9247	0.0000	0.0000	0.0000	0.0000	0.0000	0.0000	12.1063	0.0000	0.0000
11	329.9102	1678.0000	0.0000	0.0000	0.0000	329.9102	0.0000	0.0000	0.0000	0.0000	0.0000	0.0000	11.6041	0.0000	0.0000
12	360.0758	1853.0000	0.0000	0.0000	0.0000	360.0758	0.0000	0.0000	0.0000	0.0000	0.0000	0.0000	10.3352	0.0000	0.0000
13	389.9848	1986.0000	0.0000	0.0000	0.0000	389.9848	0.0000	0.0000	0.0000	0.0000	0.0000	0.0000	13.4928	0.0000	0.0000
14	419.9637	2123.0000	0.0000	0.0000	0.0000	419.9637	0.0000	0.0000	0.0000	0.0000	0.0000	0.0000	13.1268	0.0000	0.0000
15	449.9038	2261.0000	0.0000	0.0000	0.0000	449.9038	0.0000	0.0000	0.0000	0.0000	0.0000	0.0000	13.0166	0.0000	0.0000
16	479.9597	2441.0000	0.0000	0.0000	0.0000	479.9597	0.0000	0.0000	0.0000	0.0000	0.0000	0.0000	10.0019	0.0000	0.0000
17	509.9634	2621.0000	0.0000	0.0000	0.0000	509.9634	0.0000	0.0000	0.0000	0.0000	0.0000	0.0000	10.0012	0.0000	0.0000
18	540.0446	2774.0000	0.0000	0.0000	0.0000	540.0446	0.0000	0.0000	0.0000	0.0000	0.0000	0.0000	11.8083	0.0000	0.0000
19	569.9867	2947.0000	0.0000	0.0000	0.0000	569.9867	0.0000	0.0000	0.0000	0.0000	0.0000	0.0000	10.3845	0.0000	0.0000
20	600.0767	3087.0000	0.0000	0.0000	0.0000	600.0767	0.0000	0.0000	0.0000	0.0000	0.0000	0.0000	12.9138	0.0000	0.0000
21	630.0897	3254.0000	0.0000	0.0000	0.0000	630.0897	0.0000	0.0000	0.0000	0.0000	0.0000	0.0000	10.7831	0.0000	0.0000
22	660.0583	3445.0000	0.0000	0.0000	0.0000	660.0583	0.0000	0.0000	0.0000	0.0000	0.0000	0.0000	9.4142	0.0000	0.0000
23	690.0221	3658.0000	0.0000	0.0000	0.0000	690.0221	0.0000	0.0000	0.0000	0.0000	0.0000	0.0000	8.4405	0.0000	0.0000
24	719.9863	3847.0000	0.0000	0.0000	0.0000	719.9863	0.0000	0.0000	0.0000	0.0000	0.0000	0.0000	9.5124	0.0000	0.0000
25	750.0210	3973.0000	0.0000	0.0000	0.0000	750.0210	0.0000	0.0000	0.0000	0.0000	0.0000	0.0000	14.3405	0.0000	0.0000
26	779.9204	4128.0000	0.0000	0.0000	0.0000	779.9204	0.0000	0.0000	0.0000	0.0000	0.0000	0.0000	11.5740	0.0000	0.0000
27	809.9692	4276.0000	0.0000	0.0000	0.0000	809.9692	0.0000	0.0000	0.0000	0.0000	0.0000	0.0000	12.1861	0.0000	0.0000
28	839.9396	4466.0000	0.0000	0.0000	0.0000	839.9396	0.0000	0.0000	0.0000	0.0000	0.0000	0.0000	9.4500	0.0000	0.0000
29	869.9836	4591.0000	0.0000	0.0000	0.0000	869.9836	0.0000	0.0000	0.0000	0.0000	0.0000	0.0000	14.4612	0.0000	0.0000
30	900.0851	4713.0000	0.0000	0.0000	0.0000	900.0851	0.0000	0.0000	0.0000	0.0000	0.0000	0.0000	14.8069	0.0000	0.0000

31	929.9990	4857.0000	0.0000	0.0000	0.0000	929.9990	0.0000	0.0000	0.0000	0.0000	0.0000	0.0000	12.4641	0.0000	0.0000
32	959.9233	4995.0000	0.0000	0.0000	0.0000	959.9233	0.0000	0.0000	0.0000	0.0000	0.0000	0.0000	13.0145	0.0000	0.0000
33	990.0121	5131.0000	0.0000	0.0000	0.0000	990.0121	0.0000	0.0000	0.0000	0.0000	0.0000	0.0000	13.2764	0.0000	0.0000
34	1020.0748	5285.0000	3.9561	270.0000	1.1435	1020.0498	-1.1435	0.0000	0.8500	9.5419	32126.9507	0.0000	11.7041	0.7632	0.0000
35	1050.0894	5436.0000	7.3182	270.0000	3.9738	1049.9271	-3.9738	0.0000	0.0034	0.8824	2979.1655	0.0000	11.9189	0.0727	0.0000
36	1079.9151	5576.0000	9.4462	270.0000	8.1738	1079.4522	-8.1738	0.0000	0.0053	0.0000	237.2070	0.0000	12.7780	0.0057	0.0000
37	1110.0167	5710.0000	11.7126	270.0000	13.7298	1109.0318	-13.7298	0.0000	0.0044	0.0000	148.9620	0.0000	13.4769	0.0046	0.0000
38	1140.0279	5858.0000	13.8788	270.0000	20.5855	1138.2458	-20.5855	0.0000	0.0035	0.0000	122.2000	0.0000	12.1615	0.0035	0.0000
39	1169.9142	6005.0000	13.8975	270.0000	27.7567	1167.2590	-27.7567	0.0000	0.0064	0.0000	205.7396	0.0000	12.1985	0.0055	0.0000
40	1200.0328	6165.0000	17.5095	270.0000	35.7794	1196.2838	-35.7794	0.0000	0.8500	7.7657	24338.3016	0.0000	11.2838	0.5765	0.0000
41	1230.0701	6336.0000	20.5702	270.0000	45.7305	1224.6212	-45.7305	0.0000	0.8500	6.6935	20015.2862	0.0000	10.5362	0.4329	0.0000
42	1259.9307	6478.0000	22.8859	270.0000	56.6037	1252.4288	-56.6037	0.0000	0.0046	0.2313	726.5516	0.0000	12.6118	0.0216	0.0000
43	1290.0433	6631.0000	24.7240	270.0000	68.6039	1280.0441	-68.6039	0.0000	0.0020	0.1236	407.2654	0.0000	11.7997	0.0105	0.0000
44	1319.9530	6780.0000	26.0177	270.0000	81.3596	1307.0957	-81.3596	0.0000	0.0048	0.0000	163.0221	0.0000	12.0417	0.0041	0.0000
45	1350.0812	6960.0000	28.0640	270.0000	95.0053	1333.9522	-95.0053	0.0000	0.0013	0.0000	31.4026	0.0000	10.0285	0.0008	0.0000
46	1379.9267	7095.0000	28.9337	270.0000	109.2503	1360.1779	-109.2503	0.0000	0.0052	0.0000	165.5357	0.0000	13.2627	0.0048	0.0000
47	1409.9963	7240.0000	30.3606	270.0000	124.1313	1386.3049	-124.1313	0.0000	0.0049	0.0000	154.8302	0.0000	12.4340	0.0039	0.0000
48	1439.9729	7389.0000	31.7330	270.0000	139.6199	1411.9680	-139.6199	0.0000	0.0049	0.0000	158.7288	0.0000	12.0661	0.0039	0.0000
49	1470.0869	7519.0000	33.1652	270.0000	155.8197	1437.3511	-155.8197	0.0000	0.0039	0.0000	138.9348	0.0000	13.9087	0.0047	0.0000
50	1500.0998	7651.0000	34.3573	270.0000	172.5389	1462.2743	-172.5389	0.0000	0.0053	0.0000	166.6066	0.0000	13.6394	0.0047	0.0000
51	1529.9023	7790.0000	35.7701	270.0000	189.7138	1486.6280	-189.7138	0.0000	0.0039	0.0000	134.6506	0.0000	12.8609	0.0040	0.0000
52	1560.0246	7932.0000	36.8848	270.0000	207.5989	1510.8645	-207.5989	0.0000	0.0056	0.0000	170.5718	0.0000	12.7248	0.0040	0.0000
53	1589.9395	8115.0000	38.5961	270.0000	225.9709	1534.4698	-225.9709	0.0000	0.0006	0.0000	37.5415	0.0000	9.8060	0.0008	0.0000
54	1619.9204	8271.0000	39.7703	270.0000	244.9524	1557.6749	-244.9524	0.0000	0.0014	0.0000	81.5649	0.0000	11.5404	0.0023	0.0000
55	1649.9841	8423.0000	40.8696	270.0000	264.4404	1580.5655	-264.4404	0.0000	0.0029	0.0000	128.2214	0.0000	11.8676	0.0034	0.0000
56	1680.0789	8572.0000	41.9546	270.0000	284.3798	1603.1055	-284.3798	0.0000	0.0046	0.0000	149.8983	0.0000	12.1185	0.0038	0.0000
57	1709.8744	8681.0000	43.1229	270.0000	304.5381	1625.0450	-304.5381	0.0000	0.0054	0.0000	168.9978	0.0000	16.3971	0.0056	0.0000
58	1739.9425	8852.0000	44.6789	270.0000	325.4092	1646.6864	-325.4092	0.0000	0.0018	0.0000	83.4905	0.0000	10.5135	0.0019	0.0000
59	1770.0603	9008.0000	46.0406	270.0000	346.8535	1667.8316	-346.8535	0.0000	0.0006	0.0000	58.6400	0.0000	11.5883	0.0016	0.0000
60	1800.0029	9192.0000	45.9123	270.0000	368.3968	1688.6268	-368.3968	0.0000	0.0067	0.6159	-1431.2752	0.0000	9.7638	-0.0338	0.0000
61	1829.9469	9325.0000	46.6656	270.0000	389.9205	1709.4443	-389.9205	0.0000	0.0065	1.6015	5487.0014	0.0000	13.5068	0.1701	0.0000
62	1860.0853	9439.0000	48.9994	270.0000	412.3428	1729.5797	-412.3428	0.0000	0.0065	0.3675	1657.0525	0.0000	15.8769	0.0534	0.0000
63	1889.9973	9575.0000	50.8289	270.0000	435.2654	1748.7924	-435.2654	0.0000	0.0046	0.0000	154.4863	0.0000	13.1923	0.0044	0.0000
64	1919.9130	9712.0000	52.1286	270.0000	458.6733	1767.4183	-458.6733	0.0000	0.0051	0.0000	159.1158	0.0000	13.0984	0.0040	0.0000
65	1950.1008	9846.0000	53.4665	270.0000	482.7271	1785.6561	-482.7271	0.0000	0.0055	0.0000	174.0350	0.0000	13.5169	0.0048	0.0000

66	1979.9230	10015.0000	55.2805	270.0000	506.9936	1802.9859	-506.9936	0.0000	0.0011	0.0000	61.5812	0.0000	10.5848	0.0015	0.0000
67	2010.0718	10150.0000	56.3827	270.0000	531.9624	1819.8807	-531.9624	0.0000	0.0051	0.0000	158.0381	0.0000	13.4180	0.0043	0.0000
68	2040.0926	10286.0000	57.8707	270.0000	557.2156	1836.1105	-557.2156	0.0000	0.0053	0.0000	175.4752	0.0000	13.2409	0.0050	0.0000
69	2070.0975	10422.0000	59.4109	270.0000	582.8912	1851.6328	-582.8912	0.0000	0.0055	0.0000	172.8616	0.0000	13.2341	0.0045	0.0000
70	2100.0154	10581.0000	61.6965	270.0000	609.0559	1866.1328	-609.0559	0.0000	0.0020	0.0000	-92.8914	0.0000	11.2847	-0.0026	0.0000
71	2130.0580	10741.0000	62.9117	270.0000	635.7363	1879.9409	-635.7363	0.0000	0.0032	0.0000	128.8739	0.0000	11.2642	0.0029	0.0000
72	2160.0625	10895.0000	64.8114	270.0000	662.7707	1892.9537	-662.7707	0.0000	0.8500	5.8569	21690.3548	0.0000	11.6868	0.4660	0.0000
73	2189.9451	11076.0000	67.6962	270.0000	690.1640	1904.8915	-690.1640	0.0000	0.8500	10.9143	31262.3923	0.0000	9.9017	0.6246	0.0000
74	2219.9197	11232.0000	70.3334	270.0000	718.0940	1915.7683	-718.0940	0.0000	0.0043	2.9216	9312.2541	0.0000	11.5338	0.2262	0.0000
75	2250.0555	11391.0000	70.4901	270.0000	746.5032	1925.8226	-746.5032	0.0000	0.0031	0.0000	-168.3850	0.0000	11.3709	-0.0045	0.0000
76	2279.8956	11531.0000	71.9121	270.0000	774.6773	1935.6512	-774.6773	0.0000	0.0065	1.8708	5763.9767	0.0000	12.7858	0.1781	0.0000
77	2309.9468	11741.0000	76.3136	270.0000	803.5815	1943.8470	-803.5815	0.0000	0.0064	2.7567	5788.2294	0.0000	8.5630	0.1175	0.0000
78	2339.9539	11881.0000	79.1562	270.0000	832.9129	1950.1627	-832.9129	0.0000	0.0068	0.7247	2596.9240	0.0000	12.8862	0.0701	0.0000
79	2369.9409	12027.0000	82.7301	270.0000	862.5490	1954.7076	-862.5490	0.0000	0.8500	7.4226	26441.5632	0.0000	12.3118	0.6561	0.0000
80	2399.9678	12161.0000	84.5396	270.0000	892.4264	1957.6903	-892.4264	0.0000	0.0052	0.0000	163.9049	0.0000	13.4485	0.0045	0.0000
81	2429.9335	12318.0000	84.6132	270.0000	922.2580	1960.5225	-922.2580	0.0000	0.0044	0.0000	203.1405	0.0000	11.4391	0.0053	0.0000
82	2460.0085	12466.0000	84.6672	270.0000	952.2016	1963.3312	-952.2016	0.0000	0.0038	0.0000	139.5034	0.0000	12.1977	0.0043	0.0000
83	2489.9434	12634.0000	84.7209	270.0000	982.0082	1966.0990	-982.0082	0.0000	0.0032	0.0000	141.1434	0.0000	10.6910	0.0033	0.0000
84	2519.9778	12765.0000	84.7481	270.0000	1011.9159	1968.8549	-1011.9159	0.0000	0.0029	0.0000	94.2868	0.0000	13.7882	0.0028	0.0000
85	2549.9821	12928.0000	84.7867	270.0000	1041.7952	1971.5912	-1041.7952	0.0000	0.0025	0.0000	105.3785	0.0000	11.0276	0.0026	0.0000
86	2579.9511	13063.0000	84.8111	270.0000	1071.6408	1974.3076	-1071.6408	0.0000	0.0022	0.0000	74.0385	0.0000	13.3367	0.0023	0.0000
87	2610.0195	13218.0000	84.8356	270.0000	1101.5866	1977.0205	-1101.5866	0.0000	0.0019	0.0000	78.3170	0.0000	11.6284	0.0018	0.0000
88	2639.9608	13370.0000	84.8574	270.0000	1131.4069	1979.7098	-1131.4069	0.0000	0.0017	0.0000	67.3390	0.0000	11.8190	0.0017	0.0000
89	2669.9082	13513.0000	84.8718	270.0000	1161.2341	1982.3902	-1161.2341	0.0000	0.0015	0.0000	47.9946	0.0000	12.5856	0.0012	0.0000
90	2699.8997	13662.0000	84.8894	270.0000	1191.1060	1985.0663	-1191.1060	0.0000	0.0013	0.0000	47.3358	0.0000	12.0737	0.0014	0.0000
91	2730.0386	13858.0000	84.9130	270.0000	1221.1256	1987.7447	-1221.1256	0.0000	0.0011	0.0000	50.7756	0.0000	9.2116	0.0011	0.0000
92	2759.9607	14011.0000	84.9248	270.0000	1250.9301	1990.3947	-1250.9301	0.0000	0.0009	0.0000	36.1270	0.0000	11.7342	0.0009	0.0000
93	2789.9555	14168.0000	84.9363	270.0000	1280.8076	1993.0450	-1280.8076	0.0000	0.0008	0.0000	33.9535	0.0000	11.4613	0.0008	0.0000
94	2819.9521	14337.0000	84.9457	270.0000	1310.6874	1995.6901	-1310.6874	0.0000	0.0007	0.0000	27.4843	0.0000	10.6503	0.0006	0.0000
95	2850.0078	14502.0000	84.9533	270.0000	1340.6264	1998.3358	-1340.6264	0.0000	0.0004	0.0000	16.9635	0.0000	10.9310	0.0004	0.0000
96	2879.9100	14640.0000	84.9658	270.0000	1370.4128	2000.9646	-1370.4128	0.0000	0.0046	0.0000	154.7263	0.0000	13.0009	0.0048	0.0000
97	2909.9456	14757.0000	86.1984	270.0000	1400.3549	2003.3241	-1400.3549	0.0000	0.0067	0.3900	1778.2964	0.0000	15.4210	0.0541	0.0000
98	2940.0655	14925.0000	88.8665	270.0000	1430.4328	2004.8547	-1430.4328	0.0000	0.8500	8.5330	24897.3079	0.0000	10.7260	0.5725	0.0000
99	2969.9459	15062.0000	92.5556	270.0000	1460.2998	2004.2242	-1460.2998	0.0000	0.0059	0.0000	257.7446	0.0000	13.0779	0.0074	0.0000
100	3000.0368	15228.0000	91.1467	270.0000	1490.3678	2003.0788	-1490.3678	0.0000	0.0066	1.6771	-4818.1276	0.0000	10.8613	-0.1149	0.0000

101	3030.0471	15380.0000	90.4628	270.0000	1520.3762	2002.7633	-1520.3762	0.0000	0.0052	0.0000	-202.0470	0.0000	11.8456	-0.0048	0.0000
102	3050.3148	15495.0000	90.4220	270.0000	1540.6433	2002.6069	-1540.6433	0.0000	0.0047	0.0000	-182.7551	0.0000	10.5745	-0.0038	0.0000

Table C4: Deviation Control Survey Points for the 2D Study Case

	MD [m]	**V VOE [m]**	**N VOE [m]**	**E VOE [m]**	**Length VOE [m]**	**V EOU [m]**	**N EOU [m]**	**E EOU [m]**	**Length EOU [m]**	**Out EOU***
0	0.0000	0.0000	0.0000	0.0000	0.0000	0.0000	0.0000	0.0000	0.0000	0.0000
1	30.1948	30.1948	0.0000	0.0000	0.0000	29.1948	0.0000	0.0000	1.0000	0.0000
2	60.0403	60.0403	0.0000	0.0000	0.0000	59.0403	0.0000	0.0000	1.0000	0.0000
3	90.1211	90.1211	0.0000	0.0000	0.0000	91.1211	0.0000	0.0000	1.0000	0.0000
4	120.1814	120.1814	0.0000	0.0000	0.0000	119.1814	0.0000	0.0000	1.0000	0.0000
5	150.0908	150.0908	0.0000	0.0000	0.0000	149.0908	0.0000	0.0000	1.0000	0.0000
6	180.0927	180.0927	0.0000	0.0000	0.0000	181.0927	0.0000	0.0000	1.0000	0.0000
7	210.0873	210.0873	0.0000	0.0000	0.0000	211.0873	0.0000	0.0000	1.0000	0.0000
8	240.1838	240.1838	0.0000	0.0000	0.0000	239.1838	0.0000	0.0000	1.0000	0.0000
9	270.0625	270.0625	0.0000	0.0000	0.0000	271.0625	0.0000	0.0000	1.0000	0.0000
10	300.1264	300.1264	0.0000	0.0000	0.0000	299.1264	0.0000	0.0000	1.0000	0.0000
11	330.1036	330.1036	0.0000	0.0000	0.0000	331.1036	0.0000	0.0000	1.0000	0.0000
12	360.0758	360.0758	0.0000	0.0000	0.0000	361.0758	0.0000	0.0000	1.0000	0.0000
13	390.2097	390.2097	0.0000	0.0000	0.0000	391.2097	0.0000	0.0000	1.0000	0.0000
14	420.1825	420.1825	0.0000	0.0000	0.0000	419.1825	0.0000	0.0000	1.0000	0.0000
15	450.1207	450.1207	0.0000	0.0000	0.0000	449.1207	0.0000	0.0000	1.0000	0.0000
16	480.1264	480.1264	0.0000	0.0000	0.0000	479.1264	0.0000	0.0000	1.0000	0.0000
17	510.1301	510.1301	0.0000	0.0000	0.0000	509.1301	0.0000	0.0000	1.0000	0.0000
18	540.0446	540.0446	0.0000	0.0000	0.0000	541.0446	0.0000	0.0000	1.0000	0.0000
19	570.1597	570.1597	0.0000	0.0000	0.0000	571.1597	0.0000	0.0000	1.0000	0.0000
20	600.0767	600.0767	0.0000	0.0000	0.0000	601.0767	0.0000	0.0000	1.0000	0.0000
21	630.0897	630.0897	0.0000	0.0000	0.0000	629.0897	0.0000	0.0000	1.0000	0.0000
22	660.0583	660.0583	0.0000	0.0000	0.0000	659.0583	0.0000	0.0000	1.0000	0.0000
23	690.0221	690.0221	0.0000	0.0000	0.0000	689.0221	0.0000	0.0000	1.0000	0.0000
24	720.1448	720.1448	0.0000	0.0000	0.0000	719.1448	0.0000	0.0000	1.0000	0.0000
25	750.0210	750.0210	0.0000	0.0000	0.0000	749.0210	0.0000	0.0000	1.0000	0.0000
26	780.1133	780.1133	0.0000	0.0000	0.0000	781.1133	0.0000	0.0000	1.0000	0.0000

27	810.1723	810.1723	0.0000	0.0000	0.0000	809.1723	0.0000	0.0000	1.0000	0.0000
28	840.0971	840.0971	0.0000	0.0000	0.0000	839.0971	0.0000	0.0000	1.0000	0.0000
29	870.2246	870.2246	0.0000	0.0000	0.0000	871.2246	0.0000	0.0000	1.0000	0.0000
30	900.0851	900.0851	0.0000	0.0000	0.0000	901.0851	0.0000	0.0000	1.0000	0.0000
31	930.2067	930.2067	0.0000	0.0000	0.0000	929.2067	0.0000	0.0000	1.0000	0.0000
32	960.1402	960.1402	0.0000	0.0000	0.0000	961.1402	0.0000	0.0000	1.0000	0.0000
33	990.0121	990.0121	0.0000	-0.0003	0.0003	990.0121	0.0000	-1.0000	1.0000	0.0000
34	1020.0748	1020.0566	0.0000	-0.9670	0.1766	1020.0879	0.0000	-0.1443	1.0000	0.0000
35	1050.0894	1049.9708	0.0000	-3.5128	0.4630	1050.0214	0.0000	-2.9782	1.0000	0.0000
36	1080.1281	1079.7580	0.0000	-7.5362	0.6794	1079.8032	0.0000	-7.2188	1.0000	0.0000
37	1110.0167	1109.1872	0.0000	-12.9033	0.8411	1109.2165	0.0000	-12.7471	1.0000	0.0000
38	1140.0279	1138.4858	0.0000	-19.5626	1.0507	1138.4743	0.0000	-19.6119	1.0000	1.0000
39	1170.1175	1167.4379	0.0000	-27.8801	0.0768	1167.2164	0.0000	-28.7763	1.0000	0.0000
40	1200.0328	1196.1911	0.0000	-36.1144	0.3476	1196.0172	0.0000	-36.7432	1.0000	0.0000
41	1230.0701	1224.4158	0.0000	-46.3156	0.6201	1224.2899	0.0000	-46.6740	1.0000	0.0000
42	1260.1409	1252.3133	0.0000	-57.4756	0.8485	1252.2581	0.0000	-57.6168	1.0000	0.0000
43	1290.0433	1279.7678	0.0000	-69.2394	0.6929	1279.6454	0.0000	-69.5210	1.0000	0.0000
44	1320.1537	1307.0588	0.0000	-81.9081	0.5091	1306.8494	0.0000	-82.3521	1.0000	0.0000
45	1350.0812	1333.8190	0.0000	-95.2673	0.2939	1333.4991	0.0000	-95.8968	1.0000	0.0000
46	1380.1478	1360.3382	0.0000	-109.4184	0.0696	1359.8940	0.0000	-110.2360	1.0000	0.0000
47	1410.2036	1386.4731	0.0000	-124.2547	0.0215	1385.9887	0.0000	-125.1049	1.0000	0.0000
48	1440.1740	1412.1544	0.0000	-139.7001	0.0298	1412.6559	0.0000	-138.8696	1.0000	0.0000
49	1470.0869	1437.4058	0.0000	-155.7341	0.1015	1437.8892	0.0000	-154.9768	1.0000	0.0000
50	1500.0998	1462.3574	0.0000	-172.4151	0.1492	1462.8314	0.0000	-171.7085	1.0000	0.0000
51	1530.1167	1486.9224	0.0000	-189.6682	0.2091	1487.3783	0.0000	-189.0219	1.0000	0.0000
52	1560.0246	1511.0072	0.0000	-207.4055	0.2404	1511.4583	0.0000	-206.7943	1.0000	0.0000
53	1590.1029	1534.8302	0.0000	-225.7739	0.3789	1535.2118	0.0000	-225.2837	1.0000	0.0000
54	1620.1127	1558.1975	0.0000	-244.6174	0.5918	1558.4560	0.0000	-244.3015	1.0000	0.0000
55	1650.1819	1581.2003	0.0000	-264.0000	0.7484	1581.3634	0.0000	-263.8085	1.0000	0.0000
56	1680.0789	1603.6555	0.0000	-283.7582	0.8300	1603.7682	0.0000	-283.6309	1.0000	0.0000
57	1710.1477	1625.8122	0.0000	-304.1071	0.8390	1625.9212	0.0000	-303.9886	1.0000	0.0000
58	1740.1177	1647.4605	0.0000	-324.8592	0.9355	1647.5053	0.0000	-324.8128	1.0000	0.0000

59	1770.0603	1668.6427	0.0000	-346.0538	1.1391	1668.5437	0.0000	-346.1514	1.0000	1.0000
60	1800.0029	1688.7591	0.0000	-368.2691	0.1839	1689.3463	0.0000	-367.7023	1.0000	0.0000
61	1830.1720	1709.7587	0.0000	-389.9296	0.2225	1710.3176	0.0000	-389.3891	1.0000	0.0000
62	1860.0853	1729.5261	0.0000	-412.3909	0.0721	1728.8356	0.0000	-413.0108	1.0000	0.0000
63	1890.2172	1748.7812	0.0000	-435.5617	0.1958	1748.1649	0.0000	-436.0782	1.0000	0.0000
64	1920.1313	1767.4312	0.0000	-458.9420	0.1548	1766.7698	0.0000	-459.4682	1.0000	0.0000
65	1950.1008	1785.5530	0.0000	-482.8053	0.1294	1784.8592	0.0000	-483.3312	1.0000	0.0000
66	1980.0994	1803.0981	0.0000	-507.1302	0.0144	1803.9002	0.0000	-506.5575	1.0000	0.0000
67	2010.0718	1820.0056	0.0000	-531.8779	0.1508	1820.7090	0.0000	-531.4021	1.0000	0.0000
68	2040.0926	1836.2785	0.0000	-557.1076	0.1998	1836.9517	0.0000	-556.6750	1.0000	0.0000
69	2070.0975	1851.8398	0.0000	-582.7661	0.2418	1852.6283	0.0000	-582.2893	1.1633	0.0000
70	2100.0154	1866.6105	0.0000	-608.7912	0.5461	1867.1680	0.0000	-608.4822	1.1835	0.0000
71	2130.0580	1880.6472	0.0000	-635.3707	0.7952	1881.0156	0.0000	-635.1801	1.2101	0.0000
72	2160.0625	1893.7719	0.0000	-662.3768	0.9080	1894.0681	0.0000	-662.2343	1.2368	0.0000
73	2190.1105	1905.9461	0.0000	-689.8849	1.0821	1906.1084	0.0000	-689.8142	1.2591	0.0000
74	2220.1119	1917.0918	0.0000	-717.7853	1.3507	1917.0272	0.0000	-717.8104	1.2815	1.0000
75	2250.0555	1926.0025	0.0000	-746.4395	0.1909	1927.0565	0.0000	-746.0666	1.3089	0.0000
76	2280.1087	1935.7807	0.0000	-774.8578	0.0671	1936.9904	0.0000	-774.4360	1.3483	0.0000
77	2310.0895	1943.7516	0.0000	-803.7567	0.1343	1942.5674	0.0000	-804.0919	1.3650	0.0000
78	2340.1686	1949.7965	0.0000	-833.2113	0.4158	1948.8497	0.0000	-833.4148	1.3842	0.0000
79	2370.1464	1954.2924	0.0000	-862.8203	0.4461	1953.3406	0.0000	-862.9658	1.4091	0.0000
80	2400.1919	1957.6127	0.0000	-892.6594	0.0994	1956.2798	0.0000	-892.7922	1.4389	0.0000
81	2430.1242	1959.9758	0.0000	-922.5014	0.5670	1959.0700	0.0000	-922.5874	1.4770	0.0000
82	2460.0085	1962.5763	0.0000	-952.2724	0.7581	1961.8223	0.0000	-952.3431	1.5155	0.0000
83	2490.1216	1965.1967	0.0000	-982.2710	0.9226	1964.5679	0.0000	-982.3294	1.5542	0.0000
84	2520.2076	1967.8147	0.0000	-1012.2425	1.0658	1967.2893	0.0000	-1012.2909	1.5934	0.0000
85	2550.1659	1970.4216	0.0000	-1042.0868	1.1913	1969.9818	0.0000	-1042.1271	1.6328	0.0000
86	2580.1734	1973.0327	0.0000	-1071.9800	1.3003	1972.6623	0.0000	-1072.0138	1.6723	0.0000
87	2610.0195	1975.6298	0.0000	-1101.7126	1.3963	1975.3155	0.0000	-1101.7410	1.7120	0.0000
88	2640.1578	1978.2524	0.0000	-1131.7361	1.4810	1977.9829	0.0000	-1131.7604	1.7516	0.0000
89	2670.1180	1980.8594	0.0000	-1161.5823	1.5558	1980.6243	0.0000	-1161.6034	1.7919	0.0000
90	2700.1010	1983.4684	0.0000	-1191.4512	1.6223	1983.2595	0.0000	-1191.4699	1.8320	0.0000

91	2730.0386	1986.0735	0.0000	-1221.2747	1.6779	1985.8798	0.0000	-1221.2920	1.8723	0.0000
92	2760.1562	1988.6942	0.0000	-1251.2776	1.7245	1988.5068	0.0000	-1251.2943	1.9127	0.0000
93	2790.1465	1991.3039	0.0000	-1281.1538	1.7649	1991.1161	0.0000	-1281.1705	1.9535	0.0000
94	2820.1296	1993.9130	0.0000	-1311.0229	1.7998	1993.7193	0.0000	-1311.0400	1.9942	0.0000
95	2850.0078	1996.5335	0.0000	-1340.7856	1.8093	1996.3087	0.0000	-1340.8055	2.0350	0.0000
96	2880.1267	1999.1624	0.0000	-1370.7894	1.8283	1998.9158	0.0000	-1370.8111	2.0759	0.0000
97	2910.2028	2001.2134	0.0000	-1400.7788	2.1341	2001.2320	0.0000	-1400.7773	2.1155	1.0000
98	2940.0655	2004.6421	0.0000	-1430.4436	0.2129	2002.7044	0.0000	-1430.5420	2.1531	0.0000
99	2970.1639	2003.7127	0.0000	-1460.5068	0.5018	2002.0234	0.0000	-1460.4709	2.1916	0.0000
100	3000.0368	2002.6990	0.0000	-1490.3533	0.3800	2000.8472	0.0000	-1490.2829	2.2333	0.0000
101	3030.0471	2002.6400	0.0000	-1520.3749	0.1233	2000.4912	0.0000	-1520.3523	2.2722	0.0000
102	3050.3148	2002.6400	0.0000	-1540.6436	0.0331	2004.9197	0.0000	-1540.6612	2.3129	0.0000

*Out EOU: 1 = Out of the EOU, 0 = Inside the EOU.

Appendix D

Table D1 presents the comparison between the simulations coordinates with the TCO on and off using the PWP as a reference point for both cases. The mean, SD and percentile 10% are at the bottom of the table.

Table D1: Comparison Simulated Coordinates with the TCO On and Off for the 3D Case Study

	PWP			Simulation TCO ON				Simulation TCO OFF			
	V [m]	N [m]	E [m]	TVD [m]	North [m]	East [m]	Distance [m]	TVD [m]	North [m]	East [m]	Distance [m]
0	0.00	0.00	0.00	0.00	0.00	0.00	0.00	0.00	0.00	0.00	0.00
1	50.00	0.00	0.00	49.96	0.00	0.00	0.04	50.01	0.00	0.00	0.01
2	100.00	0.00	0.00	99.94	0.00	0.00	0.06	99.96	0.00	0.00	0.04
3	150.00	0.00	0.00	149.95	0.00	0.00	0.05	150.06	0.00	0.00	0.06
4	200.00	0.00	0.00	199.93	0.00	0.00	0.07	199.94	0.00	0.00	0.06
5	250.00	0.00	0.00	249.98	0.00	0.00	0.02	250.04	0.00	0.00	0.04
6	300.00	0.00	0.00	299.99	0.00	0.00	0.01	300.07	0.00	0.00	0.07
7	350.00	0.00	0.00	350.08	0.00	0.00	0.08	350.01	0.00	0.00	0.01
8	400.00	0.00	0.00	399.99	0.00	0.00	0.01	399.98	0.00	0.00	0.02
9	450.00	0.00	0.00	450.09	0.00	0.00	0.09	450.09	0.00	0.00	0.09
10	500.00	0.00	0.00	500.09	0.00	0.00	0.09	499.94	0.00	0.00	0.06
11	550.00	0.00	0.00	550.00	0.00	0.00	0.00	550.02	0.00	0.00	0.02
12	600.00	0.00	0.00	600.08	0.00	0.00	0.08	600.05	0.00	0.00	0.05
13	650.00	0.00	0.00	649.99	0.00	0.00	0.01	649.91	0.00	0.00	0.09
14	700.00	0.00	0.00	700.03	0.00	0.00	0.03	700.03	0.00	0.00	0.03
15	750.00	0.00	0.00	750.07	0.00	0.00	0.07	750.06	0.00	0.00	0.06
16	800.00	0.00	0.00	800.02	0.00	0.00	0.02	800.01	0.00	0.00	0.01
17	850.00	0.00	0.00	849.91	0.00	0.00	0.09	849.94	0.00	0.00	0.06
18	900.00	0.00	0.00	900.09	0.00	0.00	0.09	899.92	0.00	0.00	0.08
19	950.00	0.00	0.00	949.94	0.00	0.00	0.06	949.96	0.00	0.00	0.04
20	990.00	0.00	0.00	989.91	0.00	0.00	0.09	989.96	0.00	0.00	0.04
21	1010.83	-0.56	0.05	1010.72	-0.66	0.06	0.14	1010.87	-0.66	0.06	0.11
22	1032.02	-2.24	0.20	1031.96	-2.37	0.21	0.14	1031.99	-2.36	0.21	0.13

23	1053.53	-4.99	0.44	1053.55	-5.29	0.48	0.30	1053.48	-5.17	0.47	0.18
24	1075.35	-8.79	0.77	1075.38	-9.20	0.83	0.42	1075.20	-9.27	0.84	0.50
25	1097.44	-13.62	1.17	1097.32	-14.12	1.27	0.52	1097.22	-14.43	1.30	0.84
26	1119.76	-19.44	1.65	1119.71	-20.13	1.81	0.72	1119.59	-20.52	1.84	1.11
27	1142.29	-26.21	2.18	1142.10	-27.08	2.42	0.92	1142.01	-27.51	2.46	1.35
28	1164.99	-33.93	2.77	1164.63	-35.01	3.10	1.19	1164.62	-35.49	3.15	1.65
29	1187.84	-42.54	3.42	1187.73	-43.40	3.81	0.95	1187.41	-44.42	3.90	1.98
30	1210.81	-52.03	4.10	1210.87	-52.12	4.50	0.41	1210.23	-54.12	4.70	2.25
31	1233.86	-62.37	4.82	1234.24	-61.92	5.18	0.69	1233.21	-64.50	5.52	2.34
32	1256.96	-73.52	5.56	1257.36	-72.81	5.91	0.89	1256.16	-75.78	6.38	2.54
33	1280.09	-85.45	6.33	1280.63	-84.63	6.69	1.06	1279.14	-87.94	7.27	2.82
34	1303.20	-98.15	7.11	1303.87	-96.86	7.50	1.50	1302.36	-100.85	8.19	3.03
35	1326.28	-111.57	7.89	1326.98	-110.22	8.29	1.57	1325.38	-114.27	9.10	3.09
36	1349.29	-125.69	8.68	1349.77	-124.72	9.07	1.15	1348.37	-128.39	10.02	3.15
37	1372.19	-140.48	9.46	1372.73	-139.67	9.87	1.06	1371.28	-143.20	10.94	3.23
38	1394.97	-155.91	10.22	1395.39	-155.25	10.70	0.92	1393.93	-158.53	11.84	3.25
39	1417.59	-171.95	10.96	1418.04	-171.09	11.47	1.09	1416.55	-174.58	12.73	3.33
40	1440.01	-188.57	11.67	1440.43	-187.89	12.11	0.91	1438.94	-191.32	13.60	3.53
41	1462.21	-205.74	12.35	1462.65	-205.06	12.75	0.90	1461.09	-208.65	14.44	3.76
42	1484.15	-223.43	12.98	1484.45	-222.84	13.41	0.79	1482.92	-226.30	15.23	3.84
43	1505.81	-241.62	13.57	1506.00	-241.13	14.08	0.73	1504.67	-244.57	15.98	3.98
44	1527.15	-260.27	14.09	1527.30	-259.77	14.75	0.84	1525.92	-263.18	16.67	4.08
45	1548.15	-279.35	14.55	1548.23	-278.90	15.39	0.95	1546.90	-282.23	17.30	4.17
46	1568.77	-298.84	14.94	1568.71	-298.49	15.95	1.06	1567.51	-301.77	17.87	4.32
47	1588.99	-318.71	15.26	1589.22	-318.21	16.37	1.25	1587.74	-321.64	18.35	4.44
48	1608.76	-338.92	15.48	1609.01	-338.27	16.07	0.91	1607.19	-342.14	18.76	4.86
49	1628.07	-359.45	15.62	1628.28	-358.78	15.78	0.72	1626.52	-362.70	19.07	4.99
50	1646.88	-380.26	15.65	1647.04	-379.66	15.66	0.63	1645.26	-383.65	19.28	5.23
51	1665.16	-401.34	15.58	1665.35	-400.91	15.53	0.47	1663.56	-404.78	19.39	5.37
52	1682.87	-422.64	15.39	1682.90	-422.28	15.39	0.36	1681.08	-426.05	19.37	5.54
53	1699.99	-444.14	15.08	1699.85	-443.97	15.21	0.26	1698.11	-447.67	19.18	5.72
54	1716.50	-465.82	14.65	1716.26	-465.75	14.90	0.35	1714.53	-469.49	18.87	5.93

55	1732.34	-487.63	14.07	1732.00	-487.52	14.47	0.53	1730.19	-491.42	18.40	6.14
56	1747.51	-509.55	13.36	1747.16	-509.52	13.89	0.64	1745.27	-513.36	17.84	6.28
57	1761.96	-531.56	12.50	1761.54	-531.47	13.18	0.80	1759.64	-535.39	17.10	6.42
58	1775.66	-553.62	11.48	1775.19	-553.52	12.29	0.95	1773.29	-557.53	16.21	6.57
59	1788.59	-575.70	10.30	1788.10	-575.69	11.23	1.06	1786.10	-579.76	15.11	6.77
60	1800.71	-597.78	8.94	1800.69	-597.59	10.14	1.21	1798.06	-601.76	13.89	6.88
61	1811.99	-619.82	7.41	1812.61	-619.34	8.71	1.51	1809.27	-623.84	12.47	7.01
62	1822.41	-641.80	5.70	1823.20	-641.01	6.87	1.62	1819.62	-645.90	10.87	7.16
63	1831.92	-663.69	3.79	1832.66	-663.00	4.81	1.44	1828.96	-667.93	9.01	7.35
64	1840.51	-685.45	1.69	1841.29	-684.82	2.72	1.45	1837.44	-689.64	7.02	7.45
65	1848.13	-707.05	-0.63	1849.26	-706.27	0.65	1.87	1845.02	-711.30	4.80	7.56
66	1854.77	-728.48	-3.15	1856.22	-727.62	-1.64	2.27	1851.55	-732.86	2.34	7.72
67	1860.38	-749.70	-5.89	1861.95	-748.89	-4.28	2.40	1856.94	-754.03	-0.36	7.83
68	1864.94	-770.67	-8.87	1866.38	-769.86	-7.21	2.34	1861.37	-775.12	-3.28	7.98
69	1868.42	-791.37	-12.07	1869.82	-790.58	-10.35	2.36	1864.53	-795.82	-6.51	8.11
70	1870.78	-811.78	-15.52	1872.58	-810.90	-13.59	2.79	1866.53	-816.28	-9.98	8.30
71	1875.13	-860.83	-24.17	1876.85	-859.92	-22.54	2.54	1870.80	-865.32	-18.41	8.49
72	1879.48	-909.89	-32.82	1879.80	-908.81	-32.16	1.30	1875.07	-914.36	-26.86	8.66
73	1883.83	-958.94	-41.47	1883.75	-957.97	-41.28	1.00	1879.36	-963.50	-35.36	8.83
74	1888.18	-1007.99	-50.12	1887.77	-1006.91	-50.25	1.17	1883.66	-1012.56	-43.87	8.97
75	1892.53	-1057.05	-58.77	1891.89	-1055.97	-59.15	1.31	1887.97	-1061.71	-52.42	9.11
76	1896.88	-1106.10	-67.42	1896.05	-1105.02	-68.00	1.48	1892.28	-1110.79	-60.97	9.21
77	1901.23	-1155.15	-76.07	1900.29	-1153.94	-76.74	1.68	1896.59	-1159.74	-69.51	9.26
78	1905.58	-1204.21	-84.72	1905.36	-1203.12	-84.65	1.11	1900.91	-1208.83	-78.09	9.34
79	1909.93	-1253.26	-93.38	1910.18	-1252.12	-92.82	1.29	1905.25	-1258.03	-86.70	9.45
80	1915.22	-1312.12	-103.74	1915.81	-1311.03	-102.79	1.57	1910.43	-1316.74	-96.99	9.48
				MEAN			**0.8337**	**MEAN**			**3.8757**
				SD			**0.6969**	**SD**			**3.3156**
				P10			**0.0331**	**P10**			**0.0381**

Appendix E

The following is the main algorithm used in the RSS Simulator that calls and controls the inputs and results.

```
# ==================================== MAIN ========================================
# ================================ Input Parameters ================================
# --------------------------- Planned Well Path (PWP) -------------------------------
Tolerance = 0.5  # [°] Maximum range of difference for the Inclination and Azimuth tolerance to be
consider as 2 different segments in the well
Sur_pts = 50  # [m] Δ between survey points for hold section in the PWP
Step_u = 0.02  # [] u value for the Bezier algorithm (which will give the survey points in the curvature
section)
Ran_Tol = 300  # [m] The positive and negative range for evaluating different d_s and d_e combinations
for the optimization of the Bezier curves
Max_DLS = 5.5  # [°/30m] Maximum DLS set for the acceptance of the better combination of d_s and d_e

# ------------------------------- RSS Model ----------------------------------------
# Parameters for the RSS Model
# Configuration variables by the user (through GUI):
deltaT = 60  # [s] Time step for the simulation
OD_tool = 0.080  # [m] Out diameter of tool
ID_tool = 0.037  # [m] Inside diameter of tool
dist_act = 0.5  # [m] Distance from the bit to the actuator
dist_stab = 2.7  # [m] Distance from the actuator to the stabilizer
bore_D = 0.31115  # [m] Borehole diameter
# Values for the use in the Main
Delta_Sur = 30  # [m] Δ Survey point for the simulation
Error_input = 0.1  # [] Percentage of error added to the input data given by the other modules.
# Systematic default variables
Max_off = 0.9  # Maximum offset required by the user from 0 to 1 (0% to 100%)
Ela_Mod = 30000000 * (10 ** 9) / (0.145 * 10 ** 6)  # [Pa] Elasticity modulus, considering steel
Offset_L = 0.006  # [m] Max physical offset or opening of the tool (6mm)
Max_deg = 0.65 * np.pi / 180  # [rad] To determine if the offset is going to be activated or not (0.65°)

# --------------------------- Vectors of Errors (VEC)  ------------------------------
G = 9.80665  # [m/s2] Gravity
MF = 50000  # [nT] Total Magnetic Field
Dip = 72 * np.pi / 180  # [rad] Magnetic dip angle (°)
SF = 2.6  # Confidential region or confidence level for the Standard Deviation used in the Ellipse of
Uncertainty (EOU)
# Error magnitudes in the MWD tools. The values are taken from the ISCWSA Error Model - Excel Example
L_DSFS = 0.00056  # [] Depth Scale Factor - Systematic Error
L_ABZ = 0.004  # [m/s2] MWD: Z-Accelerometer Bias Error - Systematic Error
L_ASZ = 0.0005  # [] MWD: Z-Accelerometer Scale Factor - Systematic Error
L_MBXY1 = 70  # [nT] MWD TF Ind: X and Y Magnetometer Bias - Systematic Error
L_MSXY1 = 0.0016  # [] MWD RF Ind: X and Y Magnetometer Scale Factor - Systematic Error
Rho = np.array([L_DSFS, L_ABZ, L_ASZ, L_MBXY1, L_MSXY1])  # Error's magnitudes list
Min_R = 1  # [m] Minimum radius of the EOU to be compared with the Vector of Error (especially used at
the start of the drilling)

# --------------------------- Correction Parameters ----------------------------------
Max_DLS_corr = 6  # [°/30m] Maximum DLS that could be applied for the correction path
Tor_max_corr = 3  # [°/30m] Maximum Tortuosity that could be applied for the correction path
Step_u_corr = 0.02  # Step (u) for the Bezier algorithm iteration for the correction path
Reach_all = True  # True = to search for the PWP reach point on all the trajectory's sections. False = T
 search the PWP reach point only in the next closer hold section points.
CP_Active = True  # True = Correction path will be used. False = Drilling without correcting the path

# ==================================== Simulation ======================================
# --------------------------------- PWP generator ---------------------------------------
# Import data file (.xlsx) with the original given survey points
fields = ['V [m]', 'N [m]', 'E [m]']  # Names of the headers to look in the Excel file
df_data = pd.read_excel('Study Cases - Data.xlsx', sheet_name="Case3D", usecols=fields)
data_ori = df_data.to_numpy()  # Covert DF to Numpy matrix

# Analyze the data points
Analyzed_data, Data_bzr = analysis_data(data_ori, Tolerance)  # Rtn: Analyzed_data: [[[m] V, [m] N, [m] E
, [m] ΔMD, [°] Inc, [°] Azi, [°] Dif_inc, [°] Dif_azi,
# ...Curvature Change (0 or 1), Section Number]]. and ---> Data_bzr: [[[D_s, V_s, N_s, E_s, Inc_s, Azi_s
, Sec N°], [[m] D_e, V_e, N_e, E_e, Inc_e, Azi_e, Sec N°]]]
# Creates a Planned Well Path (PWP) Optimized Survey points
PWP_matrix = pwp_manager(Analyzed_data, Data_bzr, Sur_pts, Step_u, Ran_Tol, Max_DLS)  # [[V [m], N [m], E
 [m], MD [m], Inc [°], Azi [°], DLS [°/30m]]]
df_PWP = pd.DataFrame(data=PWP_matrix, columns=["V [m]", "N [m]", "E [m]", "MD [m]", "Inc [°]", "Azi
 [°]", "DLS [°/30m]"])  # Convert the PWP matrix into DF

# --------------------------------- Principal Loop ---------------------------------------
# Variables preparation
Total_L = dist_act + dist_stab  # [m] Total length of BHA
set_variables = [deltaT, OD_tool, ID_tool, dist_act, dist_stab, Max_off, Ela_Mod, Offset_L, Max_deg,
Total_L]  # Inputs from the GUI (User)
```

```
# Initialization of certain variables
RP_mtx = PWP_matrix  # Initialize the Reference Path (RP)
i_pwp = 0  # Initialize principal iterator, should follow the number of rows of the PWP matrix
Survey = True  # To know if a survey points has been reached or not
correcting = False  # Determines if the bit is in the middle of a correction path or not
MD_RP = 0  # [m] Initialize measured Depth RP
Inc_RP = 0  # [rad] Initialize inclination RP
Azi_RP = 0  # [rad] Initialize azimuth RP
given_variables = [0, 0, 0, 0, 0, 0]  # [Mu, RPM, WOB, Bore Diameter, Es, Steer] filled later
RSS_mtx = np.zeros((1, 15))  # Matrix (SI units): [[MD, Time, Inc, Azi, HD, TVD, E, N, Offset, DLS,
Tot_Force_inc, Tot_Force_azi, ROP_Ax, ROP_Inc, ROP_Azi]]
Survey_RSS = 0  # [m] Initialize Δ survey for the RSS Model Simulation
Last = False  # Boolean to tell the loop that the last PWP survey point is been analyzed

# Case 1st row
SUR = np.empty((0, 6))  # Survey points (SUR) for the simulation [[[m] MD, [m] V, [m] N, [m] E, [°] Inc
, [°] Azi]]
Bit_row = np.zeros((1, 6))  # Actual bit location [[m] MD, [m] V, [m] N, [m] E, [rad] Inc, [rad] Azi]
SUR = np.append(SUR, Bit_row, axis=0)  # Add the initial survey point (point 0) in the SUR matrix
Dr_Dp_k_mtx = np.zeros((3, 3))  # Matrix dΔr_(k)/dp_k [Depth, Inclination, Azimuth] each one [[N], [E], [
V]] 3x3 matrix
Dr_Dp_k1_mtx = np.empty((0, 3))  # Matrix dΔr_(k+1)/dp_k [Depth, Inclination, Azimuth] each one [[N], [E
], [V]] 3x3 matrix.
E_1 = np.zeros((1, 3))  # Initialize the matrix DSFS Error [[N, E, V]]
E_2 = np.zeros((1, 3))  # Initialize the matrix ABZ Error [[N, E, V]]
E_3 = np.zeros((1, 3))  # Initialize the matrix ASZ Error [[N, E, V]]
E_4 = np.zeros((1, 3))  # Initialize the matrix MBXY1 Error [[N, E, V]]
E_5 = np.zeros((1, 3))  # Initialize the matrix MSXY1 Error [[N, E, V]]
Total_Cov_mxt = np.zeros((1, 6))  # Total Covariance of the whole errors
Radii = np.zeros((1, 3))  # Radii of the EOU [[N radius, E radius, V radius]]
Deviation_mtx = np.zeros((1, 10))  # Deviation matrix (SI units) [[MD, V_vec, N_vec, E_vec, Length_vec,
V_vec, N_vec, E_vec, Length_vec, Out_or_In (Bool)]]
CP_mtx = np.zeros((1, 7))  # Correction Path (CP) matrix [[[m] V, [m] N, [m] E, [m] MD, [°] Inc, [°] Azi
, [°/30m] DLS]]
i_cp = 0  # Initialize variable for the CP matrix iterator
Reach_idx = 0  # Initialize variable for Reach point index on the PWP once the deviation is corrected
Last_corr = False  # Boolean for the final correction point (in each correction)

while i_pwp < len(PWP_matrix) - 1:  # The PWP matrix will control the duration of the whole simulation
    if not correcting:  # Case: NOT correcting path
        i_pwp += 1  # Next iteration point in the PWP
        if i_pwp == len(PWP_matrix) - 1:  # Case: Last point of the simulation (Target coordinate)
            Last = True  # Change the boolean status
    else:  # Case: Correcting path
        i_cp += 1  # Next iteration point in the CP
        if i_cp == len(CP_mtx) - 1:  # Case: Last point of the CP matrix
            i_pwp = Reach_idx  # The end point of the CP should be the same reach point on the PWP
            Last_corr = True  # Change boolean status for the final use of the correction point

    while RSS_mtx[-1, 0] < Survey_RSS + Delta_Sur:  # If a Survey point has not been reached yet
        if Survey:  # If the bit has reached a survey point then receive a new given_data from other
modules
            # Ask for new parameters given by the other modules, assumed as "mean" value
            Mu_mean = 0.23  # [] Sliding factor coefficient - assumed as mean
            RPM_mean = 143.44375  # [rpm] Rotations per minute - assumed as mean
            WOB_mean = 69866.664  # [N] Weight on bit - assumed as mean
            Es_mean = 100893789.8  # [Pa] Specific energy of the rock - assumed as mean
            Steer_mean = 0.15  # [] Steerability of the bit - assumed as mean
            # Picks a random value based on an uniform distribution and the percentage of error set by
the user, to add uncertainty
            Sign = 1 if np.random.uniform(0, 1) > 0.5 else -1  # Pick a random sign + or -
            Mu = round(Mu_mean + np.random.uniform(0, Mu_mean * Error_input) * Sign, 5)  # Add some noise
 ± to the given Mu input.
            Sign = 1 if np.random.uniform(0, 1) > 0.5 else -1  # Pick a random sign + or -
            RPM = round(RPM_mean + np.random.uniform(0, RPM_mean * Error_input) * Sign, 5)  # Add some
noise ± to the given RPM input.
            Sign = 1 if np.random.uniform(0, 1) > 0.5 else -1  # Pick a random sign + or -
            WOB = round(WOB_mean + np.random.uniform(0, WOB_mean * Error_input) * Sign, 5)  # Add some
noise ± to the given WOB input.
            Sign = 1 if np.random.uniform(0, 1) > 0.5 else -1  # Pick a random sign + or -
            Es = round(Es_mean + np.random.uniform(0, Es_mean * Error_input) * Sign, 5)  # Add some noise
 ± to the given Es input.
            Sign = 1 if np.random.uniform(0, 1) > 0.5 else -1  # Pick a random sign + or -
            Steer = round(Steer_mean + np.random.uniform(0, Steer_mean * Error_input) * Sign, 5)  # Add
some noise ± to the given Steer input.
            given_variables = [Mu, RPM, WOB, bore_D, Es, Steer]  # Put the variable into a list

        # Determines whether or not the bit is in the middle of a correction path operation
        if not correcting:  # Case: NOT correcting path
            RP_mtx = PWP_matrix  # The Reference Path (RP) is equal to the PWP
            MD_RP = RP_mtx[i_pwp, 3]  # [m] Target length
            Inc_RP = RP_mtx[i_pwp, 4] * np.pi / 180  # [rad] Target inclination
            Azi_RP = RP_mtx[i_pwp, 5] * np.pi / 180  # [rad] Target azimuth
```

```
        else:  # Case: Correcting path
            RP_mtx = CP_mtx  # The Reference Path (RP) is equal to the CP
            MD_RP = CP_mtx[i_cp, 3]  # [m] Correction target length
            Inc_RP = CP_mtx[i_cp, 4] * np.pi / 180  # [rad] Correction target inclination
            Azi_RP = CP_mtx[i_cp, 5] * np.pi / 180  # [rad] Correction target azimuth
            if Last_corr:  # Case: Last point of the CP
                correcting = False  # Change the correcting boolean to the False again
                Last_corr = False  # Change the last point of correction boolean to False again

        # Calls the RSS Model to simulate one point at each iteration
        RSS_mtx = rss_model(set_variables, given_variables, RSS_mtx, Inc_RP, Azi_RP)  # Rtn: RSS matrix
updated (1 new row with 15 columns)
        # Determines whether or not the MD_PP has been reached or the Survey point has been reached first
        if RSS_mtx[-1, 0] < MD_RP:  # If the RSS MD has not reached the Target MD from the RP
            if RSS_mtx[-1, 0] < Survey_RSS + Delta_Sur:  # If the RSS MD has NOT reached the
correspondent Δ Survey
                Survey = False  # To keep working with the Given data from the last survey
            else:  # If the RSS MD has reached the correspondent Δ Survey
                # Call Vectors_Errors_V1.0 algorithm
                inc_rad = RSS_mtx[-1, 2] * np.pi / 180  # [rad] Inclination from the simulation
                azi_rad = RSS_mtx[-1, 3] * np.pi / 180  # [rad] Azimuth from the simulation
                Bit_row = np.array([[RSS_mtx[-1, 0], RSS_mtx[-1, 5], RSS_mtx[-1, 7], RSS_mtx[-1, 6],
inc_rad, azi_rad]])  # [[m] MD, [m] V, [m] N, [m] E, [rad] Inc, [rad] Azi]
                vec_errors = voe(RP_mtx, Bit_row, SUR, Dr_Dp_k_mtx, Dr_Dp_k1_mtx, G, MF, Dip, Rho, E_1,
E_2, E_3, E_4, E_5, Total_Cov_mxt, SF, Radii, Min_R, Deviation_mtx, Last)
                SUR = vec_errors[0]  # Update SUR matrix of survey points from the RSS simulation
                Dr_Dp_k_mtx = vec_errors[1]  # Update the partial derivative matrix dΔr_(k)/dp_k [[N], [E
], [V]] 3x3 matrix each time
                Dr_Dp_k1_mtx = vec_errors[2]  # Update the partial derivative matrix dΔr_(k+1)/dp_k [[N
], [E], [V]] 3x3 matrix each time
                E_1 = vec_errors[3]  # Update the matrix DSFS Error [[N, E, V]]
                E_2 = vec_errors[4]  # Update the matrix ABZ Error [[N, E, V]]
                E_3 = vec_errors[5]  # Update the matrix ASZ Error [[N, E, V]]
                E_4 = vec_errors[6]  # Update the matrix MBXY1 Error [[N, E, V]]
                E_5 = vec_errors[7]  # Update the matrix MSXY1 Error [[N, E, V]]
                Total_Cov_mxt = vec_errors[8]  # Update the matrix for the Total Covariance of the whole
errors
                Radii = vec_errors[9]  # Update the matrix for the radii of the EOU [[N radius, E radius
, V radius]]
                Deviation_mtx = vec_errors[10]  # Update the matrix Deviation (SI units) [[MD, V_vec,
N_vec, E_vec, Length_vec, V_eou, N_eou, E_eou, Length_eou, Out EOU (Bool)]]
                # Determine whether or not a correction is needed
                if Deviation_mtx[-1, 9] == 1 and CP_Active:  # If the 'Out EOU' from the Deviation_mtx is
 1 means: Out of EOU, so correct it. and CP is active by the user
                    Bit_pos = np.array([[RSS_mtx[-1, 5], RSS_mtx[-1, 7], RSS_mtx[-1, 6], RSS_mtx[-1, 0],
RSS_mtx[-1, 2], RSS_mtx[-1, 3], RSS_mtx[-1, 9]]])  # [V_b[m], N_b[m],...
                    # ...E_b[m], MD_b[m], Inc_b[°], Azi_b[°], DLS_b[°/30m]]
                    Reach_idx, CP_mtx = correction(PWP_matrix, Bit_pos, Max_DLS_corr, Tor_max_corr,
Step_u_corr, Reach_all)  # Rtn: Reach index point on PWP, Correction Path (CP)
                    i_cp = 1  # Reset the iterator for the CP matrix
                    correcting = True  # Change boolean status to tell the algorithm that the system is
currently correcting the path
                # Update the next survey point regarding the RSS simulation
                Survey_RSS = Survey_RSS + Delta_Sur  # [m] New survey point
                Survey = True  # To receive new Given data from a new survey
        elif RSS_mtx[-1, 0] >= Survey_RSS + Delta_Sur:  # If the RSS MD has reached the Δ Survey and the
MD_RP at the same time
            # Call Vectors_Errors_V1.0 algorithm
            inc_rad = RSS_mtx[-1, 2] * np.pi / 180  # [rad] Inclination from the simulation
            azi_rad = RSS_mtx[-1, 3] * np.pi / 180  # [rad] Azimuth from the simulation
            Bit_row = np.array([[RSS_mtx[-1, 0], RSS_mtx[-1, 5], RSS_mtx[-1, 7], RSS_mtx[-1, 6], inc_rad
, azi_rad]])  # [[m] MD, [m] V, [m] N, [m] E, [rad] Inc, [rad] Azi]
            vec_errors = voe(RP_mtx, Bit_row, SUR, Dr_Dp_k_mtx, Dr_Dp_k1_mtx, G, MF, Dip, Rho, E_1, E_2,
E_3, E_4, E_5, Total_Cov_mxt, SF, Radii, Min_R, Deviation_mtx, Last)
            SUR = vec_errors[0]  # Update SUR matrix of survey points from the RSS simulation
            Dr_Dp_k_mtx = vec_errors[1]  # Update the partial derivative matrix dΔr_(k)/dp_k [[N], [E], [
V]] 3x3 matrix each time
            Dr_Dp_k1_mtx = vec_errors[2]  # Update the partial derivative matrix dΔr_(k+1)/dp_k [[N], [E
], [V]] 3x3 matrix each time
            E_1 = vec_errors[3]  # Update the matrix DSFS Error [[N, E, V]]
            E_2 = vec_errors[4]  # Update the matrix ABZ Error [[N, E, V]]
            E_3 = vec_errors[5]  # Update the matrix ASZ Error [[N, E, V]]
            E_4 = vec_errors[6]  # Update the matrix MBXY1 Error [[N, E, V]]
            E_5 = vec_errors[7]  # Update the matrix MSXY1 Error [[N, E, V]]
            Total_Cov_mxt = vec_errors[8]  # Update the matrix for the Total Covariance of the whole
errors
            Radii = vec_errors[9]  # Update the matrix for the radii of the EOU [[N radius, E radius, V
radius]]
            Deviation_mtx = vec_errors[10]  # Update the matrix Deviation (SI units) [[MD, V_vec, N_vec,
E_vec, Length_vec, V_eou, N_eou, E_eou, Length_eou, Out EOU (Bool)]]
            # Determine whether or not a correction is needed
            if Deviation_mtx[-1, 9] == 1 and CP_Active:  # If the 'Out EOU' from the Deviation_mtx is 1
means: Out of EOU, so correct it. and CP is active by the user
```

```
                Bit_pos = np.array([[RSS_mtx[-1, 5], RSS_mtx[-1, 7], RSS_mtx[-1, 6], RSS_mtx[-1, 0],
RSS_mtx[-1, 2], RSS_mtx[-1, 3], RSS_mtx[-1, 9]]])  # [V_b[m], N_b[m],...
                # ...E_b[m], MD_b[m], Inc_b[°], Azi_b[°], DLS_b[°/30m]]
                Reach_idx, CP_mtx = correction(PWP_matrix, Bit_pos, Max_DLS_corr, Tor_max_corr,
Step_u_corr, Reach_all)  # Rtn: Reach index point on PWP, Correction Path (CP)
                i_cp = 1  # Reset the iterator for the CP matrix
                correcting = True  # Change boolean status to tell the algorithm that the system is
currently correcting the path
            # Update the next survey point regarding the RSS simulation
            Survey_RSS = Survey_RSS + Delta_Sur  # [m] New survey point
            Survey = True  # To receive new Given data from a new survey
            break  # Break the Survey loop only
        else:  # If the current MD is bigger than the MD_RP
            break  # Break the Survey loop only

    # To calculate the error with the Target point only (Last point)
    if Last:
        # Call Vectors_Errors_V1.0 algorithm
        inc_rad = RSS_mtx[-1, 2] * np.pi / 180  # [rad] Inclination from the simulation
        azi_rad = RSS_mtx[-1, 3] * np.pi / 180  # [rad] Azimuth from the simulation
        Bit_row = np.array([[RSS_mtx[-1, 0], RSS_mtx[-1, 5], RSS_mtx[-1, 7], RSS_mtx[-1, 6], inc_rad,
azi_rad]])  # [[m] MD, [m] V, [m] N, [m] E, [rad] Inc, [rad] Azi]
        vec_errors = voe(RP_mtx, Bit_row, SUR, Dr_Dp_k_mtx, Dr_Dp_k1_mtx, G, MF, Dip, Rho, E_1, E_2, E_3
, E_4, E_5, Total_Cov_mxt, SF, Radii, Min_R, Deviation_mtx, Last)
        Deviation_mtx = vec_errors[10]  # Update the matrix Deviation (SI units) [[MD, V_vec, N_vec,
E_vec, Length_vec, V_eou, N_eou, E_eou, Length_eou, Out EOU (Bool)]]
    print("", end=f"\rIteration: {i_pwp} of {len(PWP_matrix) - 1}")  # Print the current iteration in
the console

print(f"\nExporting the results and plotting... Please wait")  # Print a message for the user once the
 iterations have finished
# Put the RSS simulation results into a DF
headers1 = ['MD [m]', 'Time [min]', 'Inc [°]', 'Azi [°]', 'HD [m]', 'TVD [m]', 'East [m]', 'North [m
]', 'Offset []', 'DLS [°/30m]', 'Tot F_inc [N]', 'Tot F_azi [N]',
            'ROP Ax [m/hr]', 'ROP Inc [m/hr]', 'ROP Azi [m/hr]']
df_SIM = pd.DataFrame(data=np.round(RSS_mtx, 6), columns=headers1)

# Put the deviation matrix into a DF
headers2 = ['MD [m]', 'V_vec [m]', 'N_vec [m]', 'E_vec [m]', 'Length_vec [m]', 'V_eou [m]', 'N_eou [m
]', 'E_eou [m]', 'Length_eou [m]', 'Out EOU']
df_Deviation = pd.DataFrame(data=Deviation_mtx, columns=headers2)

# Export DF to Excel
with pd.ExcelWriter('RSS_Simulator_V2.3.xlsx') as writer:
    df_PWP.to_excel(writer, sheet_name='PWP')  # Add the PWP worksheet
    df_SIM.to_excel(writer, sheet_name='SIM')  # Add the Simulation worksheet
    df_Deviation.to_excel(writer, sheet_name='DEV')  # Add the Deviation verification survey points
worksheet

# Plotting
fig1 = plt.figure(figsize=(9, 6))
PWP = fig1.add_subplot(111, projection='3d')
PWP.scatter(df_data['E [m]'], df_data['N [m]'], df_data['V [m]'], color='r', label='Survey Points')
PWP.plot(df_PWP['E [m]'], df_PWP['N [m]'], df_PWP['V [m]'], 'g', label='Optimized Path')
PWP.plot(df_SIM['East [m]'], df_SIM['North [m]'], df_SIM['TVD [m]'], 'b', label='Simulation')
plt.gca().invert_zaxis()
PWP.set_xlabel('East [m]')
PWP.set_ylabel('North [m]')
PWP.set_zlabel('TVD [m]')
PWP.legend()
PWP.set_title('RSS Simulation V2.3')
plt.show()
```